Role of Cryptochromes in Retinal Responses to Light

Jovi Chau-Yee Wong

St. Catherine's College

Nuffield Laboratory of Ophthalmology
Nuffield Department of Clinical Neurosciences

University of Oxford

Thesis submitted in fulfilment of the requirements for
the degree of Doctor of Philosophy at the University of Oxford

Hilary Term 2016

Abstract

Cryptochromes 1 and 2 (CRY1-2) are key components of the negative limb of the mammalian circadian clock. Like in many peripheral tissues, *Cry1* and *Cry2* are expressed in the retina where they are thought to play a role in regulating retinal circadian physiology.

This thesis investigates the role of Cryptochromes in the mammalian retina. The localization and expression pattern of CRY1 and CRY2 in the mouse retina are described, showing that CRY1 is expressed throughout, whereas CRY2 expression is restricted to the outer retina.

Furthermore, circadian rhythms in retinal physiology, including the photopic electroretinogram (ERG) b-wave amplitude, contrast sensitivity and the pupillary light response (PLR) are found to be all attenuated or abolished in CRY1-deficient mice. By contrast, these physiological rhythms are unaffected in mice lacking CRY2, and only photopic ERG rhythms are affected. As such, both CRY1 and CRY2 play roles in regulating normal retinal circadian rhythms, though CRY1 plays a dominant role.

The role of melanopsin in retinal rhythms is also investigated. It is found that loss of melanopsin affects contrast sensitivity rhythms but not PLR rhythms. The work in this thesis suggests that the retinal circadian clock is composed of at least two independent networks of oscillators in the retina which regulate key aspects of retinal physiology.

Lastly, this thesis investigates whether the retinal clock has any downstream effects on the SCN master pacemaker. The experimental results presented here suggest that the retinal clock is capable of rhythmically gating light input to the SCN clock, acting as a *zeitnehmer*.

Acknowledgements

"I don't like relaxing - I like science!" - Princess Bubblegum (Adventure Time)

I am lucky to have had the support and friendship of so many talented and wonderful people throughout my DPhil - I would like to express my sincere thanks to all of you.

First and foremost, I must acknowledge the inspirational mentorship I have received from my supervisors: Professors Stuart Peirson and Russell Foster over the last four years. I am lucky to have been provided this opportunity to learn from them. Stuart - thank you for being such a reliable and enthusiastic supervisor - you have always pushed me to think critically about the science, but also find time to relax! Russell - thank you for your insightful advice and positivity, as well as for always supporting opportunities for me to develop as a scientist!

I am very grateful to the Electric and Magnetic Fields Biological Research Trust for their generous support of my research project and DPhil.

Thank you to my collaborators at Public Health England – Dr. Zenon Sienkiewicz and Jackie Haines, who invested great effort towards our EMF work. To my collaborators at MRC Harwell – Dr. Pat Nolan and Dr. Gareth Banks, thank you for your warm support and expertise. I am also grateful to my collaborators at MRC LMB Cambridge – Professor Mick Hastings and Dr. Liz Maywood, as well as Mat Edwards and Nicola Smyllie, thank you for your generosity in providing me with experimental tools and patience with all my questions!

A big thank you to my research colleagues and friends: Eric, Violetta, Simona, Sibah, Laurence, Tom, David, Mathilde, Lindsay, Dany, Dominik, and Shaun. Thank you also to the wonderful BMS staff - especially Andrew and Jonathon - who have always gone above and beyond to support my experiments. Thank you also to our administrative team who have always responded kindly to my frantic emails: Toria (thank you for helping me with all my letters!), Marion, Carol, Eleanor, Rachel, Khwaja, Anne, and Claire.

An extra special thanks to Aarti Jagannath, Michelle McClements, Carrie Pothecary, Alun Barnard, Doron Hickey, Suze Broadgate and Steve Hughes, whom have each taken extra time to teach me their technical expertise and provide knowledgeable advice on my work.

Jess - thanks for being an amazing friend and colleague - I can always count on you for support and advice (and brownies!). Clio - thank you so much for being the greatest friend <3 Thomas - thank you for always keeping in touch and reminding me to stay positive! Kate and Ray – thanks for being such wonderful housemates and friends and tolerating my thesis fashion! Mom, Dad, Jory and Uncle Ray - thank you for being such a loving and supportive family - you have always encouraged me to pursue my dreams!

Lastly, to my partner, Prash - you make me the best version of myself. Thank you for supporting me always, and for 5ever.

Statement of Originality

The results in this thesis are my own work, except where this has been indicated otherwise in the thesis text and below.

The photopic electroretinogram protocol used in Chapter 3 was designed together with technical expertise from Dr. Alun Barnard (Nuffield Laboratory of Ophthalmology, University of Oxford).

Dr. Carina Pothecary (Nuffield Laboratory of Ophthalmology, University of Oxford) performed the pupillometry experiments shown in Figure 3.9.

The *Opn4*$^{-/-}$ mice used in Chapters 2 and 4 were genotyped by Simona di Pretoro (Nuffield Laboratory of Ophthalmology, University of Oxford).

The Cry1-eGFP plasmid used in Chapter 5 was constructed by Mathew Edwards (Laboratory of Molecular Biology, University of Cambridge).

The quad-mutant AAV 2/2 capsid used in Chapter 5 was provided by Doron Hickey and Dr. Samantha Da Silva (both Nuffield Laboratory of Ophthalmology, University of Oxford).

The Cry1-eGFP plasmid used in Chapter 5 was packaged into the quad-mutant AAV 2/2 capsid by Dr. Michelle McClements (Nuffield Laboratory of Ophthalmology, University of Oxford).

The GFP-only AAV used in Chapter 5 was constructed and provided by Doron Hickey.

Intravitreal injections performed in Chapter 5 were conducted with the assistance of Jessica Rodgers (Nuffield Laboratory of Ophthalmology, University of Oxford).

The EMF exposure experiments shown in Chapter 7 were performed by Jackie Haines (Public Health England). Setup of the experimental equipment used for EMF exposure experiments was performed with the assistance of Dr. Carina Pothecary, as well as Jackie Haines and Dr. Zenon Sienkiewicz (both Public Health England).

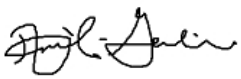

Jovi Chau-Yee Wong
June 2016

Author's Publications arising from this thesis

The work described in this thesis has contributed to the following manuscript:

Wong JCY, Smyllie NJ, Banks G, Barnard AR, Pothecary CA, Maywood ES, Jagannath A, Hughes S, MacLaren RE, Hastings MH, Nolan PM, Foster RG and Peirson SN. (*in preparation*) Differential roles for mammalian cryptochromes in the retinal circadian clock.

Table of Contents

Abbreviations

AAV	Adeno-associated virus
AII	type A II amacrine cells
AMPA	α-amino-3-hydroxy-5-methyl-4-isoxazolepropionic acid receptor
AMPK	5' AMP-activated protein kinase
ANOVA	Analysis of variance
ASPD	Advanced Sleep Phase Disorder
AU	Arbitrary Units
AVP	Arginine Vasopressin
B-Gal	beta-galactosidase
BMAL1	Brain and Muscle ARNT-Like 1
BSA	Bovine Serine Albumin
cAMP	Cyclic adenosine monophosphate
CCG	Clock-controlled Gene
cGMP	(cyclic) guanosine monophosphate
ChAT	Cholinergic Acetyltransferase
CK1	Casein kinase 1
cl	attenuated diphtheria toxin fused to cone opsin promotor
CLOCK	Circadian locomotor output cycles kaput
CMV	Cytomegalovirus (promoter)
CNS	Central Nervous System
cpd or c/d	Cycles per degree of visual angle
CRE	cyclic AMP (adenosine monophosphate) response element
CREB	cAMP response element-binding protein
CRSD	Circadian Rhythm Sleep Disorder
CRTC1	CREB-related transcription coactivator 1
Cry1	Cryptochrome 1 (mRNA)
CRY1	Cryptochrome 1 (protein)
CRY1 & 2	Cryptochrome 1 & 2
Cry2	Cryptochrome 2 (mRNA)
CRY2	Cryptochrome 2 (protein)
CT	Circadian time
C_T	PCR Cycles (Threshold)
DAPI	4',6-diamidino-2-phenylindole
DD	Constant dark
dKO	Double knockout
DNA	Deoxyribonucleotide
DRD2	Dopamine receptor D2
DSPD	Delayed Sleep Phase Disorder
DTA	diphtheria toxin subunit A
dTim, dPer, dCry	*Drosophila* Timeless, *Drosophila* Per, *Drosophila* Cry
e-Box	Enhancer box
EDTA	Ethylenediamine tetraacetic acid

EEG	Electroencephalography
eGFP	Enhanced Green Fluorescent Protein
ELISA	Enzyme-linked immunosorbent assay
EMF	Electromagnetic Fields
ERG	Electroretinogram
EYFP	enhanced yellow fluorescent protein
FAD	Flavin Adenine Dinucleotide
GABA	gamma-Aminobutyric acid
GAPDH	Glyceraldehyde 3-phosphate dehydrogenase
GCL	Ganglion Cell Layer (retina)
GDP/GTP	guanine diphosphate / guanosine triphosphate
GFP	Green Fluorescent Protein
GLT-1	Glycine Transporter 1
GNAT1	guanine nucleotide binding protein (G protein), alpha transducing activity polypeptide 1
HA (tag)	Human influenza hemagglutinin
HEK293T	Human Embryonic Kidney 293T cells
HPA	Hypothalamic-pituitary-adrenal
hr	hour
HRP	Horseradish Peroxidase
INL	Inner Nuclear Layer (retina)
IPL	Inner Plexiform Layer (retina)
IR	infrared
IRC	irradiance response curve
IS	(Photoreceptor) Inner Segements
ISI	Inter-stimulus Interval
KO	knockout
LacZ	β-galactosidase gene
LCM	Laser-capture microdissection
LD	Light/dark
LED	Light-emitting diode
LL	Constant light
LTC	Light-tight chamber
LWS	long-wave sensitive (cone opsin)
MASCO	methamphetamine-sensitive circadian oscillator
mRNA	Messenger Ribonucleic acid
MWS	middle-wave sensitive (cone opsin)
NIF	Non-Image-Forming
NIR	Near-infrared
NOR	novel object recognition
NPAS2	neuronal PAS domain-containing protein 2
OKN	Optokinetic nystagmus
OKR	Optokinetic response
ONL	Outer Nuclear Layer (retina)
OPL	Outer Plexiform Layer (retina)
OPN	Olivary pretectal nucleus
Opn4	melanopsin gene
OPN4	Melanopsin protein
OS	(Photoreceptor) Outer Segements
PACAP	Pituitary adenylate cyclase-activating polypeptide
PBS	Phosphate Buffered Saline

PCR	polymerase chain reaction
PDE	Phosphodiesterase
PER1 & 2	Period 1 & 2
PER2::LUC	Per2-Luciferase
PFA	paraformaldehyde
PIPR	Post-illumination Pupil Response
PIR	Passive-infrared
PKA	cAMP-dependent protein kinase A
PLR	Pupillary Light Response
pRGC(s)	photosensitive retinal ganglion cell(s)
qPCR	Quantitative (real time reverse transcriptase) Polymerase Chain Reaction
rd	mutation of rod photoreceptor cGMP-phosphodiesterase β subunit
REM	Rapid eye movement
REV-ERBα	Nuclear receptor subfamily 1, group D, member 1 (also known as NR1D1)
RHT	Retinohypothalamic tract
RNA	Ribonucleic acid
RNAi	Ribonucleic acid interference
ROR	Retinoic acid-related orphan receptors
RORE	Retinoic acid-related orphan receptor response element
RPE	Retinal Pigment Epithelium
RT	Room Temperature
RT-PCR	Reverse Transcriptase Polymerase Chain Reaction
SCN	Suprachiasmatic nucleus
SCRD	Sleep and circadian rhythm disruption
SDS or SDS-PAGE	Sodium Dodecyl Sulfate Polyacrylamide Gel Electrophoresis
sec	seconds
SEM	Standard Error of the Mean
siRNA	Small interfering RNA
SWS	Short Wavelength Sensitive (cone opsin)
tau	endogenous circadian period
TBP	TATA-binding protein
TBS	Tris-Buffered Saline
TH	Tyrosine Hydroxylase
TKO	triple-knockout mouse (rods, cones, and melanopsin)
TTFL	Transcriptional-translational feedback loop
UVS	Ultraviolet-sensitive (cone opsin)
VIP	Vasoactive intestinal peptide
Vipr2	Vasoactive intestinal peptide receptor 2 (gene)
VLPO	Ventrolateral preoptic nucleus
VPAC2	Vasoactive intestinal peptide receptor 2 (protein)
WT	Wildtype
ZT	Zeitgeber Time

1

General Introduction

1.1 Circadian Rhythms

Endogenous circadian rhythms enable organisms to anticipate and adapt to the predictable changes in the 24 hour solar cycle. The word “circadian” comes from the Latin *circa diem,* which means “around a day.” Evolution of species under the 24 hour light-dark cycle favours the optimization of biological resources to conserve energy and anticipate daily changes.

Virtually all organisms possess circadian rhythms. In mammals, circadian rhythms occur in a wide range of physiological and behavioural parameters, such as activity and rest rhythms, as well as daily rhythms in body temperature and hormone levels. These are direct outputs of the master circadian pacemaker in the suprachiasmatic nuclei (SCN) of the brain. Circadian rhythms also occur at a cellular level and are the product of an intracellular clock mechanism, comprised of a set of interlocking transcriptional-translational feedback loops (TTFLs) involving core clock genes. To provide any adaptive value, the circadian clock must be synchronized or entrained to the environmental light-dark cycle. In mammals, this synchronization is termed ‘photoentrainment’, as the primary entrainment signal is light. Light is detected by photoreceptors of the eye and photic information is sent to the master circadian pacemaker in the SCN (Hughes *et al*., 2015b). The SCN then synchronizes circadian rhythms throughout the body.

1.1.1 Criteria for Circadian Rhythms

A biological rhythm must fulfil the following criteria in order to be deemed a circadian rhythm (Pittendrigh, 1960, Aschoff, 1960):

1 The rhythm must be endogenously generated.

A circadian rhythm must persist in constant conditions (such as constant darkness or constant light). It is endogenously generated and not simply driven in response to a rhythmic external stimulus, such as light. For instance, an animal lacking a circadian clock may show rhythmic behaviour under a 24-hour light-dark cycle due to masking. However, under constant conditions, no rhythm would be apparent.

2 The rhythm must entrainable to environmental cycles with 24 hour periods.

A circadian rhythm must be capable of being reset to environmental 24 hour cycles by an external stimulus termed a *zeitgeber*. *Zeitgeber*s ("time-givers" in German, Aschoff (1960)) synchronize a circadian rhythm with the local environmental time in order to ensure the circadian rhythm aligns with the environmental rhythm. *Zeitgeber*s may include food, hormone signalling, and temperature, though light is the primary *zeitgeber* for mammals.

3 The rhythm must have a free running period of approximately 24 hours.

Under constant conditions, in the absence of *zeitgeber*s, the persisting endogenous rhythm must exhibit a period (tau) of around 24 hours.

4 The rhythm must exhibit temperature compensation.

Temperature compensation refers to the fact that circadian rhythms must maintain 24-hour periodicity over a broad range of physiological temperatures. At different

temperatures, the molecular kinetics of biochemical reactions can sometimes change, but a true circadian rhythm must maintain circadian periodicity despite changing temperatures, thus exhibiting temperature compensation.

1.1.2 Circadian Rhythms in Mammalian Physiology

Endogenous circadian rhythms convey a selective advantage to organisms by allowing them to anticipate the regular environmental changes between night and day (Hut and Beersma, 2011). In mammals, a variety of physiological phenomena have been observed to exhibit circadian rhythms (Refinetti, 2006). These include locomotor activity, sleep, feeding and excretion, heart rate, blood pressure and body temperature. Learning ability (Chaudhury and Colwell, 2002) and hormone release (Chung *et al*., 2011) also exhibit circadian rhythms. In particular, activity-rest cycles are perhaps the best-characterized circadian rhythms in many species. Animals that are active during the day and rest at night are termed “diurnal” (including humans), whilst animals that are active at night and rest during the day are classified as “nocturnal”. This classification has allowed for some generalizations between different species based on whether they are diurnal or nocturnal (Challet, 2007).

Characterization of physiological phenomena that exhibit circadian rhythms has been particularly valuable as it provides assays with which to examine clock function experimentally *in vivo.* For instance, measuring locomotor activity circadian rhythms is a highly useful method for evaluating circadian system function in mice (LeGates and Altimus, 2011).

1.1.3 The Suprachiasmatic Nucleus

In mammals, the master circadian pacemaker is located in the suprachiasmatic nuclei (SCN) of the hypothalamus (Klein *et al*., 1991). Lesion of the SCN results in behavioural arrhythmicity (Richter, 1971, Moore and Eichler, 1972, Stephan and Zucker, 1972), and transplantation of SCN tissue restores behavioural rhythms in SCN-lesioned animals with a circadian period matching that of the donor SCN (Ralph *et al*., 1990). Furthermore, SCN neurons were found to demonstrate a rhythm in action potential firing, where increased firing occurs during the subjective day and decreased firing in the subjective night (Inouye and Kawamura, 1979). Dissociation of SCN neurons revealed that individual SCN cells generate circadian rhythms (Welsh *et al*., 1995). Altogether, these early experiments revealed the importance of the SCN in the generation of mammalian circadian rhythms and paved the way for investigation of the molecular mechanisms governing these oscillations.

1.1.4 TTFL: the Mammalian Molecular Circadian Clock

At a molecular level, mammalian circadian rhythms are generated by an intracellular core clock mechanism, comprised of a transcriptional-translational feedback loop (TTFL) whereby clock genes (genes that form the major components of the core clock mechanism) are rhythmically transcribed and translated into proteins which negatively regulate their own expression with a period of close to 24 hours (Reppert and Weaver, 2002). In mammals, the main clock genes involved in the circadian rhythm core clock mechanism include the following genes: *Clock, Bmal1, Per1, Per2, Cry1* and *Cry2.*

This transcriptional-translational feedback loop begins with the transcription of *Clock* and *Bmal1* in the nucleus and translation of CLOCK and BMAL1 in the cytoplasm. CLOCK and

BMAL1 dimerize, translocate into the nucleus and bind E-box enhancer elements leading to the activation of transcription of Pers (*Per1* and *Per2*) and Crys (*Cry1* and *Cry2*). PERs and CRYs are translated in the nucleus, form heterodimeric complexes and translocate to the nucleus. The PER-CRY complexes then inhibit the CLOCK-BMAL1 complex binding to E-boxes, thus inhibiting their own transcription and translation. Over time, levels of PERs and CRYs decrease, and the inhibition of CLOCK-BMAL1 is lifted, thus restarting the cycle. The rhythmic expression of BMAL1 is further regulated by an additional loop involving REV-ERBα. Increases in REV-ERBα are stimulated by CLOCK-BMAL1, whereby REV-ERBα then inhibits the transcription of *Bmal1.* Additional feedback loops further regulate this core clock mechanism, such as the phosphorylation of PER and CRY by casein kinase I isoforms, ROR/REV-ERB binding element (RORE) regulation of *Bmal1*, as well ubiquitination by F-box proteins (such as CRY regulation by FBXL3). The mammalian molecular circadian clock has been recently reviewed (Buhr and Takahashi, 2013).

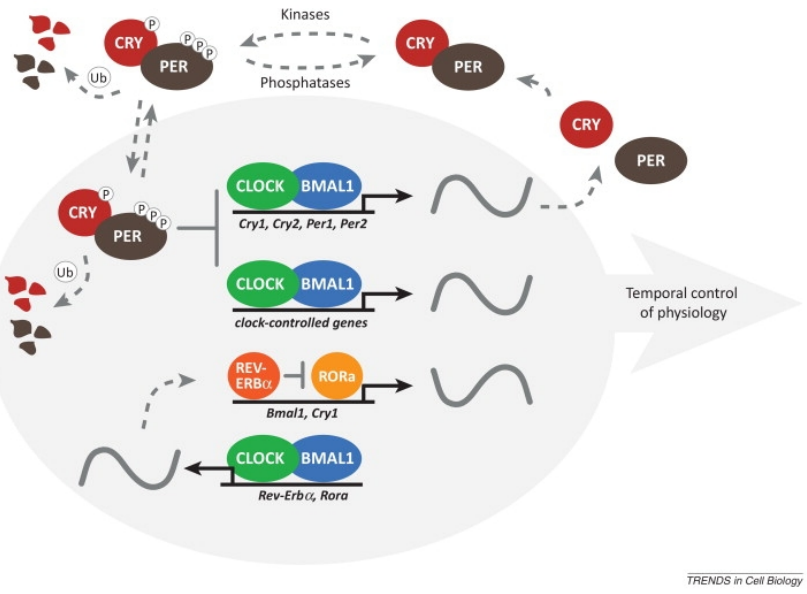

Figure 1.1. Model of Mammalian Circadian Rhythms. Molecular mechanism of mammalian circadian rhythms depicting the rhythmic cycling in the levels of the main core clock genes and proteins. Reproduced from Partch *et al*. (2014).

In addition to initiating the negative arm of the molecular clock cycle, the CLOCK-BMAL1 complex binds E-boxes controlling other genes that affect downstream behaviours. These genes are deemed clock-controlled genes (CCGs) and their transcription is thus regulated by the circadian clock. These CCGs have a wide downstream impact in that they control most aspects of physiology regulated by the circadian clock. Indeed, gene array studies have estimated that ~10% of all genes expressed in tissues exhibit circadian rhythms and thus ensure circadian regulation of physiology (Duffield, 2003).

1.1.5 Peripheral Clocks

The SCN is not the sole circadian clock in the body. The initial discovery of a circadian clock in cultured fibroblast cells (Balsalobre *et al*., 1998) led to further work that has identified clock genes expression in many peripheral tissues. Indeed, virtually all peripheral cells and tissues were found to express clock gene *Per2* in a clock gene reporter mouse, thus confirming the existence of peripheral clocks in potentially all cells (Yoo *et al*., 2004). The discovery of peripheral oscillators has caused the re-evaluation of the SCN master pacemaker as a coordinator of these peripheral oscillators, rather than the sole driver of rhythmicity in the body (Reppert and Weaver, 2002). It is now believed that SCN lesioning causes behavioural arrhythmicity because of loss of synchrony between the various peripheral oscillators, which fall out of phase with the environment as well as from one another (Buijs and Kalsbeek, 2001, Balsalobre, 2002). How the SCN synchronizes all of the peripheral clocks to the correct circadian time remains unknown, though it is thought that neural, hormonal and behavioural cues (such as feeding rhythms and body temperature rhythms) may contribute to this synchronizing signal (Dibner *et al*., 2010, Saini *et al*., 2011).

1.1.6 Analysis of Circadian Rhythmicity

In order to assess circadian rhythmicity, a variety of methods are used to determine several aspects of measurable rhythms (Refinetti, 2006). Here in this thesis, constant darkness and constant light conditions shall be used to study endogenous circadian rhythms. Then, two key analytical methods will be used to assess period (also denoted as tau, τ) of measured rhythms: actograms and chi-squared periodograms.

1.1.6.a Constant Conditions: LL and DD

Various light conditions can be used to investigate endogenous circadian rhythms. Mice are normally housed under 12:12 LD conditions, which denotes 12 hours of light followed by 12 hours of dark. The beginning of the light phase is denoted as ZT0 and the end of the light phase as ZT12. ZT6 is therefore 6 hours into the light phase (mid-day), and ZT18 is 6 hours into the dark phase (mid-night). ZT refers to *Zeitgeber* Time, indicating that a light cycle is present to convey *zeitgeber* entrainment information.

Wildtype laboratory mice display nocturnal activity patterns and generally consolidate their activity to the dark phase and rest to the light phase. A mouse that is entrained to the environmental light cycle will display stable onsets of activity from day to day (generally near the beginning of the dark phase). These entrained rhythms can be visualised using actograms (discussed below).

Whilst a cycle of light and dark can photoentrain mice, constant environmental conditions will reveal endogenous circadian rhythms. In constant darkness conditions, no photoentrainment cues are present. As such, activity-rest patterns under constant darkness reveal a mouse's internal clock rhythm. Indeed, one can then measure the free-

running natural period (tau) which is usually slightly shorter or longer than 24 hours. For instance, wildtype C57BL/6 mice have been measured to have an approximate endogenous tau of ~23.7 hours, whilst BALB/cJ mice have a free-running period of ~22.5 hours (Zheng *et al*., 2001, Legates *et al*., 2009).

In order to measure time under constant conditions, CT (circadian time) is therefore used to measure subjective time. CT0 indicates the beginning of the subjective day, CT12 the beginning of the subjective night. CT6 and CT18 therefore become subjective mid-day and subjective mid-night respectively.

Constant light conditions (LL) can also be used to reveal endogenous circadian rhythms. In constant light conditions, there is no onset or offset of the photoentrainment cue. As such, there are some caveats to using LL, as constant light exposure can sometimes alter behaviours and affect circadian rhythm measurements. For instance, mouse locomotor activity can be directly inhibited by constant bright light (Mrosovsky, 1999). Furthermore, constant light has been shown to have a period-lengthening effect, also known as Aschoff's Rule (Aschoff, 1981, Aschoff, 1979, Aschoff, 1960). In mice, a molecular mechanism for Aschoff's rule was recently reported. Constant light was found to inhibit PER2 degeneration, such that constitutively high levels of PER2 may thereby enhance phase delays and lengthen the circadian period (Munoz *et al*., 2005).

Lastly, investigation of clock gene mutant mice under different lighting conditions has yielded important information about the contribution of individual clock genes to overall circadian rhythmicity (Jud *et al*., 2005).

1.1.6.b Actograms

One of the most common methods of investigating circadian rhythms in mice is through measurement of activity-rest cycles. This has most often been facilitated through placing running wheels inside the home environment of individually-housed mice. Running wheel rotations indicate when a mouse is active and lack of wheel rotations indicate when a mouse is resting (Albrecht and Foster, 2002). Under constant conditions (DD and LL), the endogenous circadian rhythms in individual animals can therefore be examined.

Actograms are a graphical method of displaying a continuous data record of locomotor activity of one subject. Typically, data from one day (24 hours) is plotted on one line (x-axis is usually time in hours). Consecutive days are plotted one line after another (y-axis is days). By observing the vertical alignment of the onsets of activity, the period of locomotor rhythmicity may be easily visualised. If the alignment drifts towards the left, this indicates a tau < 24 hours. Alignments that drift towards the right indicate a tau > 24 hours and a completely vertical line would indicate a tau of exactly 24 hours.

Double-plotted actograms plot two days onto one line to allow for better visualization of activity patterns. The first line of a double plotted actogram would display data from Day 1 and Day 2, the second line would display Day2 and Day 3, the third line Day 3 and Day 4 and so on.

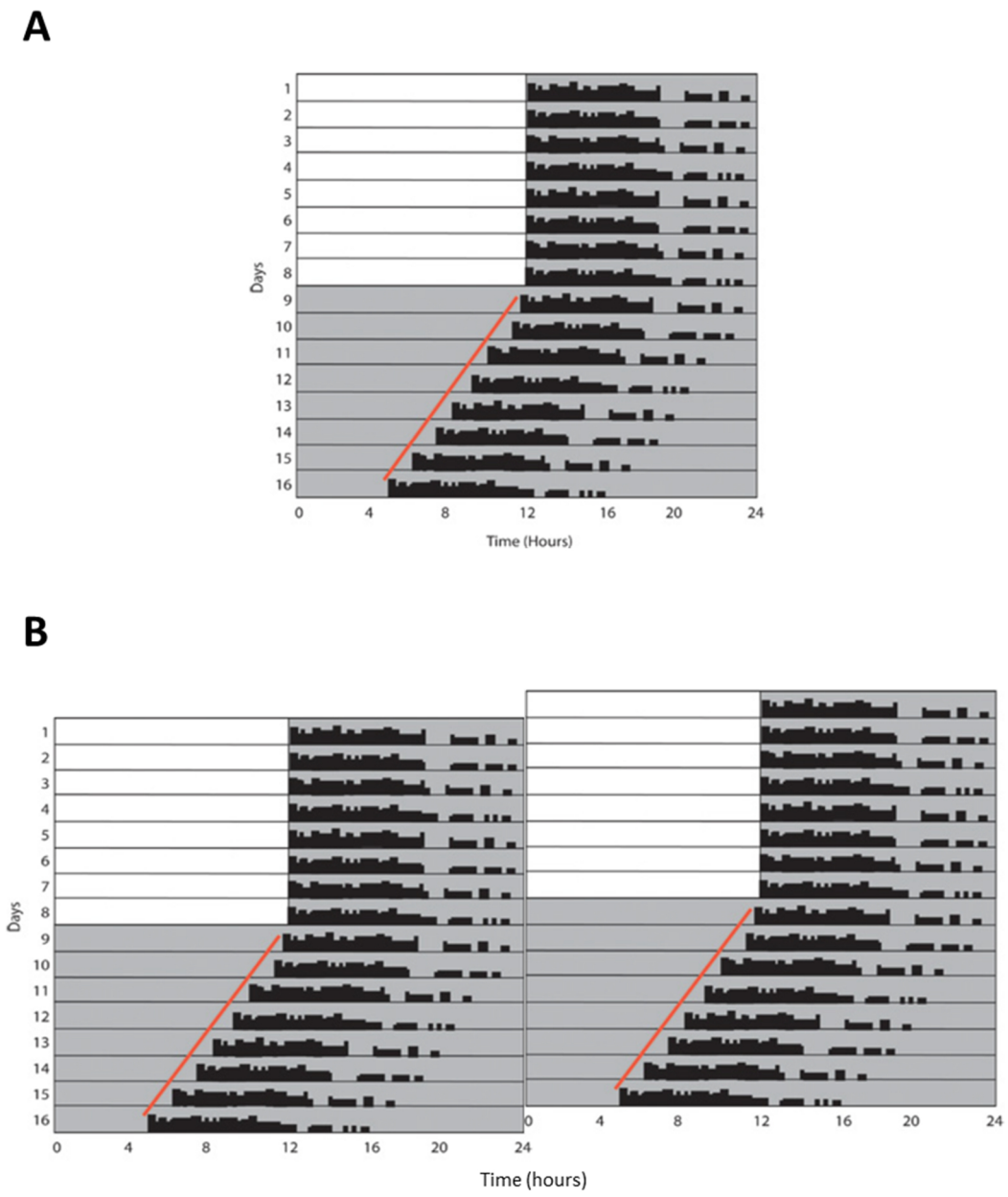

Figure 1.2. Single-plotted and double-plotted actograms. **(A)** Single-plotted actogram depicting activity of a mouse measured by running wheel activity. Black bars indicate activity (running wheel revolutions). White background indicates light, grey background indicates dark conditions. From Days 1-8, this house was housed under a 12:12 light-dark cycle and on Day 9, this mouse was released into DD conditions (constant darkness). In DD, the endogenous rhythm is revealed and the leftward drifting of the onset of activity (shown in red) over the next consecutive days indicates a tau of <24 hours. **(B)** Double plotted actogram to allow for better visualization of activity patterns. Reproduced and modified from LeGates and Altimus (2011).

1.1.6.c Chi-squared Periodograms

Whilst actograms display rhythmic locomotor activity well, determination of circadian period by measuring the slope of activity onsets over consecutive days can be subject to human bias, particularly when activity data is noisy. As such, chi-squared periodograms are ideal for displaying information about the circadian period(s) within a given actogram. Chi-squared periodograms are calculated and displayed by a computer, which adjusts the time scale of the given actogram automatically until onsets of activity align vertically. Based on how precise the fit, the computer assigns scores based on a mathematical index referring to variance (Sokolove and Bushell, 1978). When the tested period does not match that in the data, variance will be high, whereas when the tested period matches the period within the data, the variance will be low. Based on these scores, the computer can thus compute the period of the actogram. Following significance testing using the X2 statistic, the significantly highest score(s) is/are thus deemed the period(s) of the assessed actogram.

The advantage of chi-squared periodograms over manual actogram analysis include the removal of human bias in calculating period, as well as the ability to calculate several periodicities which may be superimposed and difficult to resolve by eye (for instance, ultradian rhythms, which have a period of <24 hours, superimposed on circadian rhythms superimposed on monthly rhythms). One caveat is, however, that at least ten days of data are required in order for accurate significance testing of the computed period (Sokolove and Bushell, 1978).

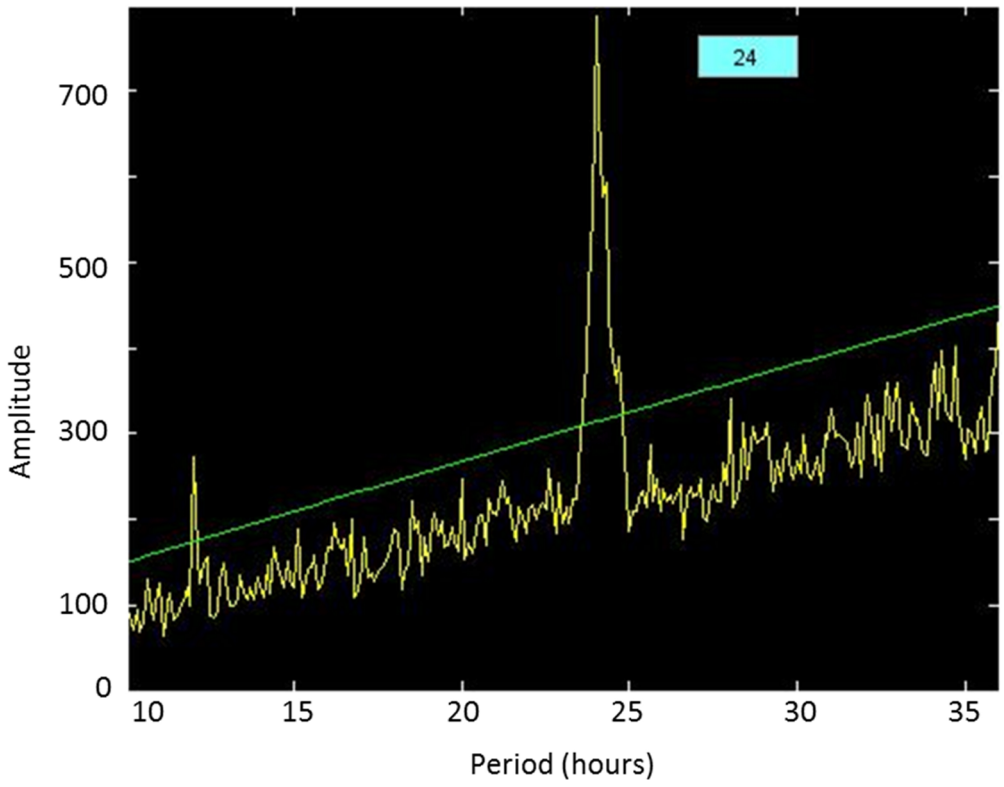

Figure 1.3. Example chi-squared periodogram. Here, the period has been calculated to be 24 hours. The level of significance is indicated by the green line. A smaller peak appears at 12 hours, a multiple of 24 hours. Source: own data.

1.1.6.d Measuring Rhythmicity of Non-continuous Data

Finally, unlike locomotor activity, sleep, heart rate or body temperature, some aspects of circadian physiology cannot be easily monitored continuously over time in the same animal. For instance, circadian rhythms of blood hormone levels (which require blood sampling) and learning ability, as well as several circadian rhythms studied in this thesis including gene and protein expression, retinal cell activity (as measured by electroretinogram), visual acuity, and contrast sensitivity, are all methods that are not easily monitored continuously in individual animals. In some cases, this can be due to the length of time it takes to measure or that repeat sampling is invasive or disturbing and may affect rhythms. Furthermore, counterbalancing between groups of animals to ensure the order of time of day sampling is not a confounding factor can complicate the ability to measure more than two timepoints from each animal. In such cases, data from two or more timepoints throughout the day can be compared within-subjects using conventional statistical methods (i.e. t-test, ANOVA) to determine whether they are significantly different from one another, and thus reflective of a significant circadian rhythm. Experiments that require tissue collection or are terminal procedures would only allow for data collection at only one timepoint per animal, thus allowing only within-groups comparisons and not within-subjects comparisons.

1.1.7 Role of Circadian Rhythms in Human Disease and Medicine

Importantly, knowledge of circadian rhythms can be used to improve human experiences. For many people, jetlag and shift work can cause a variety of symptoms due the loss of synchronization between their endogenous circadian rhythms and the environmental light-dark cycle. These include prolonged fatigue and insomnia, appetite changes, mood changes, as well as impaired alertness and performance. Shift-work with circadian disruption has recently been classified as a probable human carcinogen by the International Agency for Research on Cancer (IARC), a component organization of the World Health Organization (Straif *et al*., 2007, Erren *et al*., 2010). Circadian disruption also plays an important role in mental illness. Patients who suffer from psychiatric disease such as schizophrenia or bipolar disorder frequently display sleep and circadian rhythm disruption, and it is hoped that recent and future gains in knowledge about this association will result in therapeutic solutions for patients (Foster *et al*., 2013, Jagannath *et al*., 2013, Pritchett *et al*., 2012, Asarnow *et al*., 2013).

Furthermore, humans exhibit a range of chronotypes. Morning-types ("larks") prefer to be active in the morning, whilst evening-types ("owls") prefer activity in the evening (Roenneberg *et al*., 2003b, Zavada *et al*., 2005). Intermediate types prefer a middling activity schedule. Thus, circadian rhythms differ slightly between different chronotypes. Extreme chronotypes are thought to manifest as circadian rhythm sleep disorders (CRSD) in some people (Sack *et al*., 2007, Takahashi *et al*., 2008, Lamont *et al*., 2007), with extremely late chronotypes exhibiting Delayed Sleep Phase Disorder (DSPD). DSPD is associated with extreme eveningness and inability to sleep at socially-accepted normal

times, even when desired. DSPD sufferers exhibit onset of sleep in the early morning (0300-0600 hours), and waking times in the late morning (1100-1400 hours); this is thought to be associated with a longer-than-average endogenous period (tau) of ≥ 25 hours. Though less common, extreme morningness also occurs. This is associated with Advanced Sleep Phase Disorder and a shorter-than-average tau of < 24 hours.

Aligning shift work with chronotypes can improve work performance (Vetter *et al*., 2012, Vetter *et al*., 2015). In sports, a competition held at a certain circadian time can convey advantages or disadvantages to players based on circadian rhythms of their performance (Facer-Childs and Brandstaetter, 2015, Smith *et al*., 2013, Atkinson and Reilly, 1996). Travel across time-zones and lack of acclimation time exacerbates the effects of circadian misalignment on performance. Interestingly, the timing of academic examinations can influence performance due to circadian rhythms in memory recall and alertness, as well as chronotype (Tonetti *et al*., 2015, van der Vinne *et al*., 2015, Besoluk *et al*., 2011). Finally, even the time of day at which medicines are ingested or delivered may have an important impact on patient outcomes, as absorption and metabolism exhibit circadian rhythms (Bonten *et al*., 2014, Zhang *et al*., 2014). Understanding circadian rhythms can undoubtedly allow better optimization of outcomes for patients, workers, and families.

1.2 The Retina

1.2.1 Anatomy and function of the Mammalian Retina

The retina is a highly organized neural tissue that enables image-forming and non-image forming vision to occur. Image-forming vision refers to the sense of sight, whilst non-image forming vision refers to other retinal responses to light, including circadian photoentrainment and pupillary constriction in response to light (pupillary light response).

The retina lines the back of the mammalian eye and is composed of ten distinct layers (**Figure 1.4**). From the back of the eye to the front, they are ordered in the following way: the retinal pigment epithelium (denoted as RPE, nearest the back of the eye), photoreceptor layer (containing photoreceptor outer segments), external limiting membrane, outer nuclear layer (denoted as ONL, containing photoreceptor cell bodies), outer plexiform layer (OPL), inner nuclear layer (denoted as INL, containing bipolar, horizontal and amacrine cells), inner plexiform layer (IPL), ganglion cell layer (denoted as GCL, containing retinal ganglion cells), nerve fibre layer, and inner limiting membrane (nearest the front of the eye).

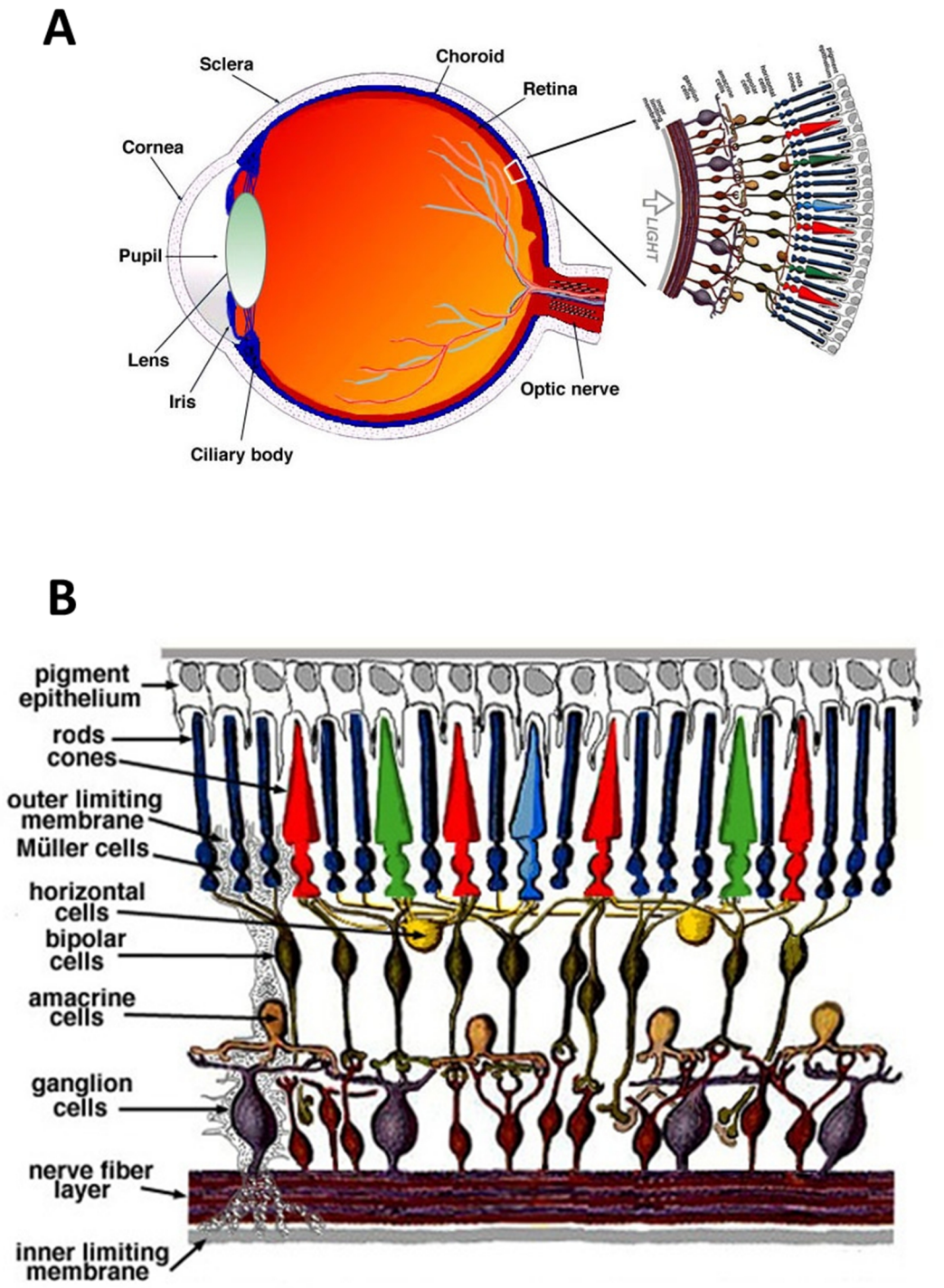

Figure 1.4. Structure of human eye and retina. (A) Schematic depicting the anatomy of the human eye and the orientation of the retina in the eye. (B) Schematic depicting the highly organized anatomical structure of the mammalian retina, as well as the morphology and organization of the various retinal cell types. Reproduced from Webvision.

There are several major neuronal cell types in the retina. These include the photoreceptor cells, bipolar cells, horizontal cells, amacrine cells, and ganglion cells. The retinal structure is highly organized, with the three neuronal cell layers (ONL, INL and GCL) containing the neuronal cell bodies separated by two layers of synaptic processes (OPL and IPL). Glial cells including astrocytes, microglia and Müller cells can also be found throughout the retina (Haverkamp and Wassle, 2000).

The function of the various components of the mammalian retina are still not yet fully understood. Here, an overview of the function of the various retinal cell types is provided.

1.2.1.a Photoreceptors

The photoreceptors capture light (photons) and transmits this information downstream as a neural signal. The outermost parts of the photoreceptor cells, the photoreceptor outer segments, contain the photopigments involved in light capture. Their high metabolic activity is supported by the adjacent retinal pigment epithelium (RPE). The RPE also supports the rest of the retina by maintaining the blood brain barrier, immune function and metabolism. Photoreceptors synapse with bipolar cells and transmit the light information to them. Bipolar cells then transmit this information to retinal ganglion cells, which project into the brain.

1.2.1.b Horizontal cells

Interestingly, a number of specialised cells located within the inner retina exist to modulate the neural signal transmitted between photoreceptors and retinal ganglion cells. Horizontal cells extend processes laterally across the retina at the level of the synapses between photoreceptors and bipolar cells. In so doing, horizontal cells communicate with

photoreceptors and modify the neural signal between photoreceptors and bipolar cells by lateral inhibition (Yang and Wu, 1991). For example, in the case of rod input onto bipolar cells, this means that the greater the stimulation of horizontal cells by rods, the smaller effect of each rod on the rod bipolar cell it synapses with. Lateral inhibition has the effect of enhancing the contrast and sharpness of a visual scene, such as by enhancing the resolution at the borders between lighter and darker parts of the image.

1.2.1.c Bipolar cells

Bipolar cells receive input from either rods or cones and are thereby deemed rod bipolar cells or cone bipolar cells. As a general rule, rod bipolar cells may be considered as a separate population from cone bipolar cells, though there is some evidence that some rods connect to OFF cone bipolar cells (Soucy *et al*., 1998). Whilst each rod may contact 2-5 rod bipolar cells, each rod bipolar cell receives input from 30-50 different rods. By contrast, there are diverse types of cone bipolar cells (mice have nine types, Ghosh *et al*. (2004)), and some cone bipolar cells receive input with only one cone cell, whilst others receive input from many. Bipolar cells can also be classed as either “ON” bipolar cells or “OFF” bipolar cells. ON bipolar cells depolarize in response to photoreceptor phototranduction, whilst OFF bipolar cells hyperpolarize. That is, ON bipolar cells maintain hyperpolarization in the dark due to glutamate (released by photoreceptors) binding mGluR6 metabotropic receptors (Masu *et al*., 1995). Reduction in glutamate following phototransduction causes ON bipolar cells to depolarize. By comparison, OFF-bipolar cells maintain depolarization in the dark due to glutamate binding to AMPA/KA ionotropic receptors (Hack *et al*., 2001). In this case, reduction in glutamate levels causes hyperpolarization in OFF bipolar cells. Rod bipolar cells are ON bipolar cells, whilst cone bipolar cells can be both ON-type or OFF-type.

Mice have five types of ON bipolar cells and four types of OFF bipolar cells (Ghosh *et al*., 2004). Having both ON and OFF types of bipolar cells allows the retina to adjust to environmental light increases and also to environmental light decreases, both of which are essential for both the image-forming and non-image-forming functions of the retina.

1.2.1.d Amacrine cells

Amacrine cells are, perhaps, the least well-understood of all the major retinal cell types. There are several types of amacrine cells, and different types can be different sizes and exhibit unique morphologies. Some amacrine cells are characterized based on the neurotransmitter they release. For instance, mice express dopaminergic amacrine cells, starburst cholinergic amacrine cells, GABAergic amacrine cells and glycinergic amacrine cells in their retinas. These amacrine cells are thought to exhibit neuromodulatory functions throughout the retina. With particular relevance to this thesis, the dopaminergic amacrine cell is thought to play a major role in the retinal clock (discussed in detail below in Section 1.4). Amacrine cells receive input from bipolar cells, and in turn, signal to both bipolar cells and ganglion cells. Amacrine cells also communicate with each other. It is thought that neuromodulatory amacrine cells use their wide lateral connectivity to modify or regulate the neural signal between bipolar cells and ganglion cells, before this information reaches the brain.

Amongst all the amacrine cells, the most common and best characterized type is the AII ("A-two") amacrine cell, which was first identified in 1974 (Famiglietti and Kolb, 1975). The AII amacrine cell is best understood as the "rod amacrine cell" as it is an important component of the rod signalling pathway of the retina. Rod bipolar cells mainly synapse with AII amacrine cells (Strettoi *et al*., 1992) – in fact, the majority of rod bipolar cells do

so, and only a minority synapse directly with ganglion cells. AII amacrine cells are also connected via gap junctions to the cone signalling pathway, and can communicate with both ON-cone bipolar cells and OFF-cone bipolar cells. In so doing, the AII amacrine cells can transmit information from the rod bipolar cells to the cone bipolar cells, though this input may be either activation or inhibition.

As AII amacrine cells depolarize in response to rod bipolar cell depolarization, this depolarization can activate ON-cone bipolar cells and thus ON-ganglion cells. By comparison, depolarization of AII amacrine cells inhibit off-cone bipolar cells (via glycine signalling). This means that increasing light levels causes depolarization of rod bipolar cells, depolarization of the AII amacrine cell, and inhibition of the OFF-cone bipolar cells. A decrease in the environmental light signal causes hyperpolarization of the rod bipolar cell, hyperpolarization of the AII amacrine cell and activation of the OFF-cone bipolar cell and thus activation of the OFF-ganglion cells. As such, the AII amacrine cells provide a way for both ON- and OFF-bipolar cells to combine rod and cone signals in an additive way. It is important to note that this is a schematic view and that the AII amacrine cell modulation of retinal circuitry seems straightforward, but in live physiology the additional inputs and outputs of the various other amacrine cells may significantly further modify the neural signal between bipolar cells and retinal ganglion cells, highlighting the complexity of this system.

1.2.1.e Retinal ganglion cells

Lastly, retinal ganglion cells (RGCs), located in the innermost cellular layer of the retina (the ganglion cell layer), generate action potentials which send information to the brain. Neural signals are transmitted from bipolar cells to the retinal ganglion cells, or via AII amacrine

cells in the case of the rod signalling pathway. More than 22 subtypes of RGCs have been described (Coombs *et al*., 2006, Volgyi *et al*., 2009). Importantly, different subtypes of RGCs are thought to project to different brain areas, including the accessory optic system, superior colliculus, pretectum, lateral geniculate nucleus, and of course, the suprachiasmatic nucleus. Different RGCs may also encode different types of visual information for both image-forming and non-image forming vision, such as the directional sensitivity of image motion and movement of borders/edges within the visual field, but also the pupillary light response, and time of day information for photoentrainment (Barlow *et al*., 1964, Olveczky *et al*., 2003, Lucas *et al*., 2003, Berson *et al*., 2002).

Altogether, the highly organized anatomy of the retina serves to enhance its function of providing light information to the brain. The phototransduction pathways that lead to image-forming and non-image-forming vision are discussed below.

1.2.2 Phototransduction and Image-Forming Vision

Although light enters the front of the eye through the cornea and lens, it is the photon-capturing rod and cone photoreceptors located in the retinal layer farthest back in the eye that capture this light signal (melanopsin phototransduction will be discussed in the section below). Photoreceptors are defined as specialized neuronal cells that can capture light information and send this information downstream (phototransduction). Indeed, the term "photoreceptor" is a slight misnomer as photoreceptors are not exactly receptors expressed by a cell, but are rather cells that are light-sensitive and can activate biological processes.

Rods and cones are the two classic types of photoreceptors in mammals and were thought to be the only two types to exist functionally in the mammalian retina prior to the discovery of melanopsin and other novel opsins (most of which remain poorly understood). In this section, discussion will be focused on rod and cone phototransduction (Rodieck, 1998).

How do photoreceptors capture light? Light-absorbing photopigments called opsins are expressed in the photoreceptor outer segments. In response to light, opsins initiate the phototransduction signalling cascade which ultimately leads to a change in the photoreceptor's cell membrane potential, thus generating a neural signal that is transmitted downstream to bipolar cells. Ultimately, these neural signals give rise to both the image-forming and non-image-forming aspects of retinal vision.

Rods express the photopigment rhodopsin, which is maximally sensitive to 497-500nm light in mammals (Toda *et al*., 1999). By contrast, there are several types of cone opsins (which are maximally sensitive to different wavelengths of the visible light spectrum, any one of which may be expressed by the cone photoreceptor. Human have three types of cones: long-wave sensitive (LWS), middle-wave sensitive (MWS) and short-wave sensitive (SWS). The three different cone opsins allow humans to achieve colour vision. Mice, however, have two types of cones: middle-wave sensitive (MWS) maximally sensitive (peak sensitivity λ_{max}) at 508nm and an ultraviolet-sensitive cone (UVS) maximally sensitive at 360 nm (Jacobs *et al*., 1991, Nikonov *et al*., 2006).

Remarkably, a mammalian rod is capable of responding to a single photon. Photoactivation of rods leads to rod phototransduction (Arshavsky, 2002). Covalently-bound to rhodopsin is a chromophore called 11-cis-retinal (11-cis refers to the geometric conformation of the retinal molecule). Upon absorption of a single photon, the chromophore 11-cis-retinal

changes conformation to become 11-trans-retinal (a straight geometric conformation). This process is termed photoisomerization. A change in conformation of the opsin protein leads to the active rhodopsin state.

In the dark, both rod and cone photoreceptors are normally depolarized and release glutamate at their synapses with bipolar cells. That is, under dark conditions, the ionic channels in the photoreceptor outer segment plasma membrane are open, allowing Na^+ and Ca^{2+} cations to flow in and maintain cell depolarization (also called the dark current). Light acts ultimately to close these channels and hyperpolarize the photoreceptor cells, thus reducing glutamate concentrations at the photoreceptor-bipolar cell synapse (Rodieck, 1998).

To do so, the active rhodopsin activates the G-protein transducin. This causes transducin to dissociate from its bound GDP, and bind GTP instead. With GTP bound to it, the alpha subunit of transducin dissociates from the beta and gamma subunits. This alpha subunit-GTP complex then activates phosphodiesterase (PDE), which causes a reduction in cyclic guanosine monophosphate (cGMP) concentrations. Thus, cGMP-gated Na^+ and Ca^{2+} ionic channels close, causing hyperpolarization of the photoreceptor and closure of voltage-gated calcium channels. Finally, this leads to a reduction in glutamate release. The reduction in glutamate concentrations at the photoreceptor-bipolar cell synapse then affects bipolar cells as well as other cell types downstream in the retinal circuitry, as previously discussed above.

The rod system can be activated by a single photon and operate at very low light levels, such that the signalling from each photon captured by the rod system is integrated by the retina in an additive manner. By contrast, the cone system operates at a different range of

light levels, where cones must respond to a far greater number of photons. Rods are saturated under bright light levels, such that their pigment is largely bleached and rods thus become unresponsive. Cones, on the other hand, can handle photoisomerization rates at least 100 times greater than rods, and do not appear to saturate at steady background light levels of any intensity (Perlman and Normann, 1998), because their high photoisomerization rates allow them to regenerate visual pigment and maintain sensitivity.

1.2.3 Photoentrainment, Non-Image-Forming Vision and Melanopsin

Photoentrainment is the process of synchronizing endogenous circadian rhythms with the environmental light-cycle (entrainment), using light as the external time cue (Roenneberg *et al*., 2003a, Johnson *et al*., 2003). In mammals, light is the main *zeitgeber* and photoentrainment therefore allows the circadian clock to be set to the external environment. The mammalian SCN, location of the master circadian pacemaker, receives light information from the retina via the retinohypothalamic tract. Photoentrainment is dependent on the eye; enucleated mammals (eyes removed) were found to no longer entrain to external light cues and displayed free-running (non-entrained or endogenous) rhythmic behaviour even under a light-dark cycle (Yamazaki *et al*., 2002).

Interestingly, mice lacking all rod and cone photoreceptors were found to retain photoentrainment ability, suggesting that a third class of retinal photoreceptors may actually facilitate photoentrainment of circadian rhythms (Foster *et al*., 1991, Freedman *et al*., 1999, Lucas *et al*., 1999). Photosensitive retinal ganglion cells (pRGCs) were identified

as the subset of retinal ganglion cells that are themselves sensitive to light and can also photoentrain the circadian system (Hattar *et al*., 2002, Berson *et al*., 2002, Sekaran *et al*., 2003). pRGCs express the photopigment melanopsin (*Opn4*) and mediate non-image forming responses to light, such as photoentrainment, the pupillary light response, negative masking and phase shifting (Hankins *et al*., 2008, Schmidt *et al*., 2011, Do and Yau, 2010). Recent studies have now revealed that pRGCs can be further subdivided into five different subtypes (named from M1 to M5), which exhibit different morphologies and express different isoforms of melanopsin (Pires *et al*., 2009, Jagannath *et al*., 2015) (Hughes *et al*., 2012b). Different pRGC subtypes appear to project to different areas of the brain and therefore regulate different aspects of physiology (Chen *et al*., 2011). Indeed, M1-type pRGCs are the main subtype that project to the SCN, along with some M2-type pRGCs (Baver *et al*., 2008). M1-pRGCs are also the main subtype projecting to the olivary pretectal nucleus shell, which controls the pupillary light response (Guler *et al*., 2008). Furthermore, pRGCs have recently been linked to a variety of physiological phenomena including pattern vision (Ecker *et al*., 2010), depression and learning (LeGates *et al*., 2012).

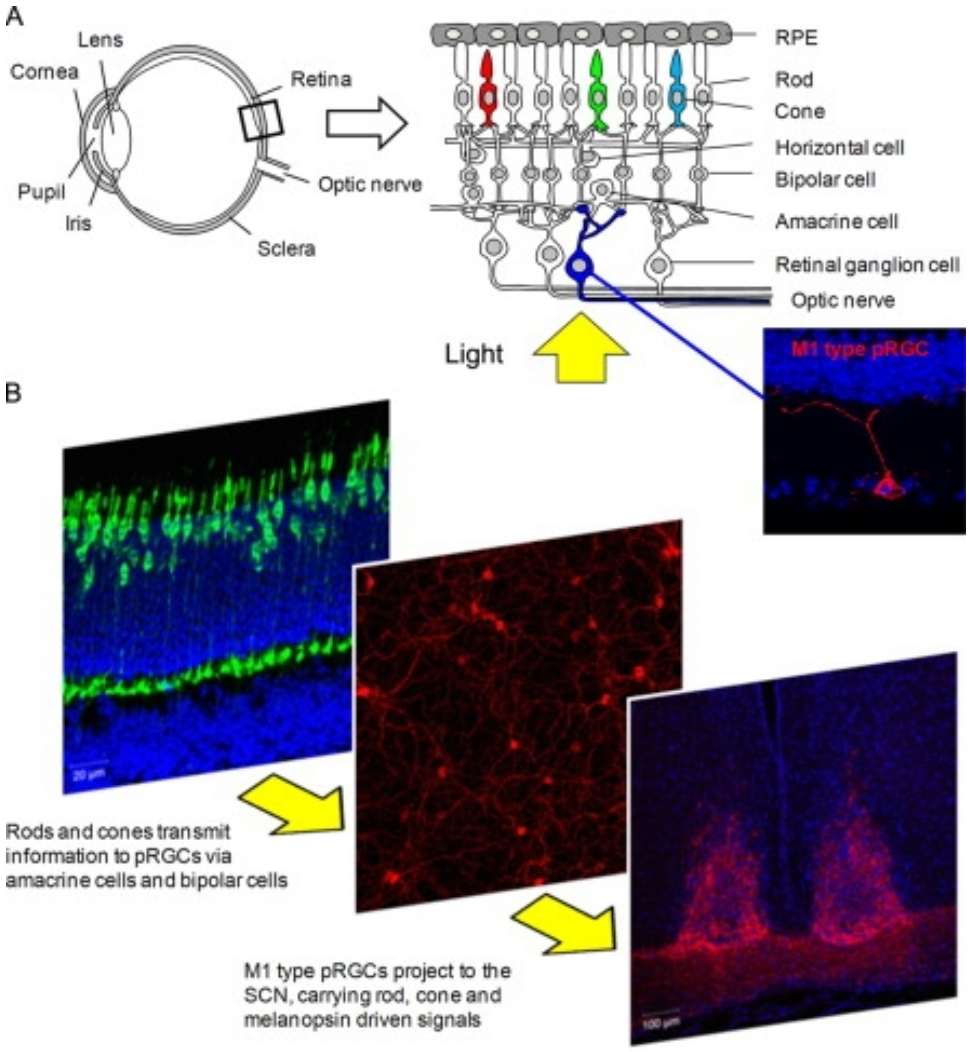

Figure 1.5. Melanopsin-expressing photosensitive retinal ganglion cells (pRGCs) represent a third class of retinal photoreceptor, and provide a conduit for transmitting rod and cone driven light input to the SCN. **(A)** Schematic representation of the eye and retina, detailing the multiple cell types of the retina and localisation of rod and cone photoreceptors (outer retina) and melanopsin-expressing pRGCs (inner retina). Right side panel shows the typical morphology of M1-type pRGCs visualized in the mouse retina. **(B)** Images depicting the transmission of rod, cone and melanopsin driven light signals from the retina to the SCN. Light input from rod and cone photoreceptors (only cones shown) travels down through the retina, via amacrine and bipolar cells, into M1-type pRGCs before the "combined" light response is transmitted to the SCN via the RHT. Figure and Legend both reproduced from Hughes *et al*. (2015b).

Melanopsin stimulation ultimately leads to depolarization, rather than hyperpolarization as in seen in rods and cones (Hughes *et al*., 2012a, Hankins *et al*., 2008, Do and Yau, 2010). The melanopsin signalling cascade involves Gq/11 type G-proteins leading to calcium influx and depolarization (Hughes *et al*., 2015c, Xue *et al*., 2011, Graham *et al*., 2008).

1.2.4 Integration of Rod, Cone, and Melanopsin Signals

Interestingly, melanopsin is not *necessary* for photoentrainment – rather, it is the pRGCs themselves that are essential (Guler *et al*., 2008). Rods and cones signal to pRGCs via bipolar and amacrine cells, thus providing light information to pRGCs (in addition to the light input pRGCs receive by expressing melanopsin). Furthermore, rod and cone photoreception can compensate for melanopsin loss and maintain photoentrainment of circadian rhythms.

In fact, rods are the main contributing photoreceptor cell type to circadian photoentrainment under low and moderate irradiances whilst melanopsin-expressing cells are mainly responsible for high irradiances such as daylight (Lall *et al*., 2010, Altimus *et al*., 2010). Surprisingly, cones do not appear to play a significant role in photoentrainment under photopic conditions despite being the main photoreceptor regulating the pupillary light response and pattern vision at those irradiances. The reason for this is likely due to light adaptation by cones in response to long light stimuli. Indeed, cones respond to light stimuli at high temporal frequency (such as a series of light flashes). Altogether, although it has been shown that the rod system, cone system and melanopsin system are each individually capable of providing photoentrainment, it may be that rods, cones and melanopsin encode different temporal and irradiance information about the

environmental light signal in order to provide an accurate time of day signal to the SCN (Lucas *et al*., 2012).

The pRGCs send photic information to the SCN via the retinohypothalamic tract using neurotransmitters glutamate (Ding *et al*., 1994) and PACAP (Hannibal *et al*., 2000). These neurotransmitters cause increased calcium influx and activate kinase signalling pathways which ultimately leads to cAMP response element binding protein (CREB) activation. CREB binding to cAMP response elements (CRE) then activates light-responsive genes. The activation of light-responsive genes acts to photoentrain the individual oscillators within SCN neurons (Meijer and Schwartz, 2003). Indeed, the acute light-induction of *Per1* and *Per2* by the aforementioned mechanism is thought to be the main mechanism by which the core molecular clock is photoentrained. Depending on the time at which light induces *Per1* and *Per2*, the circadian clock phase can therefore be shifted earlier or later. Light at the beginning of the subjective day (dawn) induces a phase advance by causing an early onset of *Per1* expression, whereas light at the end of the subjective day (dusk) induces a phase delay by causing a later offset of *Per2* transcription. Phase advances and phase delays can be measured by applying light pulses at particular times of day to manipulate the phase of a subject's circadian rhythms and measuring changes in readouts such as locomotor activity (Jud *et al*., 2005).

1.3 Cryptochromes

Cryptochromes are flavoproteins, and are evolutionarily and structurally related to photolyases, which are enzymes that repair DNA damaged by UV light (Sancar, 2003, Sancar, 2000). Given that Cryptochromes are highly conserved across several phyla, Cryptochromes in several model organisms have been studied – including mammals, non-mammals (such as European robin *Erithacus rubecula*), invertebrates (such as the fruit fly *Drosophila melanogaster*), plants (such as thale cress *Arabidopsis thaliana*), and bacteria (such as *Escherichia coli*). Cryptochromes play a role in biological timekeeping as a core clock gene and protein (Reppert and Weaver, 2002, Shearman *et al*., 2000, Kume *et al*., 1999, van der Horst *et al*., 1999), and have recently been proposed to have roles in regulating metabolism (Lamia *et al*., 2011, Lamia *et al*., 2009) and magnetoreception (Liedvogel and Mouritsen, 2010).

Cryptochromes bind FAD (flavin-adenine dinucleotide), though the molecular mechanism and function of their interaction in mammals remains unclear. Mammalian and non-mammalian cryptochromes (CRYs) are structurally and functionally different. *Drosophila* cryptochrome (dCRY) is a circadian photoreceptor in the central clock of the fly (Emery *et al*., 1998). The entrainment of the *Drosophila* clock depends on light signalling through the blue-light photoreceptor dCRY (and its chromophore FAD), which associates with TIMELESS (dTIM), promoting its degradation (Ceriani *et al*., 1999). dTIM's partner PERIOD (dPER) then becomes unstable in a light-dependent manner (Griffin *et al*., 1999). By contrast, mammalian CRYs are major components of the molecular circadian clock (as reviewed in Chapter 1.1) though their photopigment capabilities and hypothetical contribution to

mammalian circadian photoentrainment has been the subject of substantial scientific literature.

1.3.1 Mammalian Cryptochromes: Putative Mammalian Circadian Photopigments?

As CRYs function as blue light-sensitive photopigments in *Drosophila*, it was initially postulated that CRYs may be photopigments in mammals. However, such studies have often failed to separate the role of CRYs as core clock components from their putative roles as photopigments (Thresher *et al*., 1998, Selby *et al*., 2000, Thompson *et al*., 2003, Van Gelder *et al*., 2003).

CRYs are required to maintain a circadian rhythm. CRY double-knockout mice (*Cry1*$^{-/-}$*Cry2*$^{-/-}$) exhibit consolidated activity in the dark phase when exposed to a light-dark cycle (van der Horst *et al*., 1999). However, in constant conditions, *Cry1*$^{-/-}$*Cry2*$^{-/-}$ mice immediately become behaviourally arrhythmic, indicating that the consolidation of activity is due to negative masking, that is, acute suppression of locomotor activity by light. Furthermore, CRY double-knockout mice (on an *rd/rd* retinally-degenerate background) were found to have attenuated pupillary light responses compared to wild-type mice (Van Gelder *et al*., 2003), which was proposed as evidence for CRYs acting as mammalian photopigments. However, recent studies have clarified this phenotype, showing that similar pupillary phenotypes are obtained with the loss of any core clock protein (Owens *et al*., 2012), thus demonstrating that an intact clock is necessary for a normal pupillary response.

Possibly the most conclusive study regarding mammalian photoreception was conducted in a mouse model lacking rod-, cone- and melanopsin signal transduction pathways (Hattar

et al., 2003). These triple-knockout mice were found to have no remaining responses to light – they fail to display a pupillary light response, fail to entrain to a light-dark cycle and show no negative masking. Moreover, heterologous expression of melanopsin alone is sufficient to make cells photosensitive (Melyan *et al*., 2005, Panda *et al*., 2005, Qiu *et al*., 2005). These critical experiments conclusively demonstrated that melanopsin (OPN4) is the circadian photopigment in mammals.

As such, whilst *Drosophila* Cryptochromes are light-sensitive and act as a circadian photopigment, mammalian Cryptochromes are not thought to function as photopigments. Initial work assuming that mammalian Cryptochromes function in the same way as *Drosophila* Cryptochromes led to the false assumption that mammalian cryptochromes must also be photopigments.

1.3.2 Structure of Mammalian Cryptochromes

In mammals, CRYPTOCHROME1 (CRY1) and CRYPTOCHROME2 (CRY2) are light-independent components of the core molecular circadian clock mechanism. As previously described, following the heterodimerization of CLOCK and BMAL1, *Cry1*/2 and *Per1*/2 transcription is initiated. CRY1/2 and PER1/2 then heterodimerize in the cytoplasm, translocate into the nucleus and inhibit their own transcription by binding to the CLOCK-BMAL1 complex (Kume *et al*., 1999). In so doing, CRYs are critical transcriptional repressors that function to regulate the oscillation of the core circadian mechanism. Post-translational modifications of CRYs by AMPK (adenoside monophosphate-activated protein kinase), FBXL3, FBXL21, and other molecules lead to phosphorylation, ubiquitination, degradation or stabilisation of these proteins (Lamia *et al*., 2009, Yoo *et al*., 2013, Hirano *et al*., 2013).

The structure of mammalian CRY1 and CRY2 have recently been described (Czarna *et al*., 2013, Xing *et al*., 2013). Whilst dCRY has a deep binding pocket for FAD (its chromophore), mouse CRY has an open and dynamic "FAD-binding pocket" that is obscured by the mouse CRY C-terminus lid (Czarna *et al*., 2013). Furthermore, binding sites on CRY1 that were predicted in previous studies for AMPK (Lamia *et al*., 2009) and FBXL3 (Siepka *et al*., 2007) have recently been confirmed (Czarna *et al*., 2013). The findings that in mouse CRY, the homologous region to the *Drosophila* CRY FAD-binding pocket does not appear to be open and available for chromophore binding adds further evidence that mammalian Cryptochromes are not likely to contribute to mammalian phototransduction as a photopigment.

1.3.3 Differences between CRY1 and CRY2

Whilst CRY1 and CRY2 are often discussed interchangeably and are structurally similar, they play substantially different roles in the transcriptional repression of the CLOCK-BMAL1 complex. Indeed, *Cry1*$^{-/-}$ mice exhibit a shortened tau (circadian period), while *Cry2*$^{-/-}$ mice exhibit a lengthened tau (van der Horst *et al*., 1999). Furthermore, CRY levels in SCN and liver exhibit a circadian rhythm, peaking in the subjective night compared to the subjective day (Kume *et al*., 1999, Koike *et al*., 2012). However, CRY2 peaks at CT16 (early subjective night) while CRY1 peaks at CT0 (late subjective night or dawn) (Kume *et al*., 1999, Koike *et al*., 2012). Indeed, CRY1 dose-dependently lengthens the circadian period of the core clock mechanism, and CRY2, while also lengthening tau, does so at a reduced level, and acts to attenuate the potent period lengthening action of CRY1 (Anand *et al*., 2013). As such, the assumption that both mammalian CRY1 and CRY2 are completely interchangeable must be cautiously avoided. In this thesis, the individual roles of Cryptochrome 1 and Cryptochrome 2 will be considered separately in the experimental work.

1.3.4 Physiology of Cryptochrome-null Mice

The generation of *Cry1*$^{-/-}$*Cry2*$^{-/-}$ mice was first reported in a 1999 Nature article (van der Horst *et al*., 1999). When monitoring circadian locomotor rhythms of these animals under a light-dark cycle, *Cry1*$^{-/-}$*Cry2*$^{-/-}$ mice restrict their locomotor activity to the dark phase (as seen in **Figure 1.7**). This gives the appearance of 24-hour locomotor rhythms, but is actually a phenomenon known as negative masking.

Negative masking is a phenomenon by which light directly affects behaviour and in so doing, may contradict circadian clock signalling (Aschoff, 1960). Light suppresses locomotor activity in nocturnal species such as mice (Mrosovsky, 1999), such that mice that display negative masking will avoid activity under light conditions. By contrast, positive masking is observed under dim light conditions, where a nocturnal species such as a mouse will show increased activity. On an actogram, this would give the appearance of rhythmic locomotor behaviour but is in fact a reflection of direct masking responses to light.

Confirmation of light masking behaviour can be made by observation of behaviours under constant conditions. Once *Cry1*$^{-/-}$*Cry2*$^{-/-}$ mice are placed into constant darkness conditions, these mice immediately became arrhythmic (van der Horst *et al*., 1999). Interestingly, *Cry1*$^{-/-}$*Cry2*$^{-/-}$ mice demonstrate significant locomotor rhythms if transferred to constant darkness if raised under constant light conditions (Ono *et al*., 2013). This may be due to changes in AVP and VIP levels in the SCN caused by postnatal constant light exposure (Smith and Canal, 2009), which may cause circadian reorganization in the developing *Cry1*$^{-/-}$*Cry2*$^{-/-}$ mice raised under constant light conditions. However, importantly, *Cry1*$^{-/-}$*Cry2*$^{-/-}$ mice do not exhibit any locomotor activity circadian rhythms under constant

light conditions (Ono *et al*., 2013), though this has been observed in other circadian clock-deficient mice (Hughes *et al*., 2015a).

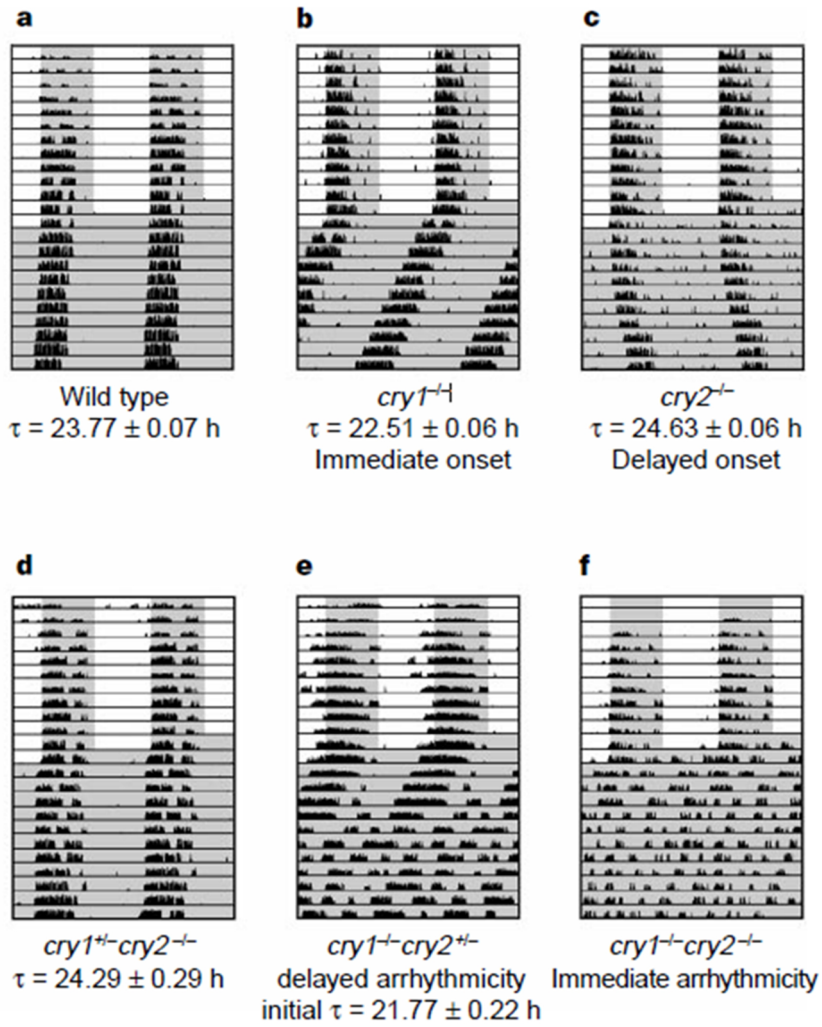

Figure 1.6. Double plotted actograms reflecting circadian locomotor activity phenotypes of *Cry*-null mice. All mouse locomotor activity was recorded under 12:12 light-dark cycles for several days and then animals were released into DD. Wildtype mice (a) exhibit a robust circadian rhythm of locomotor activity with a tau of 23.77 hours under constant darkness. By contrast, *Cry1*$^{-/-}$ mice (b) exhibit a shortened tau (22.51 hours) and immediate onset of tau changes, while *Cry2*$^{-/-}$ mice (c) exhibit a lengthened tau (24.63 hours) with a delayed onset of tau changes. Furthermore, *Cry1*$^{+/-}$*Cry2*$^{-/-}$ mice (d) show relatively stable rhythms at a slightly lengthened tau (24.29 hours). *Cry1*$^{-/-}$*Cry2*$^{+/-}$ mice become arrhythmic in constant darkness. Finally, *Cry1*$^{-/-}$*Cry2*$^{-/-}$ mice demonstrate immediate arrhythmicity once released into constant darkness conditions. Light conditions are indicated by a white background, dark conditions are indicated by a grey background. Reproduced from van der Horst *et al*. (1999).

Interestingly, actograms derived from *Cry*-null mice (as shown in **Figure 1.7**) demonstrate the differential effects of *Cry1* loss and *Cry2* loss on circadian rhythms of locomotor activity. This lends further evidence to the idea that *Cry1* and *Cry2* serve different roles in the mammalian circadian clock and should not be viewed as interchangeable despite their similar structures. As mentioned previously, $Cry1^{-/-}$ mice exhibit a shortened locomotor activity tau whilst $Cry2^{-/-}$ mice exhibit a lengthened tau. Furthermore, $Cry1^{+/-}Cry2^{-/-}$ mice which possess only one *Cry1* allele and no *Cry2* show relatively stable rhythms at a slightly lengthened tau, whereas $Cry1^{-/-}Cry2^{+/-}$ mice become arrhythmic in constant darkness. These data suggest that *Cry1* may have a significantly greater stabilizing role on the circadian clock than *Cry2*. Indeed, whilst $Cry1^{-/-}$ mice exhibit an immediate onset of shortened tau, $Cry2^{-/-}$ mice exhibit a delayed onset of lengthened tau with a smaller deviation from wildtype tau than $Cry1^{-/-}$ mice. This observation has been corroborated by an extensive study of the distinctive roles of CRY1 and CRY2 in the mouse SCN (Anand *et al*., 2013). This study revealed that CRY1 and CRY2 are both transcriptional repressors of clock controlled genes, and that CRY1 is a far more potent transcriptional repressor than CRY2. Indeed, both CRY1 and CRY2 act to lengthen the SCN rhythm, but CRY2 also represses the period lengthening activity of CRY1. These results explain the differences in $Cry1^{-/-}$ and $Cry2^{-/-}$ locomotor activity phenotype (**Figure 1.7),** which had led to the assumption that *Cry1* and *Cry2* serve opposing functions in the mammalian circadian clock, although this hypothesis did not fully explain the data from $Cry1^{+/-}Cry2^{-/-}$ and $Cry1^{-/-}Cry2^{+/-}$ mice. The results presented in the Anand *et al*. (2013) study therefore explain why $Cry2^{-/-}$ mice have a lengthened tau (*Cry2* is not present to repress the period lengthening effects of *Cry1*). Furthermore, mice a single *Cry1* allele and no *Cry2* would lead to a longer tau than wildtype,

but not as long as mice with two *Cry1* alleles and no *Cry2*. As such, *Cry1* and *Cry2* clearly have different roles in the molecular circadian architecture.

Finally, *Cry1*$^{-/-}$*Cry2*$^{-/-}$ mice do not exhibit any significant health defects, aside from developing ocular inflammation at a significantly greater rate than wildtype mice (van der Horst *et al*., 1999). Whilst other clock gene knockout mice can exhibit serious health abnormalities, particularly *Bmal1*$^{-/-}$ (Kondratov *et al*., 2006a, Kennaway, 2005, Rudic *et al*., 2004) and *Clock*$^{-/-}$ (Turek *et al*., 2005, McClung *et al*., 2005, Miller *et al*., 2004) mice, *Cry1*$^{-/-}$*Cry2*$^{-/-}$ mice were reported not to exhibit any of the premature aging symptoms displayed by other clock mutant strains (Kondratov, unpublished, cited in Kondratov *et al*. (2006a)). By contrast, loss of cryptochrome has been reported to be protective against cancer (Ozturk *et al*., 2009).

1.4 Retinal Clocks

1.4.1 A Circadian Clock in the Retina

The master circadian pacemaker found in the suprachiasmatic nuclei (SCN) of the hypothalamus entrains peripheral oscillators, such as those found in the liver, gut, and heart. The retina contains a peripheral circadian oscillator which acts to anticipate the daily dramatic changes in the light environment and optimize retinal physiology for day and night conditions, as light levels can span 8-9 log units over a single day (Green and Besharse, 2004, McMahon *et al*., 2014). The retinal clock is a complete circadian clock system; it generates autonomous oscillations which have an approximate 24-hour period and persist under constant conditions are also temperature-compensated. Unique amongst peripheral clocks, the retina can be photoentrained (Buhr *et al*., 2015, Buhr and Van Gelder, 2014) and thus synchronize retinal circadian oscillations with the environmental light-dark cycle.

The retinal clock circadian clock was first described in Xenopus (African clawed-frog) cultured retinal explants, which were found to display oscillations under constant conditions (Besharse and Iuvone, 1983). Initial retinal clock research was largely conducted on non-mammalian retinas (Cahill and Besharse, 1991, Cahill *et al*., 1991, Cahill and Besharse, 1990, Cahill and Besharse, 1989, Green and Besharse, 2004). Studies in different vertebrates has revealed that retinal clocks differ significantly between studied species, and that even in mammals, there are stark differences between what has been observed in the rat, hamster, and mouse (McMahon *et al*., 2014). Given that this thesis presents data obtained exclusively from mice, the main focus shall be placed upon published studies about the mouse retinal clock to ensure clarity and relevance.

Understanding even the basic mechanisms of the retinal circadian clock has been challenging. Despite extensive study, the identity of the exact cells or cell networks of the mouse retinal clock remains elusive and ambiguous. Furthermore, the mechanisms by which this retinal clock regulates circadian rhythms in photoreceptor disk shedding (Terman *et al*., 1993, Teirstein *et al*., 1980, Grace *et al*., 1999), dopamine synthesis (Doyle *et al*., 2002a, Doyle *et al*., 2002b, Nir *et al*., 2000), melatonin release (Tosini and Menaker, 1996, Cahill and Besharse, 1990, Besharse and Iuvone, 1983), electroretinogram b-wave amplitude (Jackson *et al*., 2012, Cameron *et al*., 2008a, Storch *et al*., 2007), visual contrast sensitivity (Hwang *et al*., 2013), gamma-aminobutyric acid (GABA) turnover rate and release (Jaliffa *et al*., 2001), extracellular pH (Dmitriev and Mangel, 2001), and rod-cone coupling (Ribelayga *et al*., 2008) have not yet been fully elucidated.

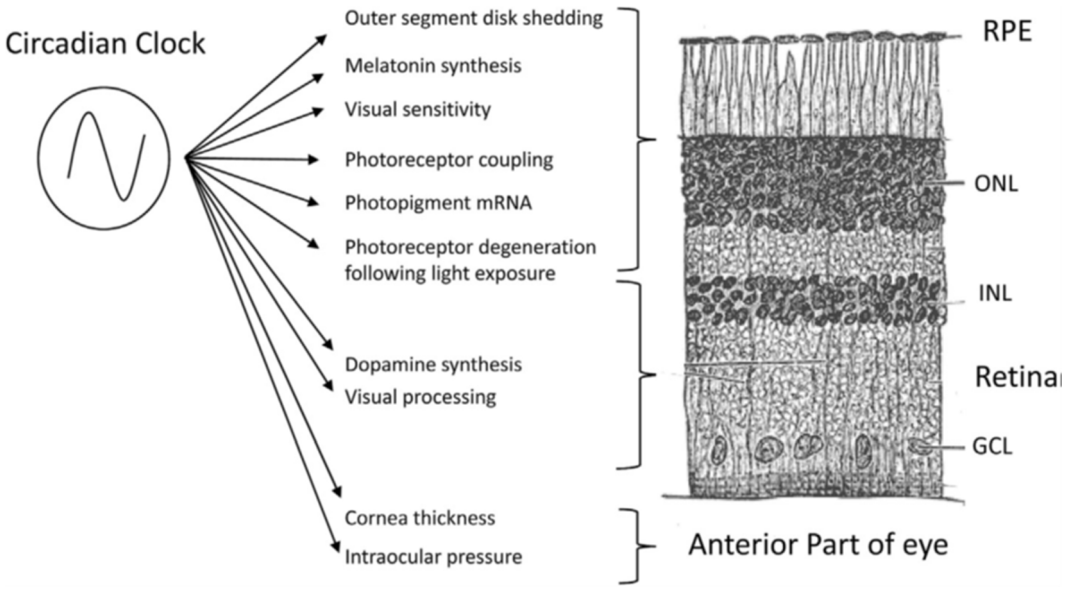

Figure 1.7. Schematic depicting the various aspects of retinal physiology shown to be regulated by the retinal circadian clock. Of note, retinal circadian physiology may be divided into both outer retinal rhythms and inner retinal rhythms, as well as extra-retinal ocular rhythms. Reproduced from McMahon *et al*. (2014).

Perhaps the strongest data on mammalian retinal clock mechanisms have been reported through PER2::LUCIFERASE rhythms in long-term retinal explants, where *Per2* oscillates in the retina on a daily basis (and this PER2::LUC rhythm can be monitored). Whilst dopamine agonists phase shift the PER2::LUC rhythm, GABA reduces the amplitude of rhythms in a dose-dependent manner (Ruan *et al*., 2008). A study by the same group recently illustrated that retinal clock rhythms (as assayed by PER2::LUC and *Per1*::LUC rhythms) are dependent on *Cry1*, *Clock* and *Per1* (Ruan *et al*., 2012). As these studies assayed bioluminescence of the whole retina, cellular resolution of the mechanism for retinal rhythms remains to be achieved.

1.4.2 Clock Gene Expression in the Mouse Retina

Recent studies on clock gene expression in the mouse retina have presented contradictory results. Given that the SCN circadian clock is regulated by a set of interlocking TTFLs, several studies investigating the retinal clock have involved attempts to understand the components of the retinal clock. The six core clock genes involved in the SCN circadian clock are *Clock*, *Bmal1*, *Per1*, *Per2*, *Cry1* and *Cry2*.

Much research has heretofore been focused on determining the expression pattern or oscillation of these six core clock genes (or their protein products) in the retina. In particular, the specific cell types expressing these core clock genes has been a subject of interest. It was hypothesized that such retinal cells could potentially be "retinal clock cells", that is, potential pacemaker cells for the retinal clock within the retina, much like the SCN cells within the hypothalamus. This involves making several significant assumptions – first of all, that the retinal clock functions similarly to the SCN clock, that both clocks use the same molecular machinery (the core clock genes), and that all six core clock genes are necessary within the same cell in order for that cell to be considered a retinal clock cell. However, recent work has called these assumptions into question, and the current understanding of the retinal clock cells that make up the retinal clock has become more nuanced over time.

1.4.2.a The core clock genes are expressed in the mouse retina

The core clock genes are expressed throughout most of the retina. Several studies have considered the overall expression of the core clock genes in the retina (in mice: Peirson *et al*. (2006); in rats: Kamphuis *et al*. (2005), Tosini *et al*. (2007b)). Altogether, the consensus

from these studies is that core clock genes are expressed in the retina – and that some show circadian oscillations. However, although some core clock genes, particularly *Cry1* and *Cry2*, were shown not to oscillate in a circadian manner using this method, this may not necessarily mean that *Cry1* and *Cry2* do not show circadian oscillations in expression levels in individual cells. Studying clock gene expression rhythms at the level of the whole retina is also complicated by the amplitude of rhythm and the fact that the retina is a heterogeneous tissue. As such, rhythms in the retina may be technically more difficult to detect than in other peripheral tissues (Peirson *et al*., 2006). *Cry1* and *Cry2* may very well exhibit a rhythmic pattern of mRNA expression that is below the threshold of detection when examined at the level of the whole retina.

1.4.2.b Clock gene expression may be retinal cell type-specific

Following this initial work, it was then determined that different retinal cell types may express clock genes with different circadian phases (Tosini *et al*., 2008). This may account for why investigating retinal mRNA expression levels in whole retina may fail to measure rhythms in some clock genes, as individual cellular mRNA levels are not measured. Indeed, lack of mRNA rhythms in whole retina could be observed if oscillations of a particular clock gene in different cells at different phases add to cause no influence on the overall rhythm.

Bearing this in mind, recent studies have now focused on cell-specific expression patterns. In initial studies of the mouse retina, CLOCK, BMAL1 and PER1 were found to be expressed widely throughout the retina, including the photoreceptors and inner retina (Gekakis *et al*., 1998). Much subsequent work has focused on the localization of *Per1*, but has yielded opposing results. Some studies have concluded that *Per1* mRNA is not expressed in photoreceptors (Witkovsky *et al*., 2003, Storch *et al*., 2007) and others have shown the

Per1 is indeed expressed in photoreceptors (Gekakis *et al*., 1998, Yujnovsky *et al*., 2006, Dinet *et al*., 2007).

The expression of *Cry1* and *Cry2* were also of great interest when cryptochromes were hypothesized to be the mammalian circadian photopigment. In human retina, *Cry2* was localized to the inner nuclear layer and ganglion cell layer (Thompson *et al*., 2003). CRY2 was also localised to the INL and GCL of mice (Miyamoto and Sancar, 1998, Dinet *et al*., 2007, Liu *et al*., 2012), whilst CRY1 has been thought to be undetectable (Miyamoto and Sancar, 1998, Liu *et al*., 2012, Hattar *et al*., 2003).

Additional studies have not clarified the situation on clock gene expression in photoreceptors. A small percentage of photoreceptor cells were found to express core clock genes when single cell quantitative real time RT-PCR was used (Ruan *et al*., 2006). Using antibodies to probe for clock proteins, cones (but not rods) were found to express clock proteins (Liu *et al*., 2012). However, another study using laser capture microdissection and qPCR found that all of the core clock genes are rhythmically expressed in the photoreceptors (Dkhissi-Benyahya *et al*., 2013).

Single-cell RT-PCR found that some dopaminergic amacrine cells express all six core clock genes (Ruan *et al*., 2006). These findings have been corroborated by several studies (Dorenbos *et al*., 2007, Witkovsky *et al*., 2003, Ruan *et al*., 2006, Gustincich *et al*., 2004). For this reason, dopaminergic amacrine cells have been suggested to act as retinal clock pacemaker cells. However, as clock proteins appear to be widely expressed in several cell types in the retina (Liu *et al*., 2012) several cell types may function as retinal clock cells. The discrepancy between these studies regarding clock gene expression may be due to low expression levels in the photoreceptors. Therefore, variable limits of detection sometimes

result in detection of clock genes and sometimes non-detection. Another hypothesis is that clock genes may be expressed in some photoreceptors and not others. In particular, it has been reported that cones, but not rods, express clock genes (Liu *et al*., 2012). If a particular study did not discriminate between rods and cones, this may lead to a discrepancy between results.

Interestingly, the study showing oscillating clock gene expression in photoreceptors but not the inner retina (Dkhissi-Benyahya *et al*., 2013), also showed that circadian rhythms in clock gene expression were lost in *Opn4*$^{-/-}$ mice. This suggests that melanopsin is important for retinal circadian rhythmicity, at least in the photoreceptors. The role of melanopsin in retinal rhythms is considered in more detail below.

A study characterizing clock protein expression in the retina reported that CLOCK, BMAL1, PER1, PER2, CRY2 and NPAS2 were expressed in cones and the inner retina (Liu *et al*., 2012). Circadian variation in clock protein expression was found only in cones and not in other cell types, suggesting that cones may be the retinal clock cells.

Finally, the localization and function of Npas2 has recently been reported (Hwang *et al*., 2013). NPAS2 (neuronal PAS domain protein 2) is a CLOCK homolog. NPAS2 is capable of substituting for CLOCK, heterodimerizing with BMAL1 and forming a complex capable of activating circadian E-box promoter elements (DeBruyne *et al*., 2007, Reick *et al*., 2001). Interestingly, the expression pattern of NPAS2 in the retina appears to be localized to a subset of retinal ganglion cells (Hwang *et al*., 2013), whilst CLOCK is widely expressed throughout the retina (Gekakis *et al*., 1998). This may suggest that NPAS2 plays a unique role in the retinal clock, potentially different from CLOCK's role in the retinal clock, and different from the synchronous function of these two proteins in the SCN circadian clock.

Altogether, currently available literature on clock gene and protein expression in the mouse retina is not conclusive about which retinal cell types express the core clock genes, and by extension, function as the primary retinal clock cells. Several different retinal cell types have been shown to express the core clock genes and, by this criteria alone, may therefore be "retinal clock cells". There are limitations as to how much may be inferred from studies using such a diverse set of experimental methods which all have different levels of resolution and detection. For instance, single cell and laser capture microdissection qPCR is a more specific method of detecting clock gene expression in the retina compared to whole retina qPCR. However, both of these methods have technical limitations (Stuart Peirson, personal communication). They can be unreproducible due to stochastic problems with low level transcript detection, and they assume all collected cells are comparable (despite that different cell subtypes may be have different functions but are categorized as the same type). Furthermore, single cell and laser capture microdissection qPCR may be prone to false positives (due to carryover of minute amounts of other material) and false negatives (due to the tiny amounts of starting material). Antibodies for protein detection can also have serious limitations as this method is completely dependent on highly specific antibodies, each of which requires substantial validation to be reliable. Also, low level expression may produce a signal indistinguishable from background noise.

Overall, the current understanding of clock gene expression in the retina remains somewhat ambiguous. Knowing the expression pattern and localization of the core clock genes, however, does not necessarily translate to understanding the function of these cells. Indeed, different retinal cell types that both express all the core clock genes may play different roles within the retinal clock. Defining retinal cells that express clock genes as

retinal clock cells may be too simplistic, as these cells may not necessarily function as circadian pacemaker cells. Furthermore, cells that express some but not all six core clock genes may not necessarily be excluded from contributing to retinal rhythms (Ruan *et al*., 2006). Indeed, most recent studies have pointed towards the existence of several types of retinal clock cells within the retinal tissue that may communicate with one another and remain synchronized through network effects. Rather than a simple set of synchronous rhythmic retinal clock cell pacemakers, the retinal clock may instead be conceptualized as a group of interlocking clock networks, where individual networks may be made up of different components (clock genes).

1.4.2.c Data on retinal clock gene expression is limited by current methods

Several methods have been used to determine how different cell types in the retina function within the retinal clock. Pharmacological studies have probed the effects of different receptor agonists and antagonists (Ruan *et al*., 2008). Physical isolation of individual cellular layers of the retina (Jaeger *et al*., 2015), and genetic manipulation of various clock and retinal genes (Storch *et al*., 2007, Barnard *et al*., 2006, Cameron *et al*., 2008a, Hwang *et al*., 2013, Ruan *et al*., 2012) have also been used to better understand the function of different retinal cell types in the retinal clock.

In order to determine which retinal cells act as circadian pacemaker cells in the retinal clock, future studies could potentially look at PER2::LUC bioluminescence patterns of individual cells of known retinal cell type. However, this method has its drawbacks – indeed, any neurochemical signalling within the retina which may strengthen existing circadian rhythms in individual cells may be lost. Furthermore, long-term retinal explants

are not necessarily representative of an *in vivo* retina under normal physiological conditions. Photoreceptor degeneration and cessation of retinal cell spiking following changes in tissue perfusion (Steven Hughes, personal communication) indicate that data obtained from PER2::LUC, whilst valuable, does not wholly represent *in vivo* retinal physiology. In order to truly identify retinal clock cell networks, an assay that can track clock gene patterns in individual cells within a whole retina in a preparation as close to *in vivo* conditions as possible will be necessary.

1.4.3 Dopaminergic Amacrine cells play a key role in entraining Retinal Rhythms

Attempts to identify the rhythm-generating cells of the retinal circadian clock have yielded conflicting results. Dopaminergic amacrine cells have been postulated as circadian pacemaker cells of the retinal clock. This is based upon several corroborating studies showing that dopaminergic cells expressed all six core clock genes and that clock gene expression exhibited circadian oscillations in these cells. *Per1* (Witkovsky *et al*., 2003) and CRY2 (Liu *et al*., 2012) have been described as oscillating in these cells. Furthermore, dopaminergic amacrine cells were found to express the highest proportion of clock genes (Ruan *et al*., 2006, Dorenbos *et al*., 2007, Gustincich *et al*., 2004). However, while dopamine acts to phase shift retinal rhythms (Ruan *et al*., 2008), retinal dopamine depletion does not affect persistence of autonomous retinal PER2::LUC rhythms (Jackson *et al*., 2012). The current model of the mammalian retinal clock is that all retinal cell types except rods contain clock genes (Ruan *et al*., 2008, Liu *et al*., 2012, Dkhissi-Benyahya *et al*., 2013) and should therefore be capable of circadian oscillations. Indeed, dopamine appears to act as a synchronizing signal (Jackson *et al*., 2012, Zhang *et al*., 2012) for the retinal clocks.

Dopamine is a key retinal transmitter, so if a clock exists in a dopaminergic amacrine cell, it is ideally placed to entrain other clocks in the retina (and affect retinal physiology). Whether all retinal cells containing clock genes act in the same manner, or can be subdivided into interacting autonomous networks remains unclear. Whilst some evidence has pointed to the presence of an outer and inner retinal clock (Ruan *et al*., 2008, Tosini *et al*., 2008), whether or how they communicate is unknown.

1.4.4 Melatonin and Retinal Rhythms

The role of melatonin in retinal circadian rhythms was one of the first to be described, based on rhythmic melatonin synthesis in retinal explants (Besharse and Iuvone, 1983, Cahill and Besharse, 1989, Cahill and Besharse, 1991, Cahill and Besharse, 1990, Cahill *et al*., 1991, Green and Besharse, 2004). Certain mouse strains are melatonin-competent, whilst others cannot synthesize melatonin (Ebihara *et al*., 1986, Goto *et al*., 1989). Given that rhythms of melatonin synthesis may be important for the retinal clock, studies have been conducted using both melatonin-competent and melatonin-incompetent mice.

Circadian rhythms of scotopic and photopic ERGs in C3H mice, which are capable of producing melatonin, are dependent on melatonin (Baba *et al*., 2009). Furthermore, circadian rhythms of the photopic ERG in melatonin-competent mice are dependent on signalling via the MT1 receptor (Sengupta *et al*., 2011). However, loss of MT1 receptors did not affect circadian rhythms of dopamine levels and as such, it appears that circadian regulation of dopamine levels does not regulate the photopic ERG rhythm. MT1 receptors are, however, expressed on pRGCs and therefore circadian rhythms in the photopic ERG are dependent on MT1 signalling on pRGCs.

Circadian rhythms of dopamine in the retina have been characterized in melatonin-producing mice (Doyle *et al*., 2002b). However, melatonin-incompetent mice (including C57BL/6) were found to lack circadian rhythms of retinal dopamine release (Doyle *et al*., 2002a).

Despite this, wildtype C57BL/6 mice and 129/Sv mice, which are genetically incapable of melatonin synthesis (Kasahara *et al*., 2010, Foulkes *et al*., 1996), demonstrate reliable retinal rhythms (Jackson *et al*., 2012, Ruan *et al*., 2008, Ruan *et al*., 2012, Cameron *et al*., 2008a, Hwang *et al*., 2013, Barnard *et al*., 2006). As such, it may be that in mice, melatonin rhythms are not essential for maintenance of the retinal circadian clock. In this thesis, all wildtype animals used are melatonin non-competent C57BL/6 mice.

1.4.5 Melanopsin and the Retinal Clock

A role for melanopsin in regulation of the retinal clock has also been suggested. Given the role of melanopsin as the mammalian circadian photopigment, it was postulated that melanopsin may play a dual role in photoentrainment of both the clocks in the brain and the retina. pRGCs express the core clock genes (Liu *et al*., 2012), though it is unclear whether the clock gene expression oscillates in pRGCs. Melanopsin expression oscillates with a circadian rhythm (Hannibal, 2006, Hannibal *et al*., 2005, Sakamoto *et al*., 2005). Furthermore, in rats, melanopsin-driven light responses in pRGCs also oscillate with a circadian rhythm (Weng *et al*., 2009), and these light responses are also affected by retinal dopamine (Van Hook *et al*., 2012), suggesting communication and feedback between pRGCs and dopaminergic amacrine cells within the retina.

Melanopsin may also be important in the development of retinal responses to light and entrainment in early life. pRGCs are the first cells in the retina responding to light after birth (Sekaran *et al*., 2005). Furthermore, light can induce c-fos expression in pRGCs one day after birth (Mateju *et al*., 2010).

Importantly, wildtype mice were found to exhibit diurnal changes in cone-based electroretinogram b-wave amplitude that were dependent on both circadian time and light history. *Opn4*$^{-/-}$ mice were found to lack circadian control of this electroretinogram response, suggesting that melanopsin may play a role possibly in synchronizing individual cellular clocks in the retina, or gating retinal clock inputs to the cone pathway (Barnard *et al*., 2006).

Furthermore, a recent study has suggested that all core clock genes are expressed in a rhythmic manner in photoreceptors and that this rhythm is lost in *Opn4*$^{-/-}$ mice (Dkhissi-Benyahya *et al*., 2013). This surprising result lends further evidence that melanopsin expression is important for proper retinal clock function. However, this study also reported no clock gene expression in the inner retina, which is similarly very surprising, as clock gene expression has been repeatedly found in different studies originating from different research groups (Ruan *et al*., 2006, Witkovsky *et al*., 2003, Liu *et al*., 2012).

Interestingly, the effect of clock loss on retinal physiology differs depending on the identity of the clock component lost. In particular, *Opn4*$^{-/-}$ mice were shown to have a cone ERG amplitude between the higher day response and lower night response seen in wildtypes (Barnard *et al*., 2006). This may suggest that loss of melanopsin causes the retina to remain at a mid-way point between the day-state and night-state. By contrast, loss of Cryptochromes places the retina in the day-state (Cameron *et al*., 2008a) whereas loss of

Bmal1 places the retina in the night-state (Storch *et al*., 2007). These results may indicate therefore that melanopsin either stops the clock midway between daytime and night time, or that dysregulation of the retinal clock caused by melanopsin loss results in a variety of phases, such that the average readout would be a middling value between the maximum at day time and minimum at night time.

Altogether, the mechanisms by which melanopsin may affect the retinal circadian clock are poorly characterized. Melanopsin involvement in the functional retinal circadian rhythms has been mainly investigated using the retinal cone ERG. Given that melanopsin-knockout mice show loss of cone ERG rhythms, this may be explained by a variety of potential mechanisms. Melanopsin may be involved in photoentrainment of the retinal clock, or perhaps in intraretinal signalling output from pRGCs that may affect dopaminergic amacrine cells. Finally, if melanopsin has a role in the development of circadian organization of retinal tissue, then melanopsin-knockout mice may have abnormal circadian organization due to lack of melanopsin since birth, leading to abnormal retinal circadian physiology. These ideas are further explored in Chapter 4.

1.4.6 OPN5: the Retinal Circadian Photopigment?

The retinal clock adapts the retina in anticipation for the immense change in illumination that occur every day between day and night. Whilst melanopsin and pRGCs photoentrain the SCN master clock, it has been a longstanding question in the retinal field as to which photoreceptors mediate the entrainment of the retinal clock (Barnard *et al*., 2006, McMahon *et al*., 2014). Recent data have provided unexpected findings in this field.

A novel photopigment, neuropsin, has been proposed to be the photopigment responsible for photoentrainment of the retinal circadian clock. *rd/rd;Opn4*$^{-/-}$;PER2::LUC retinal explants were found to have persistent retinal circadian rhythms capable of entrainment to different light-dark cycles (Buhr and Van Gelder, 2014). Loss of retinal clock photoentrainment in *Opn5*$^{-/-}$ mice suggested that *Opn5* is necessary for photoentrainment of the retinal clock (Buhr *et al*., 2015).

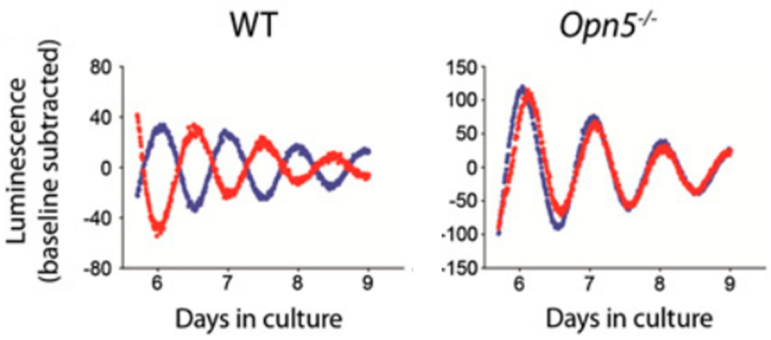

Figure 1.8. *Opn5* is necessary for mouse retinal photoentrainment. Here, PER2::LUC bioluminescence traces from wildtype and *Opn5*$^{-/-}$ retinas are depicted, where retinas have been entrained to light-dark cycles 12-hours apart (the red trace retina is entrained to the opposite light cycle as the blue trace retina). Retinas lacking *Opn5* exhibit disrupted retinal clock photoentrainment, though the amplitude of retinal rhythms is not attenuated. Reproduced and modified from Buhr *et al*. (2015).

It has been noted in previous studies that *rd/rd* mice may still have a few remaining functional photoreceptors in the retina, and that is why rodless coneless mice (*rd/rd cl*) have most often been used for functional studies investigating rod and cone loss. In the initial characterization of the retinal circadian photopigment (Buhr and Van Gelder, 2014), it is asserted that any remaining functional photoreceptors in the *rd/rd* mouse would be UV cones. Therefore, persistence of retinal circadian rhythms in *Opn1sw*$^{-/-}$ mice (which lack UV cones) was used to suggest that UV cones are not necessary for retinal photoentrainment, thus indicating *Opn5* as the retinal clock photopigment. However, irradiance response curves were not performed to rule out the involvement of other photoreceptors in retinal clock photoentrainment. Furthermore, *rd/rd;Opn4*$^{-/-}$*;Opn1sw*$^{-/-}$ mice were not studied – persistence of retinal rhythms in these mice would lend further evidence that *Opn5* may be the retinal clock photopigment and not simply an essential component of the retinal clock photoentrainment pathway.

Opn1sw$^{-/-}$ mice have intact and functional rods, MWS cones, melanopsin and *Opn5*, such that photoreceptors other than UV cones could still absorb UV light. As such, the Opn1SW experiment does not rule out the possibility that there is redundancy in the retinal photoentrainment pathway. Indeed, SCN photoentrainment still occurs in the absence of melanopsin due to a redundant rod-cone pathway. Loss of rods and cones alone, or loss of melanopsin alone is not sufficient to cause loss of SCN circadian photoentrainment. In the case of the retinal clock, it is possible that rods, cones, or melanopsin may mediate photoentrainment or that a redundant pathway via rods and cones or melanopsin exists in addition to that of *Opn5*. Remaining UV cones could still provide photoentrainment to the retinal clock in the *rd/rd*;*Opn4*$^{-/-}$;PER2::LUC retinal explants, and rod-cone photoentrainment may exist in UV cone-knockout mice. As such, whilst recent work has

suggested that *Opn5* is both necessary and sufficient for retinal clock photoentrainment, additional pathways may still exist.

Interestingly, *math5*$^{-/-}$ mice (where most retinal ganglion cells are absent developmentally) exhibited PER2::LUC retinal circadian rhythms with normal amplitude, but lacked photoentrainment ability (Buhr *et al*., 2015). This may suggest that retinal oscillations are still possible in the absence of nearly all retinal ganglion cells and nearly all *Opn5* transcripts. As such, the majority of rhythm-generating cells in the retina may not necessarily express *Opn5*. How the *Opn5*-expressing cells that might entrain the retinal clock are connected to the rhythmic retinal clock cells remains unknown.

Whilst recent work on *Opn5* has led to interesting results using PER2::LUC bioluminescence assays, it will be important to perform *in vivo* assays of retinal circadian function to determine whether *Opn5* is necessary for *in vivo* retinal rhythms. Further work is also required to distinguish whether *Opn5* is truly the sole photopigment responsible for photoentrainment of retinal circadian rhythms, or if it is merely an essential component of the retinal photoentrainment pathway.

1.4.7 Measuring Retinal Rhythms: *in vitro* and *ex vivo* methods

1.4.7.a Immunohistochemistry and RT-PCR

Both immunohistochemistry and RT-PCR are methods that have contributed greatly to the study of retinal rhythms. Although immunohistochemistry measures protein expression and RT-PCR (reverse transcriptase polymerase chain reaction) measures mRNA expression, both yield similar types of data. Tissue samples prepared for immunohistochemistry or RT-PCR are subjected to substantial physical treatment in order to yield the appropriate data.

Retinas undergoing immunohistochemistry must undergo preservation using a fixative whilst retinas being prepared for RNA extraction must be physically homogenized and the cells lysed. Both methods are therefore only capable of giving a "snapshot" of mRNA and protein expression that existed at the time the tissue was harvested. Taking tissue samples at several time points throughout the day under either diurnal or constant light conditions can then allow assessment of how a particular gene or protein's levels fluctuate throughout the day. These methods have provided substantial information regarding clock gene and clock protein expression rhythms in the retina (Peirson *et al*., 2006, Liu *et al*., 2012, Witkovsky *et al*., 2003, Storch *et al*., 2007, Gekakis *et al*., 1998, Yujnovsky *et al*., 2006, Dinet *et al*., 2007, Ruan *et al*., 2006). However, both of these methods have a substantial weakness: variability between samples can sometimes substitute artefacts for true rhythms of expression, or mask subtle, low amplitude rhythms. This weakness can be overcome by ensuring adequate numbers of samples for each timepoint to be studied – the only downside being the high animal cost of such experiments. Despite this, both immunohistochemistry and RT-PCR have provided invaluable information about the retinal circadian clock.

1.4.7.b Clock Gene Reporters

The generation of clock gene reporters has been an exciting development in circadian rhythms research. Clock gene reporters refer to clock gene promoters or clock proteins that are fused with fluorescence or bioluminescence reporters which can thereby allow researchers to visualize gene levels within cells. Tissue from a clock gene reporter mouse therefore provide a reporter signal as clock gene expression changes in that particular tissue (depending on the promoter controlling the reporter). The ability to visualize

circadian clock genes oscillating at real time and within living tissue has been a powerful new tool for circadian rhythms research. Furthermore, clock gene reporters have bridged the gap between static data individually obtained at multiple timepoints (as with immunohistochemistry and RT-PCR) and the output *in vivo* physiological rhythms (such as locomotor activity rhythms) that result from a combination of all influences on that physiology (including the circadian clock, but also other internal and external factors and motivations). By visualizing clock gene rhythms at the functional molecular level at real time in living tissue, researchers can now directly monitor clock mechanisms.

Luciferase from fire-flies and green fluorescent protein (GFP) have been used to make clock gene reporters (Hastings *et al*., 2005). *Per1*::GFP mice (Kuhlman *et al*., 2000), *Per1*::LUC (Yamaguchi *et al*., 2001), and PER2::LUC mice (Yoo *et al*., 2004) have all been used to investigate SCN circadian rhythms. However, clock gene reporter mice has allowed substantial insight into the mechanisms of the retinal clock (Ruan *et al*., 2006, Ruan *et al*., 2008, Ruan *et al*., 2012).

First of all, whole retinal explants cultured from wildtype mice (C57BL/6) could maintain circadian rhythms for at least 30 days, allowing for longitudinal studies (Ruan *et al*., 2008). With this new tool, *rd/rd* mice which also expressed the PER2::LUC reporter showed robust circadian rhythms, demonstrating that the inner retina alone is capable of retinal oscillations (Ruan *et al*., 2006). Application of pharmacological agonists and antagonists to *ex vivo* retinal cultures in order to manipulate the neurochemical signalling of the retina revealed that retinal circadian rhythms are highly robust (Ruan *et al*., 2008). Disruption of melatonin, glutamate, dopamine, acetylcholine, GABA and glycine signalling did not disrupt rhythmic PER2::LUC oscillations, and neither did blocking of signalling via connexion 36-

containing gap junctions or sodium-dependent action potentials (Ruan *et al*., 2008). However, dopamine and GABA were found to affect the retinal circadian clock oscillations, though neither was alone necessary to maintain rhythms – dopamine via D1 receptors shifts the phase whilst GABA via casein kinase affects the amplitude of the PER2::LUC oscillations (Ruan *et al*., 2008).

Importantly, PER2::LUC oscillation signals in the mouse retina appear to be originate mostly from cells within the inner nuclear layer of the retina (Ruan *et al*., 2008). However, the fact that there are few cones in the mouse retina and photoreceptors are more susceptible to degeneration in retinal culture protocol, does not negate the potential contribution of cones to retinal rhythms even if they do not contribute as much to PER2::LUC oscillation signals.

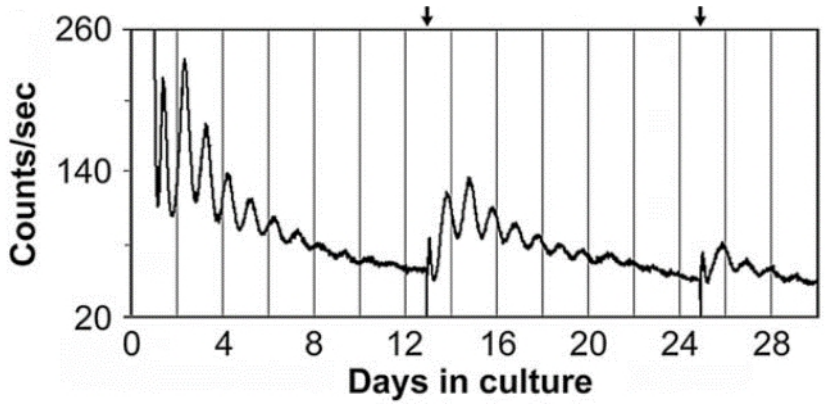

Figure 1.9. *Ex vivo* cultured retinal explants from PER2::LUC mice exhibit persistent circadian oscillations over long-term recordings. This method has been particularly informative for measuring and understanding retinal circadian rhythms. Reproduced and modified from Ruan *et al*. (2008).

Finally, comparison between the retinal circadian clock and SCN circadian clock using clock gene reporters revealed that the retina circadian clock is more dependent on *Per1*, *Cry1*

and *Clock* compared to SCN circadian clock. That is, *Per1-*, *Cry1-* or *Clock*-deficient mice exhibited significantly greater disruption to retinal circadian rhythmicity compared to SCN circadian rhythmicity (Ruan *et al*., 2012). Thus, the retinal clock may be more susceptible to disruption compared to the SCN circadian clock, though application of single pharmacological interventions (Ruan *et al*., 2008) and separation of the retinal cellular layers (Ruan *et al*., 2008, Jaeger *et al*., 2015) were both unable to abolish retinal rhythms.

Whilst retinal PER2::LUC bioluminescence rhythms are a very powerful method as it allows for longitudinal studies, there are limitations to this experimental method. In particular, retinal PER2::LUC bioluminescence rhythms are usually observed in long-term retinal explants, where *ex vivo* retinae are kept in culture media. Outside the body, intraretinal neurochemical signalling may be compromised in isolated retinae, and the tissue may not behave in a way that is representative of normal physiological conditions. Furthermore, photoreceptors degenerate in retinal explants over time (Stuart Peirson, personal communication). Thus the cell populations generating a PER2::LUC signal will change over time as photoreceptors die, and effects of treatments may differ in a retinal explant depending on how long the retina has been cultured. Also, PER2::LUC bioluminescence is a total output signal of the whole retina and cellular resolution is not possible. As such, rhythms in mouse cones will not contribute substantially to this signal as they comprise only <3% of all photoreceptors (Lyubarsky *et al*., 2004). Lastly, PER2::LUC bioluminescence is a reporter signal for PER2 rhythms, and does not represent functional retinal rhythms. As such, although PER2::LUC rhythms remain one of the most informative and useful tools for interrogating retinal circadian rhythms, its limitations must be considered during data interpretation.

1.4.8 Measuring Retinal Rhythms: in vivo methods

1.4.8.a Electroretinogram

The electroretinogram (ERG) shows field potential changes across the retina induced by light stimuli. It is a particularly useful tool given that it is relatively non-invasive for the subject. It is used in clinical medicine to assess the function of human patient retinas for both medical and research purposes.In order to record ERGs, an active electrode is placed on the cornea of the eye, and a reference electrode is placed elsewhere on the body. Field potential changes are thus recorded, which reflect extracellular currents in the retina induced by light flash stimuli. The recorded ERG waveform reflects the integrated activity of all retinal cells. Different cell populations contribute to different parts of the ERG waveform, such that it may be determined how differences in a certain aspect of the ERG waveform reflects changes in a specific retinal cell population. Using electroretinogram as a method for studying retinal rhythms has been the subject of a detailed review (Cameron *et al*., 2008b).

The flash ERG is most commonly used ERG protocol, and is also used in this thesis. The flash ERG reflects the response to a discrete light flash. As shown in **Figure 1.11**, there are several components of the flash ERG waveform: a-wave, b-wave, and oscillatory potentials.

The a-wave is the first component of the ERG waveform – it appears earliest and is shown as a negative deflection. The a-wave reflects the activation of rods and cones by light (Brown, 1968). The mouse retina contains very few cones and therefore the a-wave under photopic (bright light, rod-saturating) conditions is generally regarded as negligible as they are not thought to have enough cones to drive a significant a-wave.

The b-wave is the second component of the flash ERG. The b-wave amplitude has been shown to exhibit circadian rhythmicity and is regulated by the retinal clock (Barnard *et al*., 2006, Storch *et al*., 2007). On the ERG waveform, the b-wave is a positive peak that is thought to reflect the activity of ON-bipolar cells in the retina. The b-wave reflects second order neural activity following rod and/or cone photoreception, as both rods and cones can activate ON-bipolar cells.

Oscillatory potentials are the third component of the flash ERG waveform, and appear as superimposed waves on the b-wave. Oscillatory potentials are thought to reflect third order neural activity, such as the activation of amacrine cells or retinal ganglion cells.

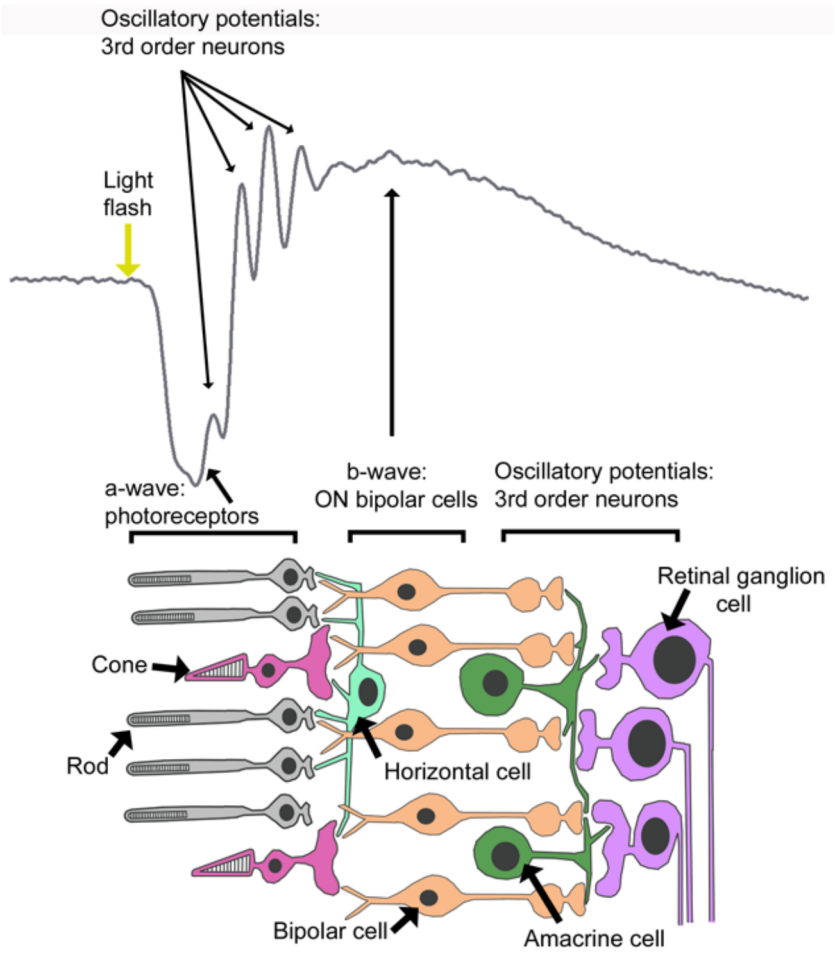

Figure 1.10. Schematic depicting the flash ERG waveform. Following a discrete light flash, the negative a-wave appears first, depicting activity from rod and cone photoreceptors. A positive b-wave follows, reflecting activity from second order neurons (ON bipolar cells). Finally, oscillatory potentials can be observed to be superimposed on the b-wave, reflecting activity from 3rd order neurons including amacrine and retinal ganglion cells. Reproduced from Cameron *et al*. (2008b).

The flash ERG protocol can be modified in order to favour rod-dependent (scotopic) and cone-dependent (photopic) responses. This allows observation of retinal activity under dark-adapted conditions and light-adapted conditions separately, thus allowing observation of responses mainly due to rod-based vision and cone-based vision separately. Under dark adapted conditions, rods are approximately 1000 times more sensitive to light than cones. Thus, use of dim stimuli can allow observation of rod-based responses under scotopic and dark-adapted conditions.

In order to examine cone-dependent (photopic) responses, one can take advantage of the fact that rods are saturated (bleached) by bright light. Application of a constant background light which is bright enough to saturate rod responses and light-adapt the retina would allow measurement of the cone responses. To do so, a very bright flash can be presented on top of a constant rod-saturating bright light, in order to probe the flash ERG waveform resulting from cone signalling. This is the method used within this thesis to probe cone responses within the photopic ERG. There are additional methods to isolate cone-dependent ERG, such as a rod-saturating flash followed by the test flash to determine cone ERG waveform, or flickering stimuli which rely on the greater temporal resolution ability of cones over rods (Cameron *et al*., 2008b). Of note, although varying light conditions favour rods or cones, they do not entirely isolate these responses; this should be taken into account when interpreting results.

Whilst the scotopic ERG was not found to exhibit any circadian rhythmicity, the b-wave amplitude of the photopic ERG shows reliable circadian oscillations (Cameron *et al*., 2008a, Barnard *et al*., 2006). As such, in this thesis, the photopic b-wave amplitude will be assayed as an output of the mouse retinal circadian clock.

1.4.8.b Contrast Sensitivity

Contrast sensitivity refers to the ability to detect differences in luminance within a visual image. That is, the ability to differentiate between the lighter areas and darker areas of an image. Whilst visual acuity, the sharpness or clarity of vision, is commonly used to assess vision in humans (which if below normal, can usually be corrected by glasses or contact lenses), contrast sensitivity is an important yet overlooked parameter of overall vision. Contrast sensitivity allows luminance differences within a visual scene to be detected over a range of overall background luminances. That is, contrast sensitivity allows for effective visual perception over the great range of environmental light levels over the day. In humans, some activities that depend highly on contrast sensitivity include night driving, interpretation of radiography (such as x-ray scans), and vision under dim light conditions.

The effective measurement of mouse spatial vision has historically been particularly challenging. An automated virtual-reality optomotor system was developed and validated in order to provide systematic, rapid and accurate visual acuity and contrast sensitivity testing for mice (Prusky *et al*., 2004). In this virtual-reality optomotor system, mice placed on a raised platform within the apparatus are shown a sine wave grating that rotates either clockwise or counter-clockwise around them (four display monitors facing one another to form a box and a mirror on the bottom create this visual reality for the mouse). The spatial frequency of the sine wave grating as well as its contrast can be changed by the user. Mice will display optokinetic tracking behaviour in response to the rotating visual stimuli if they can see it. That is, the mouse's head will follow the sine wave grating at the same speed in the same direction if it can see it – this "head-tracking" response is logged as a positive response. Lack of head-tracking indicates a negative response and inability to see the

stimulus. Of course, stimuli receiving a negative response are presented multiple times to ensure it a negative visual response is recorded rather than a lack of response due to inattention. Using this system, the peak contrast sensitivity of mice was found to be approximately 0.064 cycles/degree, whilst peak visual acuity was found to be approximately 0.4 cycles/degree (Prusky *et al*., 2004, Prusky and Douglas, 2004).

Interestingly, a recent paper has demonstrated that a circadian rhythm of visual contrast sensitivity exists and is regulated by the retinal clock (Hwang *et al*., 2013). Contrast sensitivity is dependent on retinal dopamine (Jackson *et al*., 2012) and clock gene *Npas2* (Hwang *et al*., 2013). The mechanism for this circadian phenomenon is through an interaction between dopamine D4 receptors, the clock gene Npas2 and adenylate cyclase 1 (Hwang *et al*., 2013).

Furthermore, it appears that circadian rhythms of contrast sensitivity is an inner retinal clock phenomenon. Indeed, as NPAS2 is localized to the retinal ganglion cell layer only and loss of Npas2 is sufficient to abolish rhythms in contrast sensitivity (Hwang *et al*., 2013), it appears that only the inner retinal clock is essential for maintenance of contrast sensitivity rhythms. Furthermore, mice lacking melanopsin and mice lacking pRGCs demonstrated attenuated contrast sensitivity responses (and thus lower contrast sensitivity), though this was not measured at consistent times of day (Schmidt *et al*., 2014). Indeed, given that contrast sensitivity exhibits a circadian rhythm, it is possible that the attenuated contrast sensitivity response reported in mice lacking melanopsin or pRGCs could be due to testing wildtype and mutant mice at different times of day (S. Hattar, personal communication). Given its recent validation as an output assay of the retinal clock, circadian rhythms of

contrast sensitivity are therefore measured in this thesis to probe retinal circadian function.

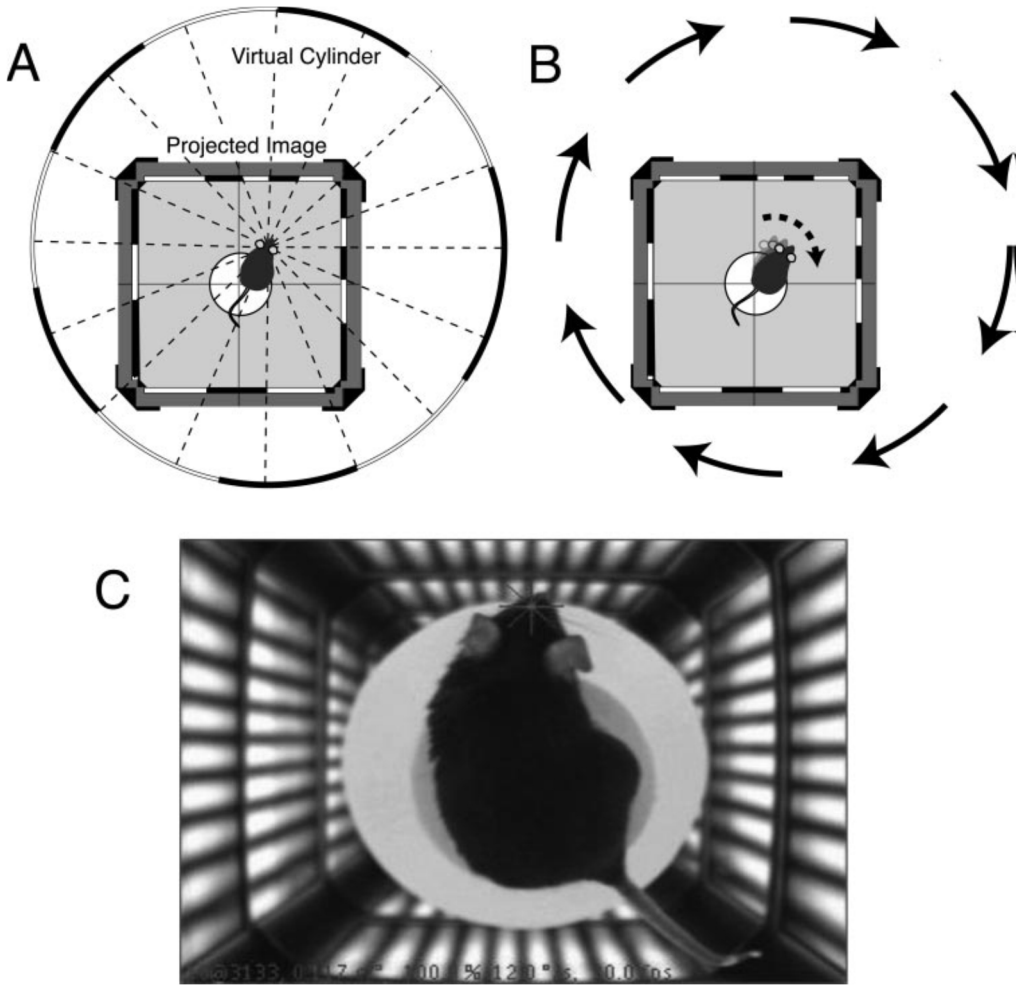

Figure 1.11. Schematic depicting virtual reality optomotor assay (also known as Optomotry) and mouse optokinetic tracking response. **(A)** A virtual 3D cylinder is projected by four monitors facing inwards towards the mouse on the platform, upon which a sine wave grating (of adjustable spatial frequency and contrast) is rotated either clockwise or counter-clockwise. **(B)** The mouse tracks the movement of the rotating grating with head and neck movement – this is the optokinetic tracking response. **(C)** Still frame of a mouse tracking the moving sine wave grating. The crosshair is placed between the eyes of the mouse by the user whilst operating the Optomotry software in order to optimize the cylinder rotation. Reproduced from Prusky *et al*. (2004).

1.4.9 Current Model for the Mouse Retinal Circadian Clock

Clock gene expression is widespread throughout the retina (Gekakis *et al*., 1998, Witkovsky *et al*., 2003, Liu *et al*., 2012). Whilst a small proportion of most major retinal cell types express all six core clock genes (Ruan *et al*., 2006), a substantial proportion of retinal cells express at least one core clock gene. The retinal clock is dependent on *Per1*, *Cry1* and *Clock* (Ruan *et al*., 2012) whilst *Per2*, *Per3* and *Cry2* appear to not be essential for maintenance of retinal circadian rhythms. Loss of *Cry1* and *Cry2* (Ruan *et al*., 2012), *Bmal1* (Storch *et al*., 2007), *Opn4* (Barnard *et al*., 2006), or melatonin receptor 1 (MT1 receptors) (Sengupta *et al*., 2011) result in loss of retinal circadian rhythms. Interestingly, loss of *Per1* alleles causes shorter periods in retinal rhythms and longer periods in SCN rhythms (Ruan *et al*., 2012). Loss of *Per3* also shortened retinal circadian rhythm periods (Ruan *et al*., 2012).

In mice, it appears that the retinal clock may contain layer-specific oscillators (Jaeger *et al*., 2015). The outer nuclear layer, inner nuclear layer and ganglion cell layer are each individually capable of independent oscillators (Jaeger *et al*., 2015, Ruan *et al*., 2008, Dkhissi-Benyahya *et al*., 2013). Furthermore, individual retinal cells (dissociated retinal cells) are capable of autonomous oscillations. Whether and how clocks within these individual nuclear layers of the retina communicate with one another remains unknown, with gap junctions thought to be one possibility (Jaeger *et al*., 2015), though pharmacological blockade of gap junctions did not disrupt retinal rhythms (Ruan *et al*., 2008). Interestingly, when the retinal layers are separated, they oscillate with longer periods correlating to the degree of separation (dissociated retinal cells have the longest period, followed by isolated retinal layers, several layers together and finally by whole retina). This suggests that communication across retinal layers contributes to circadian

period maintenance. Interestingly, dissociated retinal cells exhibited longer periods of oscillation (~29 hours) compared to dissociated SCN cells (~23.5 hours), which may reflect greater dependence on network effects for circadian period in retinal cells compared to SCN cells (Jaeger *et al*., 2015, Liu *et al*., 1997).

Dopamine and GABA play important roles in the neurochemical organization of the retinal circadian clock (Ruan *et al*., 2008, McMahon *et al*., 2014). Dopamine, especially, appears to promote a light-adapted retinal state and regulate various aspects of retinal physiology including light-adapted ERG, contrast sensitivity and visual acuity (Jackson *et al*., 2012). Furthermore dopamine is capable of phase-shifting retinal circadian rhythms (Ruan *et al*., 2008), whereas GABA contributes to the amplitude of retinal rhythms. Other neurochemical signalling pathways such as melatonin, glutamate, acetylcholine and glycine do not appear to be individually necessary for maintenance of retinal rhythms, though redundant neurochemical pathways may allow for compensation between different pathways to ensure robust rhythmicity. If this is the case, that would mask responses to pharmacological blockade of single pathways. Future studies could attempt to apply several pharmacological blockers at once to determine whether compensatory mechanisms exist.

Given current evidence, it is likely that the retinal circadian clock operates as a series of interlocking clock networks with a high level of redundancy, rather than a simple synchronized group of retinal clock cells. This would account for its sensitivity to genetic interventions (where components of the retinal clock are lost) and its resistance to network interventions (where redundancy of the retinal clocks preserve its rhythmicity).

The unique location of the retinal clock may enable it to act to gate light signal information to the brain. As a "*zeitnehmer*" (German for "time-taker" but here defined as "signal-regulator"), the retinal clock would therefore gate sensitivity of the SCN circadian pacemaker to the entraining stimuli (light). In so doing, the retinal clock may potentially affect downstream SCN clock-controlled pathways, such as sleep, locomotor activity, hormone secretion or body temperature. The retinal clock regulates the rhythmic transcription of at least 250 genes (Storch *et al*., 2007), which may explain its influence on numerous aspects of retinal physiology (**Figure 1.7**).

Although recent studies have made substantial advances in current knowledge of the retinal clock field, many questions remain to be answered. In this thesis, several of these open questions are addressed: in particular, the individual retinal expression patterns of CRY1 and CRY2, and their individual contributions to the retinal clock. The role of melanopsin in the retinal clock, and the connection between the retinal clock and downstream locomotor activity rhythm outputs are also investigated.

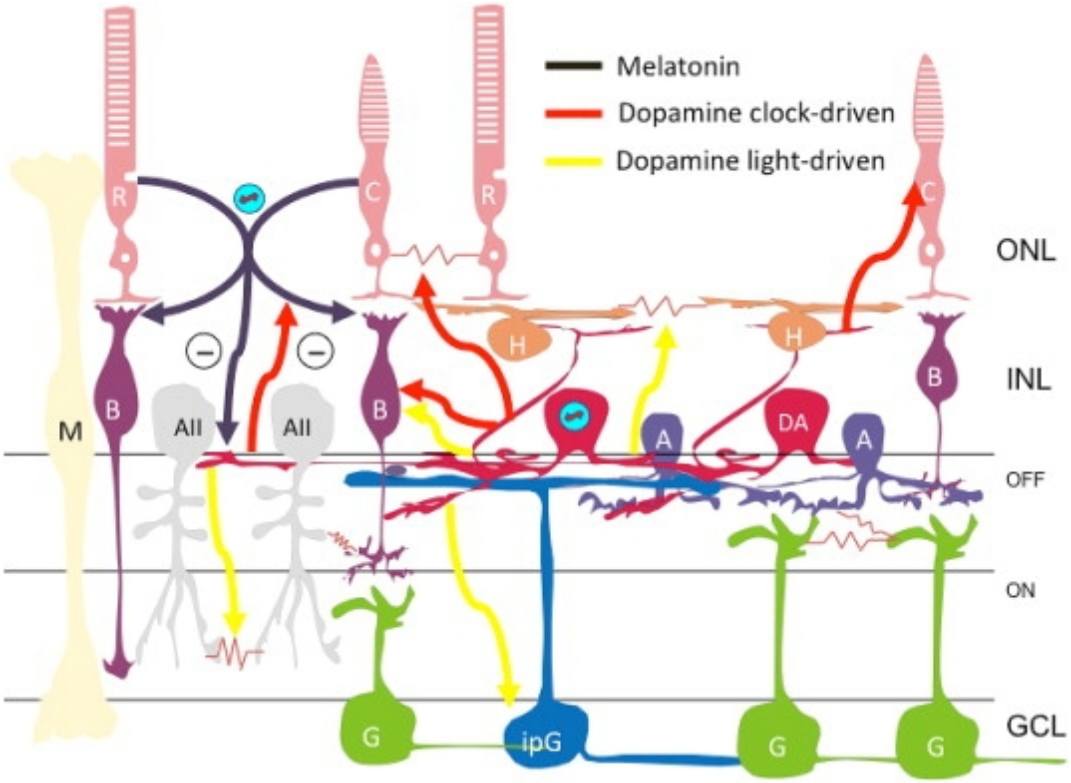

Figure 1.12. Schematic demonstrating the neurochemical outputs of the retinal circadian clock. Signalling between various retinal clock-containing cells highlights the network function of the retinal clock. Specifically, the dopaminergic amacrine cells (shown in pink) play an essential role in intraretinal communication. Circadian clock-driven signalling by dopaminergic amacrine cells are shown (in red) to affect rod-cone coupling, melatonin signalling, bipolar cell signalling and cone cell signalling, which may thereby cause increased photopic ERG b-wave amplitude. Light-driven dopamine release may affect AII amacrine cells and horizontal cells, bipolar cells and pRGCs, in order to increase photopic ERG b-wave amplitude. Effects of melatonin on the retinal clock are also shown. Reproduced from McMahon *et al*. (2014).

1.5 Thesis Aims

Given the role of mammalian cryptochromes in central circadian clock mechanisms, and the current lack of evidence for CRYs as photopigments, mammalian retinal cryptochromes may have a role as a component or modulator of the retinal circadian clock.

The primary aim of this thesis is to investigate the role of Cryptochromes in the mammalian retina. The role of melanopsin in the mouse retinal clock is also investigated, as well as whether the retinal clock may gate light input to the SCN pacemaker.

Specifically, the research presented in this thesis has four major aims:

- To determine the localization and expression pattern of CRY1 and CRY2 in the mouse retina (Chapter 2)
- To investigate a role for *Cry1* and *Cry2* in retinal circadian rhythms (Chapter 3)
- To investigate the extent and basis of a role for melanopsin in retinal circadian rhythms (Chapter 4)
- To explore whether the retinal circadian clock may have downstream effects on the SCN clock (Chapter 5)

Lastly, Cryptochrome has been proposed as a putative magnetoreceptor in several species. A pilot experiment exploring the effect of magnetic fields on sleep and associated behaviours in mice is presented in Chapter 7.

2

Localization of Cryptochromes in Mouse Retina

2.1 Introduction

2.1.1 Expression of Cryptochromes in Mammalian Retina

In order to determine the function of mammalian Cryptochromes in the mouse retina, it is first essential to determine their localization. Many studies have sought to determine which retinal cell types express clock genes and proteins (reviewed in **Section 1.4.2**), though there is a lack of consensus regarding retinal CRY expression.

Cry1 and *Cry2* mRNA expression has been reported in the mammalian retina (Miyamoto and Sancar, 1998, Thompson *et al*., 2003, Ruan *et al*., 2006, Peirson *et al*., 2006). However, studies describing CRY1 and CRY2 protein expression have been far less conclusive, notably due to the lack of antibody controls and therefore antibody specificity. Whilst CRY2 has often been reported as present in the inner nuclear layer and ganglion cell layer of the retina (see **Figure 2.1**), the presence of CRY1 in the retina has previously been reported as undetectable (Hattar *et al*., 2003, Thompson *et al*., 2003, Liu *et al*., 2012). Yet the loss of *Cry1* alone (but not *Cry2*) abolishes retinal PER2::LUC rhythms (Ruan *et al*., 2012).

These aforementioned studies have largely used the same commercially available antibody (Alpha Diagnostics CRY2 and CRY1 rabbit anti-mouse antibodies). These antibodies can be purchased along with a blocking peptide that the antibody was raised against. However, one must be cautious when using blocking peptides as the only control, as they only indicate the accuracy of the antibody binding to the blocking peptide, rather than the accuracy of the antibody binding to its endogenous target (Saper, 2005). Obviously, one should assume that blocking peptides are the same as the endogenous peptide but this is often difficult to verify as commercial companies do not always release epitope sequences.

Study	**Finding**	**Technique Used**	**Limitations**
(Miyamoto and Sancar, 1998) shown in **Figure 2.1**	*Cry1* and *Cry2* mRNA localized to inner nuclear layer and ganglion cell layer of mouse retina. No rhythms of *Cry1* or *Cry2* mRNA expression in retina.	In situ hybridization	mRNA localization does not necessarily translate to protein localization.
(Thompson *et al*., 2003) shown in **Figure 2.1**	*Cry2* mRNA is expressed at levels 11 times higher than *Cry1* and both are expressed in INL and GCL of human retina.	In situ hybridization	mRNA localization does not necessarily translate to protein localization.
(Ruan *et al*., 2006, Peirson *et al*., 2006)	*Cry1* and *Cry2* mRNA do not show rhythms in mouse retina.	RNA extraction and qPCR	Whole retinal mRNA lacks cell-type specificity
(Liu *et al*., 2012) shown in **Figure 2.1**	CRY2 protein is expressed in the inner nuclear layer and ganglion cell layer in mouse retina	Immunohisto-chemistry	Antibody controls using *Cry2* $^{-/-}$ tissue were not used.
(Ruan *et al*., 2012)	Wildtype retinas and *Cry2* $^{-/-}$ retinas demonstrate PER2::LUC oscillations but *Cry1* $^{-/-}$ have no retinal PER2::LUC rhythms.	PER2::LUC	Whole retinal PER2::LUC assay lacks cell-type specificity
(Dkhissi-Benyahya *et al*., 2013)	*Cry1* and *Cry2* are rhythmically expressed in the outer nuclear layer of the retina but not in the inner nuclear layer or ganglion cell layer of mouse retinas.	Laser-capture microdissection	LCM allows cell layer specificity, but may face problems with cell-type contamination and cross-over due to large number of PCR cycles.

Table 2.1. Summary of main findings in key studies describing the localization and/or rhythmic expression of Cryptochrome mRNA or protein in mammalian retinal tissue.

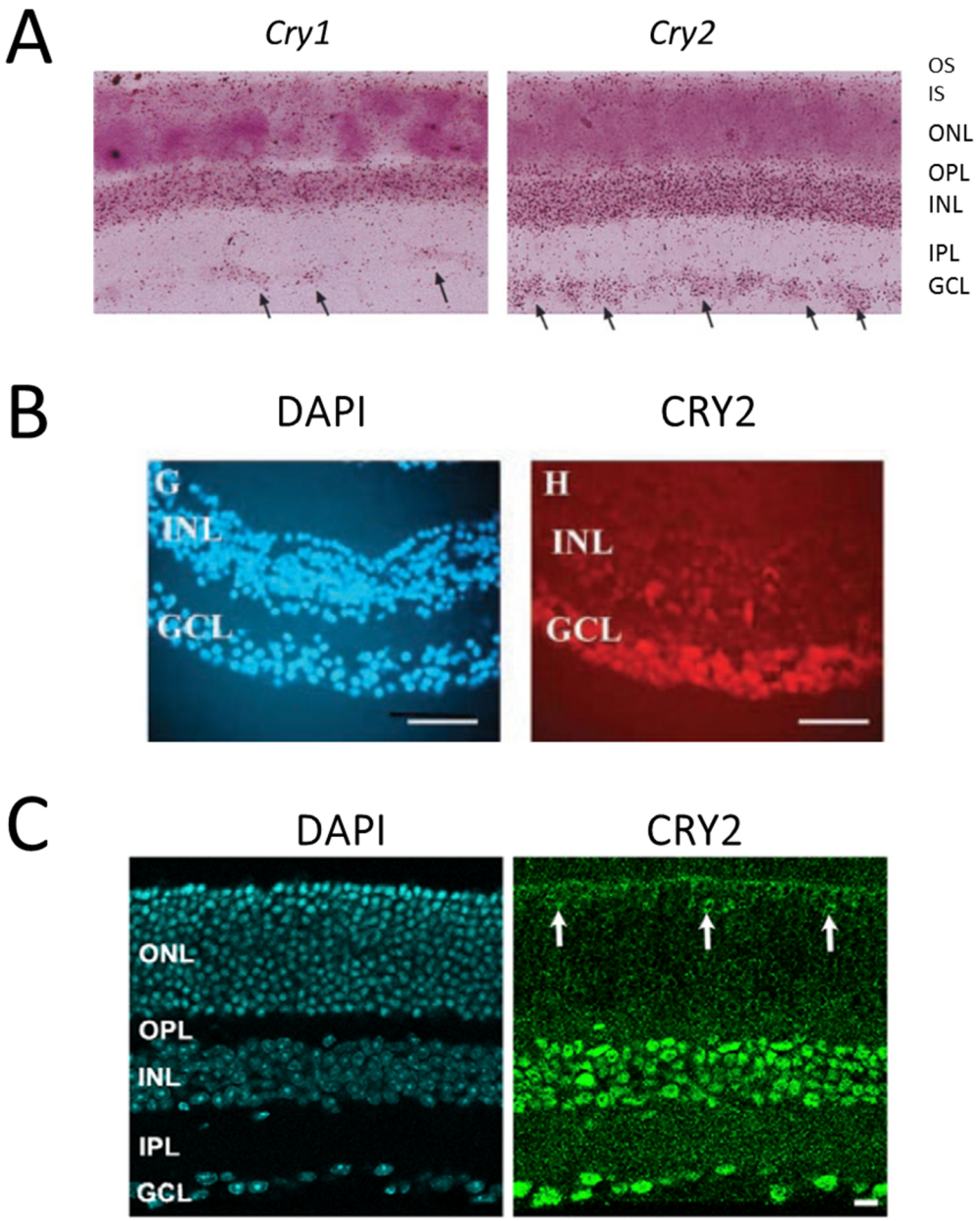

Figure 2.1. (A) *Cry1* and *Cry2* mRNA is localized to the inner nuclear layer and ganglion cell layer of mouse retina using in situ hybridization. Black arrows point to areas of increased signal indicating either increased *Cry1* or increased *Cry2* expression. OS = photoreceptor outer segments, IS = photoreceptor inner segments, ONL = outer nuclear layer, OPL = outer plexiform layer, INL = inner nuclear layer, IPL = inner plexiform layer, GCL = ganglion cell layer. Reproduced and modified from Miyamoto and Sancar (1998). Copyright (1998) National Academy of Sciences, U.S.A. **(B)** CRY2 immunohistochemistry using commercial Alpha Diagnostics antibody in human retinal tissue samples indicate CRY2 signal in the inner nuclear layer and ganglion cell layer. DAPI stain for cell nuclei is provided for reference. Scale bar = 50µm. Reproduced and modified from Thompson *et al*. (2003). **(C)** DAPI and CRY2 protein expression in mouse retina. CRY2 signal is seen in the outer nuclear layer, inner nuclear layer and ganglion cell layer. Commercial Alpha Diagnostics CRY2 antibody was used. Reproduced and modified from Liu *et al*. (2012).

Interestingly, despite the general consensus that CRY1 protein may not be expressed in significant amounts in the mouse retina, numerous studies have shown that both *Cry1* and *Cry2* mRNA are present in the retina (Peirson *et al*., 2006, Miyamoto and Sancar, 1998, Ruan *et al*., 2006). However, though they are clock genes, *Cry1* and *Cry2* do not appear to exhibit rhythmic levels of mRNA expression (Peirson *et al*., 2006). This could be due to lower amplitude rhythms in Cry mRNA expression that is below the threshold of detection, or due to rhythmic expression in certain retinal cell types, which may not all be in phase. Other canonical clock genes, however, do appear to oscillate at the level of whole retina mRNA expression, including *Per2* and *Bmal1* (Peirson *et al*., 2006). Indeed, PER2::LUC mice demonstrate autonomous *Per2* rhythms in mouse whole retinal explants and have provided useful information regarding retinal clock function at the *ex vivo*, whole retina and retinal cell layer levels (Ruan *et al*., 2008, Ruan *et al*., 2012, Jaeger *et al*., 2015). In the SCN, CRY1 peaks at CT0 and CRY2 peaks at CT16 (Kume *et al*., 1999, Koike *et al*., 2012). PER1 peaks at CT12, 4-6 hours after the *Per1* mRNA peak (Hastings *et al*., 1999).

2.1.2 Immunohistochemistry as a Tool for Localizing Proteins

Immunohistochemistry, as a method for determining the localization of proteins is largely dependent on the quality and accuracy of the antibodies used. An open letter to readers of the Journal of Comparative Neurology (Saper, 2005) addressed the growing problem of published antibodies lacking proper characterization or controls by implementing antibody validation standards.

In order to assess the specificity of an antibody, the ideal negative control to perform is reaction with a knockout sample. For example, to determine the expression pattern and localization of Protein A in wildtype mouse cerebellar tissue, the best control to use would

be cerebellar tissue from a Protein A genetic mouse knockout. With this control, the difference in signal between wildtype and knockout would indicate where the target protein is localized.

If genetic knockout tissue is unavailable, other options are available including:

- Loss of staining signal following preadsorption of antigen peptide
- Staining co-localizes with in situ hybridization signal
- Staining pattern co-localizes with another reported antibody for the same target

Furthermore, the source and the sequence of the antibody epitope are essential to report in order to ensure replicable results.

However, even these useful controls are sometimes not stringent enough in the absence of genetic knockout tissue. Antibodies that produce a signal in genetic knockout tissue provide misleading information regarding their targets and such errors may negatively affect future studies on these targets. As such, proper antibody validation is essential to protein localization studies.

2.2 Aims

The aim of this chapter is to characterise the expression pattern of CRY1 and CRY2 in the mouse retina. The consensus amongst previous studies is that CRY2 protein is present in the mouse retina, whilst CRY1 is either non-detectable or not present.

In Chapter 2, the specific aims are:

- If necessary, to validate CRY1 and CRY2 antibodies for the characterization of the retinal expression of CRY1 and CRY2
- To determine if CRY1 is expressed in the mouse retina and if so, characterize the localization and expression pattern of CRY1
- To confirm if the expression pattern of CRY2 in mouse retina is similar to previously published work
- To investigate the co-localization of CRY1 and CRY2 with specific retinal cell types

2.3 Methods

2.3.1 Animals

Wild type C57BL/6, *Cry1*$^{-/-}$ and *Cry2*$^{-/-}$ mice were used. *Cry1*$^{-/-}$ and *Cry2*$^{-/-}$ mice (kindly provided by Dr Patrick Nolan, Medical Research Council Harwell, and Prof van der Horst, Rotterdam) were maintained as homozygous lines. Control wild type C57BL/6 mice had been backcrossed (>10 generations) from the *Cry1*$^{-/-}$ and *Cry2*$^{-/-}$ mice lines. For melanopsin expression studies, *Opn4*.Cre$^{+/-}$.EYFP$^{+/+}$ mice (mixed C57BL/6 and 129/SvJ background), in which EYFP expression is enabled by expression of Cre recombinase under the control of the *Opn4* promoter, were used (Hughes *et al*., 2013).

Unless otherwise stated, all mice were housed under a 12:12 LD cycle with food and water *ad libitum*. All procedures were conducted in accordance with the UK Home Office Animals (Scientific Procedures) Act 1986 (PPL 70/6382 and 30/2812, PIL I53D8E9E7) and the University of Oxford Policy on the Use of Animals in Scientific Research. All procedures were performed in a designated establishment.

2.3.2 Genotyping

Genotyping of *Cry1*$^{-/-}$, *Cry2*$^{-/-}$ mice, and *Cry1*$^{-/-}$*Cry2*$^{-/-}$ mice followed standard protocols as previously reported (Anand *et al*., 2013). Ear notches were obtained and digested in 50mM NaOH for 90 minutes at 90°C and then neutralized with 1M Tris-HCl (pH 5).

PCR was then performed using the DNA extracted from the ear notches.

	Cry1	***Cry2***
Forward	GTGTCTGGCTAAATGGTGG	CCAGAGACGGGAAATGTTCTT
Reverse	CAGGAGGAGAAACTGACGCACT	GCTTCATCCACATCGGTAACTC
Neo-specific	TGAATGAACTGCAGGACGAG	GAGATCAGCAGCCTCTGTTCC
Expected product sizes	Wildtype 1600 bp Mutant 2200 bp	Wildtype 550 bp Mutant 310 bp

Table 2.2. Primers used for genotyping *Cry1* and *Cry2*.

Standard PCR protocols were used and products were run out on an agarose gel to confirm results. The following reagents were used for the PCR:

SYBR Green Master Mix
Forward Primer
Reverse Primer
Molecular grade water

For *Cry1*, the following PCR cycling conditions were used:

Holding stage
95°C for 10 min
Cycling stage
94°C for 30 s
61°C for 60 s
72°C for 60 s
Repeat Cycling stage x 35
Melt Curve stage
95°C 15 s
60°C for 60 s
95°C 15 s

For *Cry2*, the following PCR cycling conditions were used:

Holding stage
95°C for 10 min
Cycling stage
95°C for 30 s
55°C for 30 s
72°C for 90 s
Repeat Cycling stage x 35
Melt Curve stage
95°C 15 s
60°C for 60 s
95°C 15 s

2.3.3 Immunohistochemistry

Retinal and brain sections were prepared as previously described (Hughes *et al*., 2013). Tissue was collected at relevant time points (ZT2, ZT6, ZT10, ZT14, ZT18 and ZT22). Eyes were removed and punctured with a fine needle prior to fixation in 4% paraformaldehyde in PBS at 4 °C for 16 h. Eyes were then cryoprotected in 30% (w/v) sucrose in PBS at 4 °C for 48 h before embedding in Optimum Cutting Temperature medium (Sakura Finetek) and stored at −80 °C prior to use. 16 μm tissue sections were prepared at −23°C using a CM1850 cryostat (Leica Microsystems) and collected on poly-*l*-lysine-coated slides (Thermo Scientific).

Fluorescent immunolabelling was performed using standard techniques. Primary antibodies were incubated for 24-72h at 4°C. Primary antibodies used are listed in **Table 2.3**. Anti-Cryptochrome antibodies were incubated for 72 hours at 4°C, whilst all other antibodies were incubated overnight at 4°C. Secondary antibodies were Alexa 488, Alexa 568 and Alexa 633 conjugated donkey anti-rabbit, donkey anti-goat and donkey anti-chicken (Life Technologies) incubated for 2h at room temperature (1:200). All antibodies were diluted in PBS with 2.5% donkey serum and 1% Triton-X for retinal sections (3% Triton-X for brain sections). Wash steps were performed using PBS with 0.05% Tween-20. Tissue sections were mounted onto glass slides with ProLong Gold anti-fade reagent containing DAPI (Life Technologies).

Primary Antibody Target	**Source**	**Species raised against**	**Dilution**
CRY1	Kindly provided by Dr. Elizabeth Maywood and Prof. Michael Hastings	Rabbit antiserum	1:100
CRY2	Kindly provided by Dr. Elizabeth Maywood and Prof. Michael Hastings	Rabbit antiserum	1:100
UVS opsin	Sc-14363, Santa Cruz Biotech	Goat polyclonal	1:1000
Cone arrestin (ARRESTIN-C)	Sc-54355, Santa Cruz Biotech	Goat polyclonal	1:500
Tyrosine Hydroxylase (TH)	Ab76442, Abcam	Chicken polyclonal	1:1000
EYFP (reporting melanopsin expression)	GFP-1020, AVES Labs	Chicken polyclonal	1:1000
C-FOS	CBL440, Chemicon-Millipore	Sheep polyclonal	1:100
Cholinergic acetyltransferase (ChAT)	AB1449, Chemicon-Millipore	Goat polyclonal	1:1000
Brn3a	Sc-31985, Santa Cruz Biotech	Goat polyclonal	1:1000
GABA	A0310, Sigma-Aldrich	Mouse monoclonal	1:2500
Glycine Transporter-1 (GLT-1)	CL011, Chemicon-Millipore	Goat polyclonal	1:250
PER1	PER13-A, Alpha Diagnostics	Chicken polyclonal	1:100
CLOCK	SBS2923 (aa458-472), Source Bioscience	Goat polyclonal	1:500
CRY2	CRY21-A, Alpha Diagnostics	Rabbit polyclonal	Used various dilutions from 1:100-1:3000

Table 2.3. Summary of primary antibodies used in thesis work.

2.3.4 Image Acquisition

Images were acquired as previously described (Hughes *et al*., 2013). A LSM 710 laser scanning confocal microscope was used together with Zen 2009 image acquisition software (Zeiss). Individual colour channels were collected sequentially. 405nm, 488nm, 561nm and 633nm laser lines were used for excitation. Fluorescence emissions at 440-480, 505-550, 580-625 and 650-700nm were collected for blue, green, red and far red respectively. For all images, brightness and contrast enhancement was performed using ImageJ software (NIH; rsbweb.nih.gov/ij/).For quantitative comparisons of images, identical acquisition settings were used.

2.3.5 Western Blotting

Whole retinas from wildtype, *Cry1*$^{-/-}$, *Cry2*$^{-/-}$ and *Cry1*$^{-/-}$*Cry2*$^{-/-}$ mice were dissected at ZT 5-7 and ZT17-19. Retinal tissue was lysed in 1mL of RIPA buffer (Thermo Fisher) with protease inhibitor cocktail (Thermo Fisher). The Eppendorf tube containing the homogenized retinal tissue was spun in a centrifuge (3500g) at 4°C for 10 minutes. The supernatant comprised the protein lysate and was transferred into a new tube. 15ul of the protein lysate was added to 5ul of Laemmli buffer and heated at 95°C for 10 minutes to denature the proteins. Samples were then loaded onto a 4–12% Bis-Tris NuPAGE precast gel (Invitrogen). The gel was run in running buffer (recipe) at 100 V for one hour and then transferred to a PVDF membrane using the TransBlot (Biorad) machine. The membrane was covered in 1x TBS solution (10x TBS = 24.23g Tris, 80g NaCl, 800ml dH2O, pH to 8.0) and stored at 4°C until antibody detection.

The SNAPiD system was used for antibody detection. Membranes were incubated in blocking solution first (30ml 1% BSA in TBS) at room temperature for 30 minutes. The SNAPiD system uses a vacuum method to draw incubation solutions through the membrane to dry them. Membranes were then incubated with CRY1 or CRY2 antibodies (1:100 for 10 minutes) and control anti-GAPDH (Abcam, 1:10000 for 10 minutes), and then washed three times with 30mL of TBS-T (1x TBS + 0.1% Tween-20). Next, secondary antibodies were applied. HRP-conjugated anti-rabbit (Bio-Rad, 1:3000 in blocking solution for 1 h at room temperature) and control anti-mouse IgG (Sigma, 1:10,000, 1 h at room temperature) were used.

Signal visualization was done using Luminata Forte (Fisher), which was used to cover the membrane for 2 minutes. The membrane was then visualized onto film in a darkroom.

CRY1 and CRY2 antibodies were raised against murine peptide sequences SQEEDAQSVGPKVQRQSSN and VTEMPTQEPASKDS, respectively (Anand *et al*., 2013).

2.3.6 RNA extraction, Quantitative PCR (qPCR)

Whole retinas from wildtype, *Cry1*$^{-/-}$, *Cry2*$^{-/-}$ and *Cry1*$^{-/-}$*Cry2*$^{-/-}$ mice were dissected at ZT 5-7 and ZT17-19. Retinas were immediately snap frozen on dry ice and stored at -80°C until RNA extraction protocol.

Tissue was lysed using 100ul QIAzol Lysis Reagent (Qiagen) in a 1.5 ml Eppendorf tube and homogenized using disposable pestles (VWR). The tissue lysate was then spun in a centrifuge at 12000g at 4 °C for 5 minutes. The supernatant was removed to a clean Eppendorf tube, and 200 ul chloroform was added. The tubes were shaken and then spun in the centrifuge at 12000g at at 4 °C for 15 minutes. The supernatant was then removed

to a new tube and 500ul ethanol was added. The tubes were again shaken to mix the solutions.

RNeasy Mini Kit (Qiagen) was then used to extract RNA, and final extracted RNA concentration was determined using a Nanodrop spectrophotometer.

Quantitative gene expression was then determined using SYBR green real-time quantitative PCR (qPCR) using the following primers shown in **Table 2.4**. A geometric mean of the housekeeping genes *Gapdh, Beta-actin* and *Tbp* was used.

	Forward	**Reverse**
Cry1	GTGGATCAGCTGGGAAGAAG	CACAGGGCAGTAGCAGTGAA
Cry2	TGACCTAGACAGAATCATCGAACTG	GGCTGATGAGGGCCTGAA
Gapdh	TGCACCACCAACTGCTTAG	GATGCAGGGATGATGTTC
Beta-actin	ACCAACTGGGACGATATGGAGAAGA	CGCACGATTTCCCTCTCAGC
TBP	TGGGCTTCCCAGCTAAGTTC	GGAAATAATTCTGGCTCATAGCTACTG

Table 2.4. Primers used for Chapter 2 qPCR work.

Reverse transcription using the qScript cDNA synthesis kit (Quanta Biosciences) was performed. 1g of total RNA was used as a template. The protocol used for RNA to cDNA reverse transcription using the qScript kit was, for each reaction:

Nuclease free water	10ul
qScript reaction mix	4ul
qScript reverse transcriptase	1ul

cDNA was then diluted 1:10 before using in qPCR reaction. qPCR was performed in triplicate using Qiagen Fast SYBR Green PCR master mix. The exact reaction was as follows:

1 cycle: 22ºC, 5 min
1 cycle: 42ºC, 30 min
1 cycle: 85ºC, 5 min
4ºC hold

The PCR protocol was as follows:

Step 1: 95°C for 10 min
Step 2: 95°C for15 sec
Step 3: 60°C for 60 sec
Step 4: 76°C for 15 sec
x40 cycles repeat Step 2-4
Step 5: 95°C for 15 min
Step 6: 60°C for 60 sec

Negative controls were an RNA only sample (without qScript reverse transcription buffers), and a sample containing the qScript buffers only. These negative controls failed to reach thresholds in 45 PCR cycles.

qPCRs were run on a Fast Real-Time PCR System. Relative gene expression was then calculated using the standard $2^{-(\Delta\Delta Ct)}$ relative gene expression method with assumed efficiency = 2 (methods detailed in Peirson *et al*. (2003)), after normalizing to the geometric mean of the three housekeeping genes listed above (Vandesompele *et al*., 2002).

2.4 Results

2.4.1 Commercial CRY2 antibody generates non-specific signal

Alpha Diagnostics CRY2 rabbit antiserum antibody was used to probe for CRY2 in wildtype and *Cry2*$^{-/-}$ retinal tissue (**Figure 2.2**). A similar signal was obtained in both wildtype and *Cry2*$^{-/-}$ retinal tissues. Adjustments to immunohistochemistry protocol (detailed in **Section 2.5.4**) improved the signal-to-noise ratio of the staining results, but the Alpha Diagnostics CRY2 antibody yielded similar signals in both wildtype and knockout tissues. As the Alpha Diagnostics CRY2 antibody was found to stain *Cry2*$^{-/-}$ tissue, it was concluded that this antibody reacts with a non-specific target in mouse retinal tissue.

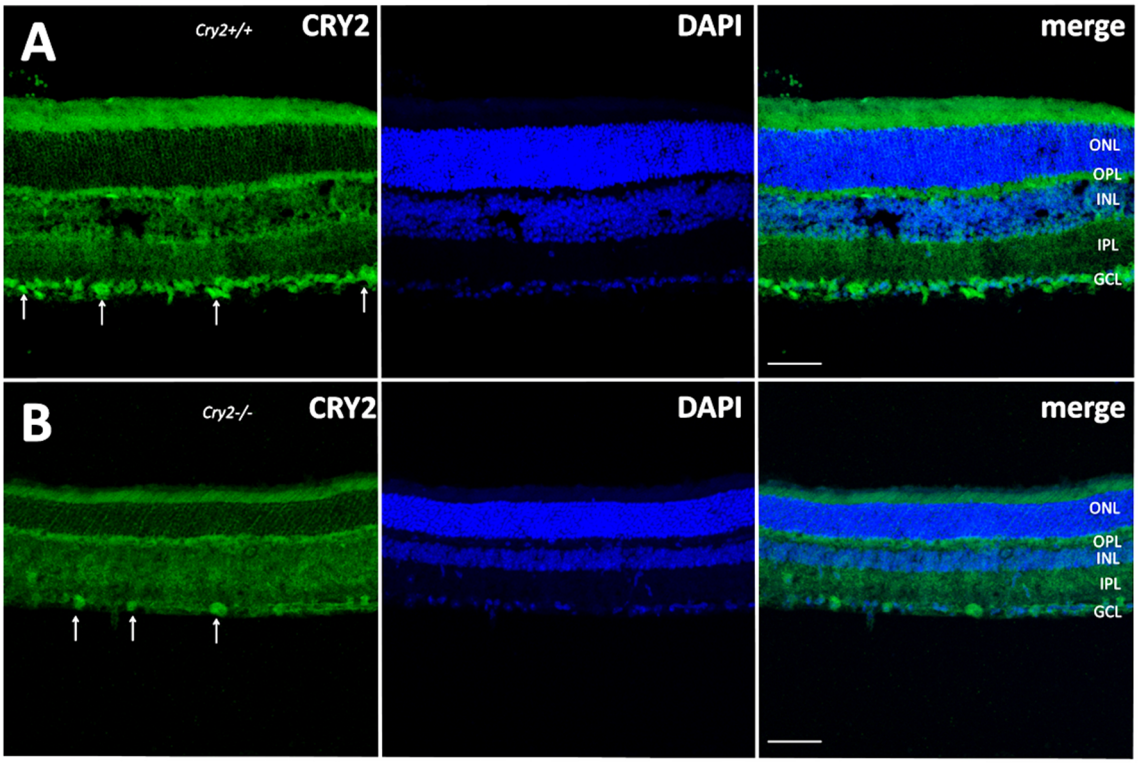

Figure 2.2. CRY2 expression was examined using the Alpha Diagnostics (ADI) commercial CRY2 antibody. ADI CRY2 antibody (green) immunoreacts with a non-specific target in wildtype **(A)** and **(B)** *Cry2*$^{-/-}$ tissue. DAPI staining (blue) in cell nuclei is also shown. Merge indicates all colour channels (green and blue) combined. Scale bar = 20µm.

Previous studies have indicated that the Alpha Diagnostics CRY1 rabbit antiserum antibody does not produce any signal in mammalian tissue (Hattar *et al*., 2003, Thompson *et al*., 2003, Liu *et al*., 2012) and so only CRY2 was studied using this commercial antibody.

2.4.2 Validation of new CRY1 and CRY2 antibodies

Newly raised rabbit antisera against mouse CRY1 and mouse CRY2 (Anand *et al*., 2013, Maywood *et al*., 2011) were used to determine localization of CRY1 and CRY2 in mouse retinal slices. Validation of CRY1 and CRY2 expression in the retina was also carried out by transfection of *Cry1*-HA and *Cry2*-HA plasmids into separate groups of HEK293T cells, and staining these cells with the CRY1 and CRY2 antibodies to ensure specific reactivity (**Figure 2.3**).

The CRY1 and CRY2 antibodies were additionally validated by staining wildtype mouse suprachiasmatic nuclei (SCN) tissue (**Figure 2.4**). Both antibodies demonstrated expression of CRY in the SCN. This was of particular importance for CRY2 as a positive control ensuring that the antibody functions in mouse tissue, as shown in previous work (Anand *et al*., 2013).

Western Blot of whole wildtype, *Cry1*$^{-/-}$ and *Cry2*$^{-/-}$ retinas confirmed that CRY1 protein is expressed in wildtype retina and detectable using the antibody used, whereas CRY2 protein could not be detected in retinal tissue using this method (**Figure 2.5**). Cells transfected with *Cry1* or *Cry2* were used as positive controls for the Western Blot. Retinal tissue from *Cry1*$^{-/-}$, *Cry2*$^{-/-}$, and *Cry1*$^{-/-}$*Cry2*$^{-/-}$ mice were used as negative controls.

Lastly, quantitative Polymerase Chain Reaction (qPCR) was performed to determine relative mRNA expression levels of *Cry1* and *Cry2* in the wildtype mouse retina at CT5 and CT17 (n=5 at each timepoint, C_T values are reported in **Table 2.5.**). Analysis across mRNA

expression levels at CT5 and CT17 (**Table 2.6**) revealed that at CT5, *Cry1* is expressed at 0.70 ± 0.077 of the level at CT17. At CT5, *Cry2* is expressed at 0.78 ± 0.079 the level at CT17.

Analysis of relative expression of *Cry1* compared to *Cry2* revealed that *Cry2* is expressed at a lower level than *Cry1* in wildtype retina at both CT5 and CT17 (**Table 2.7**). *Cry2* was expressed at 0.68 ± 0.048 of *Cry1* levels at CT5, and at 0.60 ± 0.029 of *Cry1* levels at CT17. When data from CT5 and CT17 were combined, *Cry2* was found to be expressed at 0.64 ± 0.029 of *Cry1* mRNA levels.

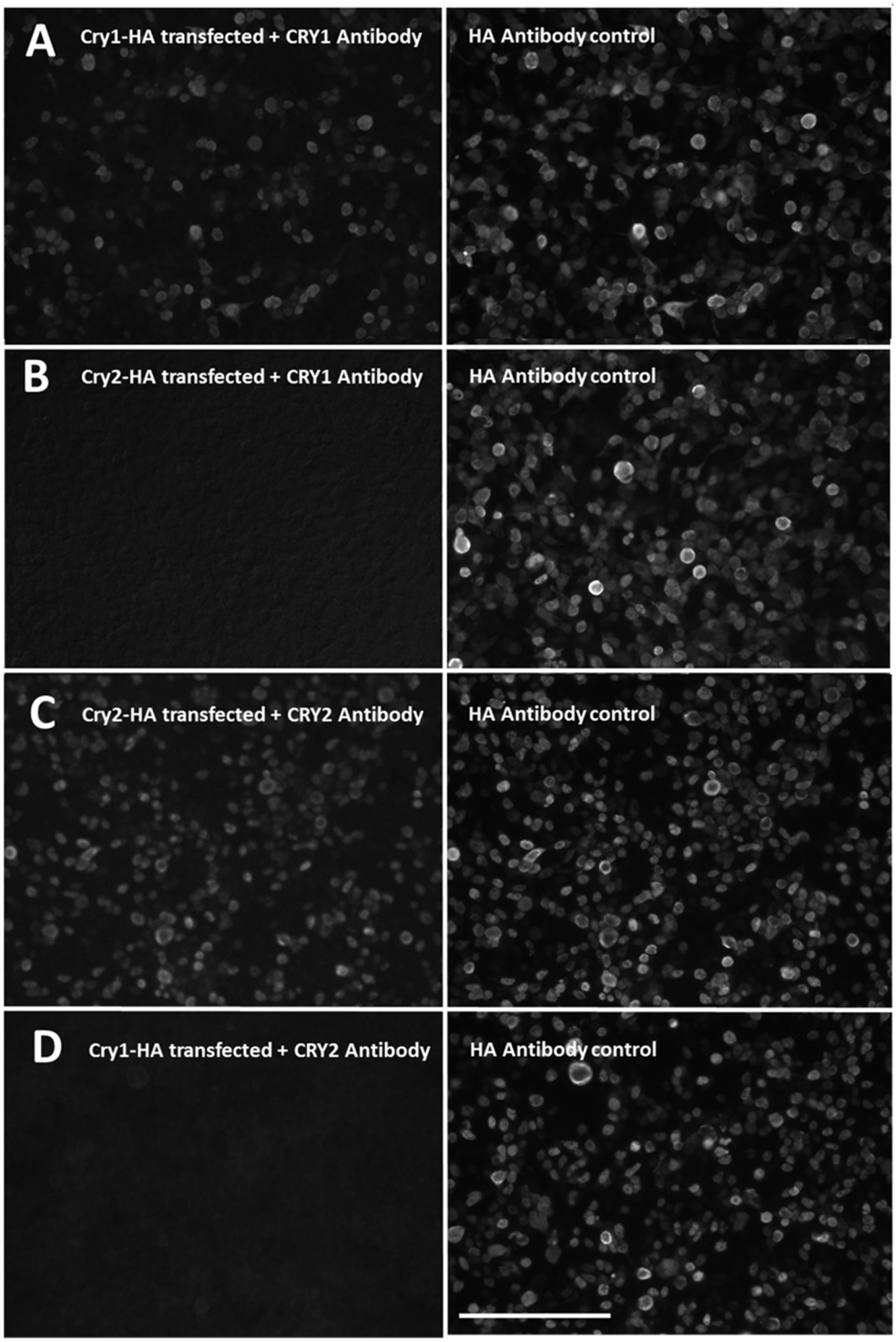

Figure 2.3. CRY1 and CRY2 antibodies are validated and confirmed to recognize CRY1 and CRY2, respectively, without non-specific reactivity in HEK293 cells transfected with CRY1 and CRY2. Scale bar indicates 10µm. **(A)** *Cry1*-HA transfected cells are recognized by CRY1 antibody (left) and HA antibody control (right). **(B)** *Cry2*-HA transfected cells are not recognized by CRY1 antibody (left), but are recognized by HA antibody control (right). **(C)** *Cry2*-HA transfected cells are recognized by CRY2 antibody (left) and HA antibody control (right). **(D)** *Cry1*-HA transfected cells are not recognized by CRY2 antibody (left), but are recognized by HA antibody control (right).

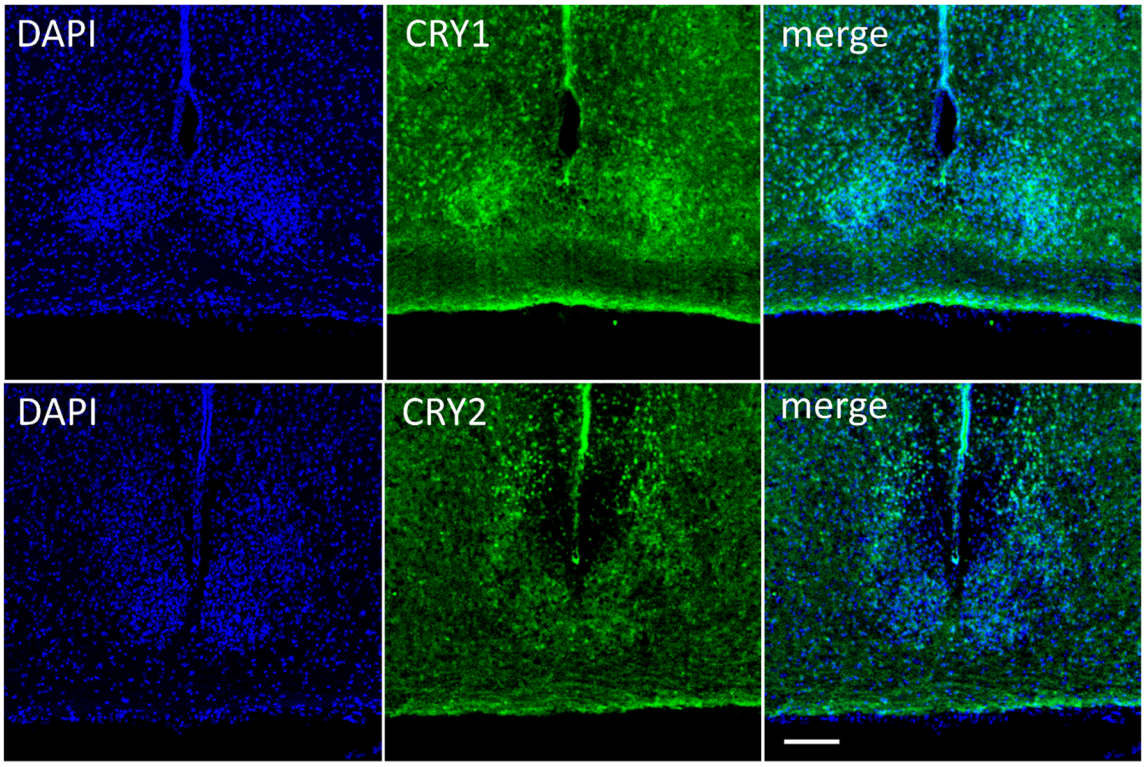

Figure 2.4. CRY1 and CRY2 expression in wildtype mouse suprachiasmatic nuclei tissue is examined using CRY1 and CRY2 antibodies obtained from Hastings lab. CRY1 **(A)** and CRY2 **(B)** antibodies (green) are both capable of recognizing their targets in wildtype SCN tissue. DAPI staining (blue) shows cell nuclei. Scale bar = 40µm.

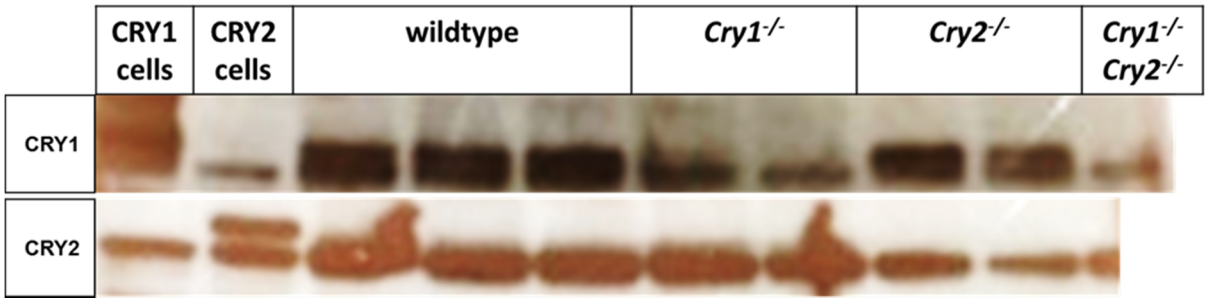

Figure 2.5. Western Blot of CRY1 and CRY2 expression in wildtype, *Cry1*$^{-/-}$, *Cry2*$^{-/-}$ and *Cry1*$^{-/-}$ *Cry2*$^{-/-}$ retinas showing that CRY1 protein is expressed in wildtype and *Cry2*$^{-/-}$ retina, whereas CRY2 protein could not be detected in retinal tissue using this method. CRY1 was detected in *Cry1*-transfected cells, and CRY2 was detected using *Cry2*-transfected cells, as a positive control ensuring the effectiveness of the probing antibody. Note that the CRY2 band on the *Cry1*$^{-/-}$ *Cry2*$^{-/-}$ retina tissue appears cut off because the membrane was cut during the experiment.

	Cry1	*Cry2*	*Gapdh*	*Tbp*	*Beta-actin*	Housekeeping geometric mean C_T	Relative expression of *Cry2/Cry1*
CT5 Retina 1	25.49	26.33	15.80	25.31	17.37	19.49	0.56
CT5 Retina 2	24.69	25.25	14.42	24.69	15.63	18.25	0.68
CT5 Retina 3	24.47	24.96	14.03	24.21	15.07	17.77	0.71
CT5 Retina 4	25.31	25.56	15.03	25.57	15.46	18.69	0.84
CT5 Retina 5	24.17	24.92	14.04	24.56	14.80	17.80	0.59
CT17 Retina 1	23.76	24.72	13.53	24.36	15.53	17.81	0.51
CT17 Retina 2	24.41	24.95	14.14	24.98	16.48	18.53	0.69
CT17 Retina 3	24.28	25.00	13.71	24.81	15.62	18.04	0.60
CT17 Retina 4	24.06	24.84	14.08	24.87	16.42	18.46	0.58
CT17 Retina 5	23.97	24.63	14.00	24.88	15.71	18.20	0.63

Table 2.5. C_T values obtained from qPCR of *Cry1* and *Cry2* in individual wildtype mouse retinas at CT5 and CT17 (n=5 at each timepoint). The geometric means of the housekeeping genes *Gapdh, Tbp*, and *Beta-actin* were calculated and displayed. The relative expression of *Cry2* compared to *Cry1* was calculated using the using the standard $2^{-(\Delta\Delta Ct)}$ relative gene expression method and displayed here.

	Cry1 Relative expression of CT5/CT17	*Cry2* Relative expression of CT5/CT17
Retina 1	0.97	1.06
Retina 2	0.67	0.67
Retina 3	0.72	0.85
Retina 4	0.49	0.71
Retina 5	0.66	0.62
Average of all retinas	**0.70 ± 0.077**	**0.78 ± 0.079**

Table 2.6. Relative expression levels of *Cry1* and *Cry2* at CT5 compared to CT17 for individual sample retinas. Mean ± SEM is shown for the averaged values.

Relative expression of *Cry2*/*Cry1* at all tested times	Relative expression of *Cry2*/*Cry1* at CT5	Relative expression of *Cry2*/*Cry1* at CT17
0.64 ± 0.029	**0.68 ± 0.048**	**0.60 ± 0.029**

Table 2.7. Relative expression levels of *Cry2* compared to *Cry1* at CT5, CT17 and at both times combined. Mean ± SEM is shown for the averaged values.

2.4.3 CRY1 is expressed throughout several layers of the mouse retina, whilst CRY2 expression is restricted to the outer retinal layer

CRY1 was localized to retinal cells in the outer nuclear layer, inner nuclear layer and ganglion cell layer (**Figure 2.6**). Co-staining with DAPI showed that both cytoplasmic and nuclear punctate staining was observed. *Cry1*$^{-/-}$ retinal tissue was used as a control and showed no specific CRY1 signal. CRY2 was localized to the outer nuclear layer. From morphological inspection, it appears that CRY2 expression is restricted to the photoreceptor outer segments. *Cry2*$^{-/-}$ retinal tissue controls again demonstrated no specific CRY2 signal.

Retinal tissue was collected at 6 different timepoints across the diurnal day: ZT2, ZT6, ZT10, ZT14, ZT18, ZT22 and immunoreacted with either CRY1 antibody (**Figure 2.7**) or CRY2 antibody (**Figure 2.8**). Neither CRY1 nor CRY2 exhibited a global change in immunofluorescence levels throughout the day.

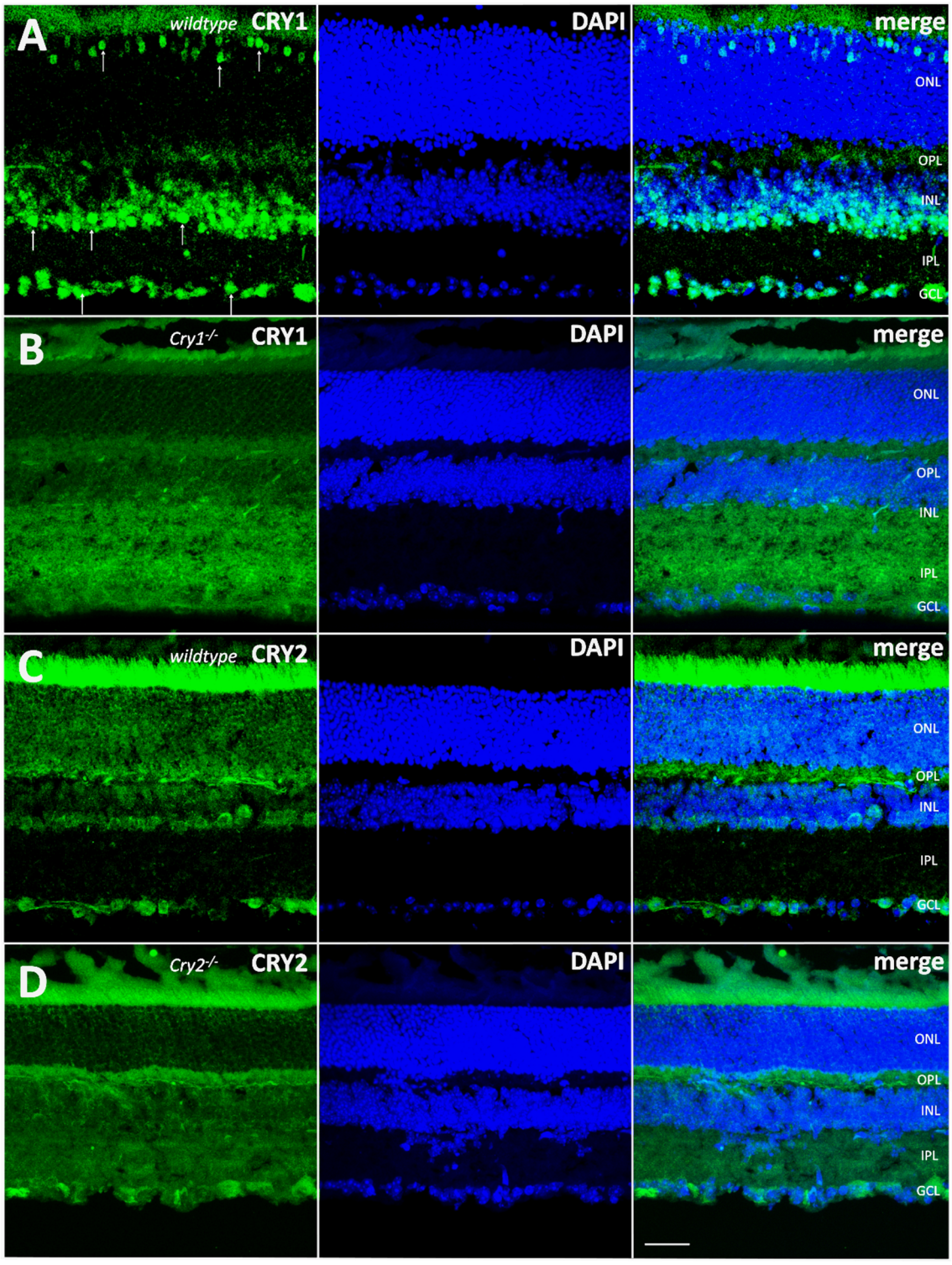

Figure 2.6. CRY1 is expressed throughout the entire mouse retina whilst CRY2 expression is restricted to the outer retina. Scale bar indicates 20µm. **(A)** CRY1 (green) is expressed in the outer nuclear layer (ONL), inner nuclear layer (INL) and ganglion cell layer (GCL) of the mouse retina. DAPI staining is shown in blue. **(B)** CRY1 (green) is not expressed in *Cry1*$^{-/-}$ retina. **(C)** CRY2 (green) is expressed only in the outer nuclear layer (ONL) of the mouse retina. DAPI is shown in blue. **(D)** CRY2 (green) is not expressed in *Cry2*$^{-/-}$ retina.

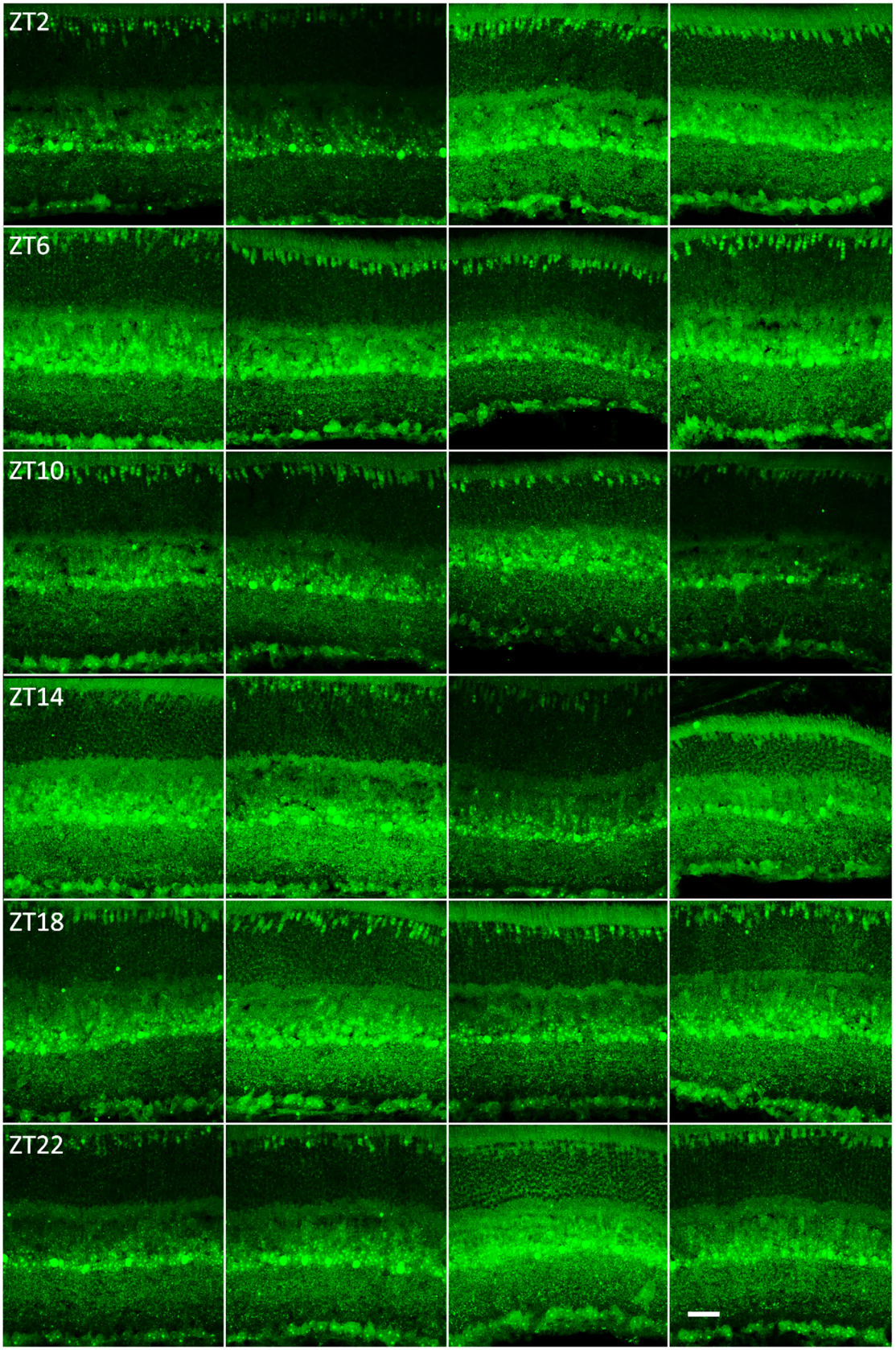

Figure 2.7. CRY1 expression in wildtype retina tissue harvested at ZT2, ZT6, ZT10, ZT14, ZT18 and ZT22 (n=4 per timepoint shown, each panel represents an individual animal). Scale bar = 20µm, all panels equally scaled.

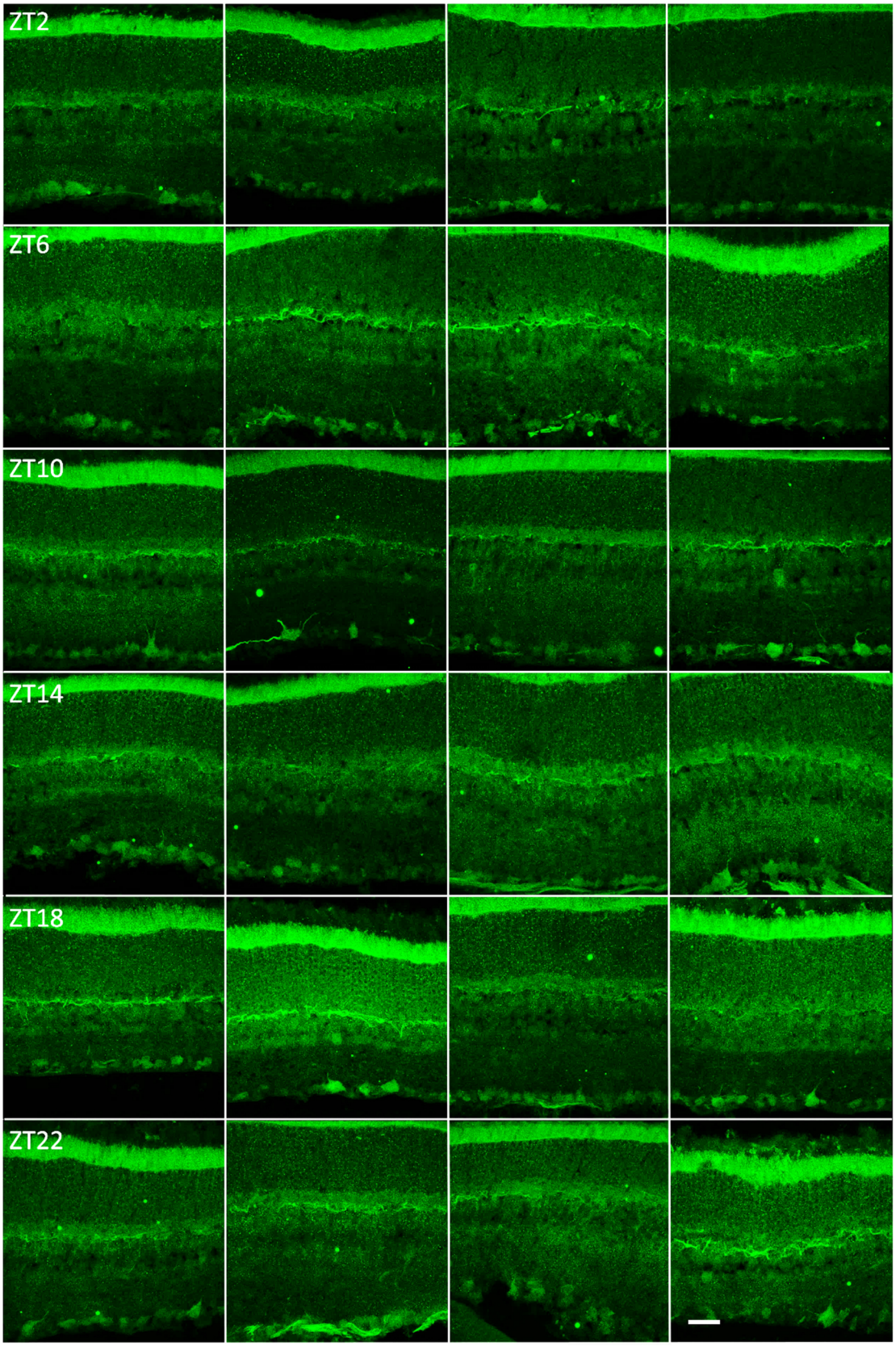

Figure 2.8. CRY2 expression in wildtype retina tissue harvested at ZT2, ZT6, ZT10, ZT14, ZT18 and ZT22 (n=4 per timepoint shown, each panel represents an individual animal). Scale bar = 20µm, all panels equally scaled.

2.4.4 CRY1 protein is expressed in all cones of the mouse retina

CRY1 was co-immunolabelled with UVS opsin, a marker for mouse UV cones (**Figure 2.9 A-B**). It was found that CRY1 completely co-localized with mouse UV cones. As UV opsin and MWS opsin are co-expressed in a gradient across the mouse retina (Applebury *et al*., 2000, Rohlich *et al*., 1994, Hughes *et al*., 2013), this suggested that CRY1 may be expressed in all cones. As such, cone arrestin, a marker of all cones, was also studied, and showed full co-localisation with CRY1 (**Figure 2.9 C**).

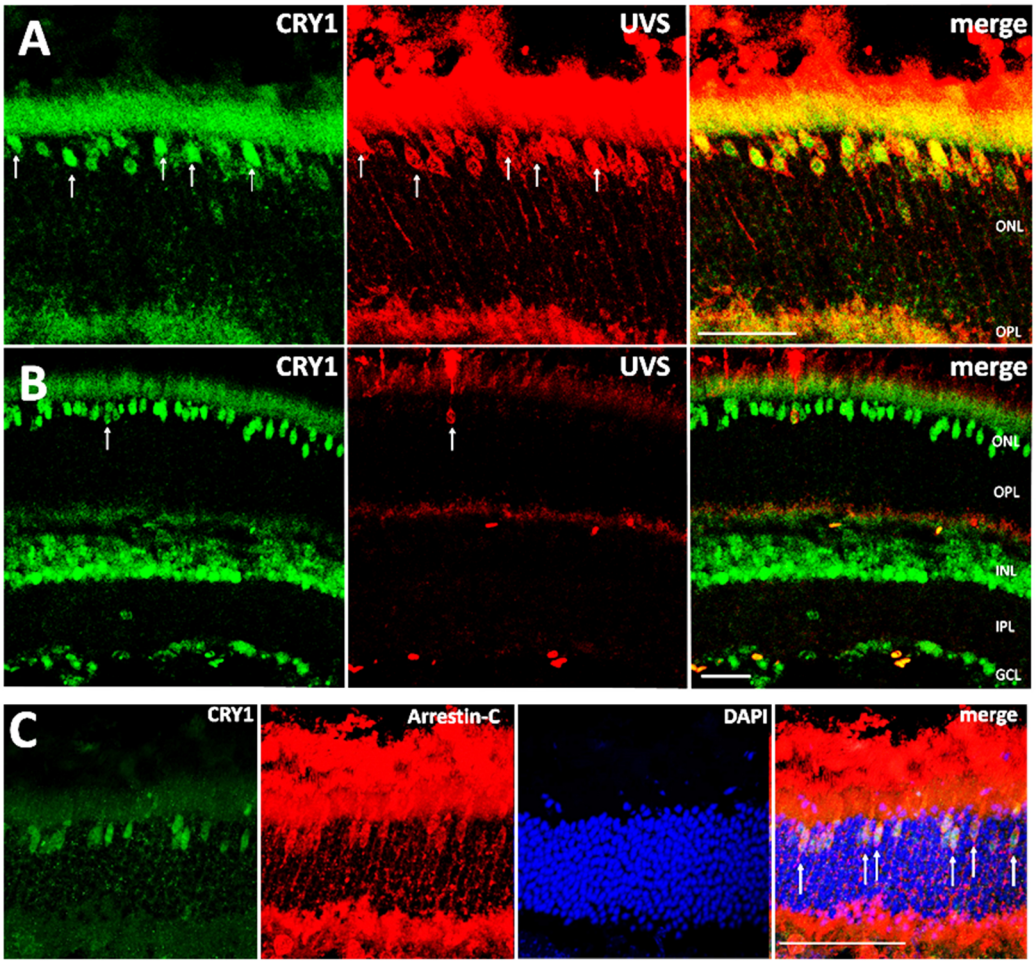

Figure 2.9. CRY1 is expressed in all cones. CRY1 (green) colocalizes with a UV cone marker, UVS opsin (red), in both the ventral **(A)** and dorsal regions **(B)** of the retina. **(C)** CRY1 (green) also colocalizes with Arrestin-C (cone arrestin, red), a marker for all retinal cones. Scale bar = 20µm.

2.4.5 CRY1 protein is expressed in amacrine cells, including dopaminergic amacrine cells

Furthermore, co-localization studies were performed with an extensive set of retinal cell markers to determine CRY1 expression in the inner nuclear layer and ganglion cell layer (**Figure 2.10 A-D**). CRY1 was found to partially co-localize with tyrosine hydroxylase (TH, a marker of dopaminergic amacrine cells), GABA (a marker of GABAergic amacrine cells) and glycine transporter 1 (GLYT-1, a marker of glycinergic amacrine cells). CRY1 was also found to partially co-localise with cholinergic acetyltransferase (ChAt, a marker of cholinergic amacrine cells, data not shown).

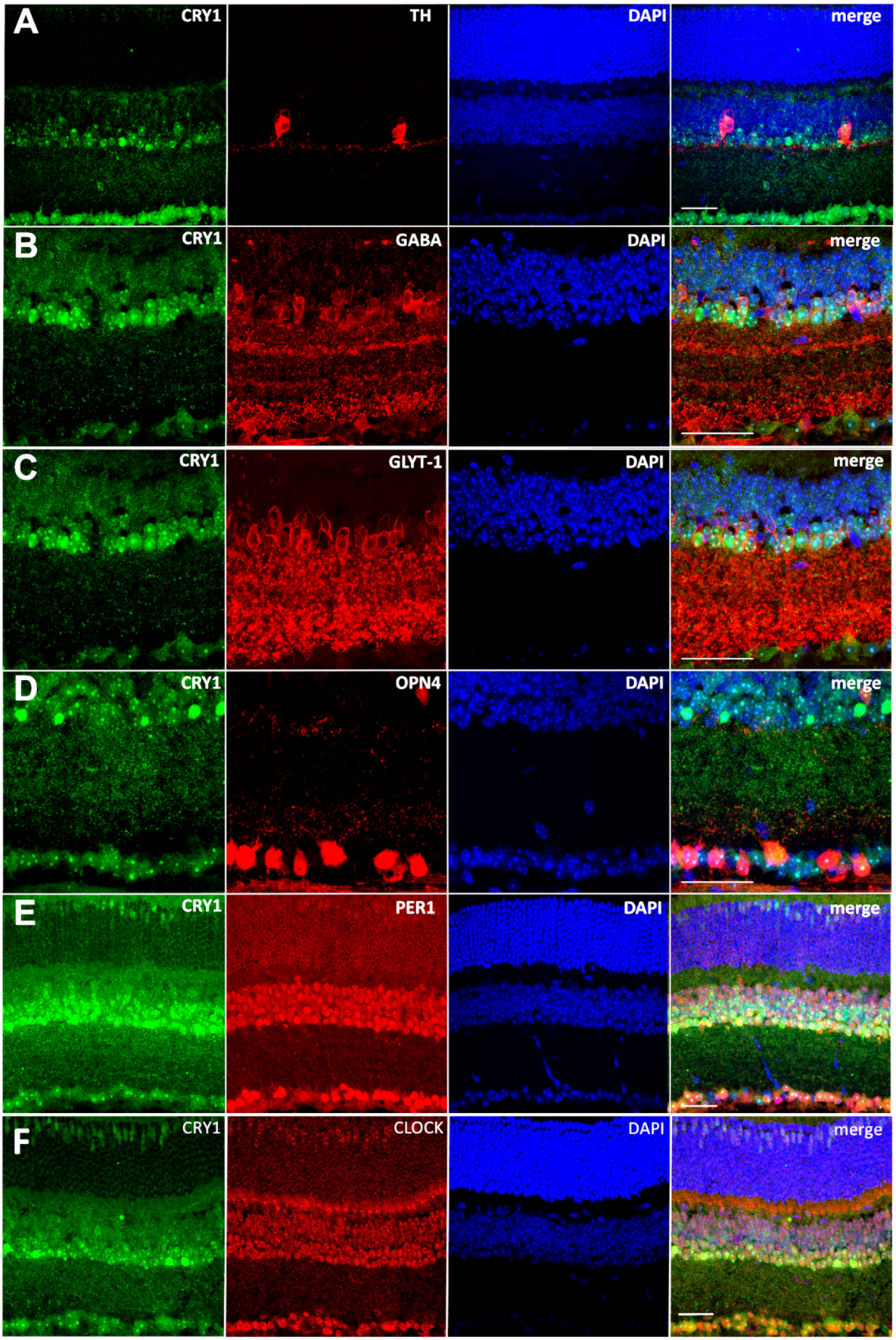
A
CRY1
TH
DAPI
merge
B
CRY1
GABA
DAPI
merge
C
CRY1
GLYT-1
DAPI
merge
D
CRY1
OPN4
DAPI
merge
E
CRY1
PER1
DAPI
merge
F
CRY1
CLOCK
DAPI
merge

Figure 2.10. CRY1 partially co-expresses with several retinal cell markers. DAPI staining is shown in blue, and merge shows all channels merged together. White arrows indicate cells demonstrating colocalization of red, green and blue signals. Scale bar indicates 20µm. **(A)** CRY1 (green) partially co-expresses with dopaminergic amacrine cells, marked by Tyrosine Hydroxylase expression (red). **(B)** CRY1 (green) partially co-expresses with GABAergic amacrine cells, marked by GABA expression (red). **(C)** CRY1 (green) partially co-expresses with glycinergic amacrine cells, marked by Glycine Transporter 1 (GLT-1) expression (red). **(D)** CRY1 (green) partially co-expresses with photosensitive retinal ganglion cells (pRGCs), marked by melanopsin (OPN4) expression (red). CRY1 (green) partially co-expresses with clock protein PER1 (**E**, red) and CLOCK (**F**, red).

2.4.6 CRY1 protein partially co-expresses with photosensitive retinal ganglion cells (pRGCs)

CRY1 protein is partially co-expressed with melanopsin (OPN4, as reported by EYFP) (**Figure 2.10 D**). This indicates that a subset of photosensitive retinal ganglion cells (pRGCs) express CRY1. Furthermore, CRY1 partially co-localises with *Brn3a*, a marker of retinal ganglion cells (data not shown). Altogether, CRY1 appears to be expressed in a subset of retinal ganglion cells, some of which are melanopsin-expressing and some of which are not. Furthermore CRY1 is expressed in a subset of pRGCs.

2.4.7 CRY1 protein partially co-expresses with circadian clock proteins CLOCK and PER1

CRY1 was furthermore found to partially co-localize with two clock proteins, CLOCK and PER1 (**Figure 2.10 E-F**). Careful study of the confocal images indicated that CRY1 expression and CLOCK expression did not fully overlap, and nor did CRY1 and PER1 expression, indicating that again CRY1 was expressed in a subset of CLOCK-expressing or PER1 expressing cells.

2.4.8 PER1 does not demonstrate diurnal rhythms in expression level detectable by immunohistochemistry

Retinal tissue collected at 6 different timepoints across the diurnal day: ZT2, ZT6, ZT10, ZT14, ZT18, ZT22 was also studied with PER1 antibody (Figure 2.11), in order to determine whether a qualitative circadian rhythm in expression level could be reliably detected by immunohistochemistry. PER1 expression as measured by immunohistochemistry did not exhibit a global change in immunofluorescence levels throughout the day. Importantly, this suggests that immunohistochemistry may not be an ideal method for studying clock protein rhythms in the retina.

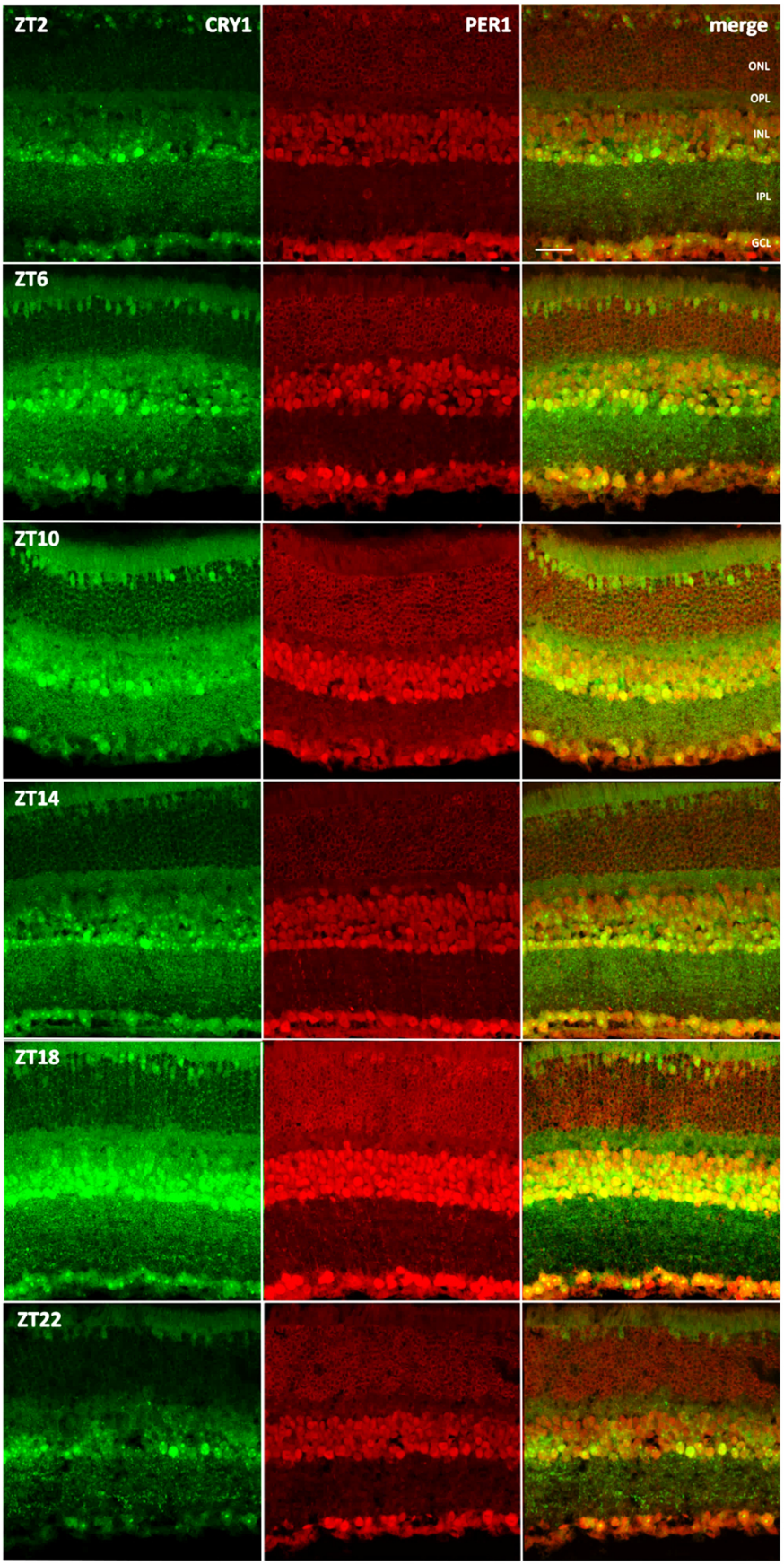

Figure 2.11. CRY1 and PER1 co-expression in wildtype retina tissue harvested at ZT2, ZT6, ZT10, ZT14, ZT18 and ZT22 (n=4 per timepoint, representative images shown). Scale bar = 20µm, all panels equally scaled.

2.5 Discussion

2.5.1 CRY1 is expressed throughout the mouse retina

Here, the presence of CRY1 in mouse retinal cones, as well as in a subset of inner nuclear layer and ganglion cell layer cells is reported. These are the first data directly showing CRY1 protein expression in the mouse retina. The presence of CRY1 in cones corroborates studies supportive of a photoreceptor clock in mammals (Tosini *et al*., 2007, Sandu *et al*., 2011). Surprisingly, CRY2 was found to be localised only to the photoreceptive outer layer and the outer segments in particular. Finally, a subset intrinsically-photosensitive retinal ganglion cells (marked by melanopsin expression) were found to express CRY1 but not CRY2, a particularly exciting finding given that melanopsin or pRGCs may play a role in regulation of the retinal clock (Barnard *et al*., 2006). This subject is further explored in Chapter 4.

Previous immunohistochemical studies have reported no CRY1 protein expression in the mouse retina (Liu *et al*., 2012, Hattar *et al*., 2003). This may be due to lack of commercial antibodies capable of recognizing CRY1. Antibodies raised in-house against CRY1 have been available for some time (Maywood *et al*., 2011, Anand *et al*., 2013) but these antibodies have not previously been used against mammalian retinal tissue. The studies reporting lack of CRY1 protein expression in the retina also reported high CRY2 expression throughout the retina. However, these studies have typically lacked knockout tissue controls, often instead using blocking peptides as the only control. Therefore, it is possible that the signal previously characterized for CRY2 in the mouse retina may be non-specific. Indeed, the non-specific target may be exclusive to the retina and expression in other tissues (such as SCN) may be correct if they are not expressing this source of non-specific binding.

Furthermore, commercially available antibodies may change over time depending on production. Initial work using the commercial CRY antibodies may have been specific to CRY but later batches may not have been. Especially given that polyclonal antibodies are produced by inoculating an animal with the antibody epitope, it is possible that different immune responses give rise to antibody batches of differing efficacy. To ensure correct characterization of Cryptochrome localization in the retina, both antibodies used in this thesis have been validated, using both heterologous expression in cell lines as well as knockout tissue controls.

CRY1 was found to partially co-localize with several retinal cell markers. This data, in particular, provides further insight regarding the identity of retinal clock cells. For instance, whilst all dopaminergic amacrine cells have previously been thought to express the six core clock genes, not every TH-positive cell (TH refers to Tyrosine Hydroxylase, a marker for dopamine neurons) co-expressed CRY1. Indeed, CRY1 was found to partially co-localize with GABAergic amacrine cells, glycinergic amacrine cells, and cholinergic amacrine cells. This pattern of partial co-localization is consistent with reports that not all individual cells within a retinal cell type express all the clock components (Ruan *et al*., 2006). Indeed, this pattern of CRY1 expression indicates that CRY1 is likely expressed in all major retinal cell types, though not in all cells of each type. This suggests that potentially most retinal cells could be retinal clock cells. However, whether CRY1 plays a functional role in the retinal clock remains unknown, and is further explored in Chapter 3.

2.5.2 Differential expression patterns of CRY1 and CRY2 in the mammalian retina suggests different functions

The findings from the work here agree with several studies that have characterized mRNA expression of both *Cry1* and *Cry2* in the mammalian retina (Miyamoto and Sancar, 1998, Thompson *et al*., 2003, Ruan *et al*., 2006, Peirson *et al*., 2006). It is interesting that although both *Cry1* and *Cry2* mRNA appear to be expressed in equal amounts throughout the retina, CRY1 protein appears to be expressed in substantially greater amounts than CRY2. Quantification of relative expression of retinal *Cry1* and *Cry2* by qPCR revealed that *Cry1* is expressed at greater levels than *Cry2* both during the subjective day and subjective night. Furthermore, western blot of whole mouse retinas yielded reliable CRY1 detection but CRY2 was not detected in significant amounts (though heterologous expression of CRY2 in cells could be detected). Differential post-transcriptional processing mechanisms for CRY1 and CRY2 may exist, which could explain why similar *Cry1* and *Cry2* mRNA expression leads to different levels protein expression in the retina. Indeed, *Cry1* and *Cry2* have often been referred to interchangeably or assumed to have the same functions, but this appears, at least at the level of the retina, to be an oversimplification. The differential functions for CRY1 and CRY2 in the mammalian retina are explored in Chapter 3.

2.5.3 CRY1 and CRY2 protein levels do not appear to fluctuate in the retina across the circadian day

Expression of CRY1 or CRY2 did not appear to exhibit dramatic time-of-day effects when observing CRY fluorescence from separate retinas taken at different time points, suggesting that a single pacemaker rhythm is unlikely and either several unsynchronized

rhythms exist or CRY levels do not oscillate in the retina. This is a tentative conclusion, however, as single cells were not observed over a period of time. Observation of CRY rhythms in live single retinal cells yet has not yet been performed. *Cry1* and *Cry2* mRNA may, however, oscillate in the outer retina (Dkhissi-Benyahya *et al*., 2013). Using laser microdissection to separate the outer and inner retinal layers, this study found rhythmic expression of both *Crys* and nearly all other clock genes in the other retina, but no *Cry* mRNA rhythm was found in the inner retina. At the level of the whole retina, both *Cry1* and *Cry2* do not appear to exhibit any detectable rhythms. Evidence for any outer retinal rhythms in CRY protein expression was investigated by comparing fluorescence in only the outer retina portion of the photographs obtained, but no obvious rhythm could be found. However, lack of an observable rhythm does not rule out the possibility that CRY proteins oscillate on a circadian basis in individual cells. Rhythms of CRY protein expression could exist in individual cells – if these rhythms are not synchronized, then assays of whole retina or entire retinal layers would yield non-rhythmic results. Further work is needed to test whether CRY rhythms exists at the single cell level, or if CRY proteins simply do not oscillate in the retina. It is also possible that rhythms in CRY1 and CRY2 expression in the retina were not found because such changes in expression were below the threshold of detection for this method. Indeed, is important to note that using immunohistochemistry to assay rhythms in protein expression may have certain limitations (discussed in detail in the next section). Though PER1 is thought to exhibit circadian rhythms of expression in the retina (Ruan *et al*., 2006, Peirson *et al*., 2006, Witkovsky *et al*., 2003), the PER1 immunohistochemistry results presented here were not able to resolve this, which may indicate that immunohistochemistry is not be an ideal method for resolving protein expression rhythms.

2.5.4 Immunohistochemistry is a semi-quantitative technique

Our findings regarding localization of Cryptochromes in the mouse retina show that proper validation of antibodies is extremely important. Adjustment of various steps in the antibody immunoreactivity process can yield results with better signal to noise ratios. The particular variables that can be altered include:

- Concentration of Primary Antibody
- Incubation time of Primary Antibody
- Concentration of detergents (Triton-X or Tween-20)
- Wash frequencies and lengths
- Use of citrate buffer solution (for antigen retrieval)
- Length of tissue fixation time
- Concentration of Secondary Antibody
- Incubation time of Secondary Antibody
- Temperature of incubation (room temperature vs 4°C refrigerator)
- Concentration, length and temperature of initial blocking step

Any change in these variables may affect the signal-to-noise ratio of the final immunohistochemistry result. Furthermore, ideally all samples are processed at the same time to ensure they are comparably treated, yet there will still be differences in incubation/wash times between the first and last sample treated, due to the time it takes to process each sample.

Significant time and effort was spent attempting to optimize the signal-to-noise ratio of the CRY2 signal obtained using the Alpha Diagnostics CRY2 antibody. As several published papers had reported that this was a reliable antibody, it was thought that replication of previous findings regarding CRY2 expression would produce similar results. Comparison of wildtype tissue immunofluorescence patterns with that of knockout tissue was performed. After initial staining results gave a relatively low signal-to-noise ratio, the listed variables above were adjusted in order to optimize staining. This included increasing incubation

times and concentrations of the primary CRY2 antibody, increasing number of washes and their lengths, using citrate buffer to de-crosslink fixed proteins and increase permeabilization by increasing the concentration of detergents (Triton-X and Tween-20).

However, even after several attempts to vary the immunohistochemistry protocol, there was an equally strong CRY2 immunofluorescence signal in the *Cry2*$^{-/-}$ mice as the wildtype mice. This led to the conclusion that the Alpha Diagnostic CRY2 antibody is not, in fact, specific to CRY2. Rather it has generated a non-specific signal present in both wildtype and *Cry2*$^{-/-}$ mouse retinal tissue. There are some potential reasons for why this could be the case. Most obviously, the Alpha Diagnostic CRY2 antibody may not recognize mouse CRY2 despite being raised against a CRY2 epitope. Another possibility is the batch of antibody received was not specific, although to rule out this case, a second aliquot was purchased with the same results. Finally, it is possible that the antibody reacts poorly in retinal tissue and has improved signal-to-noise ratio in other tissues. To rule this out, this antibody was tested in SCN brain slices. The CRY2 signal in the SCN was very poor (data not shown).

Immunohistochemistry is, at best, a semi-quantitative technique. Indeed, it is best used as an assay of presence/absence of a substance. Some quantitation is possible, for example, counting cells for presence/absence studies in order to determine approximate percentage of cells expressing a protein of interest, or approximate percentage of protein expressed in the cell membrane compared to within cell compartments. However, it is not an ideal method to gauge exact expression amounts in the context of an entire tissue, nor to assay rhythms of expression, given that signal levels may fluctuate significantly between samples due to tissue quality, impurities in incubation solutions, or other reasons difficult to control.

2.6 Conclusions

In this chapter, newly-raised CRY1 and CRY2 antibodies were extensively validated for the characterization of CRY1 and CRY2 expression in mouse retina. It was determined that CRY1 is expressed in the mouse retina and characterized the localization and expression pattern of CRY1. Although the initial aim was to confirm the retinal expression pattern of CRY2 with previously published work, the antibody validation studies presented here have revealed limitations of previous studies. By contrast with previous data, CRY1 is widely expressed throughout the retina whilst CRY2 expression is restricted to the outer retina. Furthermore, the co-localization of CRY1 with specific retinal cell types was characterized. CRY1 was found to be expressed in all mouse cones, as well as partially co-expressed with several types of amacrine cells, pRGCs and other clock proteins. CRY1 appears to be expressed at higher levels in the mouse retina compared to CRY2, and both appear to be expressed at higher levels during the subjective night compared to the subjective day. Global changes in CRY1 and CRY2 expression across the whole retina were not observed using immunohistochemistry, though this may have been due to technical limitations.

Given that this data is the first to indicate CRY1 protein expression in the mouse retina and moreover, that CRY1 appears to be expressed in higher levels and in more cell types than CRY2, this may imply that CRY1 and CRY2 perform different functions in the retina. This is of particular interest regarding the mouse retinal clock, as both CRY1 and CRY2 are core clock proteins in the SCN. Furthermore, the co-expression of CRY1 with cones and with pRGCs may indicate that CRY1 has some connection to the retinal clock, which may depend on these specific retinal cells. As such, the role of CRY1 and CRY2 in the mouse retinal clock is investigated in Chapter 3.

3

Role of Cryptochromes in retinal rhythms

3.1 Introduction

The unexpected localisation of CRY1 in the mouse retina, described in Chapter 2, gave rise to questions regarding the function of CRY1 and CRY2 in the retinal circadian clock. The following chapter describes a detailed investigation of circadian rhythms in retinal function using wildtype, *Cry1*- and *Cry2*-deficient mice.

3.1.1 Mammalian retinal cryptochromes

The function of Cryptochromes in the retina has been the subject of much interest. Their role as photoreceptive proteins in plants and insects first led to speculation that CRYs may perform a similar function in the mammalian circadian system (Sancar, 2000). A number of studies using *Cry*-null mice led to suggestions that mammalian cryptochromes act as the mammalian circadian photopigment (Thresher *et al*., 1998, Miyamoto and Sancar, 1998, Vitaterna *et al*., 1999, Selby *et al*., 2000, Sancar, 2000, Thompson *et al*., 2003). However, to date, no data currently exists to show that mammalian cryptochromes act as photopigments. Indeed, whilst CRYs are widely expressed throughout the body, loss of the eye in mammals abolishes all non-image forming responses to light (Nelson and Zucker, 1981). This would indicate that the mammalian circadian photopigment must be located within the eye, or an unlikely situation where CRY is a photopigment in the retina but not in other tissues.

Available action spectra suggested the role of an opsin-vitamin A-based photopigment (Lucas *et al*., 2001, Peirson *et al*., 2005) as the mammalian circadian photopigment. The identification and characterisation of the melanopsin (OPN4)-expressing photosensitive retinal ganglion cells (pRGCs) (Provencio *et al*., 1998, Panda *et al*., 2002, Provencio *et al*.,

2002, Panda *et al*., 2003, Hankins *et al*., 2008) resolved the question of whether melanopsin or Cryptochrome is the mammalian circadian photopigment. Loss of rod, cone, and melanopsin systems together were found to account for all non-image forming responses to light (Hattar *et al*., 2003), and heterologous expression of melanopsin was sufficient to induce photosensitivity in non-photoreceptive cells (Melyan *et al*., 2005, Qiu *et al*., 2005, Panda *et al*., 2003). Altogether, this work supported melanopsin, not Cryptochrome, as the circadian photopigment in mammals. Furthermore, these data indicate that even if mammalian Cryptochrome photoreception was possible, any contribution to mammalian responses light would be rod, cone, or melanopsin-dependent. To date, there is no evidence that this is the case. Indeed, it has been suggested that loss of photoreceptive ability in mammalian cryptochromes may be linked to the essential role of CRYs in the mammalian circadian clock. The CLOCK/BMAL1 binding site in mammalian CRY1 and CRY2 may be in the same region as the FAD co-factor binding site in *Drosophila* CRY, which is an essential region for downstream transmission of light information (Clark Rosensweig, personal communication).

3.1.2 A role for cryptochromes in retinal circadian rhythms

Given their importance in the negative regulatory arm of the TTFL, mammalian Cryptochromes are essential for maintenance of the molecular circadian clock (van der Horst *et al*., 1999). As mentioned above, mammalian CRYs are not photopigments but, as described in Chapter 2, mammalian Cryptochromes are expressed throughout the retina. Whilst they do not appear to demonstrate circadian oscillations in mRNA or protein expression levels when the retina is assayed as a whole (Peirson *et al*., 2006), this observation may be due to the lack of tools capable of recording *Cry* expression in

individual cells within an intact retina. The expression of retinal mammalian Crys combined with their essential circadian clock role may point to a role for Cryptochromes in mammalian retinal circadian rhythms. Surprisingly, loss of *Cry1* but not *Cry2* severely attenuates PER2::LUC rhythms whole retinal explants (Ruan *et al*., 2012). As such, the role of CRY in the mammalian retina appears to more plausibly relate to the regulation of retinal rhythms, rather than in any photoreceptive function. A role of CRY in the mammalian retinal clock could potentially affect retinal sensitivity to light, which may explain findings from early studies where loss of CRYs resulted in changes to retinal responses to light (Owens *et al*., 2012, Selby *et al*., 2000, Van Gelder *et al*., 2003, Thompson *et al*., 2004).

To date, studies investigating the role of cryptochromes in the mammalian retina have used mice lacking both *Cry1* and *Cry2* (*Cry1*$^{-/-}$*Cry2*$^{-/-}$ mice). The individual contributions of *Cry1* and *Cry2* to mammalian retinal physiology have not previously been explored in detail. A recent study has shown that whilst both mammalian CRYs are transcriptional repressors, in the SCN, CRY1 is significantly more potent (Anand *et al*., 2013). This accounts for the different intrinsic circadian period (taus) of *Cry1*$^{-/-}$ and *Cry2*$^{-/-}$ mice when their locomotor activity is measured under constant darkness (van der Horst *et al*., 1999). Indeed, there is growing evidence that CRY1 and CRY2 may have different functions from one another in other aspects of physiology, such as protection against DNA damage (Papp *et al*., 2015). As such, in this Chapter, *Cry1*$^{-/-}$ and *Cry2*$^{-/-}$ mice are used in order to study the individual contributions of *Cry1* and *Cry2* to retinal circadian rhythms.

Assays of retinal circadian rhythmicity have been discussed in detail (see Section 1.4.7). Of interest are three particular *in vivo* assays of retinal physiology which have previously been

shown to be under circadian control or vary with diurnal rhythmicity - the photopic ERG b-wave, contrast sensitivity and the pupillary light response (PLR).

3.1.3 Photopic electroretinogram b-wave amplitude

In addition to bioluminescent reporter gene assays, rhythms in retinal physiology also provide critical functional measures of retinal clock output. In particular, the photopic (light-adapted) electroretinogram (ERG) b-wave amplitude is a reliable output of the retinal clock (Cameron *et al*., 2008a, Cameron *et al*., 2008b, Barnard *et al*., 2006, Storch *et al*., 2007, Jackson *et al*., 2012). Wildtype mice exhibit circadian changes in cone-based ERG b-wave amplitude. Circadian rhythmicity of the ERG b-wave amplitude has been shown to be dependent on *Bmal1* (Storch *et al*., 2007), the melatonin receptor MT1 (Sengupta *et al*., 2011), as well as loss of both CRY1 and CRY2 (Cameron *et al*., 2008a).

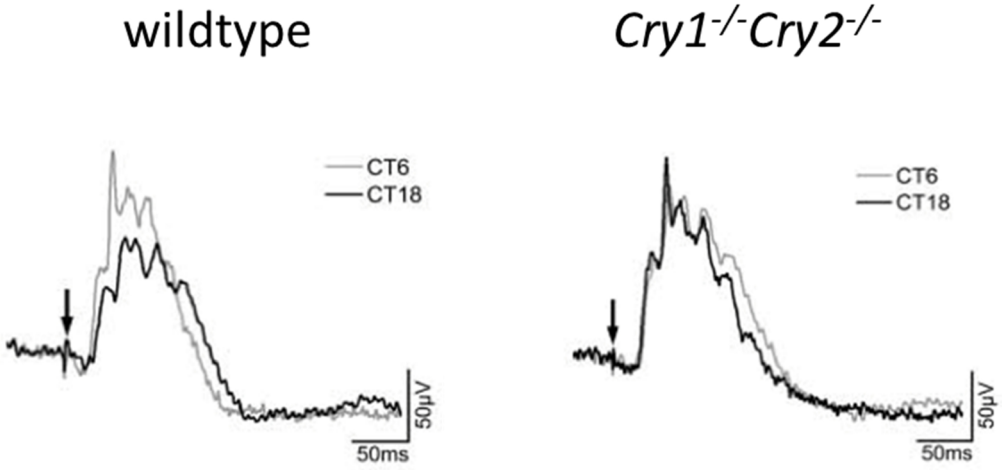

Figure 3.1. Wildtype mice exhibit a circadian rhythm in photopic ERG b-wave amplitude, where this amplitude is greater at CT6 and smaller at CT18. Mice lacking both Cryptochromes (*Cry1*$^{-/-}$*Cry2*$^{-/-}$ mice) lose this circadian rhythm and instead demonstrate a day-like greater amplitude at both CT6 and CT18. Reproduced from Cameron *et al*. (2008a).

3.1.4 Contrast sensitivity

A recent study has determined that a circadian rhythm in visual contrast sensitivity exists, which is regulated by the retinal clock (Hwang *et al*., 2013). The mechanism for this circadian phenomenon is through an interaction between dopamine D4 receptors, the clock gene *Npas2* and adenylate cyclase 1. Indeed, as NPAS2 is localized to the retinal ganglion cell layer only, it appears that loss of the inner retinal clock alone is capable of abolishing rhythms in contrast sensitivity. As such, the circadian rhythm of contrast sensitivity appears to be primarily dependent on a circadian clock in the inner retina. By contrast, circadian rhythms do not occur in visual acuity, suggesting that visual acuity and contrast sensitivity are independently regulated. The regulation of the circadian rhythm of contrast sensitivity by other clock genes remains unknown, though *Opn4*$^{-/-}$ mice were found to show attenuated contrast sensitivity responses (Schmidt *et al*., 2014).

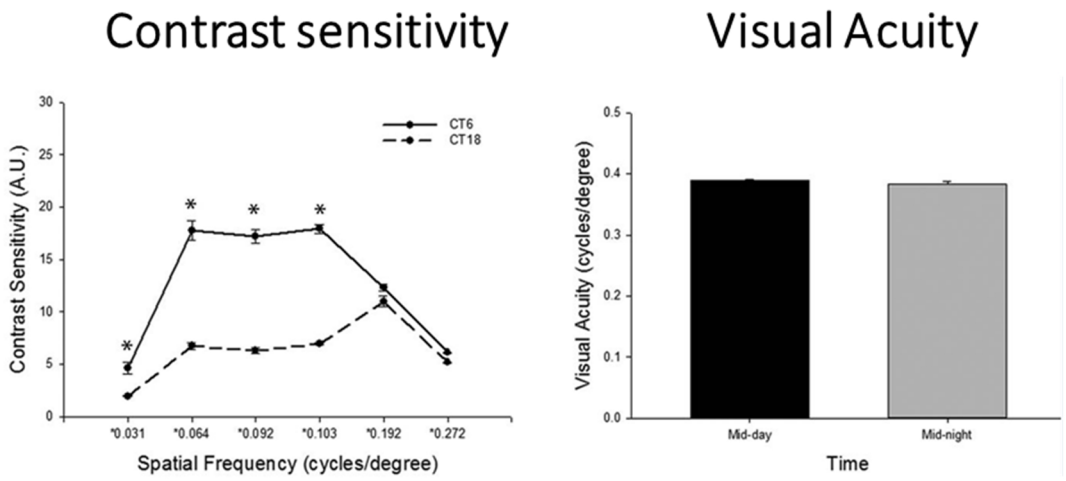

Figure 3.2. Wildtype mice demonstrate a circadian rhythm in contrast sensitivity, but not visual acuity. **(A)** Contrast sensitivity is higher at CT6 compared to CT18 across most spatial frequencies tested. **(B)** Visual acuity did not differ at CT6 compared to CT18. Reproduced from Hwang *et al*. (2013).

3.1.5 Pupillary Light Reponse

Whilst the pupillary light response (PLR) has played a key role in the characterisation of non-image forming retinal responses to light (Guler *et al*., 2008, Lucas *et al*., 2003, Semo *et al*., 2003b, Hattar *et al*., 2003, Jagannath *et al*., 2015), it is unclear if this response is regulated by the retinal clock. A diurnal rhythm of the PLR was reported in *rd/rd* mice (Owens *et al*., 2012). As such, PLR could provide an additional assay of circadian retinal physiology, though further testing is necessary to determine whether the PLR exhibits a circadian rhythm (this testing is conducted in Section 3.4.3). If so, further work would be necessary to determine if circadian rhythms in the PLR are the product solely of retinal clocks, or a combination of retinal clocks and the circadian regulation of the central pathways involved, or even circadian regulation of autonomic tone.

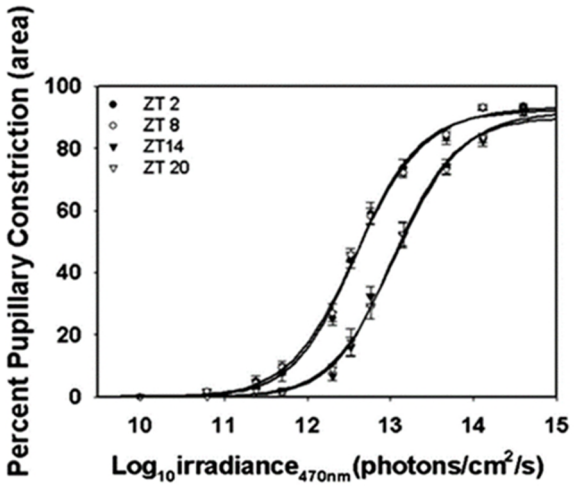

Figure 3.3. Diurnal rhythm of pupillary light response in *rd/rd* mice (which lack rods and cones). Irradiance response of pupillary light response at four times of day (ZT2, ZT8, ZT14 and ZT20). Reproduced from Owens *et al*. (2012).

3.2 Aims

Given the critical role of CRYs in central circadian rhythm generation, it is possible that CRY1 and CRY2 play different roles in retinal circadian rhythms. The aims of this chapter were to characterize retinal responses to light that exhibit circadian rhythms in wildtype mice, as demonstrated in previous studies. To do this, three independent assays of retinal physiology that have previously been shown to be under circadian control were employed - the photopic ERG b-wave, contrast sensitivity and the pupillary light response. The effects of loss of CRY1 or CRY2 on retinal circadian rhythms were then investigated. *Cry1*$^{-/-}$ and *Cry2*$^{-/-}$ single-knockout mice were used as these mice maintain central circadian rhythmicity.

In Chapter 3, the specific aims are:

- To characterise circadian rhythms of the photopic ERG b-wave, contrast sensitivity and the pupillary light response in wildtype mice
- To determine the role of CRY1 and CRY2 in circadian rhythms of the photopic ERG b-wave, contrast sensitivity and the pupillary light response

3.3 Methods

3.3.1 Animals

Methods for transgenic breeding and genotyping were conducted as described previously (Chapter 2.3).

3.3.2 Genotyping

See Chapter 2.3 for full details.

3.3.3 *In vivo* Circadian Retinal Physiology Testing

Circadian physiology testing occurred after one day in constant darkness at CT6 ± 1 hour (subjective mid-day) and CT18 ± 1 hour (subjective mid-night). Furthermore, diurnal physiology recordings were made at midday (ZT6 ± 1 hour) and midnight (ZT18 ± 1 hour) hours in the LD cycle. Unless otherwise stated, each mouse underwent all four testing times (ZT6, ZT18, CT6, CT18) in a randomized order. Finally, to reduce light adaptation effects on dark-adapted mice, each testing period for every mouse was restricted to below 25 minutes from first exposure to light.

3.3.4 Electroretinogram

Prior to electroretinography, general anaesthesia was induced in mice by a single intraperitoneal injection of medetomidine hydrochloride (Dormitor, 1 mg/kg body weight; Pfizer) and ketamine (Ketaset, 60 mg/kg body weight; Fort Dodge), and pupils were fully dilated with 1% tropicamide and 2.5% phenylephrine hydrochloride eye drops (Bausch & Lomb). Electroretinography recordings were made as described previously (Espion E2;

Diagnosys LLC) (Lipinski *et al*., 2011). After dark adaptation overnight, photopic responses were recorded (except for the case of ZT6 recordings, which were undertaken at ZT6 after 1-2 hours of dark adaptation). White flash stimuli (4ms) were superimposed on a light-adapting 30 cd/m^2 white background with 20 responses averaged using an ISI of 1 second. Averaged flash stimuli recordings were taken every 2.5 minutes ± 1 minute from the first exposure to the white background (0s) for 25 minutes in total. In a single case (*Cry1*$^{-/-}$ mouse ERG recorded at CT18 after 17.5 min light adaptation), one data point was unobtainable due to technical problems and so linear interpolation was used to estimate the missing single point. The b--wave amplitudes were quantified with specialized software (Espion; Diagnosys LLC). At the end of the procedure, general anaesthesia was reversed by intraperitoneal injection of atipamezole hydrochloride (Antisedan, 5 mg/kg body weight; Pfizer).

3.3.5 Optomotor Responses

Optokinetic head tracking (an optomotor response test) was used to measure contrast sensitivity and visual acuity using the OptoMotry system (CerebralMechanics) as described previously (Hwang *et al*., 2013). The test arena inside the OptoMotry system composed of a sine wave grating projected by four interfacing LCD monitors rotating in one direction. The direction of rotation was randomized for each mouse. Mice were placed on a raised platform inside the OptoMotry system and head tracking responses were recorded. Visual Acuity was recorded first using a staircase method for a black-and-white sinusoidal grating at 100% contrast to determine spatial frequency threshold for visual acuity. Visual acuity was recorded as the spatial frequency where head tracking stopped. For contrast sensitivity testing, a black-and-white sinusoidal grating at 100% contrast was reduced until

head tracking stopped at the contrast threshold. Six standard spatial frequencies (0.031, 0.064, 0.092, 0.103, 0.192, and 0.272 cycles/degree) were tested. Contrast sensitivity was taken as the reciprocal of the contrast threshold. For instance, a mouse that responded at 8% contrast but no lower would have a contrast sensitivity score of 12.5, whereas a mouse that responded at 4% contrast but no lower would score 25. All measurements were made under photopic conditions. At 100% contrast, 0.3 cycle/degree, 12 deg/s, light intensity as measured at the platform was 50 lux, 50% contrast was 40 lux, 10% contrast was 32 lux. The order of spatial frequency tested was randomized for each mouse.

3.3.6 Pupillometry

Pupil light response recordings were performed as described previously (Hughes *et al*., 2012, Jagannath *et al*., 2015). For recordings under diurnal conditions, mice were dark-adapted for 1–2 h prior to testing. A xenon arc lamp (150 W solar simulator, Lot Oriel, UK) with a 480 nm monochromatic filter (Andover, 10 nm half-bandwidth) was used to produce a light intensity of 14.6 log quanta/cm^2/s (173 μW/cm^2/s). Irradiance measurements were made using a radiometrically calibrated spectrophotometer (Ocean Optics, UK). Light stimuli (10 s) were transmitted to the eye via a liquid light guide as an irradiant light stimulus using a 2” integrating sphere (Pro-lite Technology, UK) and was controlled by a shutter positioned in the light path (LSZ160 shutter, Lot Oriel UK; custom software supplied by BRSL, Newbury, UK). Images of consensual pupil responses were collected with a Prosilica NIR sensitive CCD video camera (BRSL, Newbury, UK) at a rate of 10 frames per second, under infrared LED illumination (850 nm, 10 nm half-bandwidth). During pupil measurements unanaesthetised animals were temporarily restrained using normal husbandry techniques for the duration of the recording (29 s, including baseline,

stimulation and recovery phases). Each animal received handling and pupil light responses were recorded at least twice several days prior to the test in order to minimise any artefacts due to handling and procedure-related stress. Data reported was recording in one trial with all animals on test day. All images were analysed using ImageJ software (NIH; rsbweb.nih.gov/ij/) as previously shown (Hughes *et al*., 2015c).

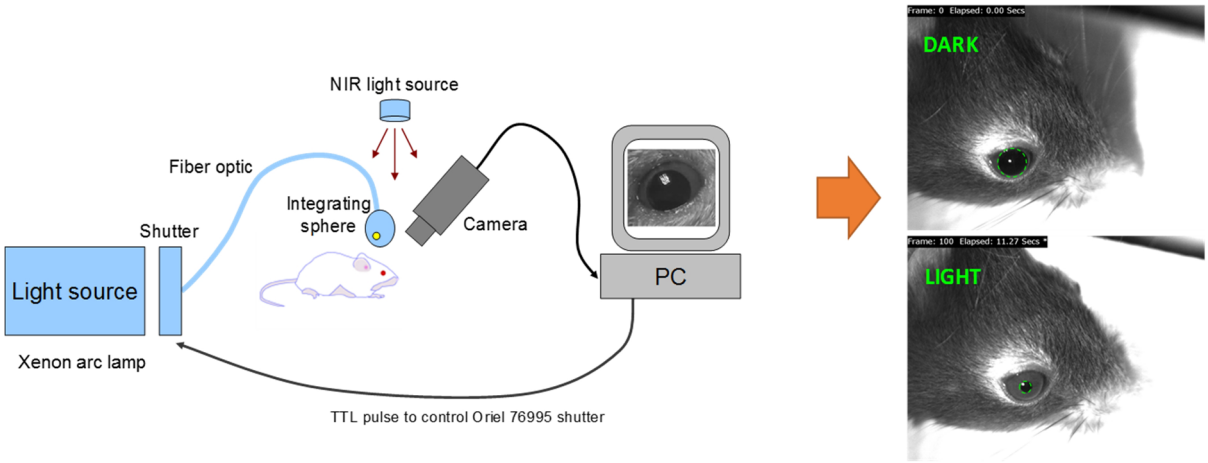

Figure 3.4. Schematic depicting equipment setup for pupillometry (left). Recorded images are then analysed using ImageJ (right). As shown, under dark conditions, wildtype mice exhibit dilated pupils (upper right), whereas under light conditions, pupils are constricted (lower right). Used with permission from Dr. Carina Pothecary (Oxford, unpublished).

3.3.7 Statistical Analysis

All data are shown with +/- SEM (standard error of the mean). Statistical analysis was performed in GraphPad Prism (version 5) using paired two-way ANOVA analysis or two-tailed Student's t-test as reported in the legend.

3.4 Results

3.4.1 Circadian rhythm in photopic ERG b-wave amplitude is abolished in *Cry1*$^{-/-}$ mice and attenuated in *Cry2*$^{-/-}$ mice

Photopic light-adapted electroretinography was performed at CT6 and CT18 as in previous studies (Barnard *et al*., 2006, Cameron *et al*., 2008a, Jackson *et al*., 2014, Storch *et al*., 2007). ERG b-wave responses were recorded over 25 minutes of light adaptation time and data were analysed by 2-way ANOVA (light adaptation and circadian time). As expected, wildtype mice (n=5) show a significant main effect of light adaptation time ($F_{(10, 44)}$ = 39.02, p < 0.0001), which peaked around 10 minutes (**Figure 3.5 A**). In addition, there was a significant effect of circadian time ($F_{(1, 44)}$ = 28.77, p < 0.0001), and a significant interaction between circadian time x light adaptation time ($F_{(10, 44)}$ = 5.006, p < 0.0001). Post-hoc Bonferroni tests showed that wildtype mice have significantly higher b-wave amplitudes during the subjective day (CT6) across the range of 5-12.5 minutes of dark adaptation. In *Cry1*$^{-/-}$ mice (n=7) significant differences of light adaptation time were still apparent ($F_{(9, 60)}$ = 22.51, p < 0.0001), peaking around 10 minutes as in wildtype animals (**Figure 3.5 B**). However, there was no significant effect of circadian time ($F_{(1, 60)}$ = 3.1, p = 0.0834), and no significant interaction between circadian time x light adaptation time ($F_{(9, 60)}$ = 1.128, p = 0.3576). Post-hoc Bonferroni tests showed no differences between circadian time at any duration of light adaptation. *Cry2*$^{-/-}$ mice (n=7) show a significant effect of light adaptation time ($F_{(9, 60)}$ = 19.79, p < 0.0001), again peaking around 10 minutes (**Figure 3.5 C**). However, in this genotype there was a significant effect of circadian time ($F_{(1, 60)}$ = 9.044, p = 0.0038) but no significant interaction between circadian time x light adaptation time ($F_{(9,60)}$ =

0.1674, p = 0.9966). However, post-hoc Bonferroni tests showed no differences between circadian times at any duration of light adaptation. As such, whilst a significant effect of circadian time was apparent, this circadian rhythm appears to be attenuated in comparison to wildtype animals.

A 10 min light adaptation protocol is most commonly used to study retinal rhythms as this provides the maximal photopic b-wave amplitude (Barnard *et al*., 2006, Storch *et al*., 2007). When summarised in this manner, differences between the genotypes are immediately apparent, with both *Cry1*- and *Cry2*-deficient mice showing attenuated circadian rhythms (**Figure 3.5 D**). Finally, rhythms in ERG b-wave amplitude were also tested in all three genotypes under entrained conditions, comparing ZT6 and ZT18. Results were found to be comparable to those obtained under constant conditions (**Figure 3.6**).

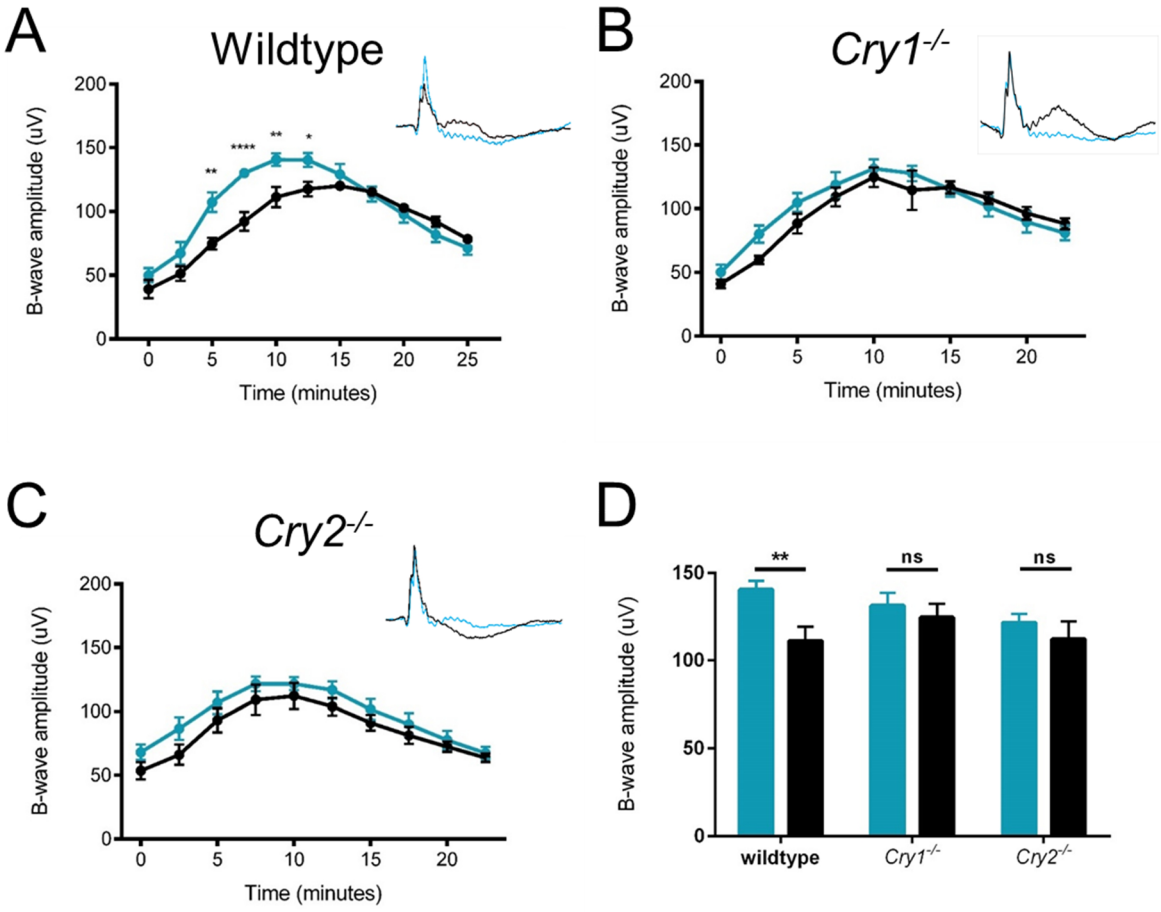

Figure 3.5. Photopic light-adapted electroretinogram b-wave amplitudes are controlled in a circadian manner and are dependent on both *Cry1* and *Cry2* expression. Data are represented as means ± SEM. **(A)** Wildtype mice (n=5) exhibit a significantly larger photopic electroretinogram b-wave amplitude at CT6 (blue) compared to CT18 (black). Retinal responses in mice were recorded over 25 minutes of light adaptation time. Representative traces (taken at 10 minutes of light adaptation) are shown inset. Post-hoc Bonferroni's multiple comparisons test show that wildtype mice have significantly higher b-wave amplitudes during the subjective day (CT6) across the range of 5-12.5 minutes of dark adaptation. **(B)** *Cry1*$^{-/-}$ mice (n=7) display no rhythm in photopic ERG b-wave amplitude. Post-hoc Bonferroni's multiple comparisons test between all circadian time and light adaptation times were not significant. **(C)** *Cry2*$^{-/-}$ mice (n=7) demonstrate a significant, but attenuated, difference in photopic ERG b-wave amplitudes at CT6 compared to CT18. A main effect of circadian time was found (see Results). However, post-hoc Bonferroni's multiple comparisons test between all circadian time and light adaptation times were not significant. **(D)** Summary of wildtype, *Cry1*$^{-/-}$ and *Cry2*$^{-/-}$ data based on 10 minutes of light adaptation are shown. Wildtype mice demonstrate a rhythm in photopic ERG b-wave amplitude between CT6 and CT18 at 10 minutes of light adaptation, whilst *Cry1*$^{-/-}$ mice and *Cry2*$^{-/-}$ mice do not. *indicates $p<0.05$, **indicates $p<0.01$, ***indicates $p<0.001$, and ****indicates $p<0.0001$.

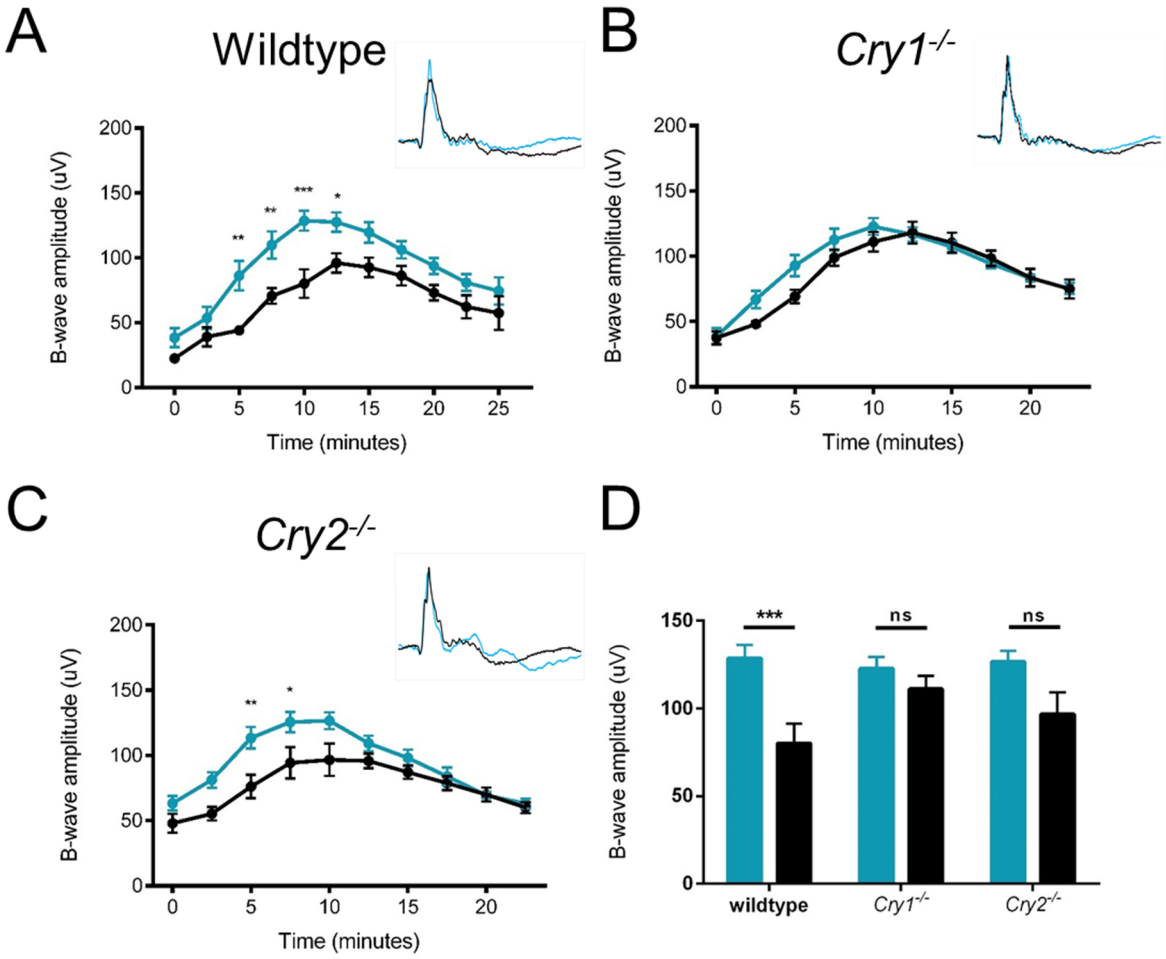

Figure 3.6. Photopic light-adapted electroretinogram b-wave amplitudes are controlled in a diurnal manner and are dependent on both *Cry1* and *Cry2* expression. Data are represented as means ± SEM. **(A)** Wildtype mice (n=5) exhibit a significantly larger photopic electroretinogram b-wave amplitude at ZT6 (blue) compared to ZT18 (black). Retinal responses in mice were recorded over 25 minutes of light adaptation time. Representative traces (taken at 10 minutes of light adaptation) are shown inset. Post-hoc Bonferroni's multiple comparisons test show that wildtype mice have significantly higher b-wave amplitudes during the day (ZT6) across the range of 5-12.5 minutes of dark adaptation. **(B)** *Cry1*$^{-/-}$ mice (n=7) display no rhythm in photopic ERG b-wave amplitude. Post-hoc Bonferroni's multiple comparisons test between all *zeitgeber* time and light adaptation times were not significant. **(C)** *Cry2*$^{-/-}$ mice (n=7) demonstrate a significant difference in photopic ERG b-wave amplitudes at ZT6 compared to ZT18. Post-hoc Bonferroni's multiple comparisons test show that *Cry2*$^{-/-}$ mice have significantly higher b-wave amplitudes at light adaptation times of 5 and 7.5 minutes of duration. **(D)** Summary of wildtype, *Cry1*$^{-/-}$ and *Cry2*$^{-/-}$ data based on 10 minutes of light adaptation are shown. Wildtype and *Cry2*$^{-/-}$ mice demonstrate a rhythm in photopic ERG b-wave amplitude between ZT6 and ZT18 at 10 minutes of light adaptation, whilst *Cry1*$^{-/-}$ mice do not. *indicates $p<0.05$, **indicates $p<0.01$, ***indicates $p<0.001$, and ****indicates $p<0.0001$.

3.4.2 Circadian rhythms in contrast sensitivity are affected in *Cry1*$^{-/-}$ but not *Cry2*$^{-/-}$ mice

We then tested the contrast sensitivity of mice at CT6 and CT18 (Prusky *et al*., 2004), where circadian differences are known to exist (Hwang *et al*., 2013). Contrast sensitivity was measured over a range of spatial frequencies ranging from 0.031 – 0.272 cycles per degree and data were analysed by 2-way ANOVA for spatial frequency and circadian time. As expected, in wildtype mice (n=7) there was a significant effect of spatial frequency ($F_{(5, 54)}$ = 39.03, p < 0.0001, **Figure 3.7 A**), with a peak around 0.064-0.092 cycles/degree in agreement with published data (Prusky *et al*., 2004). In addition, a significant effect of circadian time was apparent ($F_{(1, 54)}$ = 150.5, p < 0.0001), with higher contrast sensitivity during the subjective day (CT6). A significant interaction occurred between circadian time x spatial frequency ($F_{(5, 54)}$ = 5.441, p = 0.0004). Post-hoc Bonferroni tests show that wildtype mice have significantly higher contrast sensitivities at CT6 at spatial frequencies between 0.064 - 0.192 cycles/degree. In *Cry1*$^{-/-}$ mice (n=10) the main effect of spatial frequency was still found to be significant ($F_{(5, 36)}$ = 14.09, p < 0.0001, **Figure 3.7 B**), with a peak around 0.092 cycles/degree, but with a second peak at high spatial frequencies (0.272 cycles/degree). Whilst there was a significant effect of circadian time ($F_{(1, 36)}$ = 27.17, p < 0.0001), in comparison to wildtype animals, contrast sensitivity in *Cry1*$^{-/-}$ mice was higher during the subjective night (CT18). There was also a significant interaction between circadian time x spatial frequency ($F_{(5, 36)}$ = 5.002, p = 0.0014). Post-hoc Bonferroni tests show that *Cry1*$^{-/-}$ mice only show a significant difference in contrast sensitivity at a spatial frequency of 0.272, but not at any other spatial frequencies tested. As such, the main effect

of circadian time appears to be due to the significant difference at 0.272 cycles/degree (high acuity).

Cry2$^{-/-}$ mice (n=10) again show a significant effect of spatial frequency ($F_{(5, 36)}$ = 26.87, p < 0.0001), peaking at 0.064 cycles/degree (**Figure 3.7 C**). There was also a significant effect of circadian time ($F_{(1, 36)}$ = 91.16, p < 0.0001), with higher contrast sensitivity during the subjective day (CT6), comparable with wildtype animals. There was a significant interaction between circadian time x spatial frequency ($F_{(5, 36)}$ = 4.729, p = 0.002). Post-hoc Bonferroni tests show that *Cry2*$^{-/-}$ mice have significantly higher contrast sensitivities at spatial frequencies between 0.031 - 0.103 cycles/degree, comparable with wildtype animals.

When contrast sensitivity is compared at the peak of visual acuity, 0.064 cycles/degree as reported previously (Prusky *et al*., 2004), circadian rhythms are clearly apparent in wildtype and CRY2-deficient mice, but there is no significant circadian rhythm in CRY1-deficient animals (**Figure 3.7 D**). Rhythms in contrast sensitivity were also tested in all three genotypes under entrained conditions, comparing ZT6 and ZT18. Results were found to be comparable to those obtained under constant conditions (**Figure 3.8 A-D**).

Visual acuity in mice was found not show any circadian variation between wildtype mice and mice lacking CRY1 or CRY2 (**Figure 3.8 E-F**). Testing threshold spatial frequency, there was no significant effect of circadian time ($F_{(1, 42)}$ = 0.6298, p = 0.4319) or genotype ($F_{(2, 42)}$ = 1.267, p = 0.2923), and no interaction between circadian time x genotype ($F_{(2,42)}$ = 0.1198, p = 0.8874).

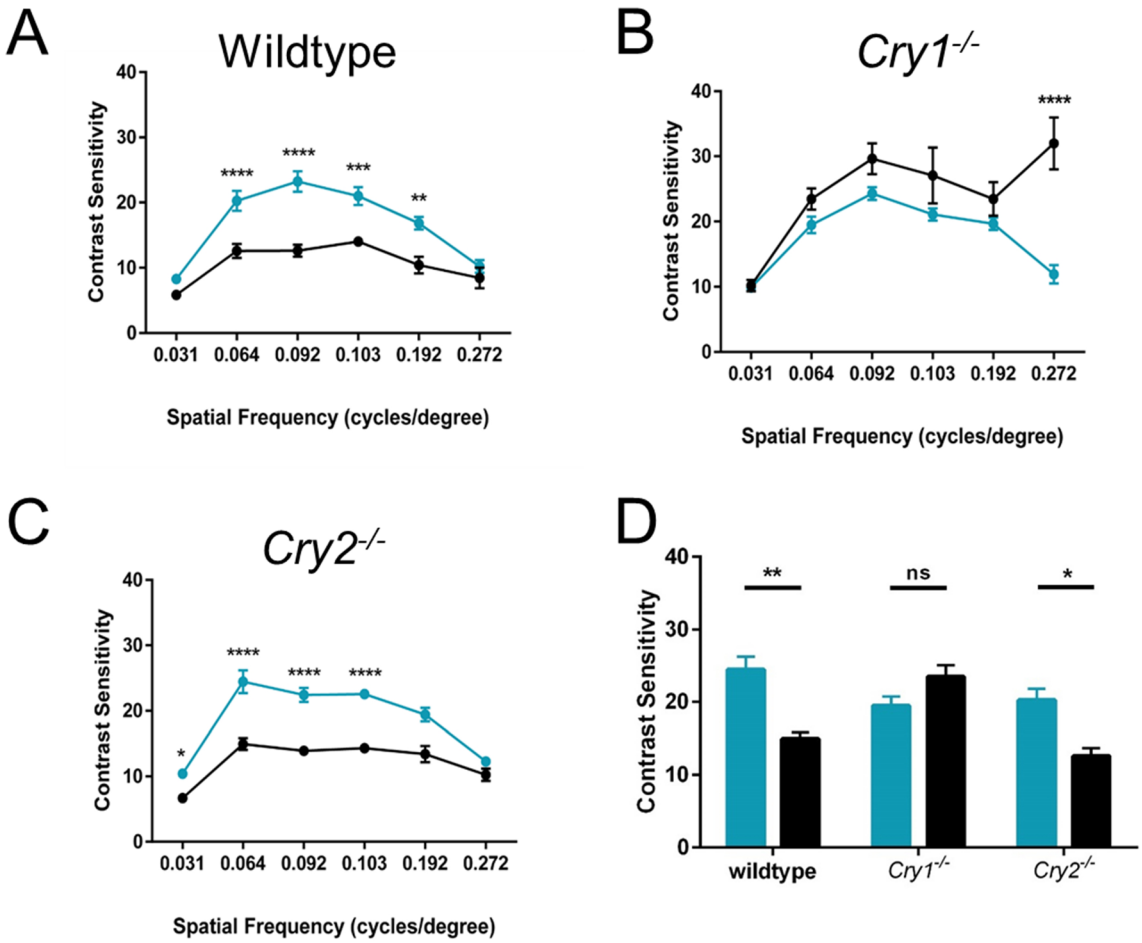

Figure 3.7. Circadian rhythm in contrast sensitivity is dependent on *Cry1*, but not *Cry2*. Data are represented as means ± SEM. **(A)** Wildtype mice (n=7) exhibit significantly higher contrast sensitivity at CT6 (blue) in contrast to CT18 (black), as measured using the optokinetic nystagmus response. Wildtype mice have significantly higher contrast sensitivities at spatial frequencies (cycles/degree) of 0.031, 0.064, 0.092, 0.103, and 0.192. **(B)** *Cry1*$^{-/-}$ mice (n=10) show no rhythms in contrast sensitivity at spatial frequencies that are rhythmic in wildtype mice. Interestingly, at the highest spatial frequency tested, *Cry1*$^{-/-}$ mice show significantly enhanced contrast sensitivity at CT18. *Cry1*$^{-/-}$ mice have significantly different contrast sensitivity at a spatial frequency of 0.272 but not at any other spatial frequencies tested. **(C)** *Cry2*$^{-/-}$ mice (n=10) show a circadian variation of contrast sensitivity similar to wildtype mice, suggesting *Cry2* does not play a necessary role for this response. *Cry2*$^{-/-}$ mice have significantly higher contrast sensitivities at spatial frequencies (cycles/degree) of 0.064, 0.092, 0.103, and 0.192. **(D)** Summary of contrast sensitivity of wildtype, *Cry1*$^{-/-}$ and *Cry2*$^{-/-}$ mice at a spatial frequency of 0.064 cycles/degree, corresponding to peak visual acuity. Wildtype and *Cry2*$^{-/-}$ mice demonstrate a rhythm in contrast sensitivity between CT6 and CT18 at 0.064 cycles/degree spatial frequency, whilst *Cry1*$^{-/-}$ mice do not. *indicates p<0.05, **indicates p<0.01, ***indicates p<0.001, and ****indicates p<0.0001.

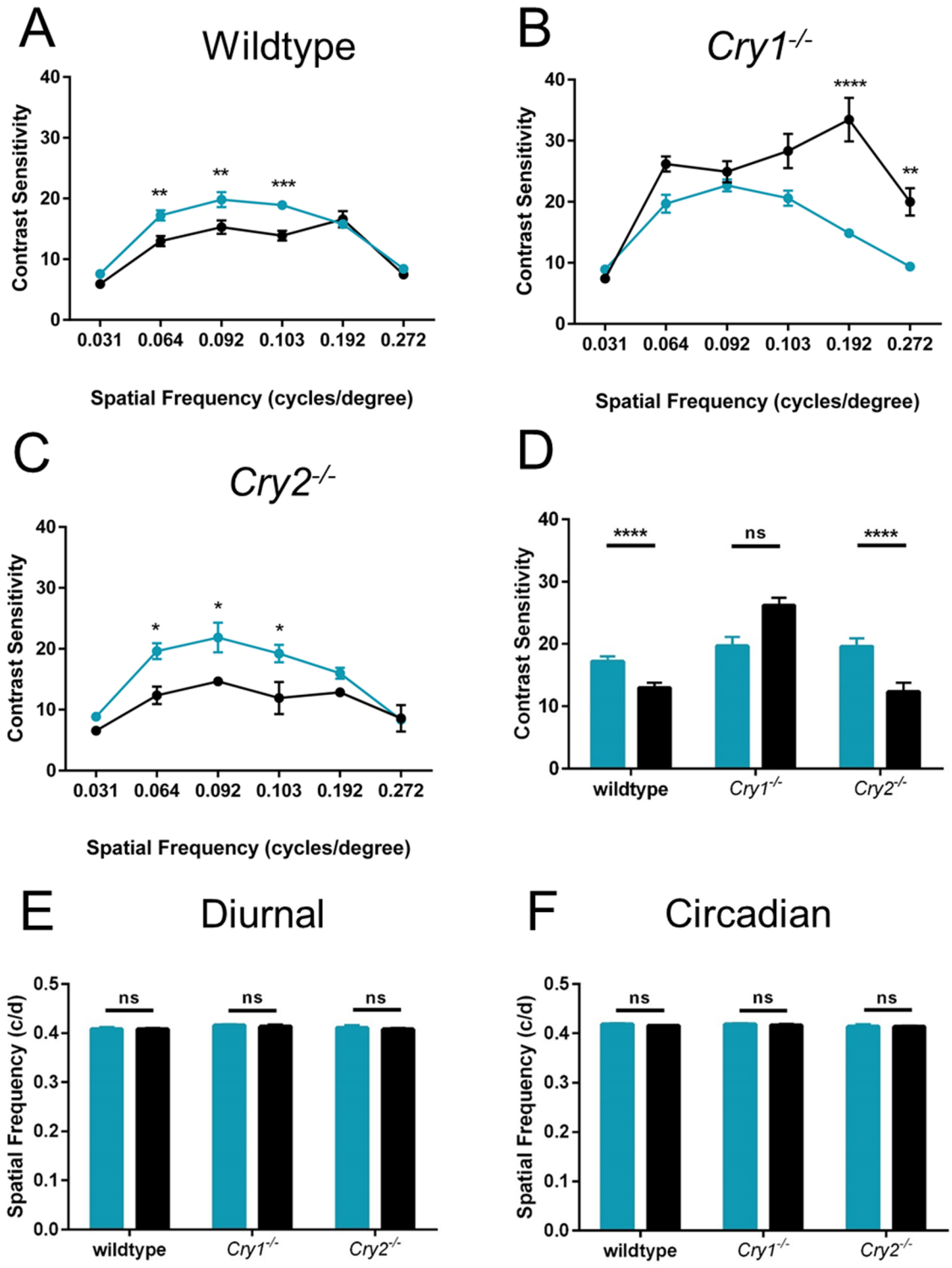
A
Wildtype
Contrast Sensitivity
40
30
20
10
0
**
**
***
0.031 0.064 0.092 0.103 0.192 0.272
Spatial Frequency (cycles/degree)
B
Cry1-/-
Contrast Sensitivity
****
**
0.031 0.064 0.092 0.103 0.192 0.272
Spatial Frequency (cycles/degree)
C
Cry2-/-
Contrast Sensitivity
*
*
*
0.031 0.064 0.092 0.103 0.192 0.272
Spatial Frequency (cycles/degree)
D
Contrast Sensitivity
****
ns
****
wildtype
Cry1-/-
Cry2-/-
E
Diurnal
Spatial Frequency (c/d)
0.5
0.4
0.3
0.2
0.1
0.0
ns
ns
ns
wildtype
Cry1-/-
Cry2-/-
F
Circadian
Spatial Frequency (c/d)
ns
ns
ns
wildtype
Cry1-/-
Cry2-/-

Figure 3.8.

Figure 3.8. Diurnal rhythm in contrast sensitivity is dependent on *Cry1*, but not *Cry2*. Data are represented as means ± SEM. **(A)** Wildtype mice (n=7) exhibit significantly higher contrast sensitivity at ZT6 (blue) in contrast to ZT18 (black), as measured using the optokinetic nystagmus response. Wildtype mice have significantly higher contrast sensitivities at spatial frequencies (cycles/degree) of 0.064, 0.092 and 0.103. **(B)** *Cry1*$^{-/-}$ mice (n=10) show no rhythms in contrast sensitivity at spatial frequencies that are rhythmic in wildtype mice. Interestingly, at the two highest spatial frequencies tested, *Cry1*$^{-/-}$ mice show significantly enhanced contrast sensitivity at ZT18. *Cry1*$^{-/-}$ mice have significantly different contrast sensitivity at spatial frequencies of 0.192 or 0.272 but not at any other spatial frequencies tested. **(C)** *Cry2*$^{-/-}$ mice (n=10) show a diurnal variation of contrast sensitivity similar to wildtype mice, suggesting *Cry2* does not play a necessary role for this response. *Cry2*$^{-/-}$ mice have significantly higher contrast sensitivities at the same spatial frequencies (cycles/degree) as wildtype mice, at 0.064, 0.092 and 0.103 cycles/degree. **(D)** Summary of contrast sensitivity of wildtype, *Cry1*$^{-/-}$ and *Cry2*$^{-/-}$ mice at a spatial frequency of 0.064 cycles/degree, corresponding to peak visual acuity. Wildtype and *Cry2*$^{-/-}$ mice demonstrate a rhythm in contrast sensitivity between ZT6 and ZT18 at 0.064 cycles/degree spatial frequency, whilst *Cry1*$^{-/-}$ mice do not. **(E)** Visual Acuity does not exhibit a diurnal variation. The main effect of circadian time is not significant $F_{(1, 42)} = 0.2965$, $p = 0.5890$. The main effect of genotype is not significant $F_{(2, 42)} = 1.933$, $p = 0.1573$. The interaction between circadian time x genotype is also not significant $F_{(2,42)} = 0.08302$, $p = 0.9205$. Post-hoc Sidak's multiple comparisons tests between all circadian time and genotype combinations were all not significant. **(F)** Visual Acuity does not exhibit a circadian variation. The main effect of circadian time is not significant $F_{(1, 42)} = 0.6298$, $p = 0.4319$. The main effect of genotype is not significant $F_{(2, 42)} = 1.267$, $p = 0.2923$. The interaction between circadian time x genotype is also not significant $F_{(2,42)} = 0.1198$, $p = 0.8874$. Post-hoc Sidak's multiple comparisons tests between all circadian time and genotype combinations were all not significant. *indicates p<0.05, **indicates p<0.01, ***indicates p<0.001, and ****indicates p<0.0001.

3.4.3 Circadian rhythms in the pupillary light response (PLR) are attenuated in *Cry1*$^{-/-}$ but not *Cry2*$^{-/-}$ mice

The pupillary light response (PLR) has played a key role in the characterisation of non-image forming responses to light (Guler *et al*., 2008, Hattar *et al*., 2003, Hughes *et al*., 2015c, Jagannath *et al*., 2015, Lucas *et al*., 2001, Semo *et al*., 2003b). However, the PLR has not previously been shown to be regulated by the retinal clock, though a diurnal rhythm in the PLR was reported in *rd/rd* mice (Owens *et al*., 2012). Here, it is shown that the PLR exhibits both circadian and diurnal rhythms in maximum pupillary constriction in wildtype mice (**Figure 3.9**). As such, the PLR may be a suitable assay for the circadian retinal clock. Bearing this in mind, this rhythm is examined in *Cry1*$^{-/-}$ and *Cry2*$^{-/-}$ mice (and *Opn4*$^{-/-}$ mice in Chapter 4).

Pupillometry was performed on wildtype mice (as shown in **Figure 3.9**) at ZT6 (n=9), ZT18 (n=8), CT6 (n=6) and CT18 (n=8). A between-groups comparison was used. Under entrained conditions, pupillary responses were significantly attenuated at ZT18 compared to ZT6 (unpaired t-test, $p<0.0001$). When circadian rhythms in maximum constriction were compared, pupillary responses were found to be significantly attenuated at CT18 compared to CT6 (unpaired t-test, $p=0.001$).

Given that the PLR demonstrates a circadian rhythm, the effect of individual Cry loss on this rhythm was then investigated. Circadian rhythms in the PLR in wildtype (n=5), *Cry1*$^{-/-}$ mice (n=7) and *Cry2*$^{-/-}$ (n=7) mice were compared (**Figure 3.10**). As previously observed above, pupillary responses were found to be significantly attenuated at CT18 in wildtype mice (paired t-test, $p=0.00022$). Whilst no significant circadian difference was

detected in *Cry1*$^{-/-}$ mice (t-test, p=0.058), *Cry2*$^{-/-}$ mice show significant circadian differences, comparable to wildtype mice (paired t-test, p=0.001).

When testing wildtype, *Cry1*$^{-/-}$ and *Cry2*$^{-/-}$ mice together, a counterbalanced design was used. Half of the mice (all genotypes) were tested at ZT6 first, and the other half at ZT18 first. CT6 and CT18 testing, respectively, then followed. Mice were then re-entrained to the opposite light-dark schedule in order to then test the other circadian time. Half of the cohort that underwent ZT6 and CT6 testing first then underwent ZT18 and CT18 testing. The other half underwent ZT6 and CT6 testing. This provided a counterbalanced approach and provided within-subject comparisons.

In summary, circadian rhythms in the PLR were detected in wildtype and *Cry2*-deficient mice, but were abolished in mice lacking *Cry1*. Rhythms in the PLR were also tested in all three genotypes under entrained conditions, comparing ZT6 and ZT18 (**Figure 3.11**). Results were found to be comparable to those obtained under constant conditions.

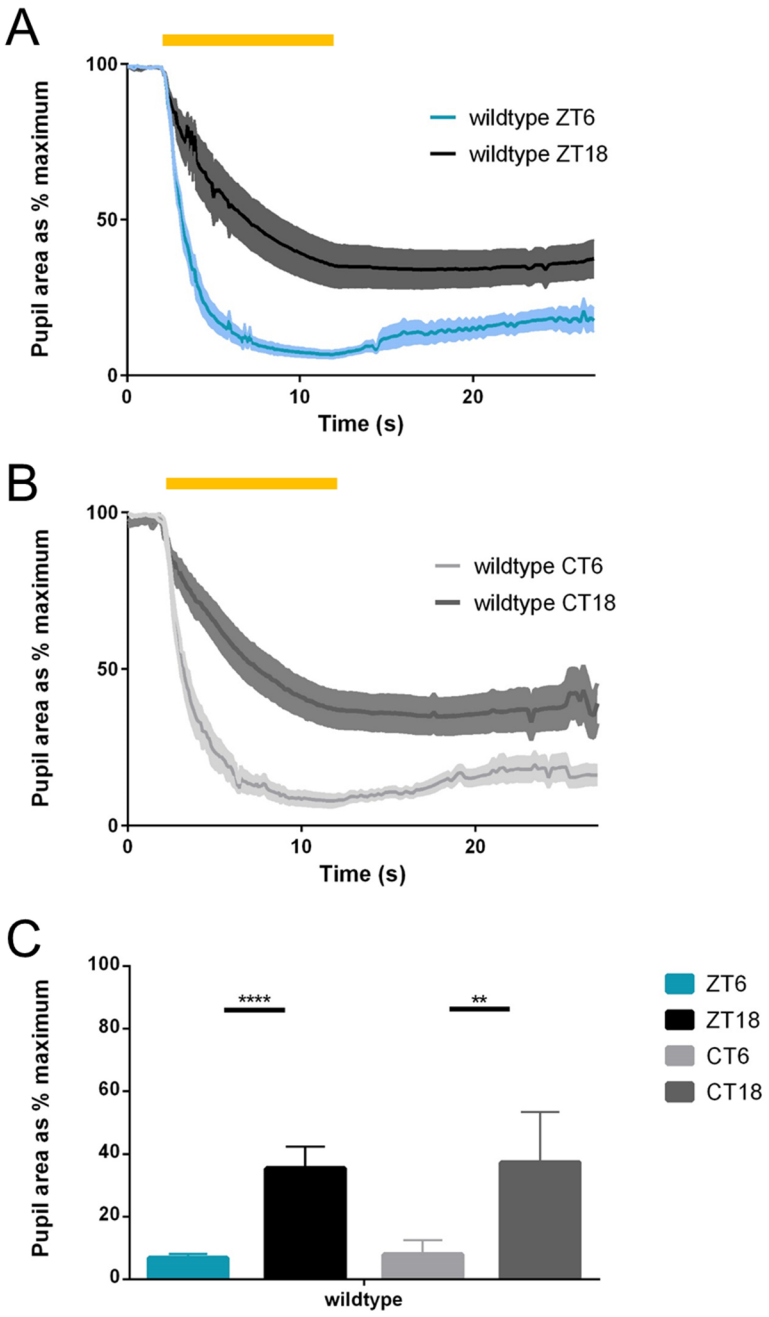

Figure 3.9. The pupillary light responses of wildtype mice exhibit both a diurnal rhythm and circadian rhythm. Data are represented as means (solid lines) ± SEM (shading). Averaged kinetics of PLR of wildtype mice at **(A)** ZT6 (blue, n=9) and ZT18 (black, n=8), or **(B)** CT6 (light grey, n=6) and CT18 (dark grey, n=8). The yellow bar indicates a bright light stimulus (480nm) switched on for 2s-12s of recording. All mice demonstrated attenuated PLR at ZT18 compared to ZT6. **(C)** Summary histogram for wildtype (n=16) mouse responses at ZT6 (blue), CT6 (light grey), ZT18 (black) and CT18 (dark grey). Data are represented as means ± SEM. Multiple t-tests were performed. The pupil area at the point of maximum constriction is significantly different between ZT6 and ZT18 (unpaired t-test, $p<0.0001$) and between CT6 and CT18 in wildtype mice (unpaired t-test, $p=0.001$). Please note that Dr. Carina Pothecary performed the experiments shown in this figure.

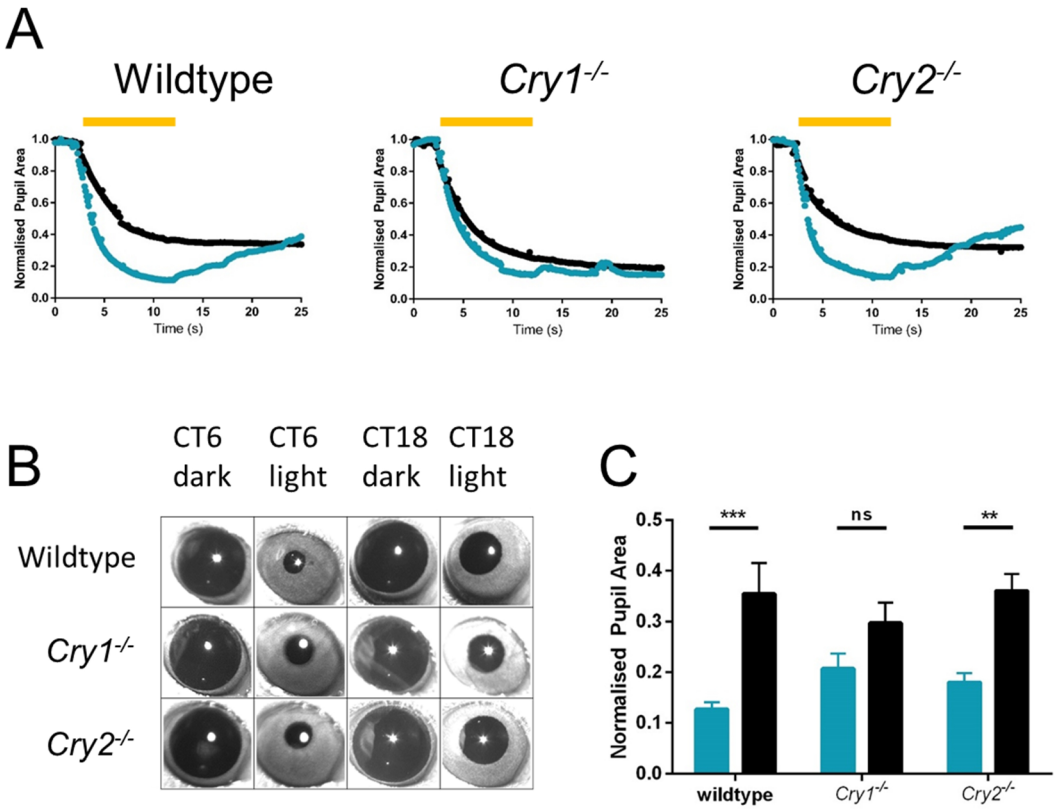

Figure 3.10. The pupillary light response is controlled in a circadian manner and is dependent on *Cry1*, but not *Cry2*. **(A)** Representative sample kinetics of PLR at CT6 (blue) and CT18 (black) for wildtype, *Cry1*$^{-/-}$, and *Cry2*$^{-/-}$ mice. The yellow bar indicates stimulus duration at 2s-12s of recording. Wildtype and *Cry2*$^{-/-}$ mice demonstrated attenuated PLR at CT18 compared to CT6. However, *Cry1*$^{-/-}$ mice have similar PLR at CT6 and CT18. **(B)** Set of pupil images demonstrating the maximum constriction of pupils at CT6 and CT18 for wildtype, *Cry1*$^{-/-}$, and *Cry2*$^{-/-}$ mice. **(C)** Summary histogram for wildtype (n=5), *Cry1*$^{-/-}$ (n=7) and *Cry2*$^{-/-}$ (n=7) mouse responses at CT6 (blue) and CT18 (black). Data are represented as means ± SEM. Maximum pupil constriction is significantly different between CT6 and CT18 in wildtype mice and *Cry2*$^{-/-}$ mice. Maximum constriction was not significantly different between CT6 and CT18 in *Cry1*$^{-/-}$ mice.

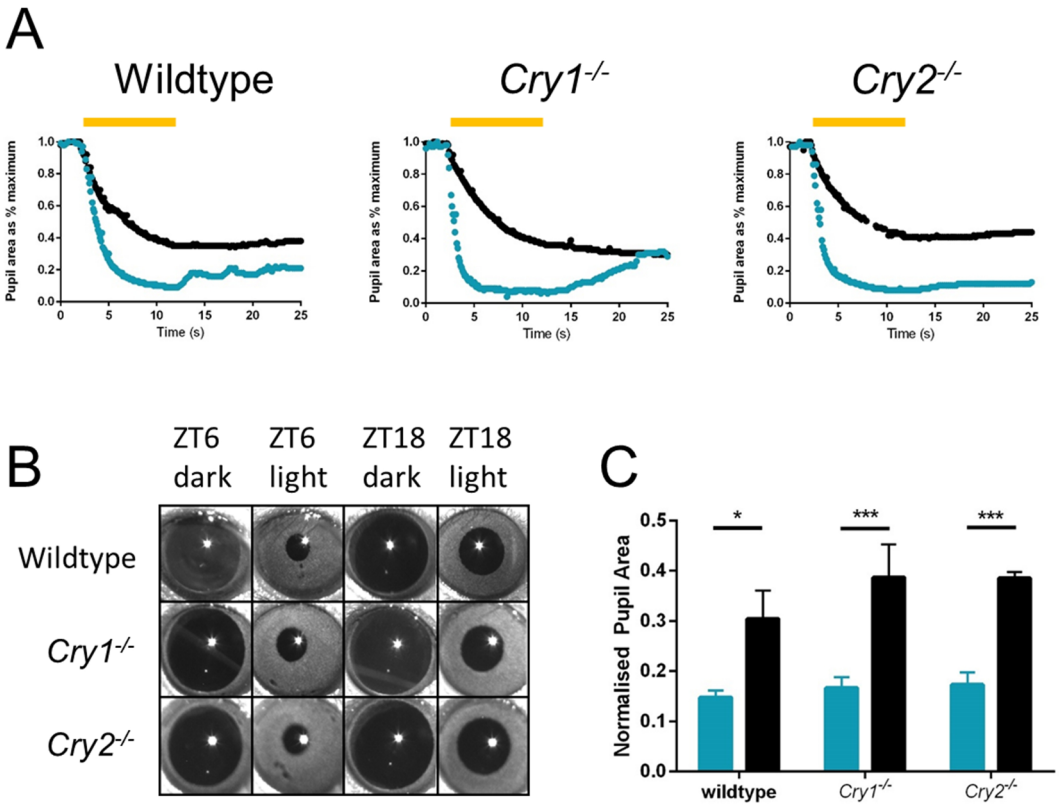

Figure 3.11. The pupillary light response exhibits a diurnal rhythm. **(A)** Representative sample kinetics of PLR at ZT6 (blue) and ZT18 (black) for wildtype, *Cry1*$^{-/-}$, and *Cry2*$^{-/-}$ mice. The yellow bar indicates stimulus duration at 2s-12s of recording. All mice demonstrated significantly attenuated PLR at ZT18 compared to ZT6. **(B)** Set of pupil pictures demonstrating that the maximum constriction of pupils at ZT6 and ZT18 for wildtype, *Cry1*$^{-/-}$, and *Cry2*$^{-/-}$ mice. **(C)** Summary histogram for wildtype (n=5), *Cry1*$^{-/-}$ (n=7) and *Cry2*$^{-/-}$ (n=7) mouse responses at ZT6 (blue) and ZT18 (black). Data are represented as means ± SEM. Maximum pupil constriction is significantly different between ZT6 and ZT18 in wildtype mice ($p = 0.017$), in *Cry1*$^{-/-}$ mice ($p = 0.00023$), and in *Cry2*$^{-/-}$ mice ($p = 0.00077$).

3.5 Discussion

3.5.1 Differential roles for mammalian cryptochromes in the retinal circadian clock

Our results indicate that not only is CRY1 widely expressed in the mammalian retina, but that it plays an essential role in the generation of functional retinal rhythms. Mice lacking CRY1 show abolition, loss, or attenuation of all aspects of retinal physiology studied - photopic ERG b-wave amplitude, contrast sensitivity and pupillary light responses. By contrast, CRY2 shows only a limited pattern of retinal expression in the photoreceptor layer (see Chapter 2), and loss of CRY2 only attenuates rhythms in ERG b-wave amplitude but has no effect on rhythms of contrast sensitivity or PLR. These findings suggest that CRY1 is the main CRY involved in retinal rhythms, whereas CRY2 may serve a redundant role. Based upon the localisation and function of CRY1 and CRY2, a model for mammalian retinal circadian rhythms is presented (**Figure 3.12**). Assuming that CRY1 and CRY2 retinal localization correlates with retinal clock function, the data presented suggest that both CRY1 and CRY2 play a role in the generation of outer retinal rhythms, reflected by rhythms in photopic ERG b-wave amplitude. By contrast, CRY1 - but not CRY2 – plays a key role in the inner retinal clock, reflected by rhythms in contrast sensitivity and pupillary constriction.

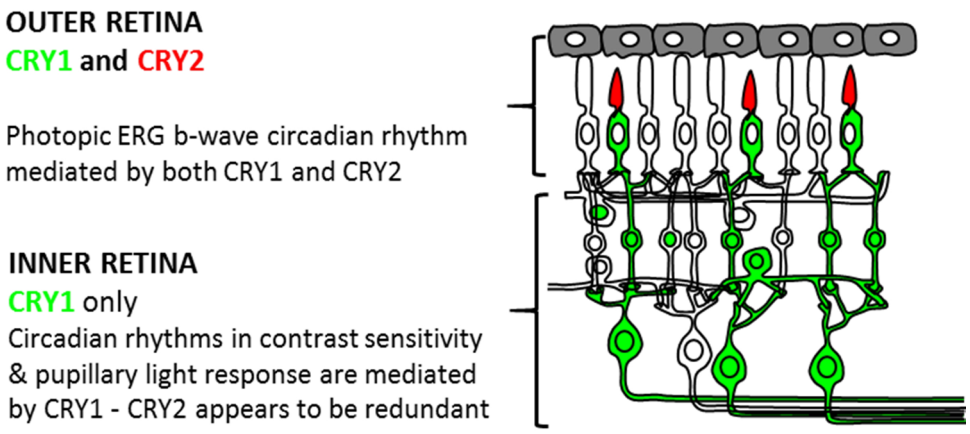

Figure 3.12. Model of mouse retinal clocks. Green cells indicate cells expressing CRY1 and red cells indicate cells expressing CRY2. CRY1 is expressed in all cones and a subset of cells in the inner nuclear layer and ganglion cell layer. CRY2 is only expressed in the outer retina. Wild-type mice demonstrate a circadian regulation of the pupillary response, contrast sensitivity, and photopic ERG b-wave response. *Cry1*$^{-/-}$ mice lack circadian rhythms in pupillary response and contrast sensitivity. Both *Cry1*$^{-/-}$ mice and *Cry2*$^{-/-}$ mice lack a circadian rhythm in photopic electroretinogram b-wave amplitude. *Cry1* and *Cry2* may play different roles in retinal rhythms, both *Cry1* and *Cry2* regulate the outer retinal clock whereas *Cry1* regulates the inner retinal clock.

It has previously been suggested that the mechanisms underlying circadian rhythm generation in the retina differs from that in the suprachiasmatic nuclei (SCN). Studies of retinal PER2::LUC rhythms have shown that the loss of *Per1*, *Cry1* or *Bmal1* is sufficient to induce arrhythmicity, whilst SCN rhythms are maintained in the absence of *Per1* or *Cry1*, albeit with a change in period (Ruan *et al*., 2012). The data presented in this chapter agree with the data of Ruan *et al*. (2012) in that retinal circadian rhythms were dependent on CRY1 but not CRY2, a result that is difficult to reconcile with previous data on CRY2 localisation in the mammalian retina. Together, these findings suggest that the retinal clock may be differentially regulated in comparison to the master clock in the SCN. This may be due to differences in how the retinal circadian clocks are synchronized as compared to the central SCN clock. Cell-cell communication involving vasoactive intestinal peptide (VIP) and

arginine vasopressin (AVP) play a critical role in the SCN neuronal network (Harmar *et al*., 2002, Hastings *et al*., 2014). By contrast, the more diffuse neuronal network of the retinal clock appears to depend upon dopamine and melatonin (McMahon *et al*., 2014), as well as coupling via gap junctions (Jaeger *et al*., 2015). Finally, it should be noted that rhythmic CRY1-expressing cones are unlikely to contribute to bioluminescent rhythms in whole retinal explants, as these cells only account for around 3% of retinal photoreceptors (Lyubarsky *et al*., 2004).

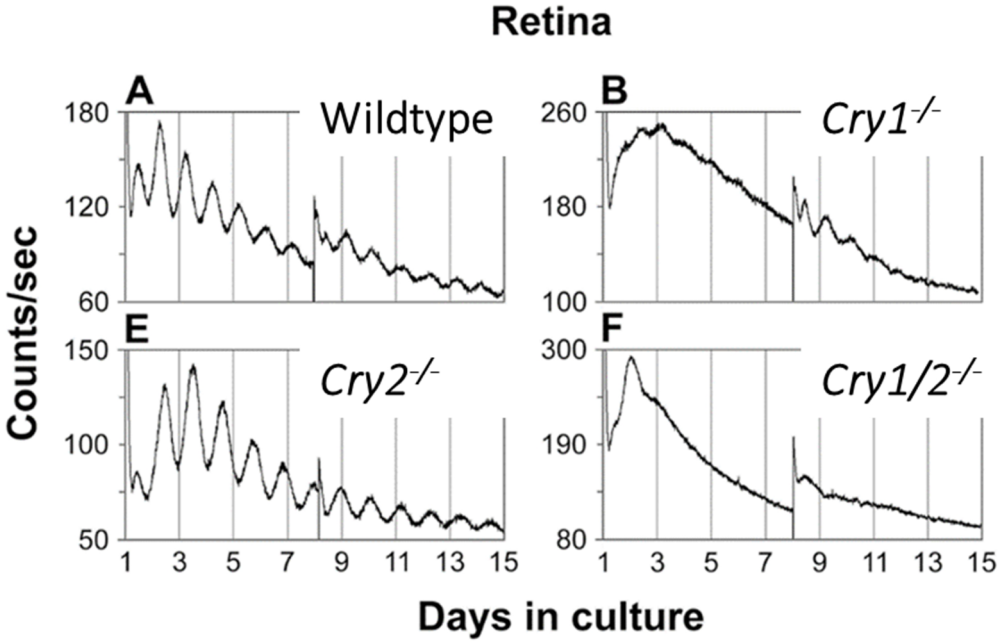

Figure 3.13. PER2::LUC rhythms in whole retinal explants are dependent on *Cry1* but not *Cry2*. Wildtype and *Cry2*$^{-/-}$ mice demonstrate consistent and robust circadian retinal PER2::LUC rhythms. However, *Cry1*$^{-/-}$ mice show severely attenuated retinal circadian rhythms, and loss of both *Cry1* and *Cry2* results in loss of retinal circadian rhythms altogether. Reproduced and modified from Ruan *et al*. (2012).

3.5.2 Loss of *Cry1* promotes the retinal daytime state

Data from rhythms in retinal physiology in *Cry1*$^{-/-}$ mice recorded in the subjective night (CT18) show comparable responses to those observed in the subjective day (CT6). Whilst loss of retinal rhythms may be expected to result in an averaging of day-time and night-time responses, *Cry1*$^{-/-}$ mice appear to display day-time responses at all phases. Similar findings have been reported in *Cry1*$^{-/-}$*Cry2*$^{-/-}$ mice (Cameron *et al*., 2008a) where these arrhythmic animals demonstrate daytime photopic electroretinogram b-wave responses at both ZT6 and ZT18. By contrast, retina-specific *Bmal1*$^{-/-}$ mice demonstrate night-like responses at ZT6 and ZT18 (Storch *et al*., 2007). This difference was attributed to the contrasting roles of *Bmal1* and *Cry1* in the transcriptional-translational feedback loop. As a transcriptional activator, BMAL1 regulates the positive limb of the TTFL, regulating clock genes and clock-controlled genes via its activity at E-box enhancers. Conversely, CRY1 forms part of the negative arm of the TTFL, inhibiting the positive drive of CLOCK and BMAL1. This antiphase activity of BMAL1 and CRY1 may account for the different phasing of retinal clocks in their absence. Further evidence comes from the contrast sensitivity data presented here, where *Cry1*$^{-/-}$ mice demonstrate a daytime response at both CT6 and CT18. NPAS2 is a homolog of CLOCK, the binding partner of BMAL1. Consistent with the differing retinal effects of positive and negative components of the TTFL, *Npas2*$^{-/-}$ mice demonstrate night-like contrast sensitivity responses at both CT6 and CT18, similar to retinal-specific *Bmal1*$^{-/-}$ mice.

It will be necessary, in future studies, to reconcile the fact that *Cry1* and *Cry2* mRNA have not yet been observed to demonstrate circadian oscillations. Of course, individual cells may demonstrate rhythmic Cryptochrome protein or gene expression over time, but this has

yet to be shown experimentally and technical limitations must be overcome. Furthermore, should *Cry* gene expression not be rhythmic, this does not preclude CRY protein expression from being rhythmic, as post-transcriptional processes may regulate circadian oscillations in protein levels whilst its gene is expressed at a constant level (Koike *et al*., 2012). Little is known about mRNA processing in different compartments of the retina, including whether *Cry2* is poorly transcribed or subject to post-transcriptional regulation, for example, by miRNAs. Alternatively, CRY2 protein may be rapidly targeted for degradation. Future transcriptomic and proteomic studies may be required to address these issues. Finally, should neither *Cry* mRNA or protein be expressed rhythmically normally, then the role of Cryptochromes in retinal rhythms may be different from that of central SCN rhythms. In this scenario, Cryptochromes may bind or act upon other rhythmic molecules that generate retinal rhythms – the availability of these binding partners may fluctuate throughout the day, thus precluding *Cry* from necessarily oscillating in retinal tissue.

3.5.3 *Cry1*$^{-/-}$ mice as a model for retinal clock deficiency

Our data also demonstrate that CRY1-deficient mice provide a valuable model to study the role of the retinal clock as, unlike *Cry1*$^{-/-}$*Cry2*$^{-/-}$ mice, these animals still possess a central circadian clock (albeit with a shorter circadian period). It should be emphasized that the different retinal phenotypes observed in clock gene knockouts may also relate to their role in the regulation of tissue-specific transcriptional profiles. As CLOCK and BMAL1 are transcription factors that drive the tissue-specific expression of numerous other target genes, loss of these critical factors may produce effects independent of their role in the circadian clock (Andrews *et al*., 2010, Hatanaka *et al*., 2010, Kondratov *et al*., 2006, Malik *et al*., 2015, Mukherjee *et al*., 2010). As such, whilst conditional targeting of retinal *Bmal1*

provides an ideal way of specifically ablating retinal rhythms (Storch *et al*., 2007), this may give rise to non-circadian changes in retinal function. Loss of CRY-mediated repression may cause fewer off-target non-circadian effects than loss of normal CLOCK/BMAL1 transcription. As such, CRY1-deficient mice may provide an alternative model in which to study the role of retinal circadian rhythms in which the positive limb of the circadian clock is preserved, but the circadian rhythm of transcriptional repression is lost.

We found a significant circadian difference in contrast sensitivity in *Cry1*$^{-/-}$ mice, with higher contrast sensitivity during the subjective night (CT18) at 0.272 cycles/degree. Not only is this response the reverse of what is seen in wildtype and *Cry2*$^{-/-}$ animals, but it occurs consistently under both entrained (ZT) and constant (CT) conditions, and only at the highest spatial frequencies (**Figure 3.7 B** and **Figure 3.8 B**). No previous studies of circadian retinal physiology have reported such changes (Cameron *et al*., 2008a, Hwang *et al*., 2013, Storch *et al*., 2007). This suggests that whilst circadian rhythms in contrast sensitivity are attenuated at most spatial frequencies, there may be some residual, although aberrant, circadian function in *Cry1*$^{-/-}$ mice. One potential explanation for this finding is that there may be a cellular subpopulation in which CRY2 is capable of partially substituting for the loss of CRY1. Given the high spatial frequencies involved and the limited overlap of CRY1 and CRY2 expression, this may reflect changes in cone function. Additional work may be required to determine the basis of this residual response.

3.5.4 Retinal versus central control of circadian rhythms in pupillary light response

Whilst the PLR has played a critical role in characterising the non-image forming responses to light, evidence for diurnal and circadian rhythms has only recently been described (Owens *et al*., 2012, Pothecary *et al*., In preparation). The PLR demonstrates clear circadian rhythms in sensitivity, with reduced responses during the subjective night. This circadian rhythm in sensitivity is attenuated in CRY1-deficient mice, but retained in CRY2-deficient animals. These data are again consistent with a principal role of CRY1 in retinal rhythms, although it should be noted that central pathways may also contribute. Future studies are needed to determine whether the PLR is regulated at the level of the retina or by either the SCN pacemaker or rhythms in the central neural pathways mediating this response. Indeed, whilst retinal rhythms may persist independently, it remains unknown as to whether these rhythms are influenced by the SCN pacemaker or other peripheral clocks. Further research is required to address these outstanding questions.

3.5.5 Differential roles for CRY1 and CRY2

CRY1 and CRY2 have frequently been assumed to play interchangeable roles within the TTFL. The results presented here indicate that at the level of the retina this appears to be oversimplification. In the retinal clock, CRY1 and CRY2 appear to be expressed in different cell types (as seen in Chapter 2), which is why they may mediate different roles in the retinal clock. This is consistent with emerging data where CRY1 and CRY2 appear to serve distinct, separable functions (Anand *et al*., 2013, Papp *et al*., 2015, Ruan *et al*., 2012). The crystal structure of mammalian CRY1 (Czarna *et al*., 2013) and CRY2 (Xing *et al*., 2013) have

recently been solved, showing structural differences in the C-terminal tail, consistent with known sequence differences in this region. Structurally, it may be the differences in C-terminal tail structure between CRY1 and CRY2 that is responsible for the differences in CRY1 and CRY2 function. Interestingly, *Cry1*-mutant mice have been generated in which a domain of the C-terminal tail structure has been deleted. These mice exhibit a shortened tau and are arrhythmic when bred with *Cry2*$^{-/-}$ mice. As they are phenotypically similar to *Cry1*$^{-/-}$ mice, this may indicate that the C-terminal tail of *Cry1* is essential for its role in the circadian clock (Prof. van der Horst, personal communication). Finally, whilst the differences between CRY1 and CRY2 that occur at the level of the retina appear to be dependent upon their differential expression pattern, further structure-function data may provide insight as to why CRY1 and CRY2 differ in their roles in circadian physiology.

3.5.6 The retinal clock as a rhythmic network

The retina is a complex and organized tissue, and the retinal clock appears no less complicated than the tissue in which it resides. Whilst liver tissue and cardiac tissue demonstrate synchronized high amplitude clock gene rhythms, it is clear that this is not the case when the entire retina is examined as a whole. Indeed, whilst some peripheral clock tissues, such as liver tissue, can be homogenized and hepatocytes treated as similar units, the retina is clearly made up of distinct cell populations whose network properties largely remain unknown. It is indeed possible, as has been previously proposed (Jaeger *et al*., 2015, Ruan *et al*., 2008, Dkhissi-Benyahya *et al*., 2013), that there are two autonomous retinal clocks, one within the outer retina (outer nuclear layer) and one within the inner retina (inner nuclear layer and ganglion cell layer). As it has been shown that all three nuclear layers of the retina are capable of independent and autonomous oscillations (Jaeger *et al*.,

2015), it is indeed possible that the retinal clock is composed of a network of independently oscillating cell layers that are normally coupled *in vivo*. The work presented in this chapter has added evidence that there are at least two independent oscillators in the retina regulating key aspects of retinal physiology. Furthermore, these oscillators may be differentially regulated (the inner retinal clock does not appear to be dependent on CRY2). It also remains possible that the rhythms observed were generated by two independent clocks that were synchronized such that individual oscillators could not be resolved.

If it is assumed that oscillations must occur at the level of cell networks, and that a cell may only be part of one retinal clock network, then long-term observation of clock gene and protein rhythms in single cells may be informative. Technical limitations currently make long term recording of single cell clock gene or protein rhythms difficult to obtain. PER2::LUC recordings have been critical in defining oscillations within the whole retina, or individual retinal layers (separated by laser microdissection). This data, however, allows a glimpse of the retinal clock only at a low resolution; the net effect of potentially several autonomous oscillations on the whole tissue can be observed, but the definition of individual networks remains unclear. The identities of specific cell networks that regulate and maintain retinal circadian rhythms, as well as if and how they interact, remain largely unknown. This is largely due to the low viability of PER2::LUC reporter mouse retinal slices (individual cell layers) such that it is very challenging to consistently record rhythms of non-intact retina using these methods (Prof Doug McMahon, personal communication). It is possible that certain cell subgroups are involved as a component in more than one retinal clock. Whilst the physiological assays used in this thesis cannot address these issues, they do provide information regarding whether *in vivo* physiological responses are affected by cryptochrome loss. Thus, it can be concluded that loss of *Cry1* is indeed sufficient to cause

an *in vivo* physiological effect on retinal circadian rhythms in mice, but the exact physiological mechanisms of retinal clockwork still remain to be characterized.

3.6 Conclusions

In this chapter, the circadian rhythms of the photopic ERG b-wave amplitude, contrast sensitivity and the pupillary light response were characterized in wildtype mice. Wildtype mice were found to exhibit attenuated photopic ERG b-wave amplitude, contrast sensitivity and PLR during subjective night compared to subjective day. The role of CRY1 and CRY2 in these three assays of circadian retinal physiology were then characterized. It was shown that *Cry1*$^{-/-}$ mice show attenuated or abolished retinal rhythms in all three assays, whereas *Cry2*$^{-/-}$ animals only show defects in ERG responses. This indicates that retinal rhythms primarily depend upon CRY1, whilst CRY2 appears largely redundant. Furthermore, these retinal functions can be correlated with the expression pattern of CRY1 and CRY2 in the mouse retina, where CRY1 is expressed throughout the retina and CRY2 expression is restricted to the outer retina. These findings suggest that CRY1 and CRY2 play distinct and separable roles in the regulation of retinal circadian physiology. Moreover, these data support the hypothesis that more than one autonomous retinal clock exists. Therefore, current knowledge contributes to a model for retinal circadian rhythms where inner and outer retinal clocks differ in their fundamental mechanisms in addition to the rhythmic physiology that they mediate.

4

Role of melanopsin in retinal rhythms

4.1 Introduction

The work in Chapter 3 contributed to further understanding of the role of CRY1 and CRY2 in retinal circadian rhythms. These data led to consideration of the role of melanopsin, which has previously been shown to have a role in retinal rhythms, as part of the mechanism governing retinal clock function. In Chapter 3, three different *in vivo* physiological assays were used to measure retinal rhythms: electroretinogram, contrast sensitivity and the pupillary light response (PLR). In this chapter, these approaches are used to further investigate the role of melanopsin in retinal rhythms.

4.1.1 Melanopsin: the mammalian circadian photopigment

As detailed in Chapter 1, the role of melanopsin as the mammalian circadian photopigment was determined in the late 1990s and early 2000s (Provencio *et al*., 1998, Hattar *et al*., 2003, Hankins *et al*., 2008). Melanopsin is an opsin-vitamin-A-based photopigment, as revealed by action spectra on rodless-coneless mice (Lucas *et al*., 2001, Peirson *et al*., 2005). Whilst there remains no evidence that mammalian cryptochromes act as circadian photopigments, multiple studies have shown that melanopsin acts in this capacity. In particular, the loss of rods, cones, and melanopsin in a triple-knockout mouse caused a complete loss of all responses to light (Hattar *et al*., 2003). Several studies further confirmed that expression of melanopsin in non-photosensitive cells rendered them photoreceptive (Melyan *et al*., 2005, Qiu *et al*., 2005, Panda *et al*., 2005). These studies critically characterised the role of melanopsin as a photopigment mediating non-image forming responses to light.

4.1.2 Melanopsin and the retinal clock

In addition to their role in non-image forming responses to light (as detailed in Section **1.4.5**), melanopsin-expressing photosensitive retinal ganglion cells (pRGCs) have also been shown to play a role in retinal rhythms. There are differing reports on whether pRGCs express the core clock genes (*Clock*, *Bmal1*, *Per1*, *Per2*, *Cry1* and *Cry2*, as discussed in Chapter 1 and 2). Some have reported that pRGCs express all core clock genes (Liu *et al*., 2012), whilst others have disputed this finding (Witkovsky *et al*. (2003) reported that pRGCs lack *Per1* expression). It was observed, as outlined in Chapter 2, that pRGCs do express CRY1. The melanopsin gene is also expressed with a daily rhythm in pRGCs (Sakamoto *et al*., 2005, Mathes *et al*., 2007). However, it is unknown if the core clock genes themselves oscillate in pRGCs. Interestingly, core clock gene oscillations in the outer retina (but not inner retina) were reported to be abolished in *Opn4*$^{-/-}$ mice (Dkhissi-Benyahya *et al*., 2013).

As has been previously noted, the light-adapted photopic electroretinogram (ERG) is dependent on the retinal circadian clock (Cameron *et al*., 2008a, Cameron *et al*., 2008b, Barnard *et al*., 2006, Storch *et al*., 2007, Jackson *et al*., 2012). The dependence of photopic ERG on CRY1 and CRY2 was also investigated in Chapter 3, and found that circadian rhythms of the cone ERG are dependent on both CRY1 and CRY2 (which corroborates results reported by Cameron *et al*. (2008)). It is also known that the photopic ERG circadian rhythm is dependent on *Bmal1* (Storch *et al*., 2007), and MT1 receptor signalling (Sengupta *et al*., 2011). Furthermore, previous studies have shown that *Opn4*$^{-/-}$ mice have abolished circadian rhythms in photopic electroretinogram amplitude (Barnard *et al*., 2006). This surprising finding led to the consideration that melanopsin and pRGCs must be able to somehow influence the cone ERG, an output of the outer retina. This may occur by way of

retrograde transmission of pRGCs to dopaminergic amacrine cells (Zhang *et al*., 2012) or potentially by gap junction communication to retinal clock cells (Sekaran *et al*., 2003). Furthermore, MT1 receptors were found on pRGCs (Sengupta *et al*., 2011) - this may be a mechanism by which MT1 signalling affects MT1 receptors on pRGCs in order to affect circadian rhythms of photopic ERG responses. In melatonin-producing mice, functional MT1 receptor signalling is necessary for circadian rhythms in photopic ERG (Sengupta *et al*., 2011). Although there has been substantial research towards understanding involvement of melatonin on retinal rhythms, it was observed in Chapter 3 that mice that do not produce melatonin (C57BL/6) were also capable of exhibiting circadian rhythms of photopic ERG, suggesting that melatonin signalling may not be essential for retinal rhythms.

Melanopsin has also been linked to light-induced dopamine increases. *Opn4*$^{-/-}$ mice showed increased retinal dopamine during the day compared to wildtype mice (Dkhissi-Benyahya *et al*., 2013). By contrast, Cameron *et al.* (2009) found that light-induced increases in dopamine were mainly driven by rods and cones and not melanopsin. Synaptic connections between pRGCs and dopaminergic amacrine cells have been reported (Vugler *et al*., 2007, Zhang *et al*., 2012).

Together, data from multiple studies has indicated that melanopsin is involved at some level in retinal clock function. Given the role of melanopsin as a circadian photopigment, there has been speculation that melanopsin may also provide light entrainment for the retinal clock (McMahon *et al*., 2014). Light-induced increases in *Per1* and *Per2* expression in the outer retina was also abolished in *Opn4*$^{-/-}$ mice (Dkhissi-Benyahya *et al*., 2013). However, *Opn4*$^{-/-}$*;rd/rd* mice were found to exhibit retinal PER2::LUC rhythms, which

indicates that melanopsin may not be essential for maintenance nor photoentrainment of molecular retinal rhythms (Buhr and Van Gelder, 2014). It has recently been suggested that novel pigment neuropsin (*Opn5*) may entrain the retinal clock to light (Buhr *et al*., 2015). There is little information regarding where OPN5 is expressed in mouse retinal tissue – most recently this has been shown to be a subset of ganglion cells in the ganglion cell layer. It remains unknown if OPN5 and OPN4 are co-expressed in any cells, or perhaps whether cells expressing OPN5 and those expressing OPN4 may communicate with one another in any way. If pRGCs expressing OPN4 also expressed OPN5, these cells may provide a dual role of entraining both the SCN and the body's circadian system, as well as the retinal tissue itself. As OPN5 antibody reagents are currently unavailable, future work will hopefully address this issue.

4.1.3 Investigating the role of melanopsin in the retinal clock

In Chapter 3, it was reported that circadian rhythms in contrast sensitivity, which are regulated by the retinal clock (Hwang *et al*., 2013), are dependent on CRY1 but not CRY2. Interestingly, the mechanism for contrast sensitivity circadian rhythms also involve D4 receptors and therefore the dopamine system of the retina. Contrast sensitivity is especially important for night vision, and is attenuated in retinal dopamine-depleted mice (Jackson *et al*., 2012) as well as in people who have Parkinson's disease, where dopamine neurons in the brain progressively degenerate (Witkovsky, 2004). The established relationship between melanopsin and dopamine, as well as that of dopamine and contrast sensitivity circadian rhythms, led to the investigation of the relationship between melanopsin and circadian rhythms of contrast sensitivity.

Wildtype mice exhibited rhythms in maximum pupillary constriction, where the PLR was attenuated at night (Chapter 3), and this response is dependent on CRY1 but not CRY2. This was also reported in *rd/rd* mice (Owens *et al*., 2012). This may imply that melanopsin expression is sufficient to provide light information for the circadian variation in PLR.

In this chapter, *Opn4*$^{-/-}$ (melanopsin-knockout) mice were tested for any deficits in retinal circadian rhythms. As circadian rhythms in photopic electroretinogram b-wave have already been tested in these mice (Barnard *et al*., 2006), circadian rhythms in contrast sensitivity and PLR were assessed.

4.2 Aims

Since melanopsin (*Opn4*) has been previously described as having a significant role in electroretinogram circadian rhythms and melanopsin-expressing photosensitive retinal ganglion cells may rhythmically express clock genes and proteins, including CRY (Chapter 2), further characterization of the role of melanopsin in the mouse retinal circadian clock was sought. To do so, two rhythmic retinal physiology assays were employed – contrast sensitivity and pupillary light response. It was shown in Chapter 3 that both of these physiological assays display a circadian rhythm in wildtype mice. As such, it was the aim of this chapter to determine whether the retinal circadian clock, as measured by these assays, would be affected by melanopsin loss. *Opn4*$^{-/-}$ mice were used to study the role of melanopsin.

In Chapter 4, the specific aims are:

- To characterise the role of OPN4 in circadian rhythms of contrast sensitivity
- To characterise the role of OPN4 in circadian rhythms of pupillary light response

4.3 Methods

4.3.1 Animals

Melanopsin knockout *Opn4*$^{-/-}$ mice (mixed C57BL/6 x Sv129 background) (Hattar *et al*., 2002, Lucas *et al*., 2003) were maintained as heterozygous breeders.

See Chapter 2.3 for details on animal care and license information.

4.3.2 Genotyping

Genotyping of *Opn4*$^{-/-}$ mice followed standard protocols as previously reported (Hattar *et al*., 2003). Ear notches were obtained and digested in 50mM NaOH for 90 minutes at 90°C and then neutralized with 1M Tris-HCl (pH 5).

PCR was then performed using the DNA extracted from the ear notches

***Opn4* Forward primer sequence (5' – 3')**	AGA AGT GGC TCT TTG GGG AGA C
***Opn4* Reverse primer sequence (5' – 3')**	GCA GAA GGC ATA GAA CTC GCA AC
LacZ Forward primer sequence (5' – 3')	AAG CAG TCA GCA GCC CAA AG
LacZ Reverse primer sequence (5' – 3')	TGT CAC CCT CCT GGT CTT GC
***Opn4* Product Size (in wildtype)**	200bp band, melting temperature of 82°C
LacZ Product Size (in knockout mice)	300bp band, melting temperature of 85°C

Table 4.1. Primers used for *Opn4* genotyping.

Standard PCR protocols were used. The following reagents were used for the PCR:

SYBR Green Master Mix (10 uL)
Forward Primer (0.5 uL)
Reverse Primer (0.5 uL)
Molecular grade water (7 uL)
Genomic DNA lysate (1 uL)

The following PCR cycling conditions were used:

Holding stage
95°C for 10 min
Cycling stage
95°C for 15 s
60°C for 60 s
Repeat Cycling stage x 35
Melt Curve stage
95°C 15 s
60°C for 60 s
95°C 15 s

Melt curve analysis was used. Wildtype mice expressing *Opn4* would give a distinct melt curve compared to the knockout mice LacZ gene melt curve. Heterozygous mice carried both wildtype and LacZ sequences, so both melt curve peaks present with the curve at 82°C significantly larger than at 85°C.

4.3.3 *In vivo* Circadian Retinal Physiology Testing

See Chapter 3.3.

4.3.4 Optomotor Responses

See Chapter 3.3.

4.3.5 Pupillometry

See Chapter 3.3.

4.3.6 Statistical Analysis

All data are shown with ± SEM (standard error of the mean). Statistical analysis was performed in GraphPad Prism (version 5) using paired two-way ANOVA analysis or two-tailed Student's t-test as reported in the legend.

4.4 Results

4.4.1 Circadian rhythms in contrast sensitivity are attenuated in *Opn4*$^{-/-}$ mice

Similarly to the work in Chapter 3, the contrast sensitivity of wildtype and *Opn4*-/- mice was tested at ZT6, ZT18, CT6 and CT18. Circadian differences in contrast sensitivity was previously shown in wildtype mice (Hwang *et al*., 2013) using a virtual optokinetic drum assay (Prusky *et al*., 2004). In parallel with Chapter 3, contrast sensitivity was measured at six different spatial frequencies (0.031, 0.092, 0.103, 0.192, and 0.272 cycles/degree, Prusky *et al*. (2004)). These data were analysed by 2-way ANOVA for spatial frequency and time. The order of times at which contrast sensitivity was tested was counterbalanced in order to allow within-subject comparisons.

As previously shown, wildtype mice (n=6) showed significantly higher contrast sensitivity at during the day (ZT6) compared to during the night (ZT18, **Figure 4.1** A). There was a significant effect of *zeitgeber* time $F_{(1, 30)} = 35.92$, $p < 0.0001$ and a significant effect of spatial frequency $F_{(5, 30)} = 24.39$, $p < 0.0001$. Furthermore, the interaction between *zeitgeber* time x spatial frequency is also significant $F_{(5, 30)} = 2.868$, $p = 0.0312$. Post-hoc Sidak's multiple comparisons test showed that wildtype mice have significantly higher contrast sensitivities at ZT6 at spatial frequencies between 0.064 and 0.092 cycles/degree. In agreement with previously published data (Prusky *et al*., 2004), peak contrast sensitivities were measured to be between 0.064-0.092 cycles/degree.

Under circadian conditions, wildtype mice again showed significantly higher contrast sensitivity at during subjective day (CT6) compared to subjective night (CT18, **Figure 4.1** C).

There was a significant effect of circadian time ($F_{(1, 30)}$ = 51.15, p < 0.0001) and spatial frequency ($F_{(5, 30)}$ = 26.77, p < 0.0001), peaking around 0.092 cycles/degree at CT6. Finally, the interaction between circadian time x spatial frequency is also significant $F_{(5, 30)}$ = 4.259, p = 0.0048. Post-hoc Sidak's multiple comparisons test showed that wildtype mice have significantly higher contrast sensitivities at CT6 at spatial frequencies between 0.092 and 0.192 cycles/degree.

Interestingly, *Opn4*$^{-/-}$ mice (n=5) exhibit no significant difference between contrast sensitivity at ZT6 compared to ZT18, or at CT6 compared to CT18 (**Figure 4.1** B and D). Under diurnal conditions (**Figure 4.1** B), the main effect of *zeitgeber* time is not significant $F_{(1, 24)}$ = 1.331, p = 0.26, but the main effect of spatial frequency is significant $F_{(5, 24)}$ = 25.65, p < 0.0001. Peak contrast sensitivities in *Opn4*$^{-/-}$ mice were measured to be around 0.092 cycles/degree, similar to those in wildtype mice. The interaction between *zeitgeber* time x spatial frequency is also not significant $F_{(5, 24)}$ = 0.5608, p = 0.7289. Post-hoc Sidak's multiple comparisons test between contrast sensitivity measurements at ZT6 and ZT18 were not significant.

Finally, when *Opn4*$^{-/-}$ mice were tested under constant darkness conditions (**Figure 4.1** D), the main effect of circadian time is not significant $F_{(1, 24)}$ = 1.957, p = 0.1746, but the main effect of spatial frequency is significant $F_{(5, 24)}$ = 36.11, p < 0.0001. The interaction between *zeitgeber* time x spatial frequency is also not significant $F_{(5, 24)}$ = 0.3807, p = 0.8570. Post-hoc Sidak's multiple comparisons test between contrast sensitivity measurements at CT6 and CT18 were not significant, and in constant conditions, peak contrast sensitivities in *Opn4*$^{-/-}$ mice were found to be at spatial frequencies around 0.092-0.103 cycles/degree.

We then compared contrast sensitivity measurements at the peak of visual acuity, 0.064 cycles/degree (Prusky *et al*., 2004) and also at the peak measured contrast sensitivity, 0.092 cycle/degree (**Figure 4.2**). It was found that in wildtype mice, diurnal rhythms of contrast sensitivity at a spatial frequency of 0.064 cycles/degree were clearly apparent (**Figure 4.2** A). Under constant conditions, rhythms were attenuated, but trended with daytime measurement showing a higher contrast sensitivity than night time measurement (**Figure 4.2** B). When contrast sensitivity was then measured at a spatial frequency of 0.092 cycles/degree, wildtype mice displayed both diurnal and circadian rhythms (**Figure 4.2** C and D). In *Opn4*$^{-/-}$ mice, contrast sensitivity at spatial frequencies of 0.064 cycles/degree and of 0.092 cycles/degree were found to have no significant rhythms under neither entrained (**Figure 4.2** A and C) nor constant conditions (**Figure 4.2** B and D).

As previously shown in Chapter 3, visual acuity of wildtype mice was found not show any diurnal or circadian variation between ZT6 and CT18, or CT6 and CT18 (**Figure 4.3**). Similarly, in *Opn4*$^{-/-}$ mice also did not show any diurnal or circadian rhythm in visual acuity. When the threshold spatial frequency detectable by the mice was tested, there was no significant effect of time ($F_{(3, 27)} = 2.147$, $p = 0.1176$) or genotype ($F_{(1, 9)} = 1.933$, $p = 0.9800$), and no interaction between time x genotype ($F_{(3,27)} = 0.3480$, $p = 0.7909$). Post-hoc Sidak's multiple comparisons tests between all circadian time and genotype combinations were all not significant.

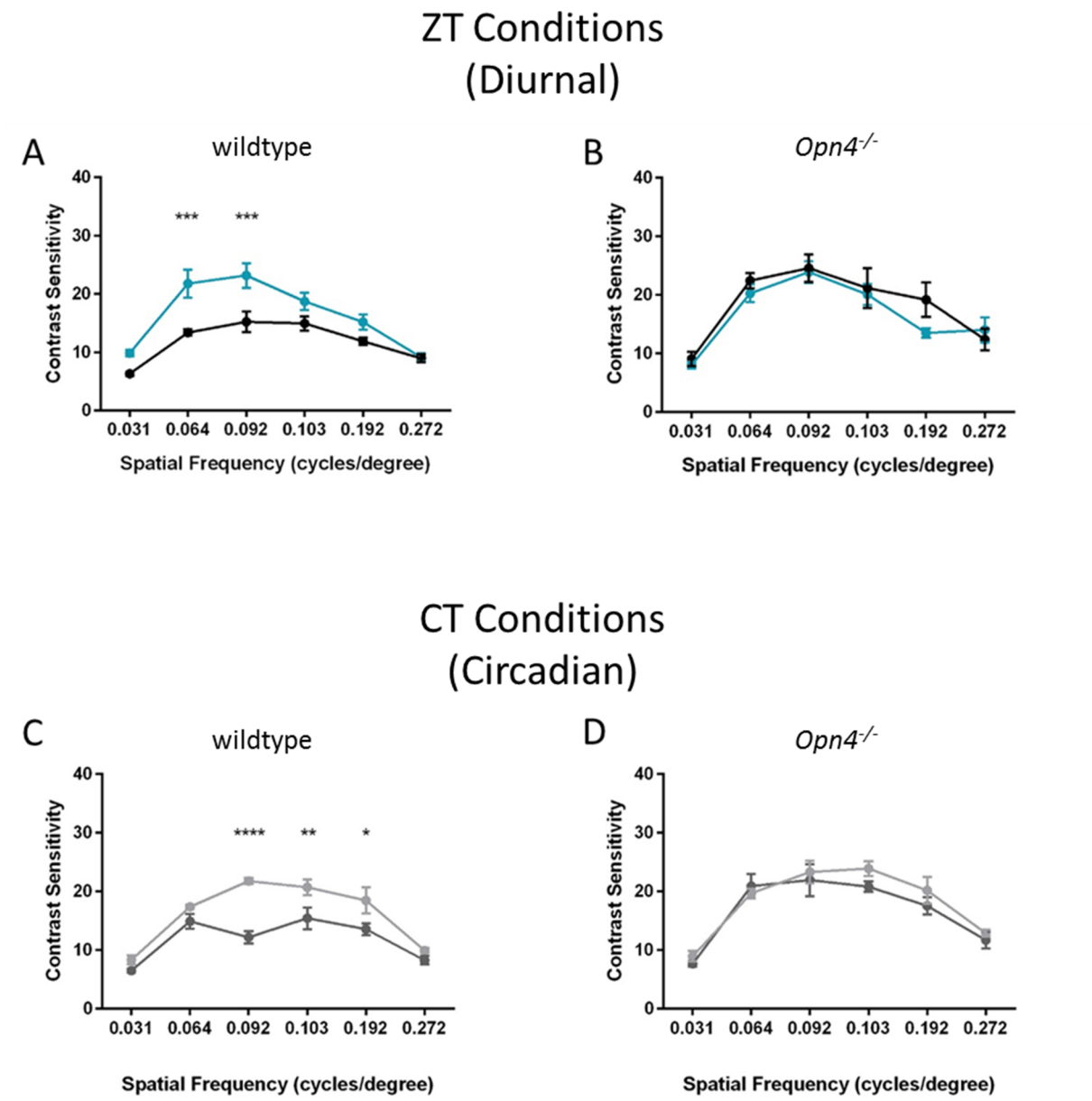
ZT Conditions
(Diurnal)
A
wildtype
B
Opn4-/-
Contrast Sensitivity
Spatial Frequency (cycles/degree)
0.031 0.064 0.092 0.103 0.192 0.272
***
***
CT Conditions
(Circadian)
C
wildtype
D
Opn4-/-
****
**
*

Figure 4.1.

Figure 4.1. Contrast sensitivity is controlled in a diurnal and circadian manner and is dependent on melanopsin. Data are represented as means ± SEM. Two-way ANOVA was performed. (A) Wildtype mice (n=6) exhibit significantly higher contrast sensitivity at ZT6 (blue) in contrast to ZT18 (black), as measured using the optokinetic nystagmus response. The main effect of *zeitgeber* time is significant $F_{(1, 30)} = 35.92$, $p < 0.0001$. The main effect of spatial frequency is significant $F_{(5, 30)} = 24.39$, $p < 0.0001$. The interaction between *zeitgeber* time x spatial frequency is also significant $F_{(5, 30)} = 2.868$, $p = 0.0312$. Post-hoc Sidak's multiple comparisons test show that wildtype mice have significantly higher contrast sensitivities at spatial frequencies (cycles/degree) of 0.064 and 0.092. ***indicates p<0.001. All other comparisons were not significant. (B) *Opn4*$^{-/-}$ mice (n=5) exhibit no significant difference between contrast sensitivity at ZT6 (blue) compared to ZT18 (black). The main effect of *zeitgeber* time is not significant $F_{(1, 24)} = 1.331$, $p = 0.26$, but the main effect of spatial frequency is significant $F_{(5, 24)} = 25.65$, $p < 0.0001$. The interaction between *zeitgeber* time x spatial frequency is also not significant $F_{(5, 24)} = 0.5608$, $p = 0.7289$. Post-hoc Sidak's multiple comparisons test between contrast sensitivity measurements at ZT6 and ZT18 were not significant. (C) Wildtype mice (n=6) exhibit significantly higher contrast sensitivity at CT6 (light grey) in contrast to CT18 (dark grey). The main effect of circadian time is significant $F_{(1, 30)} = 51.15$, $p < 0.0001$. The main effect of spatial frequency is significant $F_{(5, 30)} = 26.77$, $p < 0.0001$. The interaction between circadian time x spatial frequency is also significant $F_{(5, 30)} = 4.259$, $p = 0.0048$. Post-hoc Sidak's multiple comparisons test show that wildtype mice have significantly higher contrast sensitivities at spatial frequencies (cycles/degree) of 0.092, 0.103 and 0.192. *indicates p<0.05, **indicates p<0.01, and ****indicates p<0.0001. All other comparisons were not significant. (D) *Opn4*$^{-/-}$ mice (n=5) exhibit no significant difference between contrast sensitivity at CT6 (light grey) compared to CT18 (dark grey). The main effect of circadian time is not significant $F_{(1, 24)} = 1.957$, $p = 0.1746$, but the main effect of spatial frequency is significant $F_{(5, 24)} = 36.11$, $p < 0.0001$. The interaction between *zeitgeber* time x spatial frequency is also not significant $F_{(5, 24)} = 0.3807$, $p = 0.8570$. Post-hoc Sidak's multiple comparisons test between contrast sensitivity measurements at CT6 and CT18 were not significant.

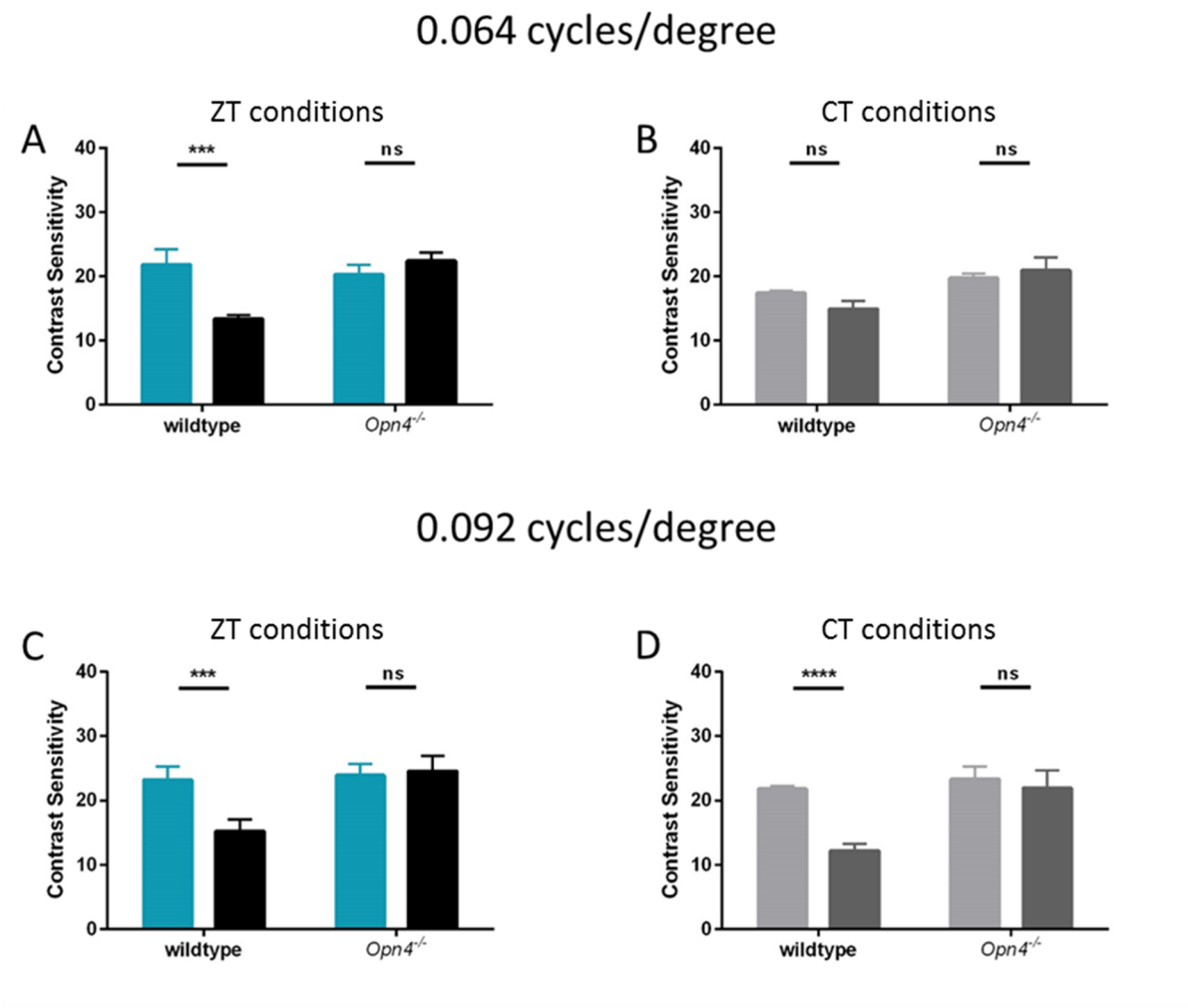

Figure 4.2. Comparison of diurnal and circadian rhythms in contrast sensitivity of wildtype and *Opn4*$^{-/-}$ mice at spatial frequencies of 0.064 cycles/degree and 0.092 cycles/degree (peak frequencies for contrast sensitivity in wildtype and *Opn4*$^{-/-}$ mice). Data are represented as means ± SEM. (A) Diurnal rhythms in contrast sensitivity of wildtype and *Opn4*$^{-/-}$ mice at a spatial frequency of 0.064 cycles/degree are shown. As drawn from the statistical analysis on wildtype and *Opn4*$^{-/-}$ mice, presented in Figure 1, wildtype mice demonstrate a rhythm in contrast sensitivity between ZT6 and ZT18 at 0.064 cycles/degree spatial frequency, whilst *Opn4*$^{-/-}$mice do not. (B) Circadian rhythms in contrast sensitivity of wildtype and *Opn4*$^{-/-}$ mice at a spatial frequency of 0.064 cycles/degree are shown. As presented in Figure 1, neither wildtype mice not *Opn4*$^{-/-}$ demonstrated a rhythm in contrast sensitivity between CT6 and CT18 at 0.064 cycles/degree spatial frequency. (C) Diurnal rhythms in contrast sensitivity of wildtype and *Opn4*$^{-/-}$ mice at a spatial frequency of 0.092 cycles/degree are shown. As shown in Figure 1, wildtype mice demonstrate a rhythm in contrast sensitivity between ZT6 and ZT18 at 0.092 cycles/degree spatial frequency, whilst *Opn4*$^{-/-}$mice do not. (D) Circadian rhythms in contrast sensitivity of wildtype and *Opn4*$^{-/-}$ mice at a spatial frequency of 0.092 cycles/degree are shown. As drawn from the statistical analysis on wildtype and *Opn4*$^{-/-}$ mice, presented in Figure 1, neither wildtype mice not *Opn4*$^{-/-}$ demonstrated a rhythm in contrast sensitivity between CT6 and CT18 at 0.092 cycles/degree spatial frequency.

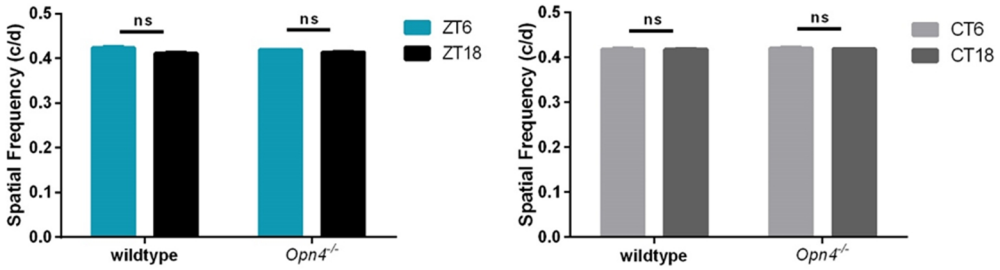

Figure 4.3. Visual Acuity does not exhibit a diurnal (A) or circadian (B) variation in wildtype or *Opn4*$^{-/-}$mice. Means ± SEM are shown. ZT6 is shown in blue, ZT18 in black, CT6 in light grey and CT18 in dark grey. Two-way repeated-measures ANOVA was performed. The main effect of time is not significant $F_{(3, 27)} = 2.147$, $p = 0.1176$. The main effect of genotype is not significant $F_{(1, 9)} = 1.933$, $p = 0.9800$. The interaction between time x genotype is also not significant $F_{(3,27)} = 0.3480$, $p = 0.7909$. Post-hoc Sidak's multiple comparisons tests between all circadian time and genotype combinations were all not significant.

4.4.2 Circadian rhythms in PLR are preserved in *Opn4*$^{-/-}$ mice

As demonstrated in Chapter 3, the pupillary light response has been shown to demonstrate a diurnal rhythm (Owens *et al*., 2012) and circadian rhythm in response magnitude.

Pupillometry was performed on wildtype mice (n=6) and *Opn4*$^{-/-}$mice (n=5) at ZT6, ZT18, CT6 and CT18. The order of times at which PLR was tested was counterbalanced in order to allow within-subject comparisons. Two-way ANOVA was performed.

As previously seen, wildtype mice exhibited attenuated PLR at ZT18 compared to ZT6 (**Figure 4.4** A). Under constant conditions, the maximum pupil constriction was attenuated at CT18 compared to CT6 (**Figure 4.4** C). *Opn4*$^{-/-}$mice also displayed similar differences in PLR, where the maximum pupillary constriction was attenuated at ZT18 compared to ZT6 (**Figure 4.4** B), and at CT18 compared to CT6 (**Figure 4.4** D).

When the average kinetics of the PLR in wildtype and *Opn4*$^{-/-}$ mice were compared between genotypes (**Figure 4.5**), the pupillary response of *Opn4*$^{-/-}$ mice was significantly attenuated compared to wildtype mice at all tested times, ZT6, CT6, ZT18, and CT18.

Two-way ANOVA statistical comparison of the maximum pupillary constriction between wildtype and *Opn4*$^{-/-}$ mice (**Figure 4.6**) revealed a significant effect of genotype $F_{(1, 56)}$ = 9.771, p = 0.0028. There was a significant effect of time $F_{(3, 56)}$ = 33.28, p < 0.0001 and no significant interaction between time x genotype $F_{(3,56)}$ = 0.5607, p =0.6432. Given that both wildtype and *Opn4*$^{-/-}$mice shown diurnal and circadian rhythms in PLR, and *Opn4*$^{-/-}$mice consistently showed attenuated PLR in comparison to wildtype, this is consistent with no interaction between time x genotype. Example screenshots displaying pupil area prior to light exposure (dark) and at maximum constriction (light) are shown in **Figure 4.7**.

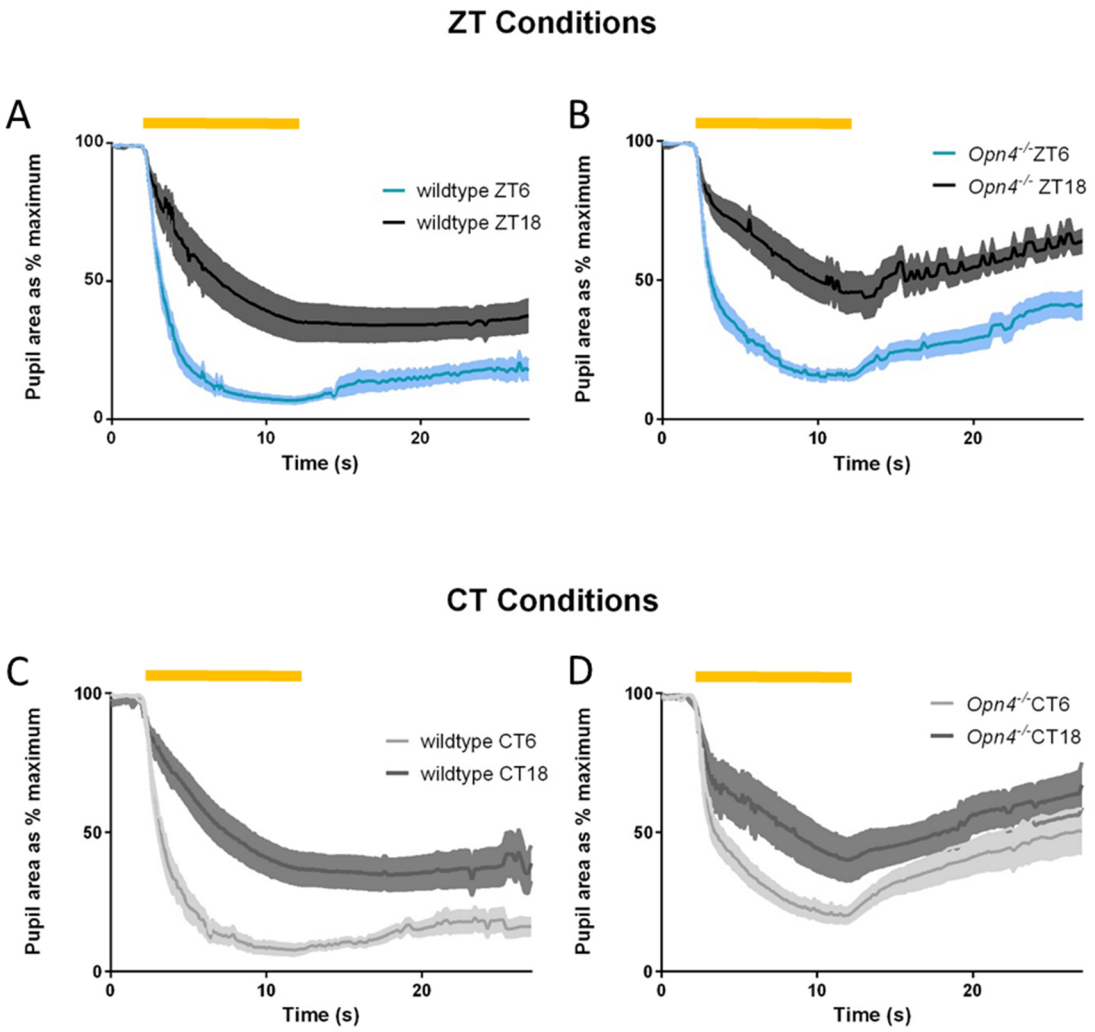

Figure 4.4. The pupillary light responses of wildtype and *Opn4*$^{-/-}$ mice exhibit both a diurnal rhythm and circadian rhythm. (A) Averaged kinetics of PLR for wildtype mice under ZT conditions (ZT6 shown in blue, ZT18 shown in grey). (B) Averaged kinetics of PLR for *Opn4*$^{-/-}$ mice under ZT conditions (ZT6 shown in blue, ZT18 shown in grey). (C) Averaged kinetics of PLR for wildtype mice under CT conditions (CT6 shown in light grey, CT18 shown in dark grey). (D) Averaged kinetics of PLR for *Opn4*$^{-/-}$ mice under CT conditions (CT6 shown in light grey, CT18 shown in dark grey). The yellow bar indicates a bright light stimulus (480nm) switched on for 2s-12s of recording. All mice demonstrated attenuated PLR at ZT18 compared to ZT6, and also at CT18 compared to CT6. Data are represented as means ± SEM.

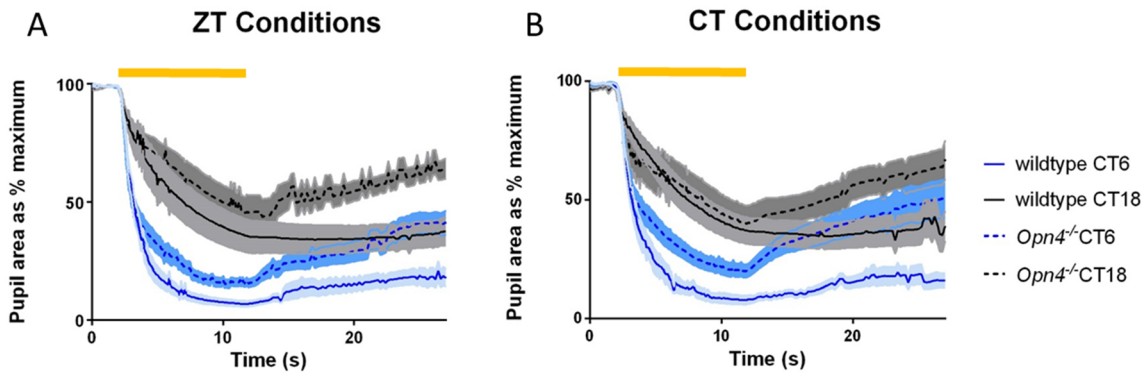

Figure 4.5. Comparison of the diurnal rhythm of wildtype and *Opn4*$^{-/-}$ mice pupillary light responses with the circadian rhythm of these responses. (A) Averaged kinetics of PLR for wildtype and *Opn4*$^{-/-}$ mice under ZT conditions (ZT6 shown in blue, ZT18 shown in black, wildtype responses shown as solid lines, and *Opn4*$^{-/-}$ responses shown as dotted lines). (B) Averaged kinetics of PLR for wildtype and *Opn4*$^{-/-}$ mice under CT conditions (CT6 shown in blue, CT18 shown in black, wildtype responses shown as solid lines, and *Opn4*$^{-/-}$ responses shown as dotted lines). The yellow bar indicates a bright light stimulus (480nm) switched on for 2s-12s of recording. All mice demonstrated attenuated PLR at ZT18 compared to ZT6, and also at CT18 compared to CT6. *Opn4*$^{-/-}$ mouse PLR are attenuated compared to wildtype PLR. Data are represented as means ± SEM. Mean responses are shown as lines, and SEM are shown as shaded colour.

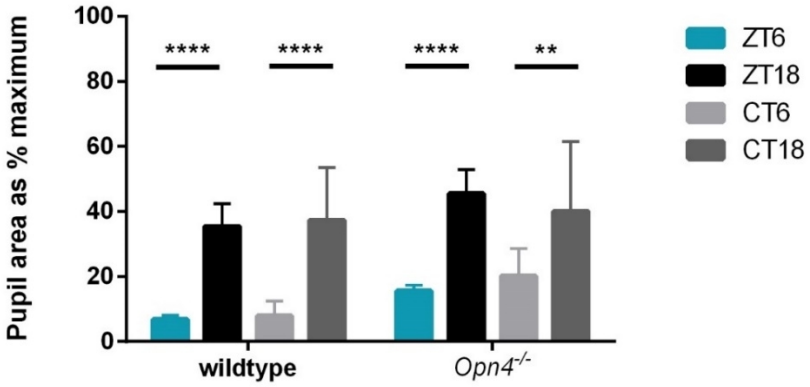

Figure 4.6. Summary histogram for wildtype (n=6) and *Opn4*$^{-/-}$ (n=5) mouse responses at ZT6 (blue), ZT18 (black), CT6 (light grey) and CT18 (dark grey). Data are represented as means ± SEM. Two-way ANOVA was performed. The main effect of time is significant $F_{(3, 56)} = 33.28$, $p < 0.0001$. The main effect of genotype is also significant $F_{(1, 56)} = 9.771$, $p = 0.0028$. The interaction between time x genotype is not significant $F_{(3,56)} = 0.5607$, $p = 0.6432$. Post-hoc Sidak's multiple comparisons tests show that both wildtype and *Opn4*$^{-/-}$ mice have significantly attenuated pupillary light response at both ZT18 and at CT18 compared to at both ZT6 and CT6. **indicates p<0.01, and ****indicates p<0.0001. All other comparisons were not significant.

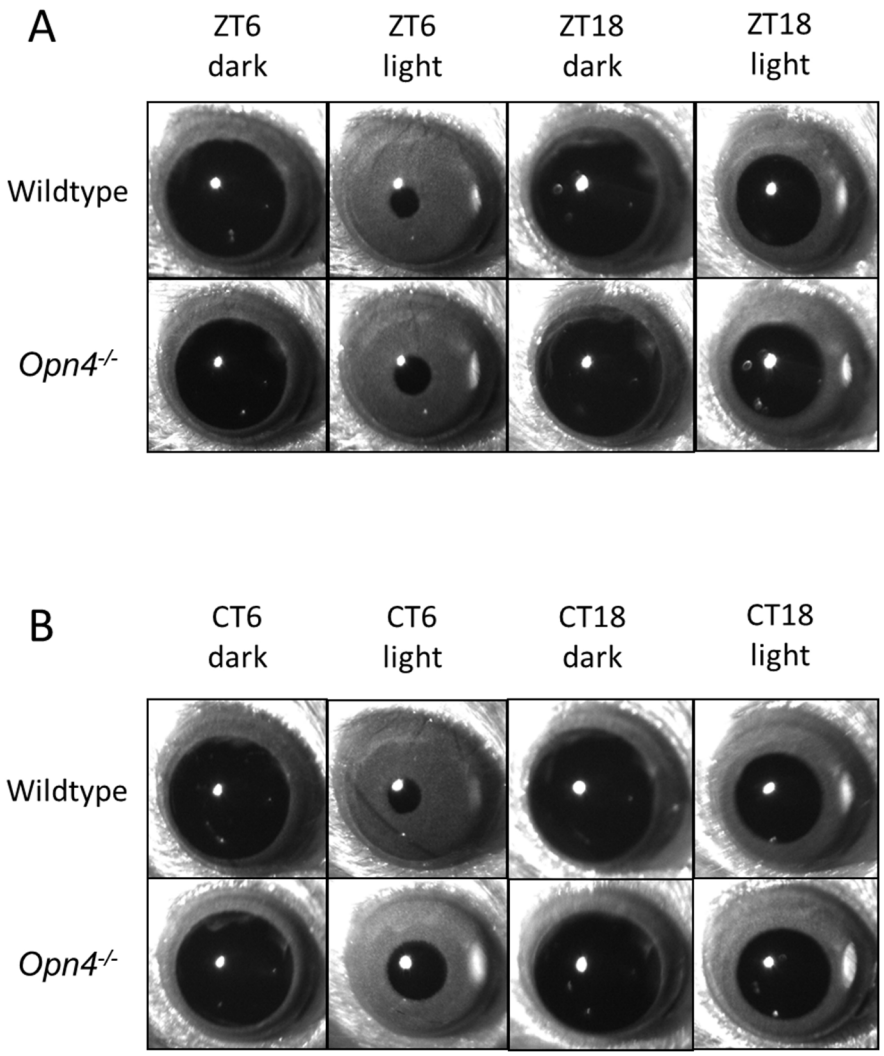

Figure 4.7. Representative pupil images showing maximum constriction of pupils at ZT6 and ZT18, as well as CT6 and CT18 for wildtype and *Opn4*$^{-/-}$ mice. Both wildtype and *Opn4*$^{-/-}$ mice display greater pupil constriction at ZT6 compared to ZT18, and greater constriction at CT6 compared to CT18. Furthermore, *Opn4*$^{-/-}$ mice display attenuated constriction compared to wildtype mice all four timepoints.

4.5 Discussion

4.5.1 Melanopsin is necessary for circadian rhythms in contrast sensitivity, but not pupillary light responses

These results indicate that whilst wildtype mice exhibit both diurnal and circadian rhythms in both contrast sensitivity and in pupillary light response (PLR), *Opn4*$^{-/-}$ mice show a loss in diurnal and circadian rhythms in contrast sensitivity but PLR was not affected. These findings demonstrate that melanopsin (*Opn4)*, is necessary for maintaining rhythms in contrast sensitivity but not in PLR.

No significant difference in contrast sensitivity measurements between CT6 and CT18 was found in wildtype mice, at a spatial frequency of 0.064 cycles/degree. However, there was a trend indicative that wildtype contrast sensitivity was greater at CT6 compared to CT18 at 0.064 cycles/degree. In Chapter 3, a significant difference in contrast sensitivity between CT6 and CT18 at 0.064 cycles/degree was found in wildtype mice. The discrepancy in results may be due to the difference in number of animals tested. In Chapter 3, 10 wildtype mice were used to explore rhythms in contrast sensitivity. In this Chapter, 6 wildtype mice were used – it is possible that a significant difference could not be resolved because of the lower number of mice tested. The trending difference may indicate that a significant difference exists but could not be resolved by the fewer number of mice tested.

The post-illumination pupil response (PIPR), defined as the recovery response of the pupil following cessation of the light stimulus, has been suggested to provide an assay of OPN4 function (Kankipati *et al*., 2010). Despite the fact that PIPR has not been systematically evaluated in the absence of OPN4, numerous research groups have used PIPR to assess

OPN4 function in humans (Zele *et al*., 2011, Feigl *et al*., 2011, Feigl *et al*., 2012, Roecklein *et al*., 2013, Adhikari *et al*., 2015, Maynard *et al*., 2015). PIPR has also been shown to have a circadian rhythm in humans (Zele *et al*., 2011). Given that PIPR has been proposed as OPN4-dependent, either a loss of PIPR or an alteration in circadian rhythms of PIPR in *Opn4*$^{-/-}$ could be expected. The data presented in this chapter indicate that *Opn4*$^{-/-}$ mice show a higher rise in PIPR than wildtype mice, but this is not a significant effect. Maximum pupil constriction is also regulated by circadian time and the PIPR magnitude may be linked directly to the amount of maximum pupil constriction. Systematic experiments examining PIPR in *Opn4*$^{-/-}$ mice under various lighting conditions are necessary to characterize the role of OPN4 in PIPR.

4.5.2 Differential regulation of circadian rhythms of contrast sensitivity and of pupillary light response

The data from the *Opn4*$^{-/-}$ mice is particularly interesting as it further separates the control of the pupillary response and the control of the contrast sensitivity response. Whilst data presented in Chapter 3 suggests that circadian rhythms in contrast sensitivity and in PLR may be regulated by the same retinal clock mechanism, the data from *Opn4*$^{-/-}$ mice show that this may not be the case. As *Opn4*$^{-/-}$ mice have functional cryptochromes, rods and cones, the data demonstrate that PLR rhythms are not dependent upon melanopsin. However, the presence of cryptochromes is not sufficient to maintain circadian rhythms of contrast sensitivity in *Opn4*$^{-/-}$ mice; melanopsin is required for this.

Whilst the PLR has been an important assay for the characterisation of non-image forming responses to light, evidence for diurnal rhythms in PLR has only recently been described

(Owens *et al*., 2012). The PLR demonstrates clear circadian rhythms of maximum pupillary constriction, with reduced responses during the subjective night. As shown in Chapter 3, this circadian rhythm in sensitivity is attenuated in CRY1-deficient mice, but retained in CRY2-deficient animals. These data are again consistent with a principal role of CRY1 in retinal rhythms, although it should be noted that central pathways may also contribute to these rhythms. Future studies are needed to determine whether the PLR is regulated at the level of the retina, SCN, or both. Indeed, whilst retinal rhythms may persist independently in isolated retinal tissue, it remains unknown as to whether retinal rhythms *in vivo* are influenced by the SCN pacemaker or other peripheral clocks. However, of note, entrainment of photoreceptor disk shedding circadian rhythms in the retina appear to depend on an intact SCN (Teirstein *et al*., 1980, Terman *et al*., 1993). Further research is required to address these outstanding questions.

4.5.3 Melanopsin is an important, though non-essential, modulator of the retinal circadian clock

The exact role of melanopsin and pRGCs in the retinal clock remains unclear, but the data presented in this chapter lends further evidence that a role definitely exists. As shown in Chapter 2, CRY1 protein was found to be expressed in a subset of pRGCs. Furthermore, previous studies have shown that *Opn4*$^{-/-}$ mice lose the ERG b-wave amplitude rhythm (Barnard *et al*., 2006), lose circadian rhythms in clock gene expression in the outer retina (Dkhissi-Benyahya *et al*., 2013), and exhibit changes in light-adaptation which compromise visual circuit optimization of spatial and temporal conditions (Allen *et al*., 2014).

Here it is shown that melanopsin loss causes loss of contrast sensitivity rhythms, but not pupillary light response rhythms. That is, circadian regulation of contrast sensitivity may be separated from that of PLR. Melanopsin may therefore be regulating the retinal clock in some way, either by gating light input to the clock, or as a component of the retinal clock network itself. Melanopsin could play a role in entraining retinal rhythms, in regulating a retinal clock oscillator in pRGCs, or influencing other retinal networks which are capable of mediating retinal rhythms (such as the dopaminergic amacrine system). However, the finding that *Opn4*$^{-/-}$ mice retain circadian rhythms in the PLR, and that mouse retinas lacking melanopsin still exhibit retinal PER2::LUC rhythms implies that although melanopsin may modulate retinal circadian rhythmicity, it is not an essential component of the retinal circadian clock. The mechanisms by which melanopsin may contribute to the retinal clock are expanded upon below.

Lastly, melanopsin and pRGCs have been found to play an important role in the development of non-image-forming retinal responses to light (Sekaran *et al*., 2005, McNeill *et al*., 2011). Melanopsin-expressing pRGCs have been shown to be the first light-sensitive cells to develop in the retina (Tu *et al*., 2005, Schmidt *et al*., 2008). Given the importance of melanopsin and pRGCs in retinal development as well as that of NIF responses, melanopsin may have a role in the development of circadian organization of retinal tissue. If this is the case, *Opn4*$^{-/-}$ mice may have developed abnormal retinal circadian organization responsible for the observed retinal rhythm defects.

4.5.4 Melanopsin may gate light input to the retinal circadian clock

As shown in the Barnard *et al*. (2006) study, melanopsin is essential for rhythms in photopic electroretinogram sensitivity. As the photopic ERG primarily measures cone function and melanopsin is localized to pRGCs in the ganglion cell layer of the retina, this would imply that melanopsin can somehow impact cone function. This study proposed two mechanisms by which melanopsin may mediate the cone ERG. First, it was proposed that pRGCs may be upstream to the retinal circadian clock and therefore melanopsin may simply regulate entrainment of the retinal clock. However, given that pRGCs receive rod and cone input, it is unlikely that loss of melanopsin would abolish the ability of pRGCs to mediate information for retinal clock function. Indeed, loss of melanopsin does not prevent circadian photoentrainment because rods and cones can compensate by sending light information via pRGCs (Panda *et al*., 2003, Guler *et al*., 2008).

Tangential to this essential melanopsin signalling theory was the potential for melanopsin, a functional photopigment, to entrain the retinal clock. However, recent studies have shown that melanopsin is not necessary for the entrainment of retinal circadian rhythms and has postulated that a novel photopigment, neuropsin (*Opn5*), may entrain the retinal circadian clock (Buhr and Van Gelder, 2014, Buhr *et al*., 2015). It was shown that whole retinas from *rd1/rd1;Opn4*$^{-/-}$ PER2::LUC mice are still able to entrain to light-dark cycles (Buhr and Van Gelder, 2014), lending evidence that melanopsin is not essential for photoentrainment of the retinal clock.

4.5.5 Melanopsin may be involved in intraretinal signalling output from pRGCs affecting the retinal dopaminergic system

The second theory for melanopsin's involvement in the cone ERG as proposed by the Barnard *et al.* (2006) study suggests that, as an alternative to photoentraining the retinal clock, perhaps melanopsin is involved in intraretinal signalling output from pRGCs and affects the cone ERG response in this manner.

However, output signalling from pRGCs must therefore somehow influence the rest of the retina. Retrograde signalling from melanopsin-expressing pRGCs to the outer retina has been a speculative issue, since, canonically, it is understood that light signalling proceeds from the outer retina to the inner retina, to the ganglion cells (Rodieck, 1998). However, gap junction coupling in the ganglion cell layer (Sekaran *et al*., 2003) could potentially affect inner retinal clock cells or dopaminergic amacrine cells, which are capable of affecting outer retinal function (Jackson *et al*., 2012, Jackson *et al*., 2014). Furthermore, pRGCs were found to signal retrogradely to dopaminergic amacrine cells, and that this was mediated by melanopsin (Zhang *et al*., 2008, Zhang *et al*., 2012). Since dopaminergic amacrine cells may influence both the inner and outer retina (Jackson *et al*., 2012), this may be a plausible mechanism by which melanopsin affects the cone ERG (as depicted in **Figure 4.8**).

As such, melanopsin could mediate retinal rhythms by contributing to an intraretinal signalling output from pRGCs which affects the dopaminergic system of the retina (perhaps by reducing dopaminergic tone or abolishing circadian regulation of dopamine secretion). Loss of melanopsin may affect pRGC signalling outputs to dopaminergic amacrine cells,

causing reduced dopamine release (and a reduced dopaminergic tone). Retinal dopamine depletion causes loss of photopic ERG circadian rhythms and attenuated contrast sensitivity responses (Jackson *et al*., 2012), similar to those observed in *Opn4*$^{-/-}$ mice. Furthermore, retinal dopamine depletion did not abolish retinal PER2::LUC rhythms (Jackson *et al*., 2012), which are also still present in mice lacking melanopsin (Buhr and Van Gelder, 2014). Thus, this mechanism would allow for a melanopsin contribution to retinal rhythmicity which is important but not essential for the generation of retinal circadian rhythms altogether. It is necessary to note, however, that the PER2::LUC data describing how retinal dopamine and melanopsin could be dispensable for rhythms, were performed in retinal explant cultures. To that point, it remains a possibility that intact, but weakened, PER2::LUC rhythms could be present in a retinal explant culture but may not be sufficient for *in vivo* rhythms. In this case, both retinal dopamine and melanopsin could be essential components for retinal circadian rhythms.

Output signalling from pRGCs may also influence the rest of the retina through changes in melanopsin expression levels. Interestingly, dopamine has also been thought to control levels of melanopsin expression (Sakamoto *et al*., 2005). Loss of melanopsin was also shown to affect light-dependent dopamine release (Dkhissi-Benyahya *et al*., 2013). However, another study has also suggested that light-dependent release of dopamine is not dependent on melanopsin and is instead driven primarily by rods and cones (Cameron *et al*., 2009).

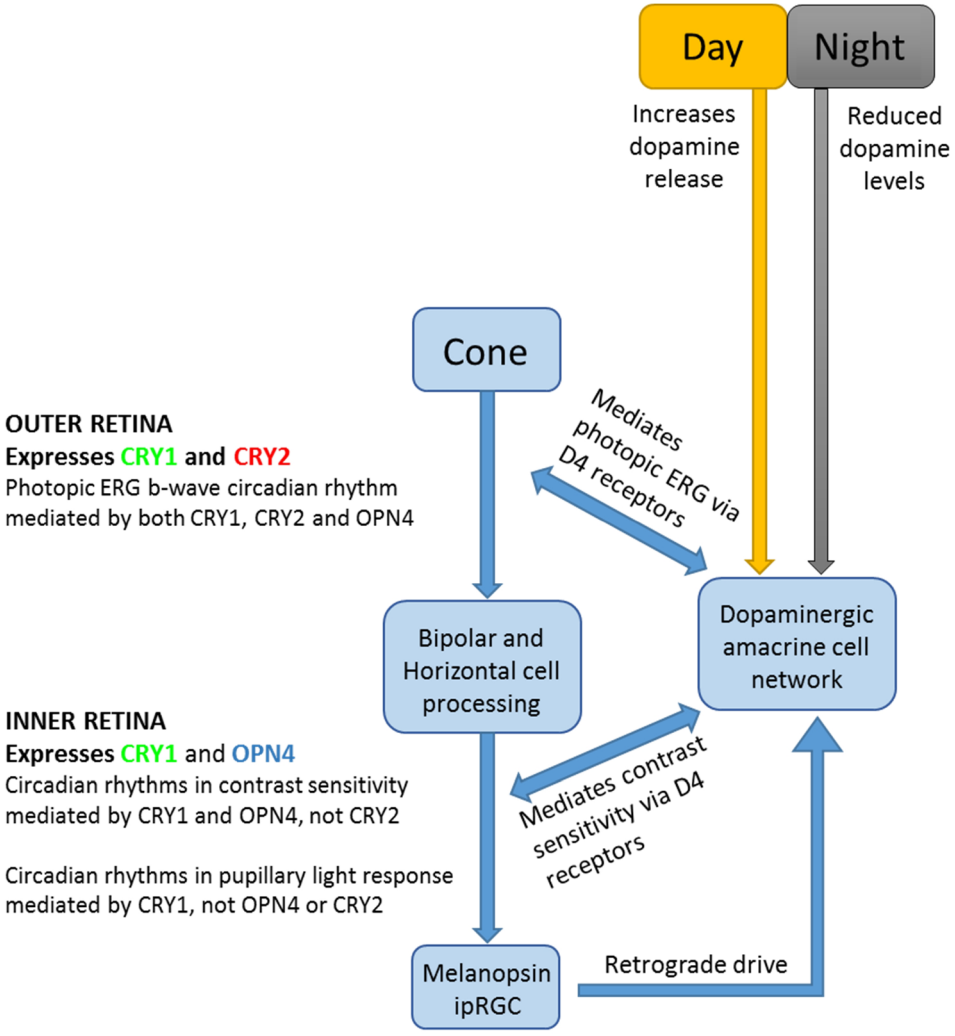

Figure 4.8. Simplified model of the interlocking roles of melanopsin and dopamine in mouse retinal clocks. Melanopsin is expressed only in photosensitive retinal ganglion cells in the ganglion cell layer, whilst dopamine is expressed in dopaminergic amacrine cells. Most retinal cell types have been shown to express clock components, such that most retinal cell types (except rods) could be considered potential retinal clock cells. Here, this figure shows these potential retinal clock cells (blue) as they relate to one another. Dopamine release is greater during the day compared to at night, and dopamine release increases in response to light. For clarity, other various effects of daytime and light are not shown on this schematic. Cones send light information to bipolar and horizontal cells, which then send information to retinal ganglion cells including melanopsin pRGCs. Melanopsin pRGCs have been shown to provide retrograde transmission to dopaminergic amacrine cells. Dopaminergic amacrine cells have a wide effect on retinal clock outputs, and are known to mediate the size and strength of the cone (photopic) ERG via D4 receptors, as well as mediate contrast sensitivity via D4 receptors. Additional effects of dopamine on visual acuity and other retinal functions are not shown. Retinal dopamine-depleted mice have been shown to exhibit persistent molecular retinal rhythms (PER2::LUC oscillations), although rhythms in ERG and contrast sensitivity are attenuated. This indicates that there are additional factors affecting retinal clocks that are not depicted here but will require further research to determine.

4.6 Conclusions

In this chapter, the role of melanopsin in circadian rhythms of contrast sensitivity and pupillary light response was characterized. It was shown that circadian rhythms in contrast sensitivity depend on melanopsin, whilst circadian rhythms in PLR do not. This suggests that these responses are mediated via different mechanisms, and OPN4 affects one but not the other. Furthermore, whilst circadian rhythms in contrast sensitivity and photopic electroretinogram are dependent on melanopsin, circadian rhythms in PLR may be partially controlled by the SCN, or this rhythmicity may be preserved due to some preserved retinal circadian rhythmicity in the *Opn4*$^{-/-}$ mice. Whilst *Cry1* was shown in Chapter 3 to be an essential component of retinal circadian rhythms, here it is shown that *Opn4* may be an important, though not essential, modulator of the retinal clock. Melanopsin may affect the retinal clock through retrograde signalling to dopaminergic amacrine neurons, and in that way, influence retinal clock cells throughout the tissue.

5

In vivo manipulation of retinal Cryptochromes

5.1 Introduction

5.1.1 The retinal clock as a *zeitnehmer*

The role of the retinal clock may not be restricted to regulating local retinal physiology. Given the unique location in the light input pathway, the retinal clock may also gate light input to the master clock in the SCN. Light is the main *zeitgeber* for the central SCN circadian clock, such that if the retinal clock were to modulate the light signal in a phase-dependent manner, this would mean that the phase and rhythmicity of the retinal circadian clock may impact the *zeitgeber* information reaching the central SCN circadian clock. This would make the retinal clock a *zeitnehmer* (German for "time-taker"), where the retinal clock would therefore regulate oscillations of the light *zeitgeber* before it reaches the SCN. In this thesis, the word *zeitnehmer* is used to mean "signal regulator", as the zeitnehmer regulates light signal information before this is sent downstream.

The *zeitnehmer* model of circadian oscillators (**Figure 5.1**) was originally proposed as an alternative hypothesis to the mainstream simple oscillator theory (Roenneberg and Merrow, 1998). The simple oscillator model describes an input (entrainment pathways) sending time information to the oscillator (the mechanism which generates rhythmicity), which then sends time information as an output (pathways which control circadian rhythms). In biological terms, a molecular circadian oscillation is generated by an autoregulatory negative feedback loop which involves a pacemaker gene as a component. The current understanding of the molecular basis of mammalian circadian rhythms makes use of this simple oscillator model, where the input (light) sends time information to the oscillator (TTFL molecular clock) which then sends time information to the rest of the body

(generating circadian rhythms such as body temperature rhythms and the sleep-wake rhythm). The autoregulatory negative feedback loop which generates molecular circadian oscillations involve the core clock genes *Clock, Bmal1, Cry1, Cry2, Per1* and *Per2*, which are deemed components of the TTFL molecular clock. However, similar autoregulatory feedback loops exist in many aspects of physiology (as negative feedback loops), but these do not necessarily lead to self-sustaining rhythmic oscillations.

The *zeitnehmer* model addresses this deficit in the simple molecular clock model by proposing that the input pathway to the oscillator itself (the *zeitgeber*) may be regulated by an autoregulatory feedback loop (Roenneberg and Merrow, 1998). If so, the *zeitgeber* itself would oscillate and its time information would oscillate prior to reaching the biological oscillator. Thus, this would form two interlocking feedback loops, which could account for why self-sustaining rhythmicity occurs in the autoregulatory feedback loops of biological clocks but not that of other negative feedback loops (Young, 2005). Instead of one clock controlling all circadian rhythms, the *zeitnehmer* model postulates that two or more separate, though coupled, oscillators may regulate different circadian rhythms. Though this model incorporates some redundancy in feedback loops, this idea seems to be borne out by biological experimentation; some biological clocks appear to be composed of multiple redundant loops (Hastings *et al*., 2014, Partch *et al*., 2014, Staiger and Green, 2011, Hardin, 2005).

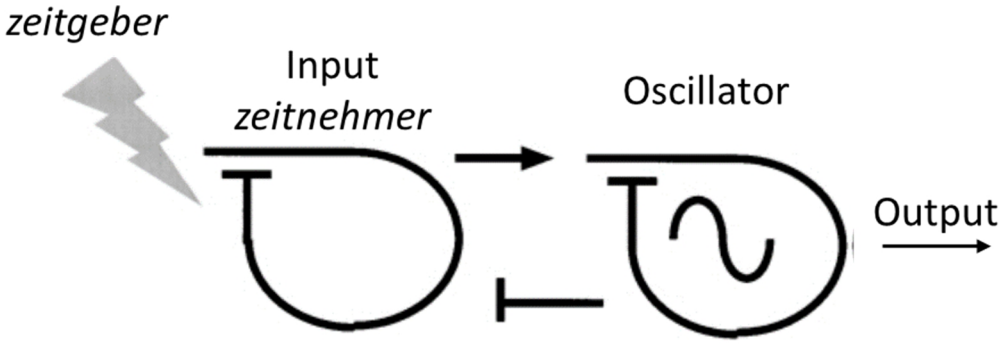

Figure 5.1. Schematic depicting the *zeitnehmer* input feedback model. The oscillator (rhythm generator), depicted as the feedback loop on the right, is downstream of a light input pathway which is itself clock-regulated (the *zeitnehmer,* or signal regulator). The *zeitgeber*, shown as the lightning bolt, is therefore gated by the *zeitnehmer*. The oscillator also provides output information downstream. Figure adapted from Merrow *et al*. (2003).

The *zeitnehmer* model has been shown in biological circadian systems, most notably the unicellular marine alga *Gonyaulax polyedra.* It was found that the *Gonyaulax* circadian system consists of at least two coupled oscillators, which can, under certain conditions, independently drive oscillations in bioluminescence and aggregation (swimming behaviour) separately (Roenneberg and Morse, 1993, Morse *et al*., 1994, Roenneberg and Taylor, 1994). Furthermore, the fungus *Neurospora crassa* receives circadian information from light and temperature cycles via a clock-regulated light input pathway to the temperature-entrainable oscillator. Temperature cycles were found to act as a *zeitnehmer* for light information reaching the *Neurospora* clock. Moreover, clock gene *frequency* (*frq*), which is necessary for a rhythmic *Neurospora* clock, has been characterized as an essential component of the *Neurospora zeitnehmer* (circadian-regulated light-input pathway) (Merrow *et al*., 1999). Loss of *frq* results in loss of the ability of the *Neurospora* clock to synchronize to light-dark cycles, indicating that it is part of the input oscillator. Lastly, the *zeitnehmer* model has also been shown in flowering plant *Arabidopsis thaliana,* where the

early flowering 3 (*elf3*) gene was found to specifically affect light input to the *Arabidopsis* circadian oscillator (McWatters *et al*., 2000).

In mammals, interactions between the retinal and SCN clock are poorly characterized, though several key studies have provided evidence that the mammalian retinal clock may gate light input to the SCN clock and that the retinal and SCN clocks are coupled oscillators. Phosphorylation of ERK (extracellular signal-regulated kinase) is a marker of photic input to the SCN, and also oscillates with a circadian rhythm in the SCN (Obrietan *et al*., 1998). In mice, this rhythm persists in DD conditions, but is lost in the SCN core (though not shell) following enucleation. This data suggests that the eye is necessary for this SCN circadian rhythm (Lee *et al*., 2003).

Furthermore, hamsters subjected to enucleation soon after birth displayed a greater variation in tau (free-running locomotor rhythm periods) under DD conditions compared to those not enucleated (Yamazaki *et al*., 2002). Animals raised in DD since birth show a shorter tau compared to those raised under LD cycles at birth, followed by DD conditions a few days after birth. Interestingly, these results suggest that exposure to LD cycles at and soon after birth lengthens tau and the presence of the eye required for this period lengthening effect, even in constant darkness. These results suggest that communication from the retina to the SCN is important even under constant darkness. Furthermore, this indicates that the coupling between the retinal clock and SCN clock is important for development of circadian organization and also that this coupling affects the free-running period (tau) every day.

Notably, whilst the *zeitnehmer* model has previously been used to understand coupled oscillators within cells, the same model can be used in the context of interlocking clock

networks expressed in separate cells or tissues. The *zeitnehmer* model may be applied to the retinal and SCN clocks as coupled oscillators, where the retinal clock is a *zeitnehmer* for the SCN pacemaker. In this model, the retinal clock might gate light input from the environment, as all light signals reaching the brain must pass first through the retina.

We hypothesized that the retinal clock may gate the environmental light signal in a circadian manner such that, under constant light conditions, the SCN would receive rhythmic light input from the retinal clock. SCN cells exhibit circadian changes in basal firing rates (Meijer *et al*., 1998), as well as in responses to light (Meijer *et al*., 1996), and in membrane conductance (Jiang *et al*., 1997). Such changes may be caused by increases in melanopsin input to both SCN and extra-SCN hypothalamic in the subjective night compared to the subjective day (Brown *et al*., 2011). Furthermore, melanopsin-expressing photosensitive RGCs also exhibit a modest circadian rhythm in sensitivity of intrinsic photoresponses (Weng *et al*., 2009). Though circadian differences in SCN light responses have usually been attributed to an SCN mechanism (Meijer and Schwartz, 2003), it is possible that retinal clock modulation of the SCN light-input pathway, and particularly melanopsin input, make a contribution.

To explore the possibility of a *zeitnehmer* function of the retinal circadian clock, a model where *Cry1*$^{-/-}$*Cry2*$^{-/-}$ global knockout mice, which have no circadian rhythms, could have *Cry1* restored in the inner retina, is therefore considered. This would result in an animal with no SCN rhythms, but with a functional clock restored in the retina. This would allow determination of whether light information is rhythmically gated by the retinal clock to the SCN. If this is the case, these animals would be expected to show circadian rhythms in activity under constant light conditions.

5.1.2 Examining circadian clock properties using constant light conditions

Whilst DD is used to study the circadian clock under free-running conditions in the absence of light *zeitgeber* input (Jud *et al*., 2005, Hughes *et al*., 2015b), studying the gating of light input cannot be conducted under such conditions. As such, constant light (LL) provides a better paradigm to study light gating under constant conditions. However, LL is known to have a range of effects on the circadian system.

Constant light produces a period-lengthening effect in nocturnal species such as mice, and the opposite effect in diurnal species, also known as Aschoff's Rule (Aschoff, 1981, Aschoff, 1960). In mice, constant light was found to inhibit PER2 degeneration, such that constitutively high levels of PER2 may thereby enhance phase delays and lengthen the circadian period (Munoz *et al*., 2005). Constant light desynchronizes SCN clock cells, though individual cellular ability to generate rhythms is not affected (Ohta *et al*., 2005). Furthermore, studies in both wildtype mice and clock-mutant mice have shown that extended exposure to constant light has often resulted in reduced or impaired locomotor activity rhythmicity (Munoz *et al*., 2005, Waite *et al*., 2012, Coomans *et al*., 2013, Sudo *et al*., 2003, Dallmann *et al*., 2011). Stress effects of prolonged LL exposure have also been suggested (Coomans *et al*., 2013), though corticosterone levels are not elevated by constant light conditions (Bhardwaj *et al*., 2015).

Cry1$^{-/-}$*Cry2*$^{-/-}$ mice raised under LD conditions do not show any rhythmicity in locomotor behaviour after exposure to either extended LL (over 45 days) or DD conditions (over 25 days) (Ono *et al*., 2013). Furthermore, previous work has found that *Cry1*$^{-/-}$ mice exposed

to constant light had arrhythmic SCN tissue, whilst *Cry2*$^{-/-}$ mice exposed to constant light remained capable of generating SCN rhythms (Evans *et al*., 2012). This study highlights that *Cry1* plays a more important role towards stabilizing the molecular clock not only in the retina, as found in Chapter 3, but also in the SCN.

Extended constant light exposure to promote and improve locomotor rhythmicity in certain mouse genotypes. Interestingly, *Cry1*$^{-/-}$*Cry2*$^{-/-}$ mice raised under LL conditions could develop rhythmic locomotor activity under DD conditions after prolonged exposure to LL (Ono *et al*., 2013). However, mice that were raised under LD conditions displayed absolutely no rhythmicity under constant light conditions or constant darkness conditions.

Other clock mutant mice have also shown improved circadian rhythms following constant light exposure. Under LL conditions, *Cry1*$^{-/-}$*Per2*$^{-/-}$ mice were found to exhibit circadian rhythms with a shortened tau (~20 hours) (Abraham *et al*., 2006). Furthermore, extended LL conditions restored clock gene rhythms in the SCN and in peripheral tissues.

Vipr2$^{-/-}$ mice were used as a model to determine the effects of constant light (LL) on arrhythmic mice (Hughes *et al*., 2015a). *Vipr2*$^{-/-}$ mice lack VPAC2, the receptor for VIP (Vasoactive Intestinal Peptide). VIP is thought to play an essential role in intercellular communication and cell coupling in the SCN, which contributes to the robustness of SCN circadian rhythmicity. However, unlike *Cry1*$^{-/-}$*Cry2*$^{-/-}$ mice, *Vipr2*$^{-/-}$ mice have intact molecular clock components. *Vipr2*$^{-/-}$ mice were found to exhibit arrhythmic locomotor activity under DD conditions. However, extended LL conditions improved the synchronization between SCN cells and ultimately caused restoration of circadian rhythms in locomotor behaviour in *Vipr2*$^{-/-}$ mice (tau ~ 24 hours).

The difference in circadian clock output resulting from lack of light *zeitgeber* input (DD conditions) and constant light *zeitgeber* input (LL conditions) implies that there are direct effects of light on the measured output (locomotor activity) or that the oscillator can differentiate between lack of input and constant input. *Zeitnehmer* effects may account for the latter by providing rhythmic input to the oscillator even under constant conditions.

5.2 Aims

To determine if the retinal clock exerts direct effects on the SCN pacemaker, restoration of the retinal clock in an arrhythmic mouse model affected circadian rhythms in locomotor activity was investigated. Specifically, it was predicted that successful genetic restoration of *Cry1* (sufficient for retinal rhythmicity – see Chapter 3) would result in a restoration of locomotor activity circadian rhythms under LL conditions. However, under DD, with no photic input, or under LD (where masking occurs), retinal *Cry1* knock-in mice would be expected to appear comparable to *Cry1*$^{-/-}$*Cry2*$^{-/-}$ mice. This work has implications regarding the nature of the retinal clock, its connection to the SCN and circadian physiology in general, as retinal clock function has never been studied in this manner.

In Chapter 5, the specific aims are:

- To generate a *Cry1* AAV suitable for *in vivo* retinal delivery
- To produce and validate *Cry1* knock-in of *Cry1*$^{-/-}$*Cry2*$^{-/-}$ mice
- To assess locomotor activity circadian rhythms of *Cry1* knock-in mice under constant light conditions (LL), light-dark cycles (LD), and constant darkness conditions (DD)

5.3 Methods

5.3.1 Retinal gene expression via AAV viral vectors

Adeno-associated virus (AAV) vectors are the most common viral vector method used to deliver retinal gene therapy, mainly due to its high transduction efficiency and lower risk of immune system response and inflammation (Bennett, 2003). Other viral methods such as lentivirus vectors are usually considered if a large transgene must be packaged (Balaggan and Ali, 2012). Non-viral methods such as unencapsulated plasmid delivery are also available but are less efficient than AAV viral vectors (Andrieu-Soler *et al*., 2006).

Finally, the route of administration regarding intraocular delivery was carefully considered. In retinal gene therapy work, often the photoreceptor layer (outer nuclear layer) is the ideal destination for the AAV viral vector. As such, subretinal injections are often used to ensure the virus penetrates the outer nuclear layer without having to first pass through the inner retina. Injection into the subretinal space is a complex technique and usually requires two separate injections – on into the upper retina and one into the lower retina to ensure adequate coverage (Samantha Da Silva, personal communication). By contrast, intravitreal delivery of viral vectors adequately yields gene expression in the inner retina with a single injection.

5.3.2 Generation of *Cry1*-eGFP AAV

Cry1-eGFP fusion plasmid (with *Cry1* promoter) was kindly provided by Mat Edwards and Prof Michael Hastings (LMB Cambridge). A map of this plasmid is shown as **Figure 5.2.**

Various AAV capsid serotypes are available and provide different tissue specificities. AAV serotype 2/2 (AAV2/2) has been shown to provide the best retinal tissue transduction compared to other serotypes (Hellstrom *et al*., 2009). Furthermore, targeted mutations to the AAV capsid can further optimize transduction efficiency. Given the desire to obtain robust transfection of the inner retina, including the ganglion cell layer and inner nuclear layer, the quad-mutant (Y272,444,500,730F) AAV 2/2 capsid was used (kindly provided by Doron Hickey and Prof Mark Hankins, Oxford), which contains four surface tyrosine (Y) amino acid residues to phenylalanine (F) residues. The quad-mutant AAV2/2 capsid has been shown to provide the most effective transduction of retinal ganglion cells and inner nuclear layer cells following a single intravitreal injection, compared to other mutant AAV2/2 capsids tested (Petrs-Silva *et al*., 2011). As such, this capsid was selected.

Repackaging of the *Cry1*-eGFP plasmid into the quad-mutant AAV 2/2 capsid was performed following a detailed protocol (Bo and Verhaagen, 2015). In summary, HyperFlasks (Corning CellBIND) were seeded with HEK293T cells. 500ug of *Cry1*-eGFP was prepared using a Qiagen Maxiprep kit, and then used to transfect the HEK293T cells within the HyperFlask. After 72 hours of incubation, cells were harvested and centrifuged. The media was then removed, and the cell pellet was treated with lysis buffer (1M Tris(hydroxymethyl) from AnalaR NORMAPUR with 150mM NaCl). Protease inhibitor cocktail is added and the sample is put through freeze-thaw cycles three times.

AAV particles were isolated using an Iodixanol (Sigma) gradient. Benzonase (Millipore) was added to the sample, which was then centrifuged for 20 minutes at 3700g. Iodixanol gradients were prepared in ultracentrifuge tubes using 15%, 25%, 40% and 60% iodixanol fractions, where larger fractions were added under smaller ones until a gradient was

created. The lysate was then added drop-by-drop to the iodixanol gradient, and the ultracentrifuge tube was then centrifuged for 1.5 hours at 59000rpm. An 18 gauge needle fitted to a 5ml syringe was then used to collect as much of the 40% iodixanol phase as possible without contaminants.

Finally, the isolated AAV vectors were purified and concentrated. Amicon 100K Ultra filters were used. The collected 40% iodixanol phase was then centrifuged in the filters until a concentrated volume of approximately 500ul was obtained (30-60 minutes). Two PBS washes were then applied to the filter and the sample was finally spun through the filter until a volume between 250-500ul was reached.

This final volume was then withdrawn, rinsed back over the filter several times, and then aliquoted into 50ul fractions. This was labelled as the *Cry1*-eGFP AAV.

After the final volume was removed, an additional 500ul PBS was rinsed back over the filter and aliquoted into 100ul fractions. This was labelled as AAV wash as they contain a lower titre compared to the initial volume obtained.

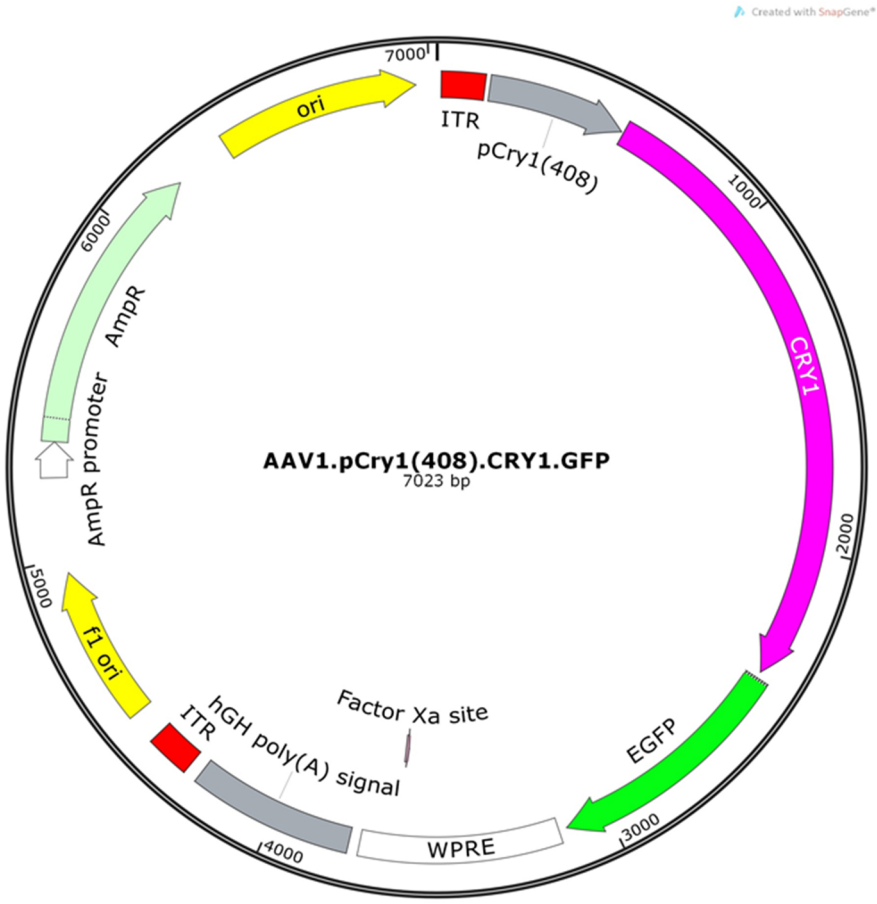

Figure 5.2. *Cry1*::eGFP Plasmid map. A *Cry1* promoter (p*Cry1*, grey) is included to ensure expression only in cells that would have natively expressed *Cry1*. The *Cry1* sequence (pink) is fused to an enhanced Green Fluorescent Protein (green) region. An ampicillin coding sequence is included. Map kindly provided by Mat Edwards (LMB Cambridge).

5.3.3 *Cry1*-eGFP AAV Virus quality controls

Three main checks were made to determine the quality of the *Cry1*-eGFP AAV:

- Virus titre
- Purity of AAV virion capsid proteins
- *In vitro* cell transfection capability

5.3.4 *Cry1*-eGFP AAV Virus Titre

qPCR was used to determine the number of genome copies of AAV present per ml of virus. A virus titre of $1x10^{11}$ or higher is ideal for *in vivo* intravitreal delivery.

To determine the virus titre, a sample of the virus was first digested with a DNase in order remove unpackaged DNA plasmids. This was done as follows:

1ul AAV or AAV wash
1ul DNase I
1ul DNase Buffer
7ul dH_2O

Next, the sample was incubated at 37°C for 30 minutes and then 95°C for 10 minutes to denature it. This sample was then diluted 1:10 in dH_2O.

qPCR primers designed to bind a region of *Cry1* within the plasmid transgene were used. *Cry1* maxiprep DNA was used as a positive template control and was diluted to the following amounts: 10ng, 1ng, 100pg, 10pg, 1pg and 0.1pg). 1 ul of the diluted denatured virus sample was then added to the PCR plate for each reaction, and each reaction was performed in triplicate. Quantifast SYBR Green was used and the qPCR was run using the StepOne Applied Biosystems qPCR machine.

For each reaction:

5ul iTaq (iTaq™ Universal SYBR® Green Supermix)
1ul Forward Primer (2uM)
1ul Reverse Primer (2uM)
2ul dH2O
1ul diluted denatured virus sample

The qPCR protocol was:

Step 1: 95°C for 3 minutes
Step 2: 95°C for 10 seconds
Step 3: 60°C for 30 seconds
Repeat Step 2-3 x40 cycles
Melt curve was obtained at 70°C

A standard curve was generated using the positive template control after converting the positive template control values from mass (g) to amplicon copies. This was done by dividing mass (g) by the molecular weight of the amplicon (g/mol), and then multiplying by Avogadro's constant (calculated using this website: **http://cels.uri.edu/gsc/cndna.html**). This gave the number of amplicon copies. The number of copies was then log-transformed and plotted against the Ct values obtained in the qPCR to form the standard curve. The number of copies in the diluted denatured virus sample could then be obtained using the standard curve. After accounting for all dilution factors, the number of virus copies was reported in units of genome particles per ml.

5.3.5 Purity of *Cry1*-eGFP AAV virion capsid proteins

The purity of AAV virion capsid proteins (VP1, VP2, and VP3) can be assayed using an SDS polyacrylamide gel protocol. For each AAV preparation, usually three samples are collected into separate Eppendorf tubes:

10 ul of AAV + 10 ul molecular grade H_2O
20 ul of AAV wash
20 ul of molecular grade H_2O (negative control)

20 ul Laemmli buffer (1:1 per sample) was then added to each sample, and the samples were heated to 95°C for 15 min. They were then placed on ice while the gel was prepared.

A 10% SDS gel was loaded into a gel tank containing running buffer (1X Tris/Glycine/SDS) buffer solution. A protein ladder (Geneflow prestained ladder S6-0024, 5 ul) was loaded, as well as all three samples. The gel was run for 2 hours at 100V.

The gel was then washed in ddH_2O on a shaker for 5 minutes. This was repeated three times. Gel stain (EX Blue) was then added to the gel to stain it for 45 minutes - 1 hour. The gel was then washed again with ddH_2O until the bands could be clearly visualized.

VP1, VP2 and VP3 capsid proteins build up the AAV virion capsid in a ratio of 1 VP1 to 1 VP2 to 18 VP3. On a stained SDS page gel containing the purified AAV preparation, only three bands should be clearly visible, with VP1 migrating at 87 kDa, VP2 at 73 kDa, and VP3 at 62 kDa. Additional bands or non-specific staining may indicate contaminants (unpackaged transgene plasmid, or nonspecific protein or cellular contaminants). Three clear bands would indicate an AAV preparation of high purity. However, it should be noted that this method cannot differentiate between AAV virion capsids containing the transgene of interest and empty AAV virion capsids. As such, it is important to also determine virus titre.

5.3.6 *Cry1*-eGFP AAV *in vitro* cell transfection

Prior to *in vivo* use of the *Cry1*-eGFP AAV, it was necessary to confirm that the virus was capable of transfecting a general cell line. HEK293T cells were used as they are a general cell line which also contain the *Cry1* promoter. As the *Cry1*-eGFP is controlled by a *Cry1* promoter, this cell line was deemed adequate.

HEK293T cells were plated into 64 well plates. These cells were then transfected with the *Cry1*-eGFP AAV and allowed to incubate for 48 hours. GFP expression was then investigated using a fluorescent microscope.

5.3.7 Animals

Wildtype (C57Bl/6) mice and *Cry1*$^{-/-}$*Cry2*$^{-/-}$ mice were used. See Chapter 2 Section 2.3 for full details.

5.3.8 Genotyping

See Chapter 3 Section 2.3 for full details.

5.3.9 *Cry1*-eGFP AAV *in vivo* intravitreal injections

Mice were anaesthetized with ketamine:medetomidine administered by intraperitoneal injection. Tropicamide (Minims) was applied to increase the pupil size to improve visibility of the fundus. Viscotears was then applied to the eye, and a circular glass coverslip (Ø6mm, VWR International) placed on the cornea. Notched forceps were then used to firmly but gently grip the superior or inferior rectus muscle of the eye in order to keep in still for injection. A small amount of air (0.5ul) was drawn first. Each eye then received an injection of 1 ul of *Cry1*-eGFP AAV or control, using a Hamilton syringe (Hamilton) of 34 gauge, 10mm, point style 2 needle. The drawn air would then be injected into the eye and form a bubble, confirming delivery of the needle contents. *Cry1*-eGFP virus and control were kept in separate syringes, and rinsed with sterile water between injections.

A GFP-only AAV packaged in a quad-mutant virus capsid was used as a negative control for these experiments (kindly provided by Doron Hickey, University of Oxford). This AAV contained a UF6.1 plasmid containing humanised GFP driven by a ubiquitous CMV enhancer, chicken beta-actin, rabbit beta-globin (CAG) promoter. Mice were allowed to recover and returned to the light-tight chambers for further experiments.

5.3.10 Immunohistochemistry

See Chapter 2.3 for immunohistochemistry methods. Chicken polyclonal anti-GFP antibody (ab13970, Abcam) was used to assay CRY1 expression. Anti-GFP primary antibody was incubated overnight at 4°C (1:1000). Alexa 488 conjugated donkey anti-chicken secondary antibody (Life Technologies) was incubated for 2h at room temperature (1:200).

5.3.11 Circadian behavioural testing

Wheel running was used to assay circadian behaviour. Twelve *Cry1*$^{-/-}$*Cry2*$^{-/-}$ mice were individually housed in cages equipped with wheels for 102 days in total (the detailed breakdown of each experiment stage based on lighting conditions, and the length of each stage is presented in **Table 5.1**). Mice were allowed to habituate to these wheel running cages under DD conditions prior to surgery. Under 6 days of DD conditions (DD1), eleven mice demonstrated behavioural arrhythmia, confirming normal *Cry1*$^{-/-}$*Cry2*$^{-/-}$ mouse behaviour under DD conditions. The one mouse (Mouse F) which showed activity rhythms under DD conditions was removed from further analysis. Given the >24 hour free-running tau observed in DD, Mouse F may have been a *Cry2*$^{-/-}$ mouse that was incorrectly genotyped.

Stage of experiment	Stage denoted as	Number of days
First stage of constant dark	DD1	6
First stage of 12:12 light-dark cycle	LD1	19
First stage of constant light	LL1	34
Second stage of 12:12 light-dark cycle	LD2	9
Second stage of constant light	LL2	25
Second stage of constant dark	DD2	9

Table 5.1. All experiment stages, their lengths and how each stage is denoted in Chapter 5.

Intravitreal injection of *Cry1*-eGFP AAV was performed on 7 mice (Mice A, B, C, D, E, G and H), with 4 additional sham controls where a GFP virus under a ubiquitous promoter was used. Mice were then returned to their wheel running cages and placed under 12:12 LD conditions for 19 days (LD1). All mice demonstrated light masking behaviour under LD conditions. That is, all mice demonstrated the majority of their daily locomotor activity in the dark phase, and demonstrated very little locomotor activity in the light phase.

After 20 days of virus incubation, mice were then released into constant light conditions (LL1) of 100 lux intensity for 34 days. 100 lux was used because it is within the dynamic range of rods, cones, and melanopsin. Previous studies have shown that 100 lux is sufficient to produce LL period lengthening effects (which are light intensity-dependent), whilst reducing likelihood of arrhythmia (Lall *et al*., 2010, Hughes *et al*., 2015a). Wheel running behaviour demonstrated the locomotor activity of individual mice under LL conditions.

After LL1, the mice were returned to 12:12 LD conditions for 9 days (LD2). Mice were then released for a second time into constant light conditions for 25 days (LL2) in order to determine whether rhythmic or arrhythmic behaviours were reproducible. Furthermore, LD2 and LL2 allowed for any delayed-onset effects of virus treatment to appear.

Finally, the mice were released directly into constant darkness (DD2) for 9 days immediately following LL2 to determine whether any observed rhythms persisted in constant dark conditions or if these effects were entirely light-dependent.

5.3.12 ClockLab Analysis of wheel running data

Wheel-running activity was automatically recorded in 1-min bins by the ClockLab interface (Actimetrics, Wilmette, IL, USA). Light-dependent resistors connected to ClockLab were used to record the light/dark conditions at all times.

Single- and double-plotted actograms, as well as chi-squared periodograms were generated by ClockLab software. Period information across an entire experimental stage (DD1, LL1, LL2, or DD2) was generated from the appropriate chi-squared periodogram and recorded. For period information within a subset of an experimental stage, onsets of activity bouts were detected automatically by ClockLab software and aligned in order to measure period (tau) of locomotor activity behaviours.

5.3.13 Statistical Analysis

All data are shown with +/- SEM (standard error of the mean). Statistical analysis was performed using paired two-way ANOVA analysis or two-tailed Student's t-test as reported in the legend.

5.4 Results

5.4.1 Construction of CRY1-eGFP AAV with quad-mutant capsid

The *Cry1*-eGFP plasmid was repackaged into the quad-mutant AAV2/2 capsid (repackaging procedures were performed by Dr. Michelle McClements, University of Oxford).

Quality-control experiments were subsequently performed to ensure the *Cry1*-eGFP AAV was of adequate quality for *in vivo* use. AAV purity was analysed using a stained SDS-PAGE gel (**Figure 5.3**). Three clear bands corresponding to approximately the correct sizes for VP1, VP2 and VP3 were found. Based on the clarity and size of the bands and lack of non-specific bands, the AAV preparation was deemed pure enough for *in vivo* delivery.

Virus titre was analysed using qPCR and found to be approximately 2.5 x 10^{11} genome copies/ml. Diluted virus (AAV wash) titre was also analysed using qPCR and found to be approximately 2.5 x 10^{10} genome copies/ml.

Lastly, to check the viability of transfection with the CRY1-eGFP AAV, the virus was transfected into HEK293T cells. Following transfection, cells were observed for GFP signal to observe positive transfection compared to sham controls. A clear GFP signal was found in CRY1-eGFP AAV-transfected cells, showing that the transfection was successful (**Figure 5.4**).

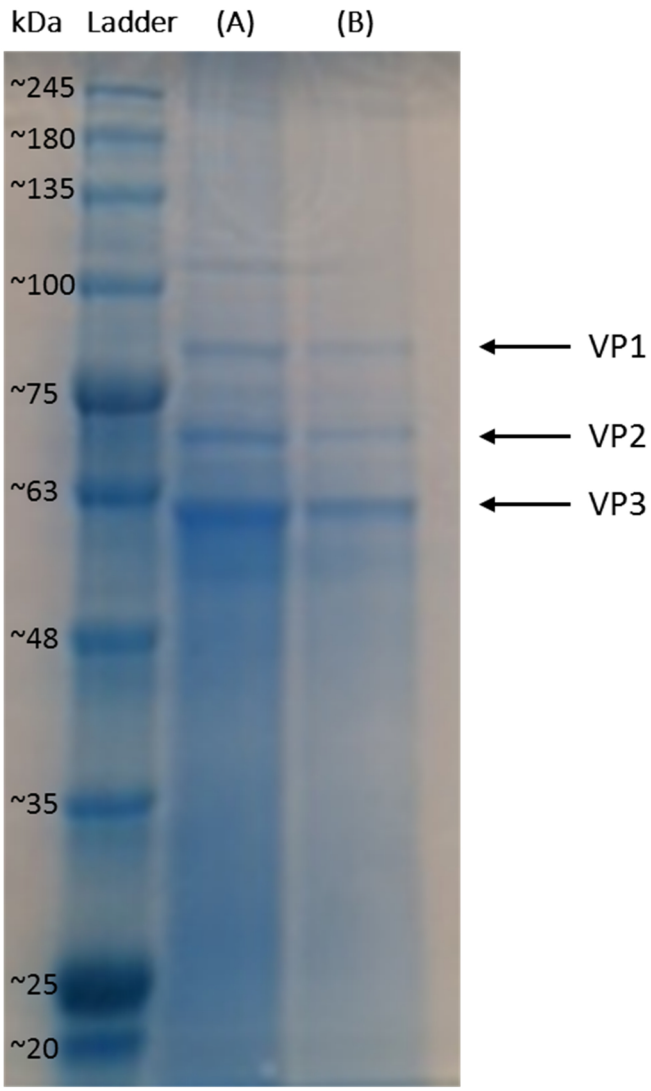

Figure 5.3. Purity of VP1, VP2, and VP3 virus capsids. Stained SDS-PAGE gel shows three distinct bands for (A) Concentrated *Cry1*-eGFP AAV and (B) Wash/Diluted *Cry1*-eGFP AAV. Correct band sizes are VP1 at 87 kDa, VP2 at 73 kDa, and VP3 at 62 kDa.

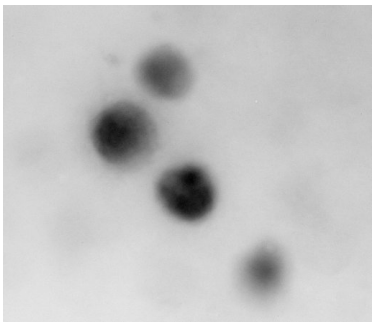

Figure 5.4. Example image of HEK 293T cells transfected with *Cry1*-eGFP virus. A clear GFP (black, due to camera settings) signal was found in CRY1-eGFP AAV-transfected cells, demonstrating successful transfection, whilst sham-transfected cells showed no GFP signal.

5.4.2 Restoration of CRY1 expression by intravitreal injection of *Cry1*-eGFP virus into *Cry1*$^{-/-}$*Cry2*$^{-/-}$ mice

Whilst intraocular AAV delivery for ocular gene therapy has often used retinal-degenerate mouse models, *Cry1*$^{-/-}$*Cry2*$^{-/-}$ mice have normal retinal anatomy, and all retinal cell layers are preserved (see Chapter 2). Importantly, the CRY1 retinal localization data (see Chapter 2) allowed the effects of AAV viral restoration of *Cry1* in the *Cry1*$^{-/-}$*Cry2*$^{-/-}$ mice to be predicted, as the inserted gene was under the control of the *Cry1* promoter. As such, *Cry1* should only be expressed in cells that would have natively expressed *Cry1*.

Cry1-eGFP was introduced to *Cry1*$^{-/-}$*Cry2*$^{-/-}$ mouse retina (n=5) by *in vivo* intravitreal injection. After 4 weeks of incubation time, mice were sacrificed and their retinae were sectioned in preparation for immunohistochemistry. CRY1 protein expression was confirmed by staining sectioned retinae with GFP antibody. CRY1 protein was found to be expressed clearly in the inner nuclear layer and ganglion cell layer (Figure 5.5). Given that the *Cry1*-eGFP virus was operating under a *Cry1* promoter, these cells would normally express *Cry1*. Upon close inspection, no photoreceptors (no rods or cones) showed a GFP signal. Otherwise, the pattern of GFP expression appears similar to that of CRY1 expression in the inner nuclear layer and ganglion cell layer seen in wildtype mice (Chapter 2). Restoration of *Cry1* expression was confirmed in all five *Cry1*-eGFP treated mice. Sham-treated mice did not display any detectable GFP signal.

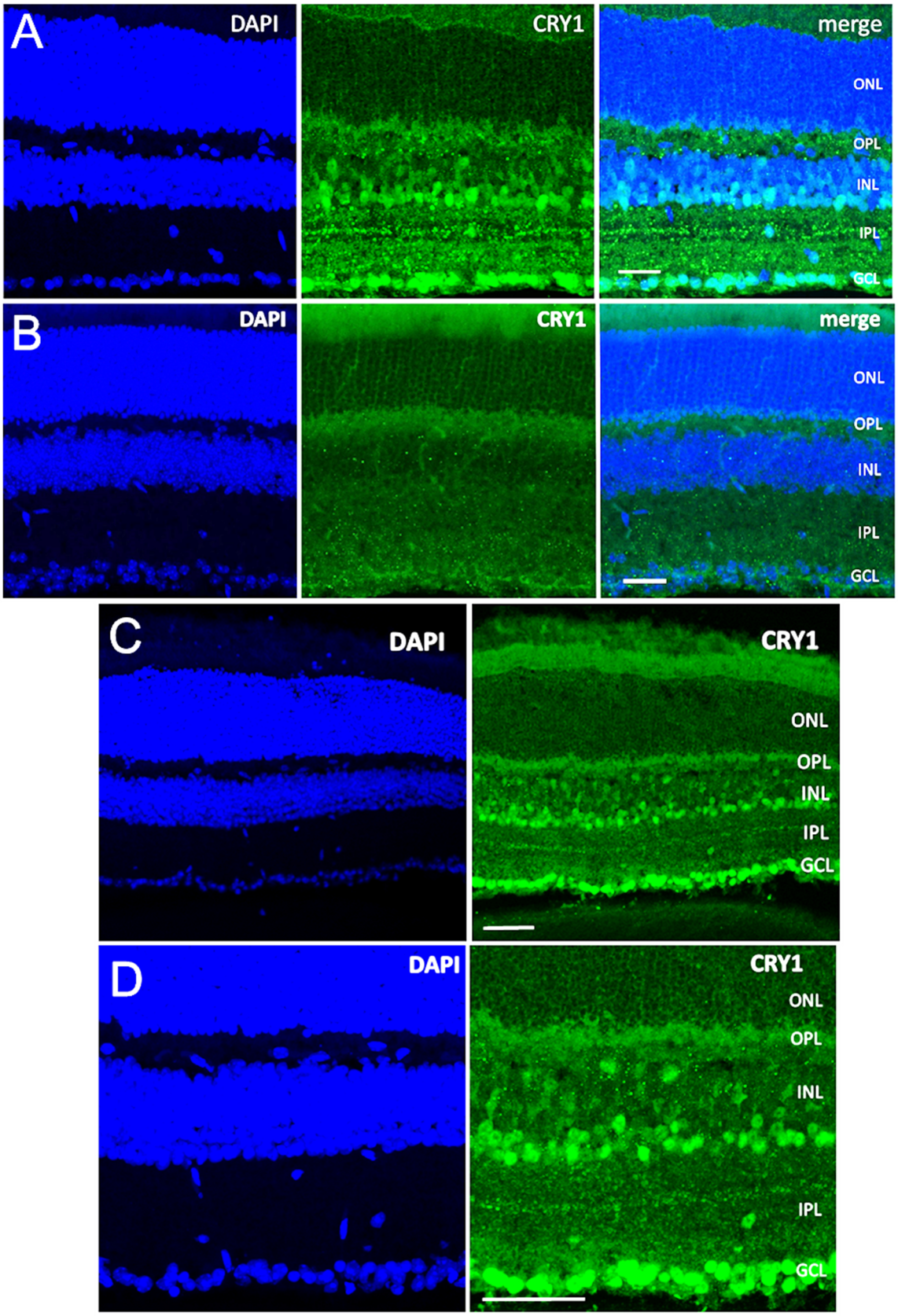
A
DAPI
CRY1
merge
ONL
OPL
INL
IPL
GCL
B
DAPI
CRY1
merge
ONL
OPL
INL
IPL
GCL
C
DAPI
CRY1
ONL
OPL
INL
IPL
GCL
D
DAPI
CRY1
ONL
OPL
INL
IPL
GCL

Figure 5.5.

Figure 5.5. CRY1 expression (as detected by GFP antibody) is restored by intravitreal injection of *Cry1*-eGFP virus into *Cry1*$^{-/-}$*Cry2*$^{-/-}$ mice. Scale bar of for all images = 20µm. (A) CRY1 (green) shows restored expression in the inner nuclear layer, and ganglion cell layer. By visual comparison with DAPI (blue), no CRY1 restoration signal is observed in the photoreceptor cell layer (outer nuclear layer). (B) No CRY1 expression is found following a sham intravitreal injection into *Cry1*$^{-/-}$*Cry2*$^{-/-}$ mice. Injection protocol was fully followed but no substances were injected, except for a small gas bubble. CRY1 is green and DAPI is blue. (C) CRY1 (green) shows restored expression in the inner nuclear layer, and ganglion cell layer. By visual comparison with DAPI (blue), no CRY1 restoration signal is observed in the photoreceptor cell layer (outer nuclear layer). (D) Higher magnification of CRY1 (green) shows restored expression in the inner nuclear layer, and ganglion cell layer. By visual comparison with DAPI (blue), no CRY1 restoration signal is observed in the photoreceptor cell layer (outer nuclear layer).

5.4.3 Separation of locomotor activity recordings into experimental stages for analysis

A sample double-plotted actogram across all stages of the entire experiment (except DD2) is depicted in **Figure 5.6.** Actograms from each experimental mouse were split into individual experimental stages then analysed. A summary of the full analysis is provided in **Table 5.2**.

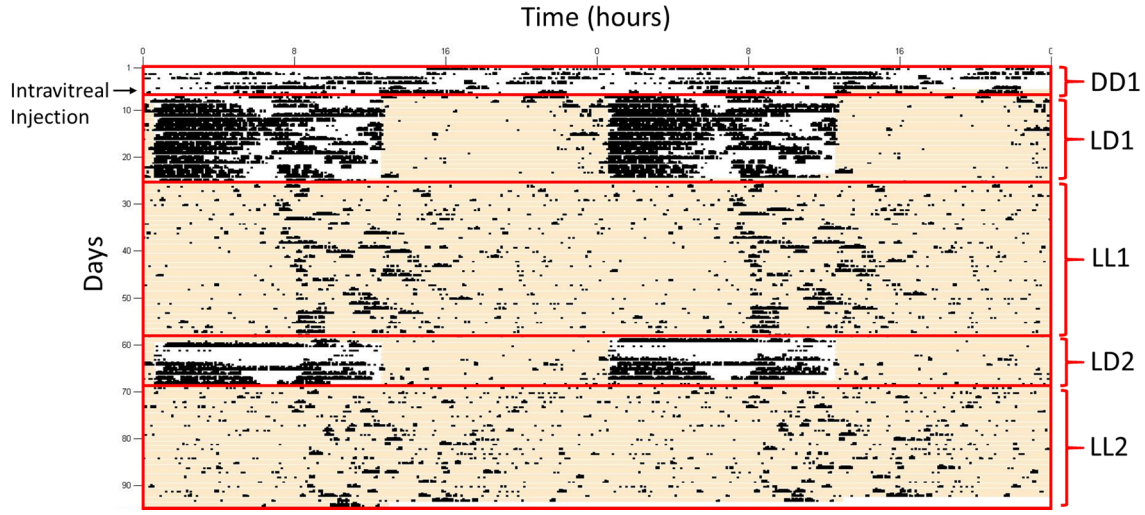

Figure 5.6. Double plotted actogram showing the activity of a single mouse over more than 90 days of continuous activity recording. Mice underwent 6 days of DD (constant darkness, DD1) to confirm the normal arrhythmic activity pattern of a *Cry1*$^{-/-}$*Cry2*$^{-/-}$ mouse. On Day 6, intravitreal injection of *Cry1*-AAV was performed. Mice were then allowed to recover under an LD cycle for 19 days (LD1) before being released into LL for 34 days (LL1). Following LL treatment, mice were returned to LD conditions for 9 days (LD2) before being released again into LL for 25 days (LL2). Finally, mice were released into DD for 9 days (DD2, not shown here). Black indicates activity as measured by wheel running. Yellow background indicates lights on, white background indicates lights off.

ID and Treatment	DD1 Rhythm	Tau (hrs)	LL1 Rhythm	Tau (hrs)	LL2 Rhythm	Tau (hrs)	DD2 Rhythm	Tau (hrs)
Mouse A CRY1 virus	No	n/a	No	n/a	No	n/a	Ultradian rhythm, 3x per day	~8
Mouse B CRY1 virus	No	n/a	arrhythmic for 12 days, then rhythmic for 10 days and then arrhythmic again, for 13 days	25	Yes, delayed	24.4	Yes	24.5
Mouse C CRY1 virus	No	n/a	Yes	24	Yes	26.5	Yes	23.5
Mouse D CRY1 virus	No	n/a	Yes, delayed	23.9	Yes, variable tau	26.5, 23.9	Yes	25.1
Mouse E CRY1 virus	No	n/a	Yes, delayed, ultradian rhythm	11.9, 13	Ultradian rhythm, 3x per day, 7.75 hrs apart	23.17 for 17 days then 25.17 for 9 days	No	n/a
Mouse F CRY1 virus	Yes	24.5	n/a	n/a	n/a	n/a	n/a	n/a
Mouse G CRY1 virus	No	n/a	No	n/a	No	n/a	Yes	24.4
Mouse H CRY1 virus	No	n/a	No	n/a	No	n/a	No	n/a
Mouse I Sham	No	n/a	No	n/a	No	n/a	No	n/a
Mouse J Sham	No	n/a	No	n/a	No	n/a	No	n/a
Mouse K Sham	No	n/a	No	n/a	No	n/a	Yes	24.4
Mouse L Sham	No	n/a	No	n/a	No	n/a	No	n/a

Table 5.2. Analysis of actograms for all experimental mice. The circadian light conditions experienced by each mouse have been denoted as DD1, LL1, LL2 and DD2 for clarity. See Table 5.1 for explanation. Green cells indicate where rhythms were observed. Four of seven *Cry1*-eGFP AAV-injected *Cry1*$^{-/-}$*Cry2*$^{-/-}$ mice demonstrated consistent rhythms under LL conditions (either LL1 or LL2 or both). Six of seven *Cry1*-eGFP AAV-injected *Cry1*$^{-/-}$*Cry2*$^{-/-}$ mice demonstrated rhythmic or weakly rhythmic activity patterns in DD2. Furthermore, one of four sham-treated mice exhibited weak activity rhythms in DD2. One *Cry1*$^{-/-}$*Cry2*$^{-/-}$ mouse demonstrated rhythms in DD1 conditions so was removed from further analysis (shown in grey).

5.4.4 Examination of circadian rhythms in locomotor activity using actograms and chi-squared periodograms

Actograms and chi-squared periodograms are used to examine whether circadian rhythmicity was restored following intravitreal injection of *Cry1*-eGFP AAV. The results from each experimental stage are depicted in the following Figures: stage DD1 is depicted in **Figure 5.7**, stage LL1 in **Figure 5.8**, stage LL2 in **Figure 5.9** and stage DD2 in **Figure 5.12**. Actograms and chi-squared periodograms from LD1 and LD2 are not depicted because all mice showed negative masking under LD conditions.

5.4.5 Behavioural screening of *Cry1*$^{-/-}$*Cry2*$^{-/-}$ mice during DD1

At the beginning of the experiment, eight mice were designated from A-H. All tested mice demonstrate arrhythmic locomotor behaviour during DD1, confirming a *Cry1*$^{-/-}$*Cry2*$^{-/-}$ phenotype, with the exception of Mouse F. As consistent rhythmic locomotor activity with a 24.5 hour period was exhibited, Mouse F was removed from the experimental cohort. After the DD1 recording, Mice A-H (except F) received *Cry1*-eGFP virus treatment, whilst Mice I-L received a sham GFP-only treatment.

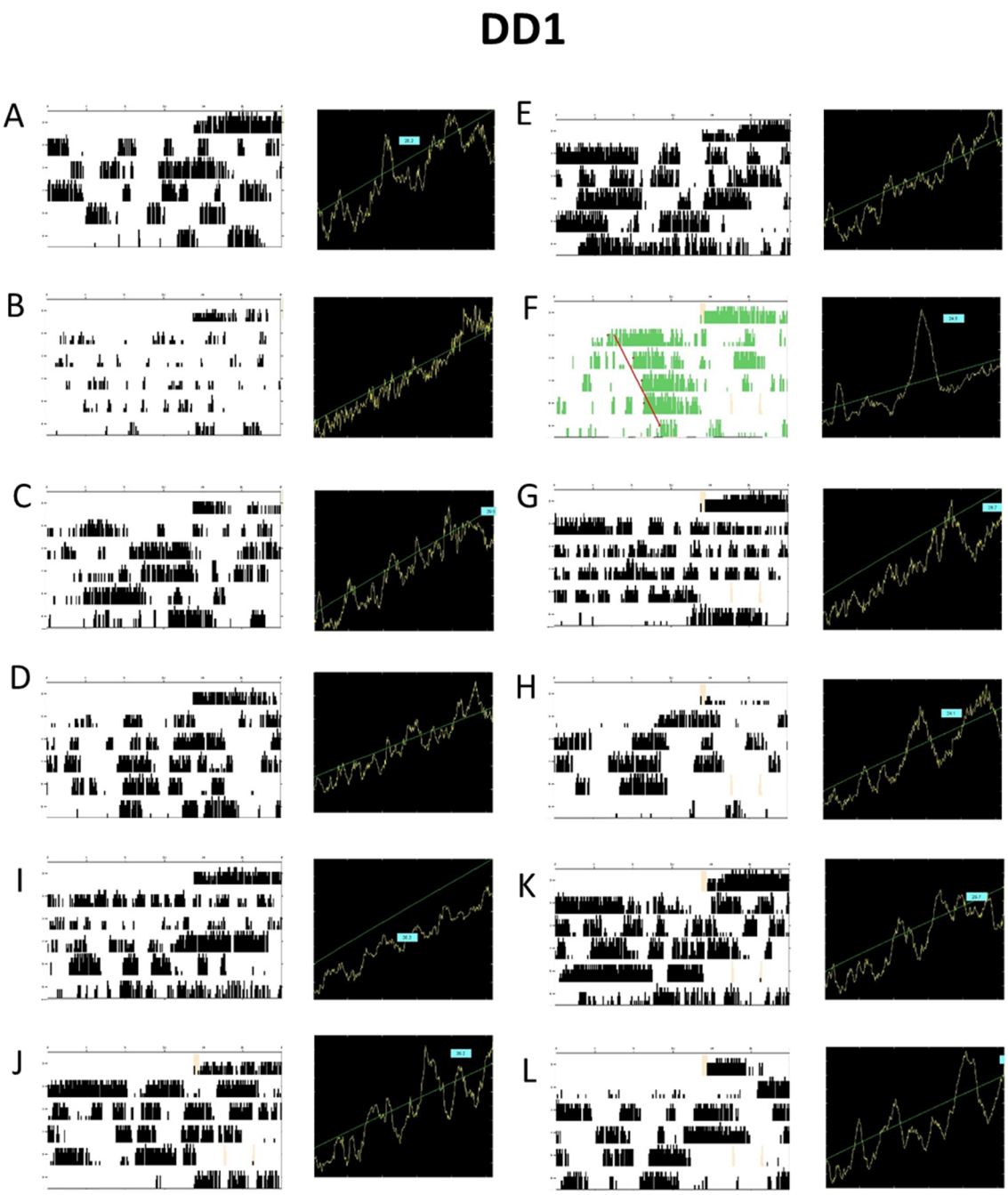

Figure 5.7. *Cry1*$^{-/-}$*Cry2*$^{-/-}$ mice do not display locomotor activity circadian rhythms in DD1 (first exposure to constant darkness, prior to virus treatment). Single-plotted actograms and chi-squared periodograms from all mice during DD1. All mice (A-L) show arrhythmic locomotor activity, which is typical for *Cry1*$^{-/-}$*Cry2*$^{-/-}$ mice, except for Mouse F, which demonstrated consistently rhythmic locomotor activity with a 24.5 hour period. As such, Mouse F was removed from the experimental cohort. After the DD1 recording, Mice A-H received *Cry1*-eGFP virus treatment, whilst Mice I-L received a sham GFP-only treatment. Black indicates activity as measured by wheel running. Yellow background indicates lights on, white background indicates lights off.

5.4.6 Rhythmic behaviour was observed in *Cry1*-eGFP virus-treated mice during LL1 and LL2

Out of the seven *Cry1*$^{-/-}$*Cry2*$^{-/-}$ mice injected with the *Cry1*-eGFP AAV, four demonstrated consistent rhythms during either LL1 or LL2 or both (**Figure 5.8** and **Figure 5.9**). However, each mouse exhibited unique characteristics despite all showing a circadian rhythm in constant light conditions. Note that where red arrows are shown in **Figure 5.8** and **Figure 5.9**, Panel 1 depicts the full actogram/periodogram whilst Panel 2 indicates the rhythmic portion of the actogram/periodogram.

Specifically, one mouse (Mouse C) demonstrated very robust rhythms (tau = 24 hours in LL1, tau = 23.8 hours in LL2) during both stages of constant light. Three mice (Mice B, D, and E) showed delayed circadian rhythmicity. Mouse C was the only mouse to show robust locomotor activity rhythmicity throughout both LL1 and LL2. An enlarged chi-squared periodogram for Mouse C in LL1 as well as the full actogram for Mouse C is shown as **Figure 5.10**.

Mouse B showed rhythmic locomotor activity patterns for 10 days (tau = 24.4 hours) in LL1 after 12 days of arrhythmicity and then became arrhythmic again for the rest of LL1. In LL2, after 15 days of arrhythmicity, this mouse then showed rhythmic activity for 7 days (tau = 25.8 hours).

Mouse D demonstrated rhythmic activity for 8 days (tau = 23.9 hours) at the end of LL1 after 26 days of arrhythmicity. In LL2, Mouse D showed rhythmicity for the entire 25 days with an average tau of 23.8 hours. On closer inspection of LL2, two distinct segments of

time had two different activity periodicities. Within LL2, Mouse D showed a tau of 26.5 hours, and also a tau of 23.9 hours.

Finally, Mouse E demonstrated rhythmicity for 11 days with two different periods at the end of LL1. For 6 days, Mouse E had a tau of 11.9 hours, which was then followed by 5 days with a tau of 13 hours. Then, in LL2, Mouse E had a consistent rhythmicity for all 25 days. Interestingly, Mouse E also demonstrated ultradian patterns (with a period <24 hours) in locomotor activity (an enlarged LL2 chi-squared periodogram and LL2 actogram for Mouse E is shown as **Figure 5.11**). Locomotor activity was confined to three bouts per day of approximately 7.75 hours apart. Furthermore, if the onsets of every 3 bouts were aligned, they gave a period (tau) of 23.17 hours for 15 days. This abruptly then changed to 25.17 hours for 10 days.

As such, whilst three *Cry1* virus-treated mice (Mice B, C and D) showed conventional approximately 24-hour periodicity in locomotor rhythms, one (Mouse E) showed an ultradian pattern of approximately three bouts every 24-hour period. By contrast, three *Cry1* virus-treated mice (Mice A, G, and H) did not demonstrate detectable locomotor activity patterns. In both LL1 and LL2, no sham-treated mice (Mice I-J) demonstrated any locomotor rhythmicity. A chi-squared test was performed to compare the proportions of mice exhibiting rhythms based on treatment (four of seven *Cry1*-virus treated and zero of four sham treated), yielding a p-value of 0.0581. Although not significant, this result indicates that a trend exists, and the *Cry1*-virus treated mice show a trend towards significantly increased locomotor activity rhythmicity compared to sham, under constant light conditions. Repeating this experiment with additional mice may indicate if any significant effect exists.

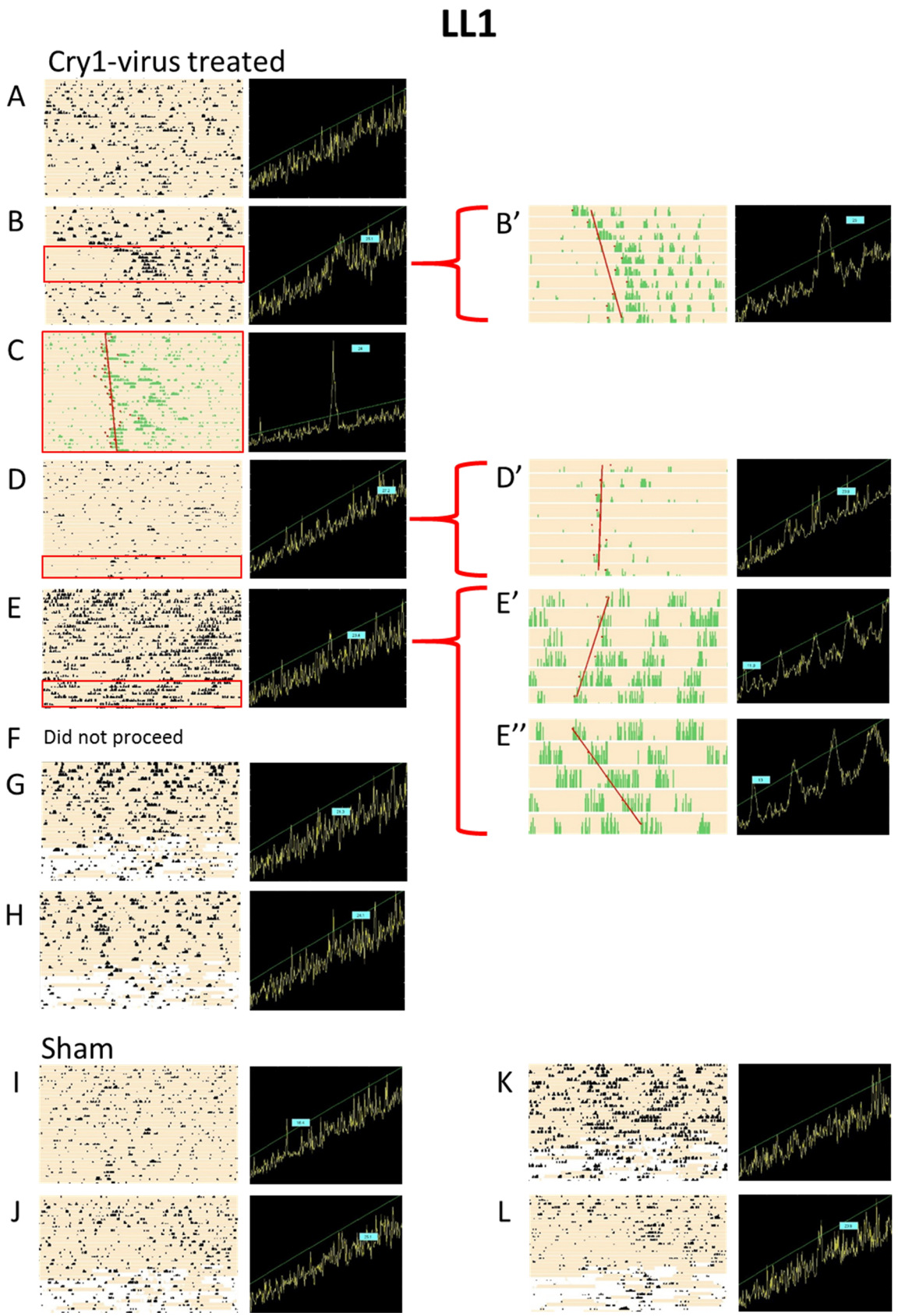
LL1
Cry1-virus treated
A
B
B'
C
D
D'
E
E'
E''
F
Did not proceed
G
H
Sham
I
K
J
L

Figure 5.8.

Figure 5.8. A subset of retinal *Cry1* knock-in *Cry1*$^{-/-}$*Cry2*$^{-/-}$ mice show circadian rhythms of locomotor activity during LL1 (first exposure to constant light after intravitreal injections). Single-plotted actograms and chi-squared periodograms from all mice during LL1. *Cry1*$^{-/-}$*Cry2*$^{-/-}$ mice A-F were subjected to *Cry1*-eGFP virus intravitreal injections, whilst *Cry1*$^{-/-}$*Cry2*$^{-/-}$ mice I-L were given sham intravitreal injections. Red rectangles indicate rhythmic portions of actograms shown. Where mice showed rhythmic behavior in a portion of the actogram, red brackets are shown: the left Panel depicts the full actogram/periodogram and the right Panel depicts rhythmic portion of the actogram/periodogram. Under LL1, only Mouse C shows consistent rhythmic locomotor behaviour throughout the entire 34 days – note the single peak in the corresponding periodogram, tau = 24 hours. Interestingly, Mice B, D and E exhibited rhythmic locomotor behaviour for several days after first exhibiting arrhythmic locomotor behaviour. Mouse B was arrhythmic for 12 days, then rhythmic for 10 days, and then arrhythmic again for 13 days (full actogram shown in Panel B, rhythmic activity shown in Panel B' where tau = 25 hours). Mouse D was rhythmic for 8 days at the end of LL1 (Panel D1 shows full actogram, panel D2 shows rhythmic activity, where tau = 23.9. Mouse E was rhythmic for 11 days with two different periods at the end of LL1 (Panel E shows full actogram, Panel E' shows rhythmic activity for 6 days at tau = 11.9 hours, and Panel E'' shows rhythmic activity for a subsequent 5 days at tau = 13 hours). All sham-treated mice exhibited arrhythmic locomotor behaviour during LL1. Note that Mouse F was removed from the experimental cohort. On actograms, black indicates activity as measured by wheel running. On periodograms, green line indicates threshold of significance.

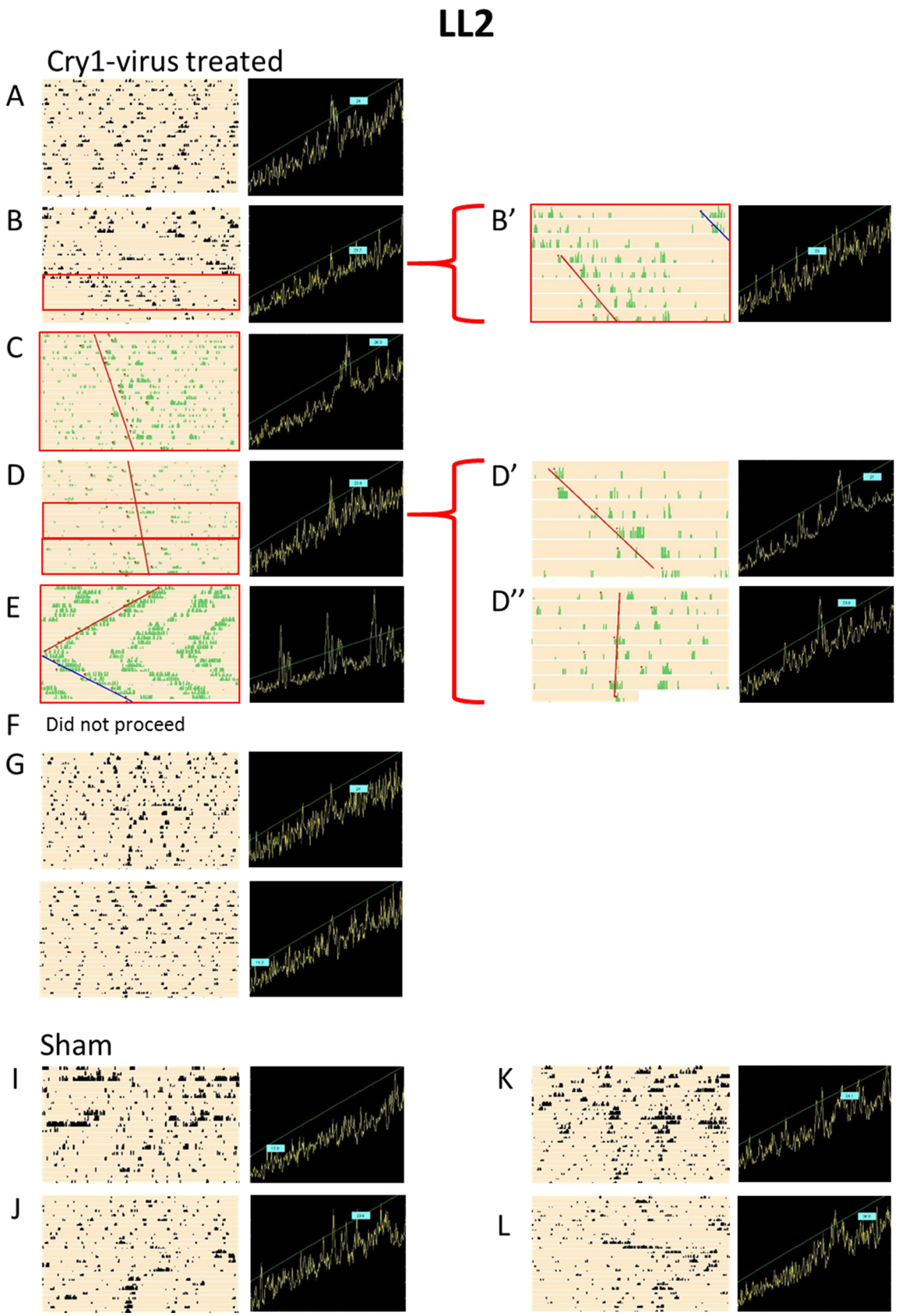
LL2
Cry1-virus treated
A
B
B'
C
D
D'
D''
E
F
Did not proceed
G
Sham
I
J
K
L

Figure 5.9.

Figure 5.9. A subset of retinal *Cry1* knock-in *Cry1*$^{-/-}$*Cry2*$^{-/-}$ mice repeatedly show circadian rhythms of locomotor activity during LL2 (second exposure to constant light after intravitreal injections). Single-plotted actograms and chi-squared periodograms from all mice during LL2. *Cry1*$^{-/-}$*Cry2*$^{-/-}$ mice A-F were subjected to *Cry1*-eGFP virus intravitreal injections, whilst *Cry1*$^{-/-}$*Cry2*$^{-/-}$ mice I-L were given sham intravitreal injections. Red rectangles indicate rhythmic portions of actograms shown. Where mice showed rhythmic behavior in a portion of the actogram, red brackets are shown: the left Panel depicts the full actogram/periodogram and the right Panel depicts rhythmic portion of the actogram/periodogram. Under LL2, Mouse C shows consistent rhythmic locomotor behaviour throughout the entire 25 days, tau = 26.5 hours. Similarly to LL1, Mice B, D and E again exhibited rhythmic locomotor behaviour for several days after first exhibiting arrhythmic locomotor behaviour. Mouse B became rhythmic for 8 days at the end of LL2 (full actogram shown in Panel B, rhythmic activity shown in Panel B' where tau = 24.4 hours). Mouse D demonstrated an average locomotor rhythm tau of 23.8 hours (Panel D), but this could be broken down into segments of time where Mouse D showed a tau of 26.5 hours (Panel D') and also a tau of 23.9 hours (Panel D''). Mouse E demonstrated a consistent rhythmicity with two different periods. A tau of 23.17 hours for 17 days was followed by a tau of 25.17 for 9 days. In addition to this, Mouse E demonstrated ultradian patterns in locomotor activity, with bouts every ~7.75 hours. All sham-treated mice exhibited arrhythmic locomotor behaviour during LL2. Note that Mouse F was removed from the experimental cohort. On actograms, black indicates activity as measured by wheel running. On periodograms, green line indicates threshold of significance.

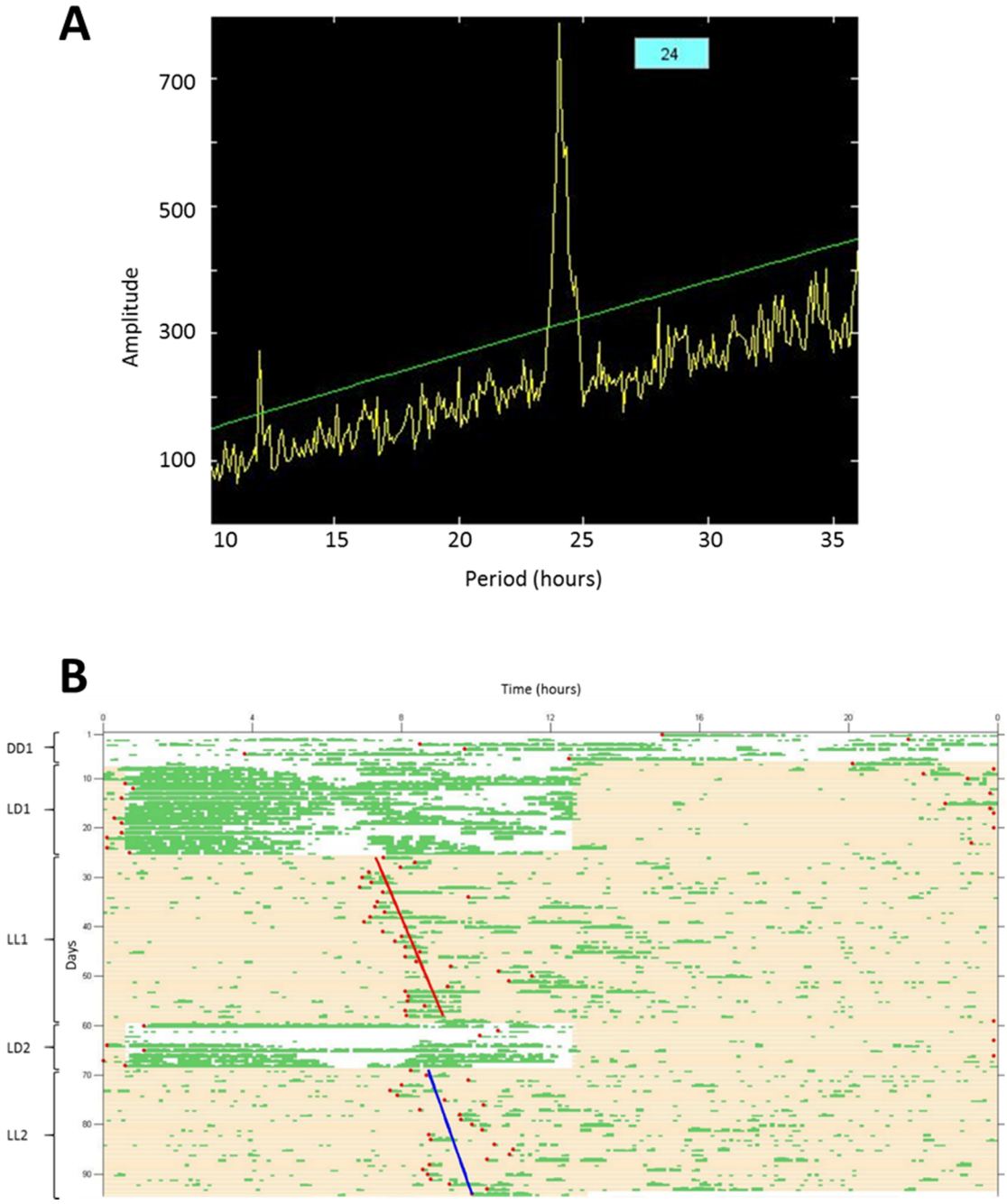

Figure 5.10. Retinal *Cry1* knock-in can restore behavioural rhythms under constant light conditions in arrhythmic *Cry1*$^{-/-}$*Cry2*$^{-/-}$ mouse model. Mouse C demonstrates circadian rhythms of locomotor activity during LL1 and LL2. (A) Example chi-squared periodogram of Mouse C during LL1, demonstrating that it exhibited rhythmic locomotor behaviour with a period of 24 hours (yellow peak). Green line indicates threshold level for statistically significant rhythms. A minor peak is also visible at tau = 11.95 hours. (B) Single-plotted actogram showing Mouse C activity patterns over the course of the experiment. Red dots indicate onset of activity. Red line indicates a period (tau) of 24.06 hours as calculated over LL1. Blue line indicates a period (tau) of 24.05 hours as calculated over LL2. Green indicates activity as measured by wheel running. Yellow background indicates lights on, white background indicates lights off.

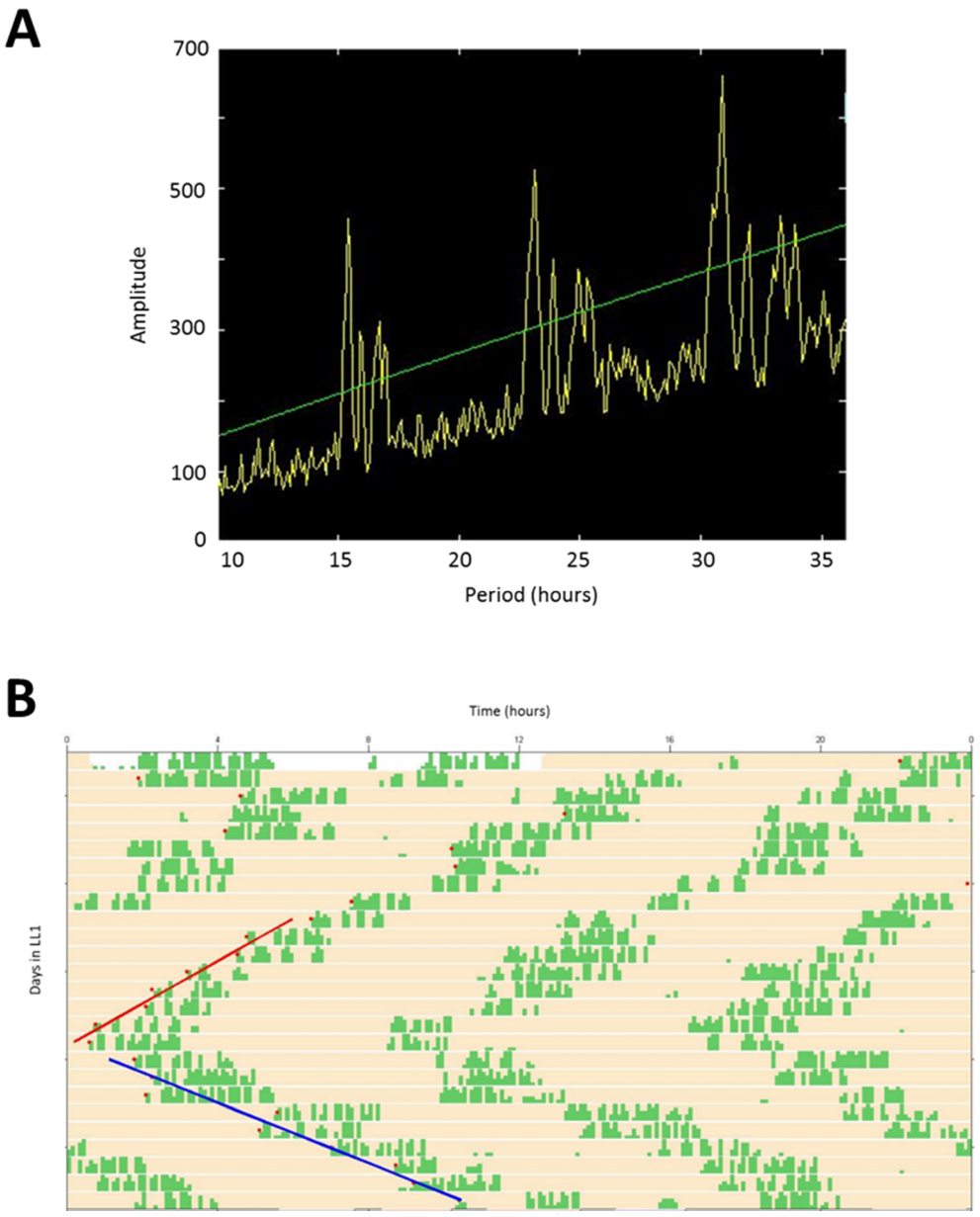

Figure 5.11. Restored behavioural circadian rhythms under constant light following retinal *Cry1* knock-in in *Cry1*$^{-/-}$*Cry2*$^{-/-}$ mice show variable period length. Mouse E demonstrates ultradian rhythms of locomotor activity during LL2. (A) Chi-squared periodogram of Mouse E during LL2 demonstrating that it exhibited rhythmic locomotor behaviour with three significant periods (yellow peaks) at tau = 15.41 hours, tau = 23.31 and tau = 30.91 hours. Green line indicates threshold level for statistically significant rhythms. Minor peaks are also visible at periods of 15.90, 16.68, 16.89, 23.88, 24.91, 25.30, 31.99, 33.3, and 33.89 hours. (B) Single-plotted actogram showing Mouse E activity patterns over the course of LL2, where consistent ultradian rhythms were exhibited. Red dots indicate onset of activity. Red line indicates a period (tau) of 23.17 hours. Blue line indicates a period (tau) of 25.17 hours. Green indicates activity as measured by wheel running. Yellow background indicates lights on, white background indicates lights off.

5.4.7 Circadian rhythms in locomotor activity were detected in both *Cry1-eGFP* virus-treated and sham-treated mice under DD following constant light exposure (DD2)

Examination of mouse activity during DD2 (constant darkness conditions following LL2) yielded further interesting results. Five of the seven *Cry1* virus-treated mice (Mice A, B, C, D, and G) demonstrated circadian rhythms of locomotor activity during DD2. One of the sham-treated mice (Mouse K) also exhibited rhythmic locomotor activity during DD2.

In the periodogram for Mouse A (as seen in **Figure 5.12** A) more than one significant peak could be identified. Mouse A demonstrated ultradian rhythms of approximately three bouts for every 24-hour period in DD2. This mouse exhibited rhythmic locomotor behaviour with three significant periods (yellow peaks) at tau = 14.69 hours, tau =22.0 and tau = 29.3 hours (**Figure 5.12** A, actogram). When activity bouts are aligned and the tau is measured, two different periods can be measured at the same time – tau = 22 hours and tau = 26.08 hours (**Figure 5.12** A, chi-squared periodogram).

An example DD2 actogram and chi-squared periodogram (from Mouse B) demonstrating clear circadian rhythms in locomotor activity (tau=24.56 hours) is enlarged and depicted in **Figure 5.13**.

A chi-squared test was performed to compare the proportions of mice exhibiting rhythms based on treatment (five of seven *Cry1*-virus treated and one of four sham treated), yielding a p-value of 0.1369. This indicates that there is no significant difference in rhythmicity between *Cry1*-virus treated and sham-treated mice under constant dark conditions.

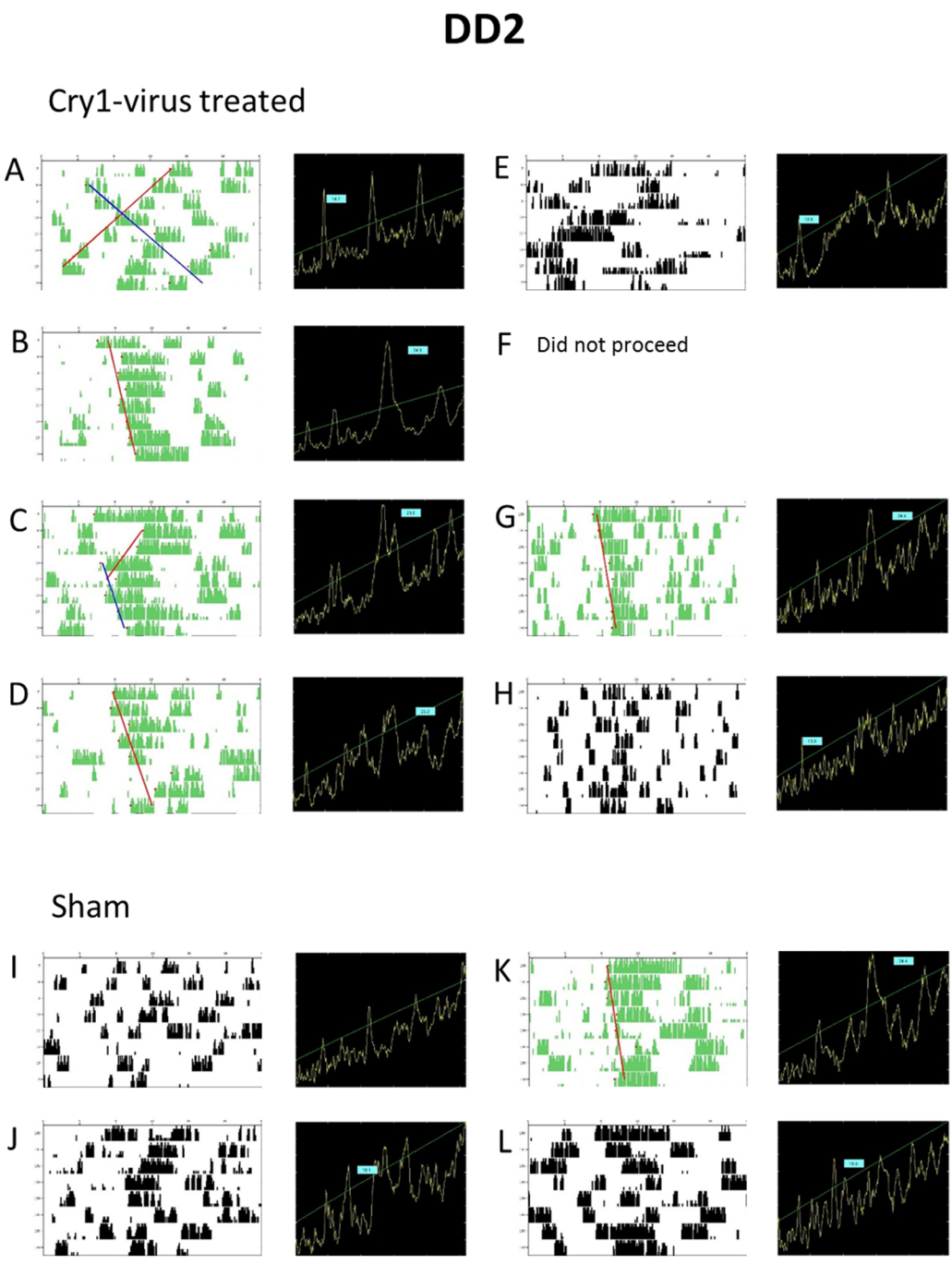

Figure 5.12. A subset of retinal *Cry1* knock-in *Cry1*$^{-/-}$*Cry2*$^{-/-}$ mice show circadian rhythms of locomotor activity during DD2 (second exposure to constant darkness after intravitreal injections). Single-plotted actograms and chi-squared periodograms from all mice during DD2. Mice A-F were subjected to *Cry1*-eGFP virus intravitreal injections, whilst mice I-L were given sham intravitreal injections. Under DD2, Mice A, B, C, D, and G all exhibited rhythmic locomotor activity during the 9 days of constant darkness. One sham-treated mouse, Mouse K, also showed rhythmic locomotor activity in DD2. See **Table 5.2** for details on tau and periodicity information. Note that Mouse F was removed from the experimental cohort. On actograms, black indicates activity as measured by wheel running. On periodograms, green line indicates threshold of significance.

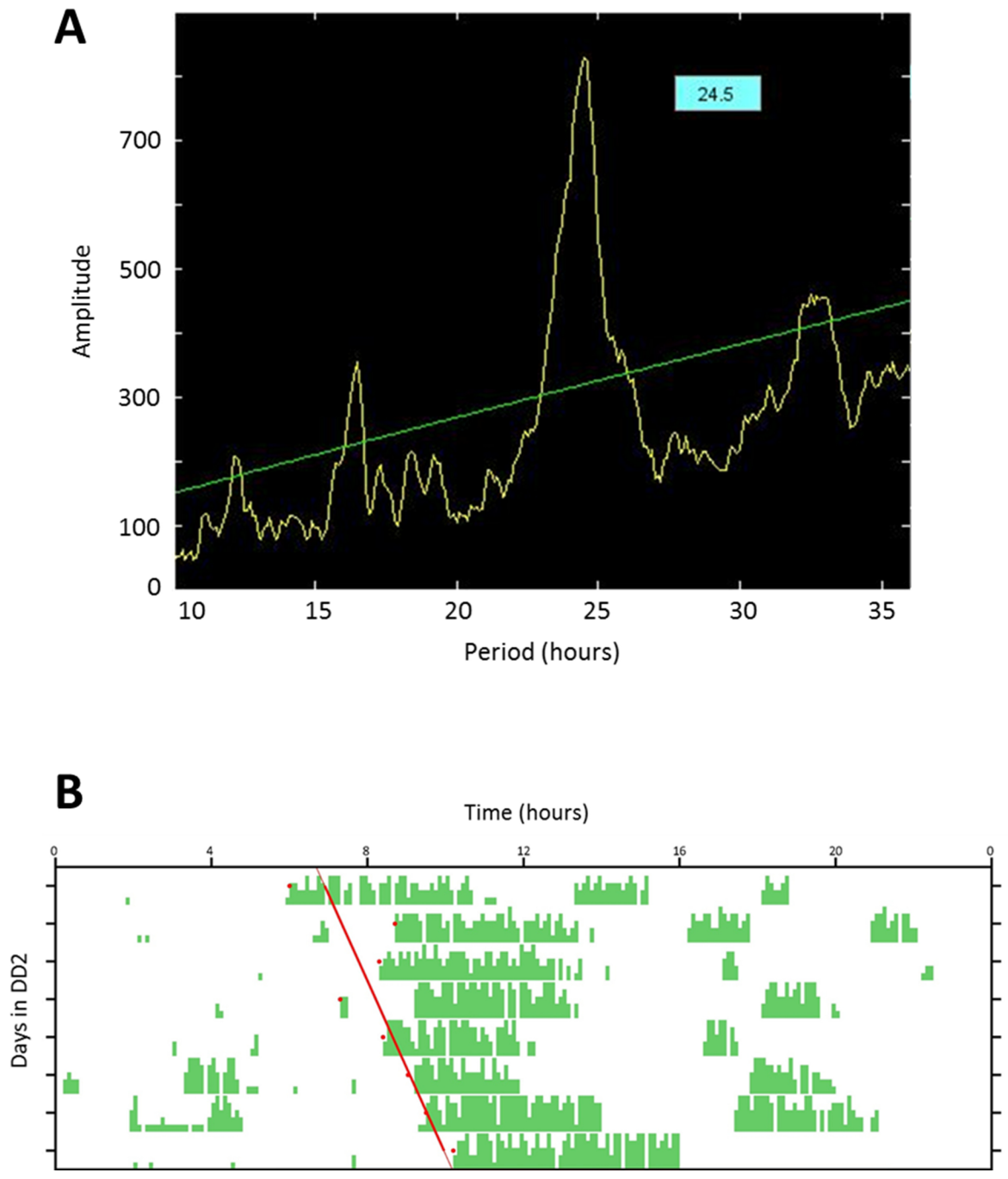

Figure 5.13. Retinal *Cry1* knock-in can restore behavioural rhythms under constant darkness conditions in arrhythmic *Cry1*$^{-/-}$*Cry2*$^{-/-}$ mouse model. Mouse B demonstrates circadian rhythms of locomotor behavior during DD2. (A) Chi-squared periodogram of Mouse B demonstrating that it exhibited rhythmic circadian locomotor behaviour (yellow peak) at tau = 24.56 hours during DD2. Green line indicates threshold level for statistically significant rhythms. Minor peaks are also visible at periods of 12.19, 16.51, and 33 hours. (B) Single-plotted actogram showing Mouse B activity patterns over the course of DD2, where the mouse exhibited consistent circadian rhythms. Red dots indicate onset of activity. Red line indicates a period (tau) of 24.56 hours. Green indicates activity as measured by wheel running. White background indicates lights off.

5.5 Discussion

5.5.1 Restoration of the retinal clock in an SCN arrhythmic animal is capable of inducing locomotor circadian rhythms

In this chapter, *in vivo* manipulation of *Cry1* was performed with the aim of determining whether the retinal clock is capable of acting as a *zeitnehmer* for the SCN pacemaker. The restoration of *Cry1* into a *Cry1*$^{-/-}$*Cry2*$^{-/-}$ mouse is the first experiment of its kind, as restoration of retinal circadian rhythms in an arrhythmic mouse model has never previously been attempted. Here, the *in vivo* restoration of CRY1 into *Cry1*$^{-/-}$*Cry2*$^{-/-}$ inner retina by intravitreal delivery of AAV vectors has been validated. It was then shown that restoring *Cry1* into the inner retina of the *Cry1*$^{-/-}$*Cry2*$^{-/-}$ mouse can restore circadian rhythms of locomotor activity under constant light conditions in a proportion of animals. These exciting results imply that, under certain conditions (LL), a retinal clock alone is capable of regulating light signals to the SCN to produce rhythmic locomotor activity. Furthermore, although the hypothesized *zeitnehmer* model predicted that constant light input would be necessary for the retinal circadian clock to modulate its signal downstream to the SCN clock, surprisingly, it was found that *Cry1*-knock-in mice also demonstrated rhythmic locomotor activity when subsequently released into constant darkness conditions. This may be explained by a free-running retinal clock continuing to provide rhythmic input to the SCN clock. Together, these findings suggest that the retinal clock acts as a *zeitnehmer* where the light input to the SCN is regulated in a rhythmic manner by the retinal clock (schematic shown as **Figure 5.14**). Given that this was a pilot experiment, the

plan is to replicate these results to further characterise the mechanisms of the behavioural rhythms observed.

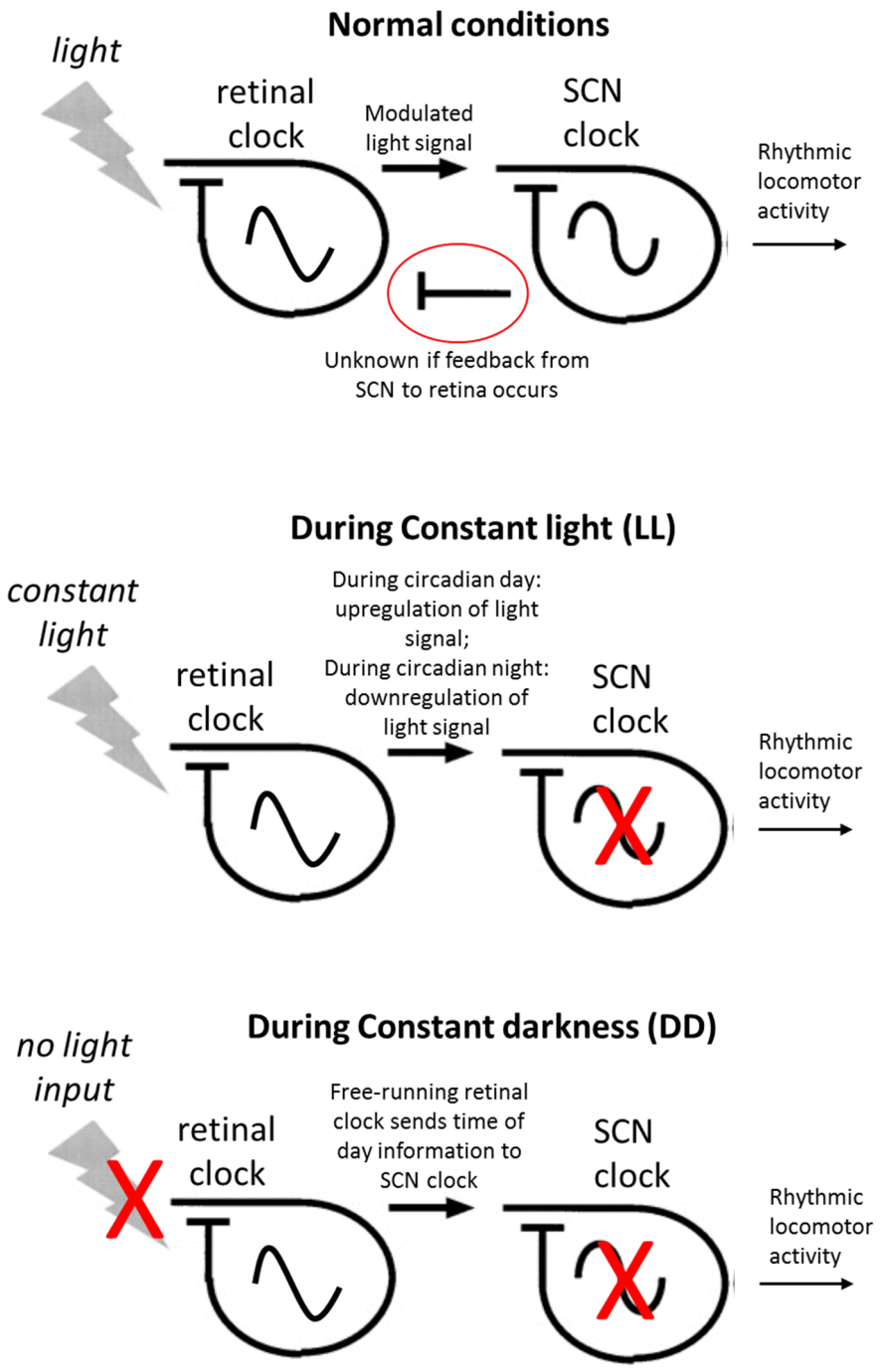

Figure 5.14. Model of retinal clock *zeitnehmer* effects on the SCN under normal physiological conditions as well as during the experimental conditions used in this Chapter, where this model was tested under conditions of SCN arrhythmicity during constant light and during constant darkness. Figure adapted from Merrow *et al*. (2003).

Additional controls are necessary to verify the effects of *Cry1*-eGFP AAV knock-in. In particular, qPCR could confirm whether levels of *Cry1* restoration are comparable to wildtype native *Cry1* levels. Furthermore, comparison of *Cry1*-eGFP signal with CRY1 antibody in wildtype retinas would allow comparison of the *Cry1* knock-in expression with native retinal *Cry1* expression. Lastly, comparison of *Cry1*$^{-/-}$*Cry2*$^{-/-}$ mouse locomotor activity rhythms under constant light conditions before and after *Cry1* knock-in would allow confirmation that restoration of locomotor rhythms are due to restoration of the retinal clock.

5.5.2 *Cry1* restoration effects during constant light conditions

Four of seven mice transfected with *Cry1*-eGFP AAV demonstrated some degree of rhythmic locomotor activity under constant light conditions (during LL1, LL2 or both). However, there have been variable onsets and period measurements (tau) in the restored locomotor activity rhythms during experimental constant light conditions. Indeed, one mouse demonstrated robust circadian locomotor rhythmicity in both LL1 and LL2 (Mouse C). Mouse B showed delayed onset rhythmicity in both LL1 and LL2. Mouse D showed delayed onset rhythmicity in LL1 and circadian locomotor rhythmicity in LL2 with variable period. Finally, Mouse E showed ultradian rhythmic behaviour in both LL1 and LL2. None of the sham-treated mice showed rhythmic locomotor activity during LL1 or LL2.

Previous work has found that *Cry1*$^{-/-}$ mice exposed to constant light have arrhythmic SCN tissue, whilst *Cry2*$^{-/-}$ mice exposed to constant light remain capable of generating SCN rhythms (Evans *et al*., 2012). This may be due to the impaired retinal clock and therefore impaired retinal light-gating properties in *Cry1*$^{-/-}$ mice, which are revealed under constant

light. The *Cry1* knock-in model may mimic a *Cry2*$^{-/-}$ mouse under LL conditions, which has preserved rhythmicity under these constant conditions.

Cry1 knock-in mice are expected to have a tau similar to that of a *Cry2*$^{-/-}$ mice (longer than 24 hours) given that it expresses *Cry1* but not *Cry2*. Furthermore, period lengthening effects of LL (Aschoff's Rule) allow the prediction of a >24 hour tau in *Cry1* knock-in mice. This was observed in mice that demonstrated rhythmicity in either LL1, LL2 or both. All mice showing a circadian rhythm in locomotor activity, did so with a periodicity of greater than 24 hours, as expected. Under LL1, taus of 23.9, 24, 25 and 26 hours were observed (though 26 hour tau may have been caused by ultradian rhythms with 13 hour tau). Under LL2, taus of 24.4, 25.17, and 26.5 hours were observed (the 26.5 hour tau was observed in two different mice). This is consistent with the period lengthening phenomena associated with constant light conditions. As such, this lends further evidence that the restoration of circadian rhythms in LL1 and LL2 in virus-treated mice resulted in restoration of a phenotype similar to that of *Cry2*$^{-/-}$ mice under constant light conditions.

At a mechanistic level, the retinal clock modulation of the light signal could be achieved through upregulation or downregulation of neural transmission of the light signal at different times of day. For instance, the light signal may be upregulated during the day (resulting in increased SCN firing) and downregulated at night (resulting in decreased SCN firing). Of note, the converse is not true: loss of the retinal clock is not sufficient to result in loss of SCN rhythmicity. *Cry1*$^{-/-}$ mice have attenuated retinal rhythms, as shown in Chapter 3, but they have a working SCN circadian clock (albeit with a shorter tau). However, lack of a retinal clock may produce small changes on activity rhythms which may have previously been attributed to other causes.

This study used similar constant light conditions as those previously used to assess locomotor activity rhythmicity in *Vipr2*$^{-/-}$ mice (Hughes *et al*., 2015a). Whilst *Vipr2*$^{-/-}$ mice have intact clock components but have severely attenuated SCN coupling, resulting in behavioural arrhythmicity under LD conditions, prolonged LL conditions were found to induce rhythmic locomotor in these mice due to improved SCN cell synchronization. Prolonged LL conditions were also necessary to retain rhythmic behaviour in these animals. *Cry1*-retinal knock-in mice behave similarly to *Vipr2*$^{-/-}$ mice in that constant light was able to induce rhythmic locomotor activity. This could be explained as the improved SCN coupling could be due to a rhythmic retinal signal. If loss of VPAC2 affects the SCN clock, but does not impair the retinal clock, LL may be expected to provide a rhythmic signal due to retinal gating, which would account for why it can restore locomotor rhythms in *Vipr2*$^{-/-}$ mice. However, it may only work in models that spare the retinal clock. In models where the retinal clock is also disrupted, rhythmic gating will no longer occur, so LL will not restore rhythms in the SCN (and behaviour).

The differences in rhythmic locomotor activity patterns during LL1 and LL2 may have been due to the variation in retinal transfections achieved. Indeed, the different patterns of rhythm restoration (such as immediate onset, delayed onset, and circadian versus ultradian rhythms in activity) may have resulted from differences in the types of cells or networks that were transfected by the *Cry1*-eGFP AAV. As the composition of individual retinal clock networks has not been characterized, further information will be needed regarding how retinal networks control the retinal clock in order to understand the links between a particular pattern of viral transduction and its resultant locomotor rhythm pattern. Future experiments could use Cre-lox viral systems in order to control the types of retinal cells that *Cry1* is restored into. For instance, restoration of *Cry1* into retinal cones

alone could indicate the role of the cone clock (outer retinal clock) restoration downstream on locomotor rhythms. Similarly, restoration of *Cry1* into TH-expressing cells or OPN4-expressing cells could reveal whether clocks in dopaminergic amacrine cells alone or pRGCs alone, respectively, could drive rhythmic behaviour.

5.5.3 *Cry1* restoration effects during constant darkness conditions following constant light exposure

We were initially surprised to find the five of seven *Cry1* retinal knock-in *Cry1*$^{-/-}$*Cry2*$^{-/-}$ mice expressed circadian locomotor rhythms in DD following LL exposure (DD2), as this suggests there may be long-term effects of *Cry1* retinal knock-in. The *zeitnehmer* model for the retinal clock had implied that a constant light signal was necessary in order for the retinal clock to modulate the light input pathway to the SCN clock. However, circadian rhythms of locomotor activity may have arisen during DD2 due to the restored retinal clock sending time of day information to the SCN. Indeed, preservation of coupling between the retinal oscillator and SCN oscillator may explain why several *Cry1*$^{-/-}$*Cry2*$^{-/-}$ mice appear to have retained or developed rhythmic locomotor activity when released into DD conditions after extended LL exposure. Although dampening of the retinal clock was not observed, this may have been due to the recording length, which will be extended in future studies. Alternatively, circadian-like rhythms in DD2 may reflect rhythmic locomotor activity in response to an environmental stimulus (that is not light) which coincides with a 24 hour period. These two explanations are detailed below in Section **5.5.4** and **5.5.5**.

Five of seven *Cry1* knock-in mice exhibited circadian rhythms of locomotor activity with periods between 23.5 hours – 25.1 hours under constant darkness conditions. One mouse

also showed ultradian rhythms with 3 bouts per day (bouts every 8 hours). Finally, one sham-treated mouse exhibited activity rhythms with a 24.4 hour tau. This may indicate that the observed locomotor rhythms in constant darkness are the product of an artefact.

5.5.4 Explaining DD2 circadian rhythms as the consequence of the retinal clock and SCN clock operating as coupled oscillators

In previously studied *Vipr2*$^{-/-}$ mice, observed rhythmicity was dependent on LL conditions – these mice were no longer rhythmic once released into DD conditions (Hughes *et al*., 2015a). Similar extended LL exposure protocols were used: 36 days in the Hughes *et al*. (2015) study; 34 in LL1 and 25 in LL2 for this study. As such, the restoration of SCN cell-cell communication in *Vipr2*$^{-/-}$ mice was dependent on constant light conditions. This may have been due to the SCN requiring a greater signal and the dampening retinal clock is insufficient to drive rhythms in a *Vipr2*$^{-/-}$ SCN.

In the experiment presented in this chapter, the restored retinal *zeitnehmer* may have been free-running under constant dark conditions. If the retinal clock is coupled to the SCN clock, the retinal clock may therefore be capable of sending time of day information to the SCN clock regardless of input to the retinal clock. This hypothesis depends on the ability of the retinal clock to send time of day information to the retinal clock in the absence of light input. Furthermore, coupled oscillators would be expected to communicate both ways, in which the SCN must therefore communicate to the retinal clock. Indeed, circadian rhythms in photoreceptor disk shedding could no longer be entrained to a new light cycle following SCN ablation, though a free-running rhythm persisted in the retina (Teirstein *et al*., 1980,

Terman *et al*., 1993). This implies that the SCN is necessary for photoentrainment of the retinal photoreceptor disk shedding rhythm and therefore may send time information to the retinal clock. Further work is necessary to establish the extent of which the retinal clock and SCN clock are connected and whether they can be designated as coupled oscillators.

5.5.5 Explaining DD2 circadian rhythms as an artefact

Given that the mice were all screened in DD1 for circadian rhythmicity and all showed a lack of rhythms, it can therefore be assumed that the SCN circadian pacemaker was not intact at the beginning of this experiment. Similarly, as one sham-treated mouse (Mouse G) along with several *Cry1* virus-treated mice show circadian rhythms in DD2, this may suggest that the *Cry1*-eGFP AAV treatment itself may not have caused any restoration of the SCN pacemaker.

Furthermore, if it is assumed that light is essential for the retinal clock to gate light input to the SCN, then free-running locomotor activity rhythms would require restoration of a working SCN pacemaker in DD conditions. Restoration of *Cry1* in the retina was not expected to cause restoration of the SCN TTFL in DD conditions. The AAV2 virus used in the *Cry1* virus-treated mice is not expected to infect cells beyond the locus of infection. That is, the virus cannot cross neural synapses to infect other cells projected to from the retina. However, in the future, the SCN will be assayed for *Cry1* virus re-expression to exclude this possibility.

Circadian-like rhythms in $Cry1^{-/-}Cry2^{-/-}$ SCN-arrhythmic animals may have therefore arisen as a result of a consistent running wheel response to a rhythmic external stimulus. Given that the mice showing behaviour at approximately the same time of day (rather than

several mice in different phases of activity), it is possible that uncontrollable experimental setup factors, such as the sound of other running wheels, entry of staff or other colleagues into the room, daily scheduled maintenance or work, or other stimuli with a rhythmic occurrence may have induced the mice to run on the wheels, thus "entraining" them to display circadian-like locomotor rhythms despite having no endogenous SCN clock that should be able to function in DD conditions. Although all efforts had been made to avoid rhythmic stimuli for the mice used in this experiment, it is possible that such external factors (such as regular housekeeping of other mice housed in the same room but different Light Tight Chamber) may have had an effect on the wheel running.

However, future experiments may allow a more detailed analysis regarding the potential causes of the observed circadian-like rhythmicity in DD2. First of all, the recording must be extended. Ideally DD2 should be recorded for at least 2 weeks in order to ensure trends can be measured accurately and any dampening of rhythms observed. Indeed, as LL1 and LL2 were recorded for 4 weeks, it was therefore possible to find even rhythms delayed by several days of arrhythmicity. Further, longer recordings permitted further findings that sometimes this delayed rhythmicity devolved once again into arrhythmicity. As such, in future, every light condition will be applied for at least two weeks each.

Also, DD2 conditions followed immediately after LL2, without an intermediate LD state. The manifestation of rhythmic behaviour may have arisen as a result of the stresses associated with such substantial changes in light environment. In a future experiment, an intermediate LD state between any periods of constant conditions will be tested. Although, previous studies have used LL immediately followed by DD (Ono *et al*., 2013). Still, in future it would be important to measure the effects of a transition from LD to DD.

5.5.6 Ultradian locomotor rhythms following *Cry1* restoration

One of the *Cry1*-virus treated *Cry1*$^{-/-}$*Cry2*$^{-/-}$ mice (Mouse E) showed consistent ultradian locomotor rhythms. In particular, during both stages of LL exposure (LL1 and LL2), this mouse demonstrated approximately 3 bouts of activity every day, where onsets of each bout were ~8 hours apart. Aligning the onset of every third bout revealed circadian period information, which changed over the course of LL exposure. At the beginning of LL2, a tau of 23.17 hours was observed. This subsequently changed to a tau of 25.17 hours. These ultradian bouts of activity may have been the result of the lack of circadian control revealing ultradian rhythmicity in locomotor behaviour. Interestingly, Mouse E also showed ultradian-like rhythms in LD2 (under light-dark conditions).

By contrast, *Cry1*-virus treated Mouse A showing a similar ultradian pattern of activity in DD conditions following LL exposure (DD2, see **Figure 5.12**) but not during LL exposure (LL1 or LL2). Furthermore, the periodicity of the ultradian bouts did not change throughout the recording, although DD2 was recorded for only 9 days (as compared to 34 days of LL1 and 25 days of LL2 recording). *Cry1*$^{-/-}$*Per2*$^{-/-}$ mice under extended DD conditions develop ultradian rhythms (Abraham *et al*., 2006). This are similar to those recorded in Mouse A during DD2.

The observation of the development of ultradian rhythms was an unexpected finding but there are a few possibilities for why such patterns may have arisen. Firstly, these *Cry1*$^{-/-}$*Cry2*$^{-/-}$ mice may have an underlying intact ultradian oscillator despite their lack of circadian control. Furthermore, it is possible that an environmental stimulus induced wheel running activity and if this stimulus occurred periodically, this may have resulted in a pattern of wheel running activity unrelated to any endogenous rhythmic activity.

In mice, two oscillators that persist in the absence of SCN or circadian rhythmicity have been characterized. The first is the methamphetamine-sensitive circadian oscillator (MASCO), which regulates methamphetamine-induced locomotor activity rhythms with an approximate circadian periodicity (Honma *et al*., 1986), despite SCN lesion (Honma *et al*., 1987) or loss of circadian clock control (Mohawk *et al*., 2009). The second is an ultradian oscillator (Dowse *et al*., 2010), which appears to be dopamine-dependent and regulate rhythms in behavioural arousal and locomotor activity (Blum *et al*., 2014). It was suggested that the ultradian oscillator that persists in the *Cry1*$^{-/-}$*Per2*$^{-/-}$ mice gates clock gene induction in response to constant light (Abraham *et al*., 2006). Furthermore, previous work in rats has suggested that the ultradian rhythms in corticosterone secretion remain intact following SCN lesion and constant light exposure (Waite *et al*., 2012). The *Cry1*$^{-/-}$*Cry2*$^{-/-}$ mice exhibiting ultradian rhythms that have been observed in this chapter may therefore demonstrate ultradian locomotor rhythms driven by the dopamine-dependent ultradian oscillator, though more experiments would need to be done to support this theory. As not all mice exhibited ultradian rhythms, extension of the DD2 phase may reveal ultradian rhythms in other (virus treated and non-treated) mice. This would indicate whether *Cry1*$^{-/-}$*Cry2*$^{-/-}$ mice still have a functional ultradian oscillator or if the oscillator was restored by the *Cry1* virus treatment in the retina. Future work could also investigate modulation of the dopaminergic tone in the brains of *Cry1*$^{-/-}$*Cry2*$^{-/-}$ mice to determine whether their ultradian oscillations of locomotor rhythms are dopamine-dependent and regulated by the dopamine ultradian oscillator.

5.6 Conclusions

The retinal clock may not be restricted to regulating local retinal physiology, but may also gate light input to the master clock in the SCN. To explore the possibility of a *zeitnehmer* function of the retinal circadian clock, a *Cry1* AAV suitable for *in vivo* retinal delivery was generated and retinal *Cry1* knock-in in an arrhythmic *Cry1*$^{-/-}$*Cry2*$^{-/-}$ mouse was produced. *Cry1* knock-in of *Cry1*$^{-/-}$*Cry2*$^{-/-}$ mice was validated using multiple quality controls and locomotor activity circadian rhythms of *Cry1* knock-in mice was assessed under constant light conditions (LL), light-dark cycles (LD), and constant darkness conditions (DD). A significant proportion of the *Cry1* knock-in mice showed locomotor activity circadian rhythms under both LL and DD conditions.

These results are the first of their kind in attempting to determine the role of the retinal clock in the context of downstream locomotor circadian rhythms. These data suggest that the retinal clock is capable of functioning as a *zeitnehmer* as predicted by Merrow and Roenneberg. Moreover, these findings may provide a tentative explanation as to why LL can be permissive for circadian rhythms in specific models with normally disrupted SCN function.

In the context of the other retinal clock work performed in Chapters 2 and 3, here *Cry1* restoration in the inner retina of a *Cry1*$^{-/-}$*Cry2*$^{-/-}$ mouse was found to be very likely sufficient to restore retinal circadian rhythms, indicating the inner retinal clock alone is already capable of being a *zeitnehmer*. The impact of an intact retinal clock downstream indicates that the retinal clock does, under these conditions, affect the light signals reaching the brain. Further work is required to determine what effect the outer retinal clock restoration would have on locomotor circadian rhythms, and also how exactly the retinal clock

modulates the light signals reaching the brain. Finally, *Cry1* knock-in animals also exhibited circadian rhythms of locomotor activity under constant darkness conditions following prolonged constant light conditions, suggesting long-term effects of retinal clock restoration. Future studies will address whether this surprising result is due to free-running (but dampening) retinal clock rhythms and coupling of the retinal and SCN clocks or an artefact of the experimental environment.

6

General Discussion

6.1 Potential links between the roles of Cryptochromes and melanopsin in the retinal clock

In both Chapters 3 and 4, mouse retinal clock function has been examined through performing retinal rhythm assays on mouse models that lack *Cry1*, *Cry2*, or melanopsin. Each mouse model has provided some insight as to the functional contributions of *Cry1*, *Cry2* and melanopsin to the retinal circadian clock, suggesting that these contributions may be linked.

Notably, Cryptochromes and melanopsin may contribute in different ways to retinal circadian rhythmicity. *Cry1* and *Cry2* are constitutive clock genes, whilst melanopsin is a mammalian circadian photopigment. *Cry1* may be an essential component of the retinal molecular clock (in the retinal TTFL) present in both outer retinal clock cells and inner retinal clock cells. *Cry2* may play a similar role but only in outer retinal clock cells. Melanopsin, by contrast, may exert influence of the retinal circadian clock as a modulator of intraretinal signalling, such as retinal dopaminergic signalling, rather than as a component of the molecular TTFL. Furthermore, melanopsin expression is restricted to the inner retina, though melanopsin may influence outer retinal clock function by modulating intraretinal signalling.

A summary of the data obtained in Chapters 2-4 determining the roles of *Cry1*, *Cry2* and *Opn4* in retinal circadian rhythms is provided as **Table 6.1** below. Interestingly, it appears that the observed retinal rhythms can be attributed to *Cry1*, *Cry2* and *Opn4* specific retinal expression patterns. Furthermore, it was surprising to find that melanopsin appears more necessary than *Cry2* for maintenance of retinal rhythms. This may be due to physical

isolation of *Cry2* to the photoreceptor outer segments and outer retinal clock, whilst melanopsin appears to be involved in intraretinal signalling.

	***Cry1*$^{-/-}$ mice**	***Cry2*$^{-/-}$ mice**	***Opn4*$^{-/-}$ mice**
Retinal protein expression	Widespread: Cones, INL (including subset of amacrine cells), GCL (including subset of pRGCs)	Outer retina: Photoreceptor outer segments	Inner retina: pRGCs
PER2::LUC rhythms (previous studies)	Unstable, attenuated	Rhythmic	Rhythmic
Photopic ERG b-wave amplitude rhythms	Attenuated	Attenuated	Attenuated
Contrast sensitivity rhythms	Attenuated	Rhythmic	Attenuated
Pupillary light response rhythms	Attenuated	Rhythmic	Rhythmic

Table 6.1. Summary of data obtained in Chapters 2-4 regarding the roles of Cry1, Cry2 and Opn4 in retinal circadian rhythms. Data on PER2::LUC studies is taken from Ruan *et al*. (2012) and Buhr and Van Gelder (2014).

Loss of *Cry1*, *Cry2*, or melanopsin resulted in loss of the photopic ERG circadian rhythm. It was hypothesized that loss of the photopic ERG rhythm could be due to either loss of rhythmicity within the outer retinal clock cells (when either *Cry1* or *Cry2* is lost), or due to loss of input from dopaminergic amacrine cells (when melanopsin is lost). Interestingly, if the inner retinal clock (of which *Cry1* is a component, but not *Cry2*) includes an oscillator in pRGCs modulated by melanopsin, loss of inner retinal rhythmicity may also influence the photopic ERG via the dopaminergic system. This may account for why loss of both outer and inner retinal rhythms in *Cry1*$^{-/-}$ mice causes a more profound loss of photopic ERG rhythm, whilst loss of only outer retinal rhythms in *Cry2*$^{-/-}$ mice attenuates the photopic ERG rhythm to a lesser magnitude (see **Figure 3.5**).

Contrast sensitivity, on the other hand, appears to be regulated by the inner retinal clock alone. Loss of the outer retinal clock via loss of *Cry2* did not affect circadian rhythms of contrast sensitivity. On the other hand, loss of outer and inner retinal rhythms together (via *Cry1* loss) or loss of inner retinal rhythms alone (via melanopsin loss or *Npas2* loss, Hwang *et al*. (2013)) was sufficient to abolish contrast sensitivity rhythms. Contrast sensitivity is also modulated by retinal dopamine (Jackson *et al*., 2012), providing a potential mechanism. To clarify, the inner retinal clock may directly connect with the retinal dopaminergic system via melanopsin-expressing retinal clock cells.

As such, it is possible that melanopsin-expressing pRGCs that act as retinal clock cells are the same pRGCs that were observed to express CRY1 (Chapter 2). The function of these specific cells could not be isolated using the experimental approaches in Chapters 3 and 4, but it is possible to speculate that these cells could potentially play an important role in regulating retinal circadian rhythms by providing a cellular location for the retinal clock roles of *Cry1* and *Opn4* to intersect.

The effects of *Cry1* loss on retinal circadian physiology may therefore be due to modification of the retinal dopaminergic system via a subset of melanopsin-expressing pRGCs which express CRY1. As such, CRY1-expressing pRGCs may mediate the effects of CRY on the retinal clock. Of note, *Opn4*$^{-/-}$ mice demonstrated daytime contrast sensitivity responses at both tested circadian times, similar to those found in *Cry1*$^{-/-}$ mice (though intermediate, not daytime, photopic ERG responses were found in *Opn4*$^{-/-}$ mice). This may imply that loss of *Cry1* and loss of melanopsin affects the same retinal circuitry.

In future studies, use of melanopsin-Cre mice may yield useful information regarding the role of CRY1-expressing pRGCs in the retinal clock. For instance, does *Cry1* loss or any clock

component loss in CRY1-expressing pRGCs alone affect retinal rhythms? If that were true, this may indicate that CRY1-expressing pRGCs are essential to the circadian organization of the mammalian retinal clock, as deficits in both contrast sensitivity and ERG may be regulated by these cells. This would imply that CRY1-pRGCs are one of the main cell types that regulate the retinal clock, although the fact that some retinal rhythms, including the PER2::LUC rhythms and the pupillary light response, are still present in mice lacking melanopsin would imply that there are additional retinal clocks that have preserved rhythmicity despite melanopsin loss. These additional networks may have lesser significance, as despite their preserved rhythmicity, neither contrast sensitivity rhythmicity nor photopic ERG rhythmicity is preserved.

Lastly, given the important role of melanopsin and pRGCs in the development of non-image-forming retinal responses to light (Sekaran *et al*., 2005, McNeill *et al*., 2011, Tu *et al*., 2005, Schmidt *et al*., 2008), it is possible that melanopsin may have a role in the development of circadian organization of retinal tissue. Additional experiments could verify whether effects on retinal circadian physiology in *Opn4*$^{-/-}$ mice are due to a role of melanopsin in the retinal clock or a developmental abnormality caused by absence of melanopsin. For instance, *Opn4* siRNA could be used to knockdown melanopsin in wildtype mice. This would allow investigation of the effects of retinal melanopsin loss on a background of normal development. Furthermore, development of an *Opn4*-AAV could be used to restore melanopsin expression in *Opn4*$^{-/-}$ mice. In this mouse model, retinal rhythms would be expected to be restored – however, if rhythms are still affected, this may indicate developmental abnormalities in circadian organization of the retina in *Opn4*$^{-/-}$ mice.

Several components of the retinal clock TTFL (such as Bmal1, Npas2, Cry1, and Cry2) as well as several circadian rhythms in retinal physiology (such as photopic ERG b-wave amplitude, contrast sensitivity and PLR) have now been identified. However, it is necessary to investigate and better understand the mechanisms by which the endogenous clock regulates physiology in the retina.

6.2 Future work towards understanding retinal rhythms

6.2.1 Confirming the role of *Cry1* in retinal rhythms

The *Cry1*-eGFP AAV knock-in method (described in Chapter 5) could be used to confirm the function of CRY1 in the retina (Chapter 3). It could be predicted that retinal circadian rhythms would be restored in *Cry1*$^{-/-}$ mice following *Cry1*-eGFP AAV knock-in. With intravitreal injection, only the inner retinal *Cry1* expression is restored. The photopic ERG rhythm appears to depend on the outer retinal clock. Thus, only inner retinal rhythms: contrast sensitivity rhythms and possibly the PLR rhythm would be expected to be restored. This experiment would provide confirmation that *Cry1* is necessary for contrast sensitivity rhythms (and possibly PLR rhythms as well).

Furthermore, investigating the role of *Cry1* in retinal rhythms at the molecular level is essential. Retinal explants from *Cry1*$^{-/-}$;PER2::LUC mice display severely attenuated bioluminescence circadian rhythms (Ruan *et al*., 2012). Intravitreal injection of *Cry1*-eGFP AAV knock-in method in *Cry1*$^{-/-}$;PER2::LUC mice would allow confirmation that retinal rhythm restoration has occurred at a molecular level. This experiment would also confirm that *Cry1* is necessary for the molecular mechanisms underlying normal retinal rhythms.

6.2.2 Investigating retinal clock networks

Altering the route of administration for retinal AAV delivery of virus could also allow examination of *Cry1* restoration in the outer retinal clock. Subretinal injection would restore *Cry1* only in the cones, and therefore potentially only restore the electroretinogram b-wave amplitude circadian rhythm. These experiments may allow confirmation that the retinal clock model presented in Chapter 3 is correct. It is possible that such physiological outputs require *Cry1* expression in both inner and outer retina in order for both inner and outer retinal clocks to function properly. Testing *Cry1* knock-in mice following both intravitreal and subretinal viral delivery may determine whether this is necessary. Furthermore, subretinal injection is technically challenging and may only transduce regions of the retina, rather than cones specifically. Lastly, this approach may result in transduction of rods as well. Although rods were not observed to express *Cry1,* it is still possible that rods could express *Cry1* at very low levels or that they have the necessary molecular machinery to activate the *Cry1* promoter.

The use of floxed clock genes in retinal Cre transgenic mouse lines may yield further insight as to the specific cell networks involved in generating retinal clock rhythms. Previous work has validated this approach; retina-specific *Bmal1* knockout mice were created by breeding CHX10-Cre mice with conditional *Bmal1* knockdown mice (Storch *et al*., 2007). Retina-specific dopamine-depleted mice were created by breeding CHX10-Cre mice with conditional *Tyrosine hydroxylase* knockdown mice (Jackson *et al*., 2012). Given that over fifteen retinal Cre transgenic mouse lines exist (Ivanova *et al*., 2010), this approach has a wide variety of applications.

Retinal Cre transgenic mouse lines could also be used to restore the retinal clock in specific cell types. For instance, retinal cone photoreceptor–Cre lines (Le *et al*., 2004, Akimoto *et al*., 2004) could be used to generate *Cry1*$^{-/-}$*Cry2*$^{-/-}$;Cone-Cre mice. Retinal delivery of floxed *Cry1* AAV would therefore restore *Cry1* specifically in retinal cones to allow *in vivo* investigation of the cone clock cells in an otherwise arrhythmic system. Melanopsin-Cre mice (Ecker *et al*., 2010) and TH-Cre mice could be used similarly to investigate the role of CRY1-pRGCs and CRY1-expressing dopaminergic amacrine cells, respectively.

6.2.3 Circadian regulation of the pupillary light response

Cry1 AAV knock-in using *Cry1*$^{-/-}$ mice would also allow confirmation of whether circadian rhythms in the PLR are driven by the retinal clock or if circadian rhythms in central mechanisms mediate these responses. If central mechanisms are involved, the pupillary light response rhythm may be due to a circadian rhythm in autonomic tone. That is, if sympathetic and parasympathetic regulation change with a circadian period, this may account for the differences in PLR at CT6 compared to CT18 observed in Chapter 3 and 4. The influence of autonomic tone rhythms on PLR rhythms are likely to be driven by the SCN and mediated via the paraventricular nucleus (Dibner *et al*., 2010). This pathway also mediates circadian rhythms in melatonin synthesis and corticosterone (Ishida *et al*., 2005, Lehman *et al*., 1987).

Determining whether the circadian rhythm in PLR is regulated by the retinal clock or central mechanisms will be extremely valuable in either validating a novel retinal clock assay or providing further insight regarding retinal clock mechanisms. Indeed, if central mechanisms are found to regulate the PLR rhythm, this would suggest that there is a

central pathway dependent on *Cry1* for circadian rhythmicity, which has not previously been shown.

6.2.4 A role for *Opn5* in retinal clock *zeitnehmer* effects

The proposed mechanisms by which the retinal clock functions remain poorly characterized. There is a substantial amount of evidence pointing to dopamine as having neuromodulatory effects on several retinal layers, enabling communication and possibly synchrony between retinal clock neurons. However, retinal dopamine-depleted mice maintain retinal oscillations (as read out by PER2::LUC oscillations, Jackson *et al*. (2012)). As such, there may be additional factors that enable robust oscillations of the retina.

The discovery of novel photopigment *Opn5* (neuropsin) as a potential entraining photopigment specifically for the retinal clock (Buhr and Van Gelder, 2014, Buhr *et al*., 2015) encourages further inquiry into its contribution to downstream effects of the retinal clock *zeitnehmer*. Do neuropsin expressing cells project to the SCN? This is not yet known, but may be particularly interesting as neuropsin may entrain the retinal clock. If the retinal clock communicates with the SCN, neuropsin-expressing cells may be conveying light information to the SCN by an, as yet, uncharacterized mechanism. Furthermore, the retinal clock is capable of maintaining retinal oscillations even in the absence of most *Opn5* transcripts (Buhr *et al*., 2015) (although *Opn5* was necessary for retinal rhythm photoentrainment). This adds yet another layer of complexity to retinal clock networking structure. Can the retinal clock act as a *zeitnehmer* in the absence of *Opn5*, the entraining photopigment? Further experiments into this area using *in vivo* tools may add valuable information to existing *ex vivo* retinal explant work. Future work may thereby bring about

further understanding regarding the exact relationship between *Opn5* and rhythmic cells of the retina.

In summary, future work shall include the following experiments using AAV or siRNA tools to further understand mechanisms of retinal rhythms:

- Role of melanopsin in retinal rhythms
    - *Opn4* siRNA for loss, *Opn4* AAV for restoration
- Retinal or central control of PLR circadian rhythm
    - *Cry1* AAV in *Cry1*$^{-/-}$ mice, if PLR rhythm restored, there is retinal clock control
- Role of CRY1-expressing pRGCs
    - *Cry1* AAV in *Cry1*$^{-/-}$*Cry2*$^{-/-}$*;Opn4-Cre* mice
- Role of outer retina/inner retina CRY1 expression on retinal rhythms
    - Subretinal vs intravitreal injections
    - Cone-Cre mice
    - Other Cre mice to investigate other cell populations (TH-Cre, Melanopsin-Cre)
- IN PROGRESS: Restoration of *Cry1* in *Cry1*$^{-/-}$ PER2::LUC retina to see if rhythms are restored (collaboration with N. Smyllie)

6.3 Conclusions

In this thesis, the primary aim was to investigate the role of Cryptochromes in the mammalian retina. The work presented here has determined the localization and expression pattern of CRY1 and CRY2 in the mouse retina. Furthermore, both CRY1 and CRY2 have essential roles in regulating normal retinal circadian rhythms. It is shown for the first time that not only is CRY1 expressed in the mammalian retina, but that it plays a dominant role in the regulation of retinal circadian physiology. Whilst *Cry1* and *Cry2* are individually dispensable for SCN circadian rhythms, this work suggests that retinal circadian rhythms are dependent on *Cry1*. This thesis has added further evidence that the retinal clock is not a simple group of synchronized pacemakers but a complex network, where at least two independent networks of oscillators in the retina regulate key aspects of retinal physiology.

Investigation of the role of melanopsin in retinal rhythms in this thesis found that melanopsin is necessary for circadian rhythms of contrast sensitivity, but not PLR rhythms. Taken together with previous studies, melanopsin may affect the retinal clock through retrograde signalling to dopaminergic amacrine neurons, and in that way, influence retinal clock cells throughout the tissue. As such, melanopsin may be an important, though not essential, modulator of retinal circadian rhythms.

The final aim of this thesis was to investigate whether the retinal clock has any downstream effects on the SCN clock. Altogether, the data presented in Chapter 5 suggest that the retinal clock is capable of functioning as a *zeitnehmer* as predicted by Merrow and Roenneberg. It was found that *Cry1* restoration in the inner retina of a $Cry1^{-/-}Cry2^{-/-}$ mouse is very likely sufficient to restore retinal and locomotor activity circadian rhythms,

indicating the inner retinal clock alone is already capable of being a *zeitnehmer*. Furthermore, these findings may provide a tentative explanation as to why constant light conditions can be permissive for circadian rhythms in specific mouse models with normally disrupted SCN function.

Altogether, this work has revealed distinct and separable roles of CRY1 and CRY2 in mammalian retinal circadian physiology. Furthermore, this thesis has also contributed to a more nuanced understanding of the complexities of the mammalian retinal clock, as well as its important role in the light input pathway to the SCN. Future development of experimental tools that monitor clock protein expression in individual retinal cells in a physiological setting will provide further insight regarding underlying mechanisms of the retinal clock.

In summary, the work in this thesis has provided the following significant advances to current knowledge:

- The role of mammalian cryptochromes in the retina has previously been controversial and unclear. CRY1 was thought to not even be expressed in the retina. The results from work performed in this thesis suggest that *Cry1* is essential for maintenance of both inner and outer retinal circadian rhythms, whilst *Cry2* is important for outer retinal rhythms only.
- Furthermore, this work has examined the role of melanopsin in retinal rhythms in greater detail and *Opn4* appears to be important for some, but not all retinal rhythms.
- Lastly, *Cry1* retinal knock-in of *Cry1*$^{-/-}$*Cry2*$^{-/-}$ mice will be the first time the role of the retinal clock alone in a clockless animal has been tested – the preliminary results indicate a functional retinal clock is sufficient to drive locomotor rhythms. However, further work is needed to corroborate these results.

Lastly, understanding mammalian retinal circadian rhythms will hopefully lead to greater comprehension of how retinal responses to light can be optimized for therapeutic improvements to vision and non-image forming light responses. Clinically relevant research following from this thesis work could investigate whether loss of retinal rhythms causes any significant retinal pathologies. For instance, placing *Cry1*$^{-/-}$ mice under prolonged constant bright light could allow examination of retinal light-damage effects, and whether any such effects are hastened or aggravated by retinal clock loss. Mouse strains with retinal disease or degeneration (such as the *rds* model which exhibits slow rod and cone degeneration) could be crossed with *Cry1*$^{-/-}$ mice to determine if disease progression is

affected by loss of retinal rhythms. In such cases, it would also be worthwhile to determine if strong entrainment stimuli help preserve rhythms and can slow disease. Finally, characterization of retinal disease parameters that exhibit circadian rhythms are necessary to provide assays upon which the impact of retinal clock loss may be tested. As such, clinically-relevant retinal rhythms research may allow for development of treatments to preserve healthy retinal circadian rhythms and any associated physiology.

7

Pilot Experiment: Evaluation of sleep and associated behaviours in response to magnetic fields

7.1 Introduction to Magnetoreception

Magnetoreception is the ability of animals to sense and respond to the Earth's magnetic field. Magnetoreception ability has been described in over fifty species of animals (Wiltschko and Wiltschko, 2012). Evidence for magnetoreception has been found in diverse groups of animals, from *Drosophila* and monarch butterflies to dolphins, dogs, cows, turtles, mice and even humans. The majority of magnetoreception work in non-mammals has been performed in migratory birds and *Drosophila melanogaster* (fruit flies), though there is now emerging data on mammalian magnetoreception.

In migratory species, the use of magnetoreception has been associated with navigation and orientation during long-distance migration (Mouritsen *et al*., 2016, Wiltschko and Wiltschko, 2002). In non-migratory species, it is thought that magnetoreception may provide information for local orientation and navigation (Wiltschko and Wiltschko, 2002, Wiltschko and Wiltschko, 2013, Lefeldt *et al*., 2014). Magnetoreception may be a redundant sense in some species, and may not be the only sense used in navigation, particularly where other senses are well-developed, such as vision or olfaction. In such cases, magnetoreception may be used in complement with other sensory modalities. Furthermore, in certain species, magnetoreception ability may only be engaged when other senses are deprived, or when other senses are not capable of providing useful information for navigation and orientation.

One of the main challenges of magnetoreception research has been to determine the mechanism by which animal magnetoreception occurs. The Earth's magnetic field is approximately 50μT in intensity. By comparison, the magnetic field 3cm away from appliances such as a hair dryer can range from 6-2000 μT, whilst 3cm from an electric

shaver can generate a magnetic field ranging from 15-1500μT (World Health Organization). The magnetic field exposure safety limit for the public is 100μT at 50Hz, and 500μT for working conditions (World Health Organization) As such, has been particularly challenging to hypothesize a biochemical process or interaction that would be affected by the Earth's relatively low magnetic field strength.

Despite over 40 years of work on this subject, the identity and mechanism of the magnetoreceptor which senses and transduces information regarding the Earth's magnetic field remains inconclusive. However, two main hypotheses have arisen: the magnetite hypothesis and the radical pair hypothesis. The latter support the role of Cryptochrome as a putative candidate magnetoreceptor.

In this section, these two main hypotheses for the magnetoreception mechanism will first be discussed. An overview of Cryptochrome-based magnetoreception, which is suggested to be mediated via a radical pair mechanism, will then be provided. Magnetoreception studies in various species will then be reviewed, beginning first with migratory birds, whose use of the magnetoreception for orientation and migration has been of particular interest. Secondly, magnetoreception studies in *Drosophila melanogaster* (fruit fly) will be reviewed, where genetic tools have been able to provide essential information regarding the molecular mechanisms of magnetoreception. Finally, magnetoreception in mammals will be discussed, which provide the most relevant data for application to humans, as well as studies using mice, which are most relevant to the work performed in this thesis. Notably, studies in *Drosophila* and mice enable specific mechanistic hypotheses to be tested because of available genetic tools.

It is important to consider that whilst often studies have taken conclusions from one species and translated it to others (such as data from *Drosophila* being translated to mammals), it is possible that magnetoreception may operate by different mechanisms in different species. Furthermore, whilst the Earth's magnetic field has an intensity of 50μT, many experimental studies have used much higher intensities, which has made comparison of various studies difficult. In addition, removal of background magnetic fields for experimental controls can be challenging, which leads to further challenges in data interpretation.

As such, cautious methodology is applied to the experiments presented in order to ensure the data provided in this thesis adds more information to the magnetoreception field, rather than confuse it any further.

7.1.1 Magnetite Hypothesis

Magnetite is a mineral (also called Fe_3O_4 or iron (II, III) oxide) hypothesized to be present in certain biological cells as iron-rich crystals. The magnetite hypothesis suggests that biological magnetite, innately sensitive to magnetic fields, physically moves within a biological cell in response to a magnetic field, thus triggering downstream pathways responding to any changes in magnetic field orientation (Kirschvink *et al*., 2001).

Magnetite-based magnetoreception has been demonstrated in magnetotactic bacteria (Frankel *et al*., 1979). Such bacteria contain magnetite crystals and align themselves along magnetic field lines (this is also known as magnetotaxis and may be either north-seeking or south-seeking). This led to the hypothesis that animal magnetoreception may depend on magnetite-containing cells or tissues in animals (magnetosomes) which could mediate

magnetoreception (Kirschvink and Gould, 1981). Animal magnetite-based magnetoreception (Kirschvink *et al*., 2001, Cadiou and McNaughton, 2010, Wiltschko and Wiltschko, 2013, Shaw *et al*., 2015) has been described as a potential mechanism for magnetoreception in the beaks of birds such as homing pigeons and chickens, and in other animals including salmon and bats.

Magnetite-based magnetoreception has been best characterized in birds. Early work by Beason and Semm suggested that the trigeminal nerve of birds mediates magnetic information and that this information may be used as a navigational map (Semm and Beason, 1990, Beason and Semm, 1991, Beason and Semm, 1996). Recent work has suggested that perhaps magnetite-based receptors are expressed in the upper beaks of pigeons and that magnetite-based magnetoreception conveys information regarding the intensity of the magnetic field in order to aid navigation (Wiltschko and Wiltschko, 2013). In particular, pigeons with their upper beaks anaesthetized perform significantly differently than control animals in a magnetic orientation task within an area containing an anomalous magnetic field (Wiltschko *et al*., 2010). However, the trigeminal magnetite system in birds may also be a redundant system for navigation, as lesioning the trigeminal nerve did not prevent successful navigation in pigeons (Gagliardo *et al*., 2008).

Furthermore, as elaborated upon below, evidence does not support a magnetite hypothesis for *Drosophila* or mammalian magnetoreception. Data from experiments in *Drosophila* (reviewed below in Section 1.5.6) have provided strong evidence for a role of Cryptochrome in radical pair magnetoreception. It is possible that magnetite magnetoreception is the main mechanism by which some animals can sense magnetic fields. In other animals, particularly birds, it has been hypothesized that both magnetite-

based magnetoreception and radical pair magnetoreception exist as separate systems in the same organism, though whether and how they interact remains uncertain (Mouritsen and Hore, 2012). A recent study (Qin *et al*., 2016) has suggested that the magnetite and radical pair systems may operate in conjunction via a novel putative magnetoreceptor MagR (see section I.i.d).

7.1.2 Radical Pair Hypothesis

The radical pair magnetoreception hypothesis is based on the idea that biological sensing of magnetic fields could progress via a biochemical reaction generating a radical pair, whose products are sensitive to the environment's magnetic field (first described by Schulten *et al*. (1978)). The radical pair mechanism involves light-activated electron transfer which creates a radical pair (molecules with a single unpaired electron) as either a singlet or triplet excited state (depending on electron spin correlation). The production of either the singlet or triplet state is dependent upon the magnetic field. This means that a magnetic field orientation in a certain direction could lead to more singlet products compared to triplet products, whilst another field orientation would then lead to more triplet products compared to singlet products. The singlet and triplet states convert to one another based on the orientation of the radical pair in the magnetic field. Finally, the ratio of singlet to triplet state products is thought to affect the magnetoreceptor in such a way that it affects downstream chemical signalling pathways, hence allowing magnetoreception to occur. **Figure 7.1** provides a schematic for the radical pair mechanism and this topic has been recently reviewed (Ritz *et al*., 2000, Rodgers and Hore, 2009).

Importantly, application of radiofrequency fields which are thought to disrupt radical pair singlet-triplet product formations (without affecting magnetite) significantly disrupted

magnetic orientation behaviour of European robins (Ritz *et al*., 2004, Thalau *et al*., 2005), though no evidence of a specific mechanism was presented.

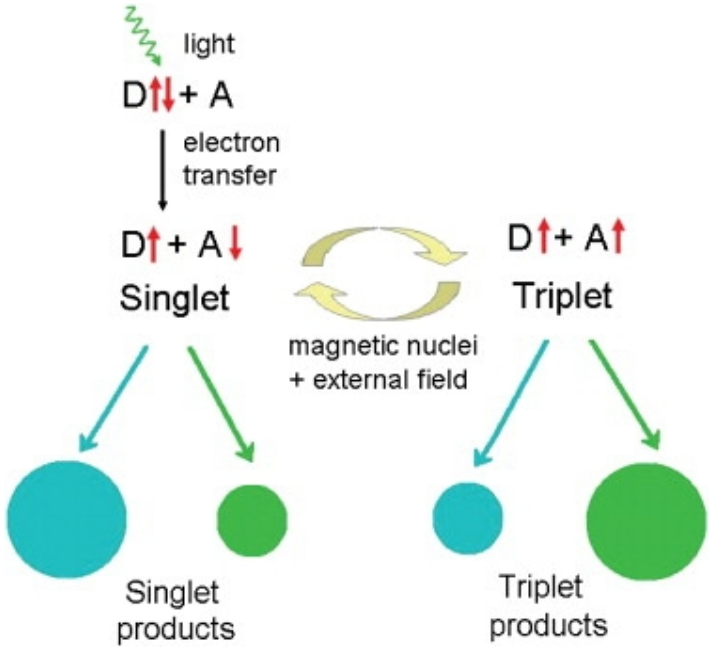

Figure 7.1. Schematic of the radical pair mechanism. Light-activated electron transfer creates a radical pair as either a singlet or triplet excited state. The ratio of singlet and triplet products generated depends on the environmental magnetic field. The electron donor molecule is designated with the letter D and the electron acceptor molecule with the letter A. Reproduced from Ritz *et al*. (2009).

The spin chemistry behind the radical pair mechanism has been the subject of much study and has been especially relevant in the search for a candidate magnetoreceptor that can mediate radical pair reactions (Rodgers and Hore, 2009). The majority of work on radical pair magnetoreception has endorsed Cryptochrome as an appropriate candidate magnetoreceptor, as Cryptochromes fit the necessary chemical criteria, and also recent studies of Cryptochrome and animal magnetoreception have not refuted this hypothesis.

7.1.3 Cryptochromes as magnetoreceptors

Cryptochrome has been proposed to be a candidate magnetoreceptor in several species. The Cryptochrome hypothesis was first proposed in (Ritz *et al*., 2000), because it was thought that Cryptochrome may be capable of mediating the spin chemistry required for the radical pair mechanism. In addition, given that cryptochrome is thought to be a photopigment in some species (particularly *Drosophila* and *Arabidopsis*), Cryptochrome may therefore fit the hypothesis of a light-sensitive receptor capable of sensing Earth's magnetic fields via the radical pair mechanism (Cry magnetoreception findings are summarized below in **Table 7.1**).

Species	Cry homolog	Magnetoreceptive ability	References
Thale cress (*Arabidopsis Thaliana*)	*AtCry1*	Differences in Cryptochrome-mediated plant growth in response to a magnetic field were detected (Ahmad *et al*., 2007) but were not reproduced in a subsequent study (Harris *et al*., 2009)	(Ahmad *et al*., 2007) (Harris *et al*., 2009)
Fruit fly (*Drosophila melanogaster*)	dCry	Loss of magnetoreception when the blue-light range that activates dCRY is omitted	(Gegear *et al*., 2008)
Garden warbler (*Sylvia borin*)	*gwCry1a*	Colocalization of gwCry1 with c-fos following migratory behavior; isolated gwCry1 absorbs blue light and forms radical pairs	(Mouritsen *et al*., 2004) (Liedvogel *et al*., 2007)
European Robin (*Erithacus rubecula*)	*Cry1a*	Immunohistochemistry signal from light-activated Cry1a found following exposure to blue but not red light	(Niessner *et al*., 2013)
Chicken (*Gallus gallus*)	*Cry1a*	Immunohistochemistry signal from light-activated Cry1a found following exposure to blue but not red light	(Niessner *et al*., 2013)
Mouse (*Mus musculus*)	*Cry1* and *Cry2*	Not yet shown	Not yet shown
Human	CRY2	*Cry*-deficient *Drosophila* respond to magnetic fields when human CRY2 is knocked-in	(Foley *et al*., 2011)

Table 7.1. Summary of Cryptochrome homologs in model species used to study magnetoreception, and the extent of characterized magnetoreceptive ability.

Specifically, the CRY magnetoreception hypothesis describes a mechanism whereby CRY, once activated by light (especially blue light, given its peak sensitivity, VanVickle-Chavez and Van Gelder (2007) Tu *et al*. (2004)), forms protein-bound Flavin or Tryptophan radical pairs where the spins of the unpaired electrons are affected by the Earth's magnetic field. The length of time Cryptochrome remains activated would depend on the how the radical pair spins are affected by the magnetic field. In invertebrates such as *Drosophila melanogaster,* Cryptochrome activation by magnetic fields would affect downstream signalling pathways involved in magnetoreception. In vertebrates such as migratory birds and mammals, this activation of Cryptochrome may potentially affect the light-sensitivity of the retinal neurons expressing Cryptochrome. As such, the retina may modulate the light-dependent magnetosensitive signal, such that an organism can visualise the magnetic field (or the visual field is modified depending on the intensity and orientation of the magnetic field). The Cryptochrome radical pair-based mechanism is thought to provide a magnetic sense that organisms may use as a visual map or compass. In long-distance migration, this would allow organisms to orientate themselves in the correct direction using the Earth's magnetic field, and perhaps "see" the correct direction. Finally, it is thought that whilst Cryptochrome radical pair-based magnetoreception can provide compass and directional information regarding the magnetic field environment, some animals (such as homing pigeons) may plausibly possess both this system and a magnetite system to detect the intensity of the field around them (Mouritsen and Hore, 2012).

Experimentally, CRY1, as detected using antiserum raised against the chicken CRY1a C-terminus, has been proposed to be localized in the retina of several species, including dogs, bears and primates (Niessner *et al*., 2016). However, there are some notable limitations to

this study, as the lack of knock-out tissue controls. Furthermore, although the study proposed that the antiserum recognized chicken CRY1a homologs in other species because of few sequence differences between those homologs and the epitope, the antiserum could not recognize CRY1a homologs in several species despite similar target sequences. Lastly, because no signal was achieved in mouse retinal tissue, the study claimed that the mouse magnetoreceptor may not express a *Cry1a* homolog, although this could have been due to technical limitations with the antibody.

Drosophila have been shown to lose the ability to sense a magnetic field when the blue-light range that activates CRY is omitted (Gegear *et al*., 2008). Magnetosensitive activity is restored when *Cry*-deficient *Drosophila* have dCry knocked back in (Gegear *et al*., 2010). Surprisingly, *Cry*-deficient *Drosophila* were also found to respond to magnetic fields when human CRY2 was knocked-in (Foley *et al*., 2011). Recent evidence has supported the idea of cryptochrome as a magnetoreceptor in birds (reviewed in Liedvogel and Mouritsen (2010)). Notably, increased c-fos, a marker for recent neuronal activity, was found in cryptochrome-expressing cells following magnetic orientation behaviour in garden warblers (Mouritsen *et al*., 2004). Furthermore, the light-activated conformation of Cry1a in chickens and European robins was found to be expressed following exposure to blue light, but not red light (Niessner *et al*., 2013). While these studies suggest at first glance that Cryptochromes may be blue-light sensitive magnetoreceptors across most tested species, no study has yet been able to confirm this role unequivocally. Indeed, further review of some studies indicates that certain CRY-dependent responses may light-dependent, circadian clock-dependent, or dependent on both light and clock. In addition, Cry may play a necessary part of the magnetoreception signalling pathway, but may not

necessarily be the light-sensitive magnetoreceptor. The major Cryptochrome magnetoreceptor studies are reviewed critically below.

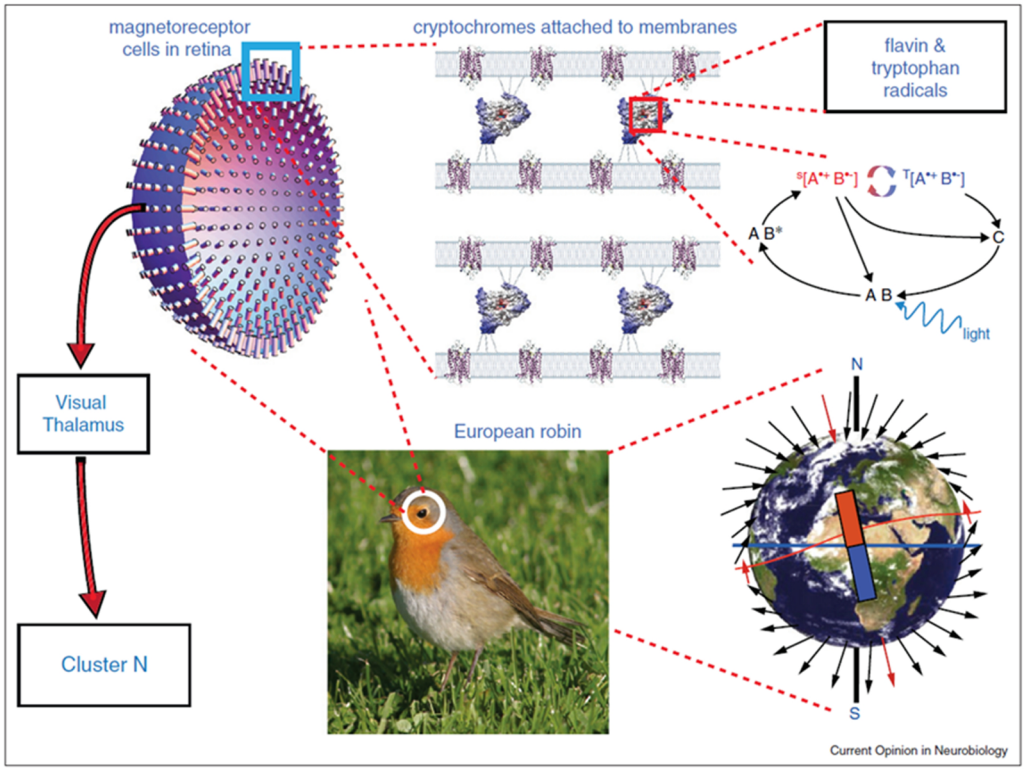

Figure 7.2. Schematic depicting Cryptochrome magnetoreception. Starting at the top right, Cryptochrome is thought to be a light-sensitive magnetoreceptor which forms Flavin and Tryptophan radical pairs (A and B are the electron donor and electron acceptor molecules, respectively), that can be influenced by magnetic fields via the radical pair mechanism. Cryptochrome is attached to membranes and is expressed in the retinas of birds such as the European robin. Retinal Cryptochrome magnetoreceptors to convey information about the surrounding magnetic field to the brain areas that process magnetic information (thought to be the Visual Thalamus and Cluster N in birds). Reproduced from Mouritsen and Hore (2012).

To date, cryptochromes remain the main candidate magnetoreceptor for the radical pair hypothesis (Rodgers and Hore, 2009, Solov'yov *et al*., 2010, Ritz *et al*., 2010a, Liedvogel and Mouritsen, 2010, Ritz *et al*., 2010b), though a recent study has now proposed a second candidate, MagR (Qin *et al*., 2016). However, solid evidence showing cryptochrome as a biological magnetoreceptor has been sparse. Below, the major studies investigating

cryptochrome magnetoreception in several model species are described and critically examined.

7.1.4 MagR: an alternative magnetoreceptor

Recently, a new candidate putative magnetoreceptor protein, deemed MagR, has been proposed. MagR is thought to form a rod-like complex with CRY and also bind iron, thus combining the radical pair mechanism and magnetite mechanism in a single system (Qin *et al*., 2016). MagR capable of binding CRY was found in *Drosophila* heads and therefore proposed as the *Drosophila* candidate magnetoreceptor. Whilst loss of MagR has not yet been shown to cause loss of magnetoreception in *Drosophila*, further experiments showing both loss and restoration of function would further support to this hypothesis.

Interestingly, MagR was shown to be expressed widely throughout the avian retina (tested in homing pigeons *Columba livia*) and colocalizes with CRY4 in the retina. CRY4 is a bird cryptochrome with no mammalian ortholog but has previously been associated with bird magnetoreception (Mitsui *et al*., 2015, Watari *et al*., 2012). Given the widespread expression of MagR in the retina, it will be necessary to determine whether the Cry-MagR complex is localized elsewhere in the body, as that may identify either other magnetosensitive structures or suggest that Cry-MagR is a magnetoreceptor in retinal tissue but not elsewhere in the body (which would be unlikely unless special conditions or components in the retina were not present elsewhere). Furthermore, the Cry-MagR complex was found in six different species across a great range of phyla: fruit fly, monarch butterfly, pigeon, mole rat, minke whale and human. As such, the Cry-MagR complex may have the potential to mediate magnetoreception in different types of species, though functional testing has yet to be performed.

The discovery of Cry-MagR complexes is the first direct finding to support a combined radical pair mechanism and magnetite mechanism theory of magnetoreception. However, this work is still in early stages and functional studies are essential to establish whether Cry-MagR complexes are truly capable magnetoreceptors in *Drosophila* and in other species.

7.1.5 Magnetoreception in non-mammals

7.1.5.a Magnetoreception in Drosophila melanogaster

Drosophila melanogaster (fruit fly, hereby denoted as *Drosophila*) are a particularly useful species in which to study magnetoreception, as genetic tools are available to probe the mechanisms by which *Drosophila* sense magnetic fields. In a groundbreaking study, Cry-deficient *Drosophila* were shown to lose the ability to sense magnetic fields (Gegear *et al*., 2008). In the same study, magnetoreception was also lost when the blue-light range that activates CRY was omitted. As such, this work was the first definitive study linking Cryptochrome to magnetoreception in *Drosophila.* Given that *Drosophila* Cryptochrome is a blue-light photoreceptor that entrains the fly circadian system, this data neatly fits into current knowledge of fly Cryptochrome. However, it is important to critically review this initial *Drosophila* magnetoreception study, as it has set the basis for the majority of subsequent work on this topic. First of all, the data from the study allows for two main conclusions – that *Drosophila* magnetoreception is *Cry*-dependent, and that *Drosophila* magnetoreception is dependent on blue light. However, given that it is possible for light at other wavelengths to stimulate a photopigment maximally sensitive in the blue-range, it is indeed possible for other wavelengths of light to stimulate Cryptochrome. Indeed, the

action spectra of *Drosophila* Cryptochrome peaks at 390nm (VanVickle-Chavez and Van Gelder, 2007), though 420nm light provides minor excitation (<5%).

Later work by the Reppert group showed that, through genetic knock-in, *Drosophila* will respond to magnetic fields using either *Drosophila* or monarch butterfly *Cry1* and monarch butterfly *Cry2* (Gegear *et al*., 2010). CRY-deficient *Drosophila* were also found to respond to magnetic fields when human CRY2 was knocked-in. Restoration of human CRY2 (but not human CRY1) is able to rescue the loss of magnetoreception in *Cry*-deficient flies (Foley *et al*., 2011). Importantly, this study show that magnetoreception is Cry-dependent and that human CRY2 is capable of mediating magnetoreception, though it does not prove that CRY is a magnetoreceptor, just that this response is CRY-dependent. Furthermore, as mammalian Cryptochromes do not function as photopigments, this study lends further evidence that Cry may not be a light-dependent magnetoreceptor, but may instead play an essential component of the magnetoreception pathway, perhaps by interacting with another photosensitive component, rather than being photosensitive itself.

Climbing, or negative geotaxis, was next found to be another *Drosophila* behaviour affected by magnetic fields (Fedele *et al*., 2014b). This study found that *Drosophila* climbing is disrupted by static electromagnetic fields (500 μT intensity) and that this is mediated by Cryptochrome, specifically the C-terminus of Cryptochrome. Finally, this study also showed that CRY expression in certain structures alone (antennae, photoreceptors, or a subset of clock neurons) is sufficient for magnetosensitivity of the climbing response.

In *Drosophila*, the Cryptochrome radical pair mechanism is thought to involve light activation of Flavin adenine dinucleotide (FAD), which is bound near a triad of Tryptophan residues (also called the Trp-triad). Electron transfer via the Trp-triad is thought to be an

essential component of a radical pair mechanism, such that Cryptochrome-based radical pair mechanism is hypothesized to depend on it (Aubert *et al*., 2000, Brazard *et al*., 2010). However, several studies have already shown that mutation of the Trp-triad in *Drosophila* does not affect magnetoreception abilities, casting doubts that the Trp-triad is truly a necessary part of the magnetosensing mechanism (Gegear *et al*., 2010, Fedele *et al*., 2014a). Specifically, removal of the Trp-triad motif does not block magnetoreception responses. Further work on this subject revealed that a CRY C-terminus structure that does not encode the Tryptophan triad or the FAD binding domain can still mediate magnetoreception, indicating that neither of these structures appear to be necessary for *Drosophila* magnetoreception (Fedele *et al*., 2014a). However, now a fourth Tryptophan residue has been found to be located nearby the Trp-triad exclusively in animal cryptochromes (Muller *et al*., 2015), such that it may play a role in electron transfer with the previously characterized Trp-triad. Perhaps this fourth residue could have compensated for the loss of the Trp-triad in previous studies that did not find loss of magnetoreception with loss of the Trp-triad (Gegear *et al*., 2010, Fedele *et al*., 2014a).

7.1.5.a Magnetoreception in migratory birds

Migratory birds are useful model organisms because they have a magnetoreception-relevant behaviour that can be easily observed. Furthermore, migratory orientation behaviour in birds can be observed and measured. Linking migratory behaviour in migratory bird species to Cryptochromes has therefore been one of the main goals in magnetoreception research using these model species.

Recent evidence has supported the idea of cryptochrome as a magnetoreceptor in birds (Liedvogel and Mouritsen, 2010, Ritz *et al*., 2010b). Furthermore, CRY can be detected in

the retinae of birds and other species, including mammals (Mouritsen *et al*., 2004, Bolte *et al*., 2016, Niessner *et al*., 2016). Increased C-FOS, a marker for recent neuronal activity, was found in cryptochrome-expressing cells following night-time magnetic orientation behaviour in garden warblers (Mouritsen *et al*., 2004). However, CRY is expressed in many cells throughout the mammalian retina, including cells that express C-FOS in response to light without any change in the magnetic field environment (own data). As such, though some studies conclude that their data support Cryptochrome as blue-light sensitive magnetoreceptors, it is essential to critically review this data in the context of circadian rhythm and retinal physiology literature.

Importantly, whilst bird species may have a clear physiological assay from which researchers can assess magnetoreception, there are some drawbacks to using birds as a model species to study the mechanism of magnetoreception. In particular, most birds used in such studies must be captured from the wild are not genetically controlled. Furthermore, genetic tols are poorly developed in birds, such that it remains very challenging to determine the specific mechanism by which bird magnetoreception occurs. For instance, Cry-knockout migratory birds would be most useful to assess the effects of loss of Cry on migratory behaviour.

7.1.6 Magnetoreception in mammals

A few high profile studies have indicated that mammals can sense magnetic fields. However, the data underlying this claim has been relatively weak and based more on associative observations rather than functional mechanisms.

For instance, cattle and deer were suggested to orientate preferentially in the North-South direction whilst resting or grazing (Begall *et al*., 2008), and that this orientation was disrupted by proximity to power lines due to low-frequency electromagnetic fields (Burda *et al*., 2009). However, these studies were both based on analysis of aerial images of pastures, rather than controlled experiments. Furthermore, a follow up study by another research group suggested that cattle do not show any significant magnetic orientation preference along geomagnetic lines (Hert *et al*., 2011). A subsequent article (Begall *et al*., 2011) was then issued in defense of the original cattle magnetoreception study, claiming that differences in methodology and poor image quality were responsible for the two study's different findings. This subsequent article claimed that adding the Hert *et al.* (2011) data to their own study still showed that cattle prefer to orientate North-South when resting. Another study from the same group and using similar methodology as (Begall *et al*., 2008) indicated that dogs prefer to align North-South while defecating but not while urinating (Hart *et al*., 2013). These results are again mainly associative, and although they generate public interest in magnetoreception research, the data provided from these studies have not been replicated nor yielded solid conclusions upon which to base further experimentation.

In humans, the potential adverse effects of unavoidable exposure to electromagnetic fields has been of public interest (Crumpton, 2005, Crumpton and Collins, 2004). In particular,

speculation regarding the association between mobile phone use and brain cancer garnered much public interest and resulted in the establishment of the Electromagnetic Fields (EMF) Project at the World Health Organization in 1996 (McGregor, 1998, Ban, 1998). The EMF project aims to characterize the effect of electromagnetic fields on human health and set guidelines for safe EMF exposure. Currently, the WHO has set magnetic fields of 100μT at 50Hz to be the upper limit of intensity and frequency for safe long-term exposure. The International Agency for Research on Cancer (IARC) classified extremely low-frequency magnetic fields as "possibly carcinogenic to humans" (IARC, 2002). However, longitudinal studies conducted by the EMF Project (INTERPHONE study) as well as by other groups concluded that mobile phone use is not correlated with increased risk of various brain cancers (Aydin *et al*., 2011, INTERPHONE study group, 2010, Hepworth *et al*., 2006, Lonn *et al*., 2005). However, it was noted that mobile phone use (particularly by young individuals) has increased since when initial studies began, and that given the recent development of mobile technologies and networks such as 3G and 4G, any longitudinal findings can report only on any effects within the time frame of the study. Not enough time has yet elapsed to determine an effect with certainty. Furthermore, other studies have suggested a link between human residences near power lines and certain cancers such as childhood leukaemia (Kheifets *et al*., 2010, Ahlbom *et al*., 2000, Greenland *et al*., 2000), though such studies remain inconclusive (Lacy-Hulbert *et al*., 1998, Baldi *et al*., 2011, Morgan *et al*., 2015). As such, it remains of relevance to human health whether exposure to EMF causes any effect on humans, and indeed if such effects are detrimental. Before such a question can be approached, however, it is essential to first understand mammalian magnetoreception and its mechanisms. Because of the widely available genetic and

experimental tools to ensure appropriate replication, mice are an ideal animal model by which to investigate mammalian magnetoreception.

7.1.7 Magnetoreception in mice

Only a handful of studies have reliably described magnetoreception in mice. So far, only two mouse behaviours involving magnetoreception have been reliably characterized using laboratory mice: nest building and learned magnetic direction in a 4-armed water maze.

C57BL/6J mice were found to build their nests based on magnetic orientation (Muheim *et al*., 2006). Mice were trained to build nests in one of four magnetic directions by applying a light gradient in a rectangular cage, such that mice would build in the dark end of the cage. Mice were then tested in a circular arena, and were found to build their nests consistently in the same magnetic direction as that in which they were trained. Similar work has been performed in mole rats (Ansell's mole rats, *Cryptomys anselli*, and blind mole rats, *Spalax ehrenbergi*) and Siberian hamsters (*Phodopus sungorus*). Mole rats appear to have an innate preference to nest-build in magnetic east to south-east directions and rotation of the magnetic field rotates the locations of where their nests are built (Burda *et al*., 1990, Kimchi and Terkel, 2001). In Siberian hamsters also use magnetic cues to decide nest position and are also capable of learning a magnetic direction in which to build their nests (Deutschlander *et al*., 2003).

C57BL/6 mice were also found capable of learning the magnetic direction of a submerged platform in a 4-armed (plus) water maze following two training trials (Phillips *et al*., 2013). The magnetic field was rotated between trials to ensure that magnetic orientation was tested. Furthermore, extreme care was taken to ensure that other directional cues were

not available or at least randomized in order to ensure only magnetic cues could be used by the mice. Lastly, directional preference of each mouse was taken into account to ensure this did not bias results. Importantly, electromagnetic shielding was also employed to minimize any interference. Notably, other commonly used rodent spatial cognition tasks such as the water maze and radian arm maze have not yielded observations of magnetic cue-guided behaviour in mice, despite their extensive laboratory use. This may be due to the many directional cues available to mice, such that magnetoreception may not always be employed when mice orient themselves.

Although these two studies (performed by the same research group) have shown significant promise in providing reliable and accessible assays for laboratory studies of mouse magnetoreception, their results have yet to be replicated and validated by independent groups.

Given that genetic tools are readily available, mice are the best available model organism to investigate mammalian magnetoreception at a mechanistic level. Indeed, recent studies have investigated mouse CRYs as magnetoreceptors. As the best characterized function of Cryptochromes in mice is its role as a core clock protein, the impact of magnetic fields on the SCN under blue light was tested (Fedele *et al*., 2014a). However, no significant effect of magnetic fields was found on mouse SCN, suggesting that any mouse magnetoreception ability may be via other pathways (Mat Edwards and Michael Hastings, personal communication).

There are some scientific issues that need to be addressed regarding the possibility that mammalian cryptochromes function as magnetoreceptors. Firstly, the cryptochrome-based magnetoreception and radical pair magnetoreception relies on the assumption that

magnetoreception is light-dependent. There is currently no scientific evidence showing that mammalian cryptochromes are capable of acting as photoreceptors, or that they are able to modulate signals in response to light. Indeed, mammalian cells used for heterologous melanopsin (OPN4) expression experiments were found to be non-light sensitive, but became photosensitive after melanopsin transfection (Panda *et al*., 2005, Qiu *et al*., 2005, Fu *et al*., 2005). Yet, most mammalian cells express Cryptochromes (Aarti Jagannath, personal communication), thus suggesting that Cryptochromes are not capable of acting as photoreceptors in mammals. Similarly, mice without rods, cones and melanopsin lack all responses to light, though Cryptochromes were still expressed in these mice (Hattar *et al*., 2003). Together, this suggests that mammalian Cryptochromes are not functional photoreceptors in mammals. Non-mammalian cryptochromes, however, have been shown to function as photopigments (Stanewsky *et al*., 1998, Emery *et al*., 1998, Somers *et al*., 1998, Cashmore *et al*., 1999) and can therefore be seen to fit the radical pair hypothesis. In mammals, the Cryptochrome-based magnetoreception could still be reconciled with the lack of photoreceptor function in mammalian Cryptochromes. Cryptochromes may not be mediating the magnetoreception response (as the light-sensitive magnetoreceptor), they may instead play an essential role magnetoreception response in a light-independent manner. Furthermore, light-dependent and Cry-dependent magnetoreception in mammals could occur if Cry were to interact with a photoreceptive system as part of the magnetoreception signalling cascade.

Secondly, there is a lack of replicable evidence showing that mammals can sense magnetic fields. There has yet to be a standardized physiological assay to test mammalian magnetoreception. Lastly, despite the availability of Cry-deficient mice since 1999 (van der Horst *et al*., 1999), investigation of magnetoreception in wildtype mice compared to mice

lacking cryptochromes has never been undertaken. Since highly-specific genetic knockout tools are not yet available in other species, mice are the best candidate species to test whether Cryptochromes mediate magnetoreception in mammals.

7.2 Aims

The aim of this pilot experiment are to determine whether low frequency magnetic fields affect sleep and associated behaviours in wildtype mice. The coordination of several brain regions and neurotransmitters regulates sleep in mammals. Importantly both circadian pacemaker and homeostatic inputs affect the sleep-wake cycle. Even slight disturbances to physiology can affect sleep and as such, sleep is both an essential function and a useful physiological readout.

Furthermore, in mice, sleep is immediately induced in response to light. This makes light-induced sleep a potentially useful assay for studying mammalian magnetoreception, as the radical pair mechanism is proposed to be light-dependent. As such, this light-induced sleep response provides a rapid way of studying the effects of light on sleep and how electromagnetic fields may affect this.

In this pilot experiment, the specific aims are:

- To determine whether CRY1 co-localizes with C-FOS expressing cells following a light pulse
- To assess how a 100μT and 50Hz magnetic field affects latency to sleep and distance travelled in wildtype mice using a non-invasive and sensitive assay of sleep (videotracking and immobility assessment)
- To determine if any magnetic responses are light-dependent, and to quantify these responses.

Depending on whether this pilot study on sleep and associated behaviours yields a reliable and non-invasive assay to study mouse magnetoreception, future experiments using *Cry*-null mice to determine whether mammalian cryptochromes mediate mouse magnetoreception may be pursued.

7.3 Methods

7.3.1 Mice

C57BL/6 mice from Harlan were used for all the experiments in this chapter.

7.3.2 Light Tight Chambers

For light pulse studies, mice were individually housed in cages placed in ventilated light-tight chambers so that the light environment could be controlled. Chambers were lit using LEDs with light levels of ~300lux when measured at the bottom of the cage.

Figure 7.3. Photograph of individual cages inside lit and ventilated light-tight chambers. Used with permission from Professor Stuart Peirson (Oxford, unpublished).

7.3.3 Light pulses

For light pulse studies, mice were dark adapted for 4 hours and then subjected to a white LED light pulse at ZT16 for 30 minutes in a new cage (Semo *et al*., 2003b, Lupi *et al*., 2008). Tissue was then collected at ZT17, 30 minutes after the white light pulse finished. The light

intensity of the white light pulse was approximately 300 lux. As a negative control, tissue was also collected at ZT16 from mice who were moved to a new cage but were not exposed to the white light pulse. The light pulse was approximately 300 lux in intensity.

7.3.4 Immunohistochemistry

Immunohistochemistry experiments were performed as in previous experiments (described in Chapter 2.3). C-FOS primary antibody (CBL440, Chemicon-Millipore) was incubated overnight at 4°C (1:100). Alexa 568 conjugated donkey anti-sheep secondary antibody (Life Technologies) was incubated for 2h at room temperature (1:200).

7.3.5 Hatbox Cages for magnetic coil experiments

Specialized cages were used for the magnetic coil experiments, using no metal parts to ensure no interference with the application of the magnetic field. These cages, termed "hatbox" cages because of their shape, were custom-made from black Perspex. The dimensions and shape of the "hatbox" cages is outlined in **Figure 7.4**. Two mice could be housed separately in each hatbox. A food hopper and water bottle were made available, as well as flowing air exchange, such that mice had continuous access to food and water during the experiments.

7.3.6 Magnetic Coil

The Helmholtz magnetic coil was custom-made for the Electric and Magnetic Fields Biological Research Trust and the Health Protection Agency/Public Health England. A field intensity of 100 μT at a frequency of 50Hz was used in magnetic field testing as this is the

safe exposure limit proposed by the World Health Organization. Light intensity within the hatbox was 150 lux during both regular light exposure and during light pulses.

7.3.7 Study design

Wildtype mouse behaviour was recorded from ZT13-16 in response to an acute light pulse and a 100µT magnetic field. 18 male C57 Bl6 mice were used in this experiment. In order to make within-subject comparisons, all 18 mice were subjected to 4 different conditions whilst their activity was recorded between ZT13-16. All mice were moved to the novel hatbox cages at ZT13 and returned to their home cage at ZT16.

Condition A: No light, No magnetic field
Condition B: Light pulse from ZT14-15, No magnetic field
Condition C: Light pulse from ZT14-15 in the presence of 100µT magnetic field from ZT 13-16
Condition D: No light, 100µT magnetic field from ZT 13-16

In all mice, Condition A was recorded first. Order of Conditions B, C, and D were randomized for each of the 18 mice to counterbalance any effects of order of conditions. Furthermore, equal numbers of mice received each particular order of Conditions B, C, and D to ensure counterbalancing.

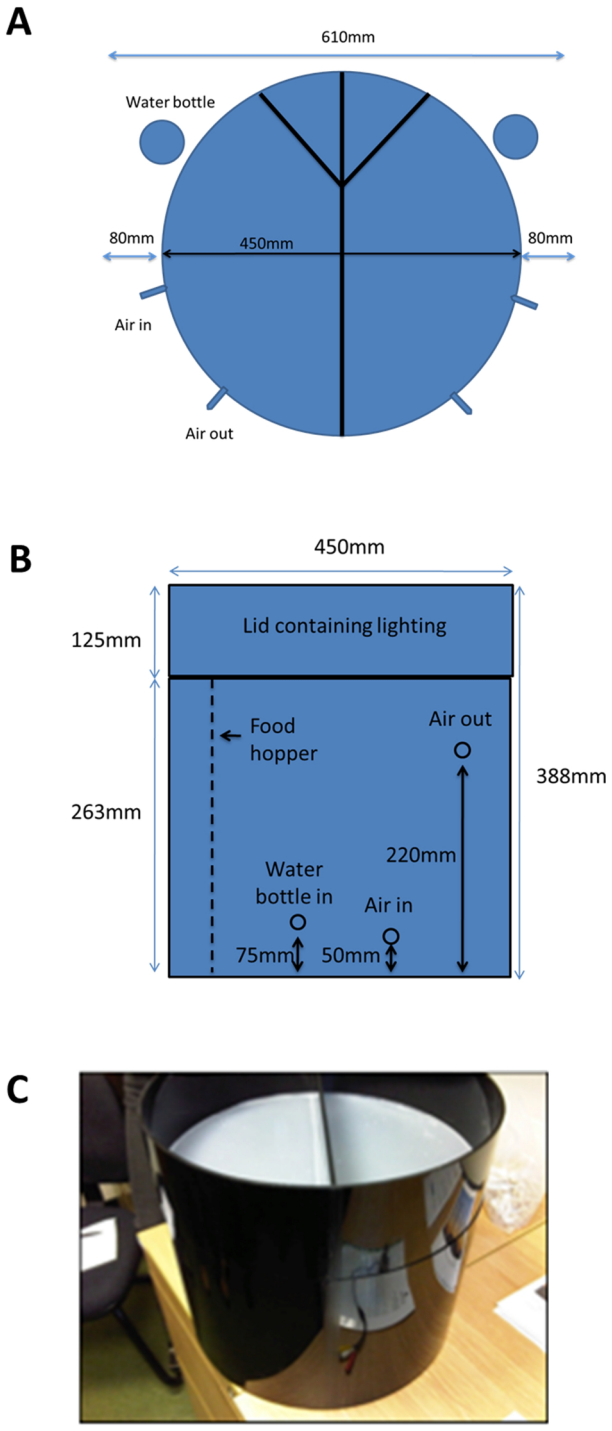

Figure 7.4. Hatbox dimensions and image of hatbox cage. **(A)** Top view of hatbox cages. Each cylindrical cage is divided into two compartments which can each house one mouse. Water and food are provided *ad libitum*. Filtered air is passed to and from the cage as the tops are sealed. The dimensions of each hatbox cage is detailed in the diagram. Used with permission from Dr. Jackie Haines (Public Health England). **(B)** Side view of hatbox cages. The lids of each hatbox cage contain lighting and also an infrared video camera in order to videorecord mouse activity under both light and dark conditions. Used with permission from Dr. Jackie Haines (Public Health England). **(C)** Image of hatbox cages used. Used with permission from Professor Stuart Peirson (Oxford, unpublished).

7.3.8 Camera setup

Miniature near infrared video cameras (Sentient Mini-night vision CCTV camera, Maplin, UK), were mounted 30cm above every cage to record mouse activity in both light and dark conditions. A wide angle lens (130o, 2.8mm, Open Twenty Four Seven Ltd, UK) was used to ensure the entire cage area could been recorded. Any light reflection from the NIR light source was diffused using tracing paper if necessary. All cameras were connected to a 16-channel digital hard-drive recorder (Samsung SRD 470D). Custom made Perspex blocks (LivAcrylic) were used to prevent mice from entering an area of the cage that could not be recorded by the camera.

7.3.9 Analysis of immobility-defined sleep and distance travelled

Prior to any video recording, background shots were taken of the cage under the camera with no mouse inside, under both light and dark conditions. After the experiment videos were recorded, video files were downloaded from the digital hard-drive recorder and cut using editing software (Video Edit Master, freeware) to include before and after background shots for individual mouse recording. Using ANY-maze software (Version 4.70, Stoelting, USA), background subtraction using the background shots without the mouse in the cage. This background subtraction enabled accurate video-tracking of the mouse. When cage bars were present, ANY-maze could be used to remove these bars from the video, as well as adjust contrast to improve mouse tracking. Furthermore, the exact area within the video that depicts the cage floor could be denoted and a scale bar drawn to ensure accurate calculations.

ANY-maze measured immobility automatically, as well as several other behaviours, including the latency to immobility and distance travelled.

Use of ANY-maze software to measure immobility-defined sleep has previously been validated against electroencephalography, the gold standard for measuring sleep status (Fisher *et al*., 2012). This protocol uses immobility of 40s or more to define a sleep bout. 95% sensitivity of immobility detection was used to provide the best results.

Distance travelled was used as an assay instead of time spent mobile, as it gives a better indicator of mouse activity. A grooming mouse may largely remain in one spot in the enclosure, though it will be deemed "mobile" according to ANY-MAZE software. Grooming on the spot is a very different activity compared to exploration of the enclosure. As such, distance travelled was chosen as a better indicator of overall mouse activity.

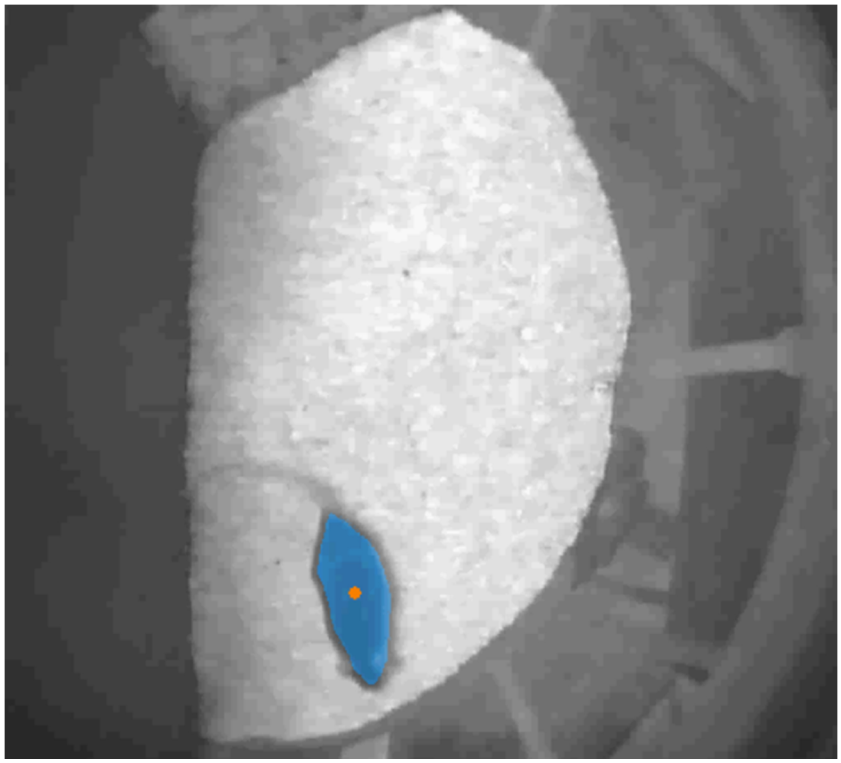

Figure 7.5. A screencapture of a mouse inside a hatbox cage. The mouse's body is tracked by the Any-MAZE software (blue).

7.4 Results

7.4.1 CRY1 is partially co-expressed with cells expressing light-induced C-FOS in the retina

To address previous studies where CRY colocalization with C-FOS in retinal cells following magnetic orientation behaviour in birds (Mouritsen *et al*., 2004), CRY1 co-localization with retinal cells responsive to an acute light pulse, a marker of light activation *in vivo* (Hannibal *et al*., 2001, Pickard *et al*., 2009, Semo *et al*., 2003a) was studied. CRY1 was found to partially co-express with light-responsive retinal cells that express the immediate early gene *c-fos* after a 1 hour bright white light pulse at ZT14. As such, a subset of cells expressing light-induced C-FOS in the retina also express CRY1, but some do not.

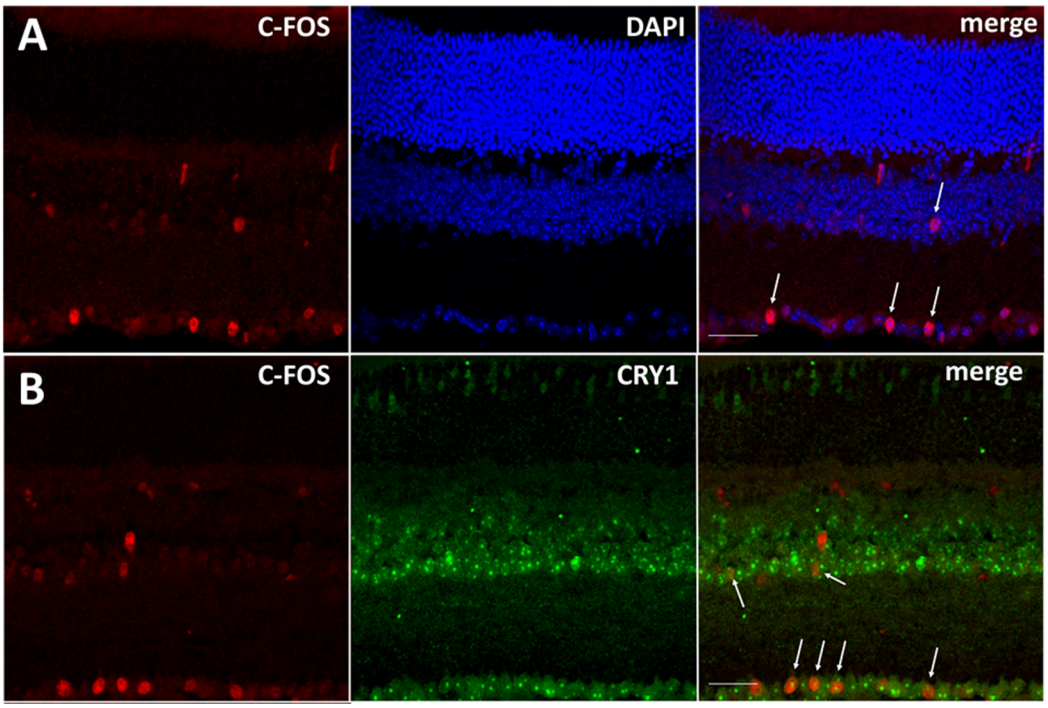

Figure 7.6. CRY1 partially co-localizes with C-FOS expressing cells following a white light pulse. White arrows indicate cells demonstrating colocalization in individual cells. Scale bar indicates 20µm. **(A)** A subset of retinal cells express C-FOS following a white light pulse. **(B)** CRY1 colocalizes with C-FOS expressing cells following a white light pulse.

7.4.2 Wildtype mice are awake and active between ZT13-15

Wildtype mouse behaviour under sham conditions, without application of a light pulse or electromagnetic field (EMF), was recorded (n=18) between ZT13-15 in order to determine baseline amounts of time spent asleep and distance travelled. As later assessment of light-induced sleep and associated behaviours in mice between ZT13-15 was planned, a baseline on which to reference any observed behaviours was therefore required.

Mice were removed from their home cage at ZT13 and placed directly into the hatbox cages with *ad libitum* access to food and water. They were singly housed and individually monitored by video. Anymaze animal tracking software was used to then analyse mouse behaviours. Mice were found to spend 20 ± 6.4 seconds asleep and travel 71 ± 3 m in the first hour (ZT13-14). Mice increased their sleep to 128 ± 67 seconds in the second hour (ZT14-15) and decreased distance travelled to 37 ± 4 m. Finally, mice slept most (345 ± 101 seconds), and travelled least (27 ± 3 m) in the third hour (ZT15-16). At ZT16, the experiment ended and mice were returned to their home cages. Mice likely demonstrated increased sleep behaviour over time in the new enclosure as they spent more time exploring in the first hour compared to the last hour.

This data is shown in **Figure 7.7** and **Figure 7.8** as Condition A (EMF off, Light off). These baseline sham recordings were used to determine whether acute light or magnetic field pulses had any effects on wildtype mouse behaviour.

7.4.3 Wildtype mice demonstrate a higher sleep duration in response to a 100µT magnetic field in addition to a ZT14-15 acute light pulse

Sleep duration data is presented in **Figure 7.7** and distance travelled data is presented in **Figure 7.8**.

Mice did not sleep for significantly different amounts of time, nor travelled significantly different distances under all four test conditions (A, B, C, and D) between ZT13-14.

Wildtype mice were found to sleep in response to a ZT14-15 acute white light pulse without any EMF (Condition B). As in Condition A, mice were moved to hatbox cages at ZT13. From ZT14-15, a light pulse of 150 lux was applied. Time spent asleep trended upwards immediately in response to the light pulse compared to sham ($p = 0.07$).

At ZT14-15, surprisingly, wildtype mice were found to spend significantly higher time asleep ($p < 0.0001$) in the presence of both EMF and light pulse (Condition C), compared to light pulse alone (Condition B), EMF alone (Condition D), or the sham control (Condition A). Furthermore, when exposed to EMF alone (Condition D), mice travelled a significantly greater distance between ZT14-15 compared to all other conditions (Conditions A, B and C).

At ZT15-16, when subjected to EMF alone (Condition D), mice spent significantly less time asleep than under all other conditions (Condition A, B and C). Furthermore, mice travelled a significantly greater distance during ZT15-16 when subjected to light pulse alone (Condition B), EMF alone (Condition D) or both (Condition C), compared to sham treatment (Condition A).

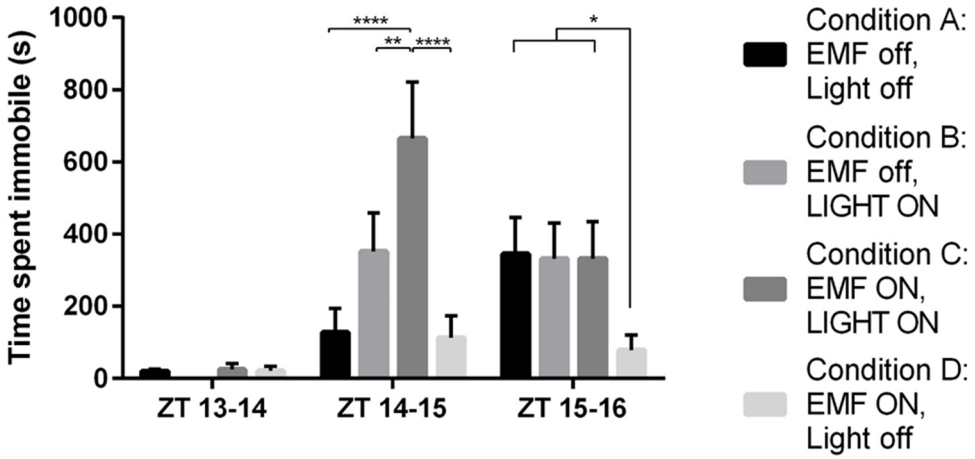

Figure 7.7. Wildtype mice demonstrate a higher sleep duration in response to a 100µT magnetic field in addition to a ZT14-15 acute light pulse. Mice did not sleep for significantly different times under all four conditions between ZT13-14. Between ZT14-15, mice tended to sleep a greater amount of time when a light pulse was applied compared to the sham or EMF only condition ($p = 0.07$). When both an acute light pulse and EMF were applied, mice slept for a significantly greater amount of time ($p < 0.0001$) than under the light pulse only condition. Finally, during ZT15-16, mice slept for a significantly smaller amount of time under the EMF only condition compared to all other conditions ($p < 0.0001$). During EMF ON conditions, the magnetic field was applied from ZT13-16. EMF = electromagnetic field, LIGHT = light pulse. Please note that Jackie Haines performed this experiment.

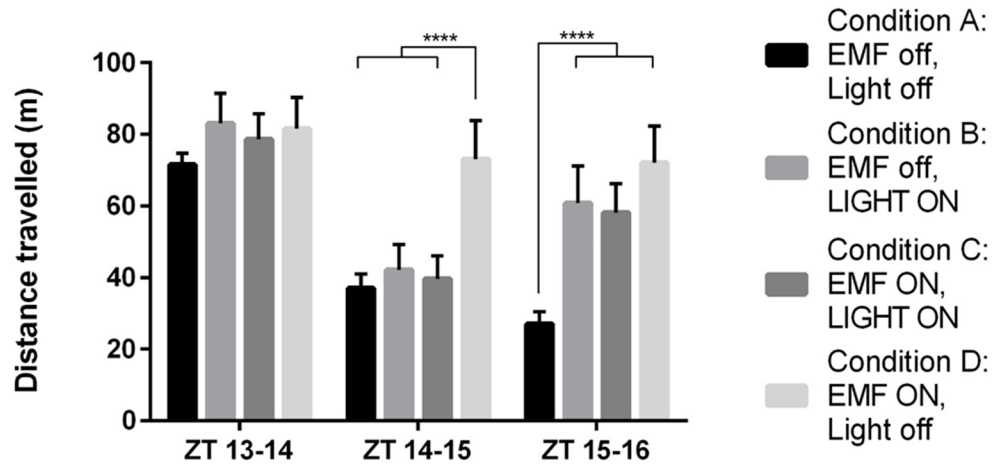

Figure 7.8. Wildtype mice exposed to the 100µT magnetic field but not light pulse, travelled a significantly greater distance between ZT14-15 compared to all other mice. Mice did not travel for significantly different distances under all four conditions between ZT13-14. At ZT14-15, mice under the EMF only condition travelled for a significantly greater distance than all other conditions ($p < 0.0001$). At ZT15-16, mice under the light pulse only, EMF only and light pulse and EMF together travelled for a significantly greater distance compared to the sham condition ($p < 0.0001$). During EMF ON conditions, the magnetic field was applied from ZT13-16. EMF = electromagnetic field, LIGHT = light pulse. Please note that Jackie Haines performed this experiment.

7.5 Discussion

7.5.1 Effects of EMF on sleep and associated behaviours in mice

These results are the first data indicating effects of magnetic fields on sleep in mammals. Sleep is a light-sensitive physiological phenomenon in mice, and is thus a potentially informative assay for mouse magnetoreception. Sleep duration and latency to sleep is dependent on a variety of factors, including homeostatic needs, circadian drive, and emotional state. Light-induced sleep at ZT14 is a well-characterized response in mice (Lupi *et al*., 2008, Semo *et al*., 2003a, Heise *et al*., 2015). Given that a reliable and established sleep response in mice was available, this response was therefore examined under the effect of low-frequency magnetic fields. Sleep has not previously been shown to be affected by the application of low-frequency magnetic fields in any animal models.

7.5.2 Light-dependent effects of EMF on mice

Perhaps the most striking result from these experiments is demonstrated in **Figure 7.7**. Here, it is shown that wildtype mice sleep for a greater duration of time (as assayed by time spent immobile) in response to a 100 µT magnetic field applied together with an acute light pulse at ZT 14-15. Acute light-induction of sleep independent of magnetic field application was observed, though this response is somewhat attenuated compared to previous studies (Lupi *et al*., 2008). This may be caused by removing mice from their home cage one hour prior to the light pulse, whereas previous studies recorded mice sleeping within their home cages. The latter was not possible for the work presented here as the

mice were placed within the magnetic coil at ZT13. Neither time spent asleep nor the latency to sleep are affected by cage disturbance (assayed by physical cage shaking, data not shown). As such, it was assumed that the time spent asleep nor the latency to sleep would not be affected in these magnetoreception experiments when mice were transported from the home cage to the hatbox cages. However, the effects of removing mice from their home cages on subsequent light-induced sleep were not tested. This will be necessary in future studies.

The acute nocturnal light-induction of sleep is potentiated by the application of a 100μT magnetic field. The mechanism for this response may be cryptochrome-based, as discussed below, or by an as-yet undetermined mechanism. Previous studies, particularly in avian species, have suggested that retinal Cryptochromes sense changes in magnetic fields and affect retinal light sensitivity (Ritz *et al*., 2000). As such, certain changes in the magnetic field may cause the environment to appear either brighter or darker. Given this hypothesis, it may be speculated that the application of the 100 μT magnetic field may cause the light environment to appear significantly brighter to mice, leading to increased sleep. However, current knowledge is still far from proving such a hypothesis and this will require further work, though it will be inherently limited by the inability to assay how the environment appears to animal subjects.

In **Figure 7.8**, increased distance travelled between ZT15-16 was observed after the one-hour light pulse as compared to sham-treatment. This may be rebound exploration of the environment following the light pulse. There was no difference observed in distance travelled between light-pulsed mice treated with or without EMF.

7.5.3 Light-independent effects of EMF on mice

Application of the 50 Hz 100 µT magnetic field also caused mice to spend less time asleep at ZT15-16 compared to sham-treated mice at the same time point. This may have been caused by several potential factors. As EMF was applied for all three hours of testing, low frequency magnetic fields may attenuate sleep in the absence of light. Furthermore, it was found that application of EMF alone from ZT13-16 results in increased distance travelled compared to sham treated mice. It may be that EMFs potentiate locomotor activity, thus causing reduced sleep at the measured times.

This is the first report of light-independent effects of EMF affecting sleep and locomotor activity of mice. The mechanism for light-independent EMF effects in mammals remain unknown, and magnetite-based magnetoreception studies have been performed mainly in non-mammals. Perhaps, as in other species, mammals express magnetosensitive molecules that contain magnetite crystals. Furthermore, both light-independent and light-dependent magnetoreception may be plausible in a mammalian magnetoreception mechanism that depends on the Cry-MagR complex. However, particularly as sleep has not previously been investigated in response to EMF effects, further work will be required to determine the mechanism of light-independent EMF-reponses.

7.5.4 A role for mammalian Cryptochromes in magnetoreception

We have shown CRY expression in mouse retinal cone photoreceptors as well as in pRGCs. The role of CRY in light-dependent mammalian magnetoreception may therefore involve Cryptochrome interaction with the photoreceptor systems of the retina. Mammalian CRYs are not photopigments, and therefore it is important to consider that there is no need to assume that mammalian CRYs must be light-dependent magnetoreceptors. Rather, it is possible that mammalian CRYs are an essential component of the mammalian magnetoreception pathway, but not necessarily light-dependent magnetoreceptors.

The mechanism for magnetoreception in mice has not yet been characterized. Future work will determine whether *Cry1*$^{-/-}$, *Cry2*$^{-/-}$ and *Cry1*$^{-/-}$*Cry2*$^{-/-}$ mice demonstrate any differences in light-induced sleep within the same magnetic field. This work would aim to determine whether the observed mouse magnetoreception behaviours are CRY-dependent. If so, this would lend further evidence to the magnetoreception field that CRYs are essential to the magnetoreception signalling pathway, if not the magnetoreceptors themselves. However, the issue of light-responsiveness in mammalian Cryptochromes would still need to be resolved, as there remains to date no evidence that mammalian Cryptochromes are light sensitive. It was observed that CRY1 is expressed in light-activated cells (marked by C-FOS expression following a nocturnal light-pulse, see **Figure 7.6**). CRY1 is expressed in cones and light-induced C-FOS expressing cells, whilst CRY2 can be found in the outer segments of photoreceptors. As such, whilst mammalian Cryptochromes may no longer function as photoreceptors, they are located in light-sensitive cells in the mammalian retina and therefore their putative function as magnetoreceptors could thus be governed by light.

If Cryptochrome is mediating magnetoreception either as the magnetoreceptor or as an essential part of the pathway, the mechanisms by which it may do so remain to be elicited. Investigating CRY retinal function in a magnetic field environment requires some experimental creativity. Electrophysiological recordings such as electroretinography on live anaesthetized mice, or multi-electrode array recordings in whole retinal explants are not possible within the magnetic field environment as the recordings themselves will be perturbed by the electromagnetic fields. Similarly, digital contrast sensitivity testing (such as those detailed in this thesis using the Optomotry setup) cannot be performed within the magnetic field arena as the recording equipment would be located within the arena and may be affected by EMF.

A potential future area of exploration, should Cryptochrome be found to mediate magnetoreception, would be to look at the effects of the magnetic field on the retinal clock, since mammalian Cryptochromes play a vital role in the retinal clock. This thesis has presented three different physiological assays for the mouse retinal clock, all of which have been shown to be CRY-dependent. As such, contrast sensitivity, using a non-digital setup, could be tested within the magnetic field arena without concerns that the magnetic field may affect the recordings. This would involve standardized printed posters of black bars on a white background at the correct spatial frequency and contrast differences (dark grey bars on a light grey background with the appropriate saturation). These posters could be rolled into a cylinder and placed on a rotating drum base to replicate the stimuli of the digital contrast sensitivity apparatus. The rotating drum base should be outside the magnetic field whereas the mouse and the rotating laminated poster are within the field. Indeed, as a circadian rhythm in contrast sensitivity appears to be dependent on *Cry1*, this

setup could be used to explore the effects of a magnetic field on the contrast sensitivity circadian rhythm in both wildtype and *Cry1*$^{-/-}$ mice.

Furthermore, exploration of other magnetic field intensities would give additional information regarding whether magnetoreception in mice exhibits any dose-dependent effects. It would be especially informative to know what the magnetic field intensity threshold for magnetoreception in mammals is, as this may affect public health guidelines. In these experiments, 100µT 50Hz EMF stimulation was used in order to produce results comparable to previous studies (Saha *et al*., 2014, Kabacik *et al*., 2013) and also because it is the limit imposed by the World Health Organization regarding safe exposure to EMF for humans. Previous studies on various species have used magnetic exposures of very diverse intensities, from 150 nT (Mouritsen *et al*., 2004) to 50 µT (Phillips *et al*., 2013) to 500 µT (Fedele *et al*., 2014b). Given the large range in which magnetoreception studies have used different field strengths in the past, it would be useful as a future experiment to understand dose dependent effects of magnetic fields.

In addition, other effects of magnetic fields on mammals have yet to be studied. Given the highly significant effect on mouse sleep depicted in **Figure 7.7** it may be informative to determine whether magnetic fields affects sleep in humans. Insomnia and sleep disorders remain prevalent in human society, with more than one-third of the UK population experiencing them at one time in their lives (UK National Sleep Foundation). If exposure to magnetic fields has any temporary or lasting effects on sleep and associated behaviours in humans, this is of particular interest for public health reasons.

7.6 Conclusions

In this pilot experiment, a non-invasive and sensitive assay of sleep was used in order to measure the effects of EMF on light-induced sleep in mice. It is shown that there are both light-dependent and light-independent effects of EMF on mice. In particular, it was found that wildtype mice sleep for a greater duration of time in response to a magnetic field applied together with an acute light pulse. These results are the first data indicating effects of electromagnetic fields on sleep in mammals.

In future experiments, the question of whether mammalian CRYs mediate mouse magnetoreception will be explored using *Cry*-null mice. Further work will elucidate whether the role of mammalian CRYs in magnetoreception is a role as the light-dependent magnetoreceptor or as an uncharacterized role as an essential pathway component.

References

ABRAHAM, D., DALLMANN, R., STEINLECHNER, S., ALBRECHT, U., EICHELE, G. & OSTER, H. 2006. Restoration of circadian rhythmicity in circadian clock-deficient mice in constant light. *J Biol Rhythms,* 21**,** 169-76.

ADHIKARI, P., PEARSON, C. A., ANDERSON, A. M., ZELE, A. J. & FEIGL, B. 2015. Effect of Age and Refractive Error on the Melanopsin Mediated Post-Illumination Pupil Response (PIPR). *Sci Rep,* 5**,** 17610.

AHLBOM, A., DAY, N., FEYCHTING, M., ROMAN, E., SKINNER, J., DOCKERTY, J., LINET, M., MCBRIDE, M., MICHAELIS, J., OLSEN, J. H., TYNES, T. & VERKASALO, P. K. 2000. A pooled analysis of magnetic fields and childhood leukaemia. *Br J Cancer,* 83**,** 692-8.

AHMAD, M., GALLAND, P., RITZ, T., WILTSCHKO, R. & WILTSCHKO, W. 2007. Magnetic intensity affects cryptochrome-dependent responses in Arabidopsis thaliana. *Planta,* 225**,** 615-24.

AKIMOTO, M., FILIPPOVA, E., GAGE, P. J., ZHU, X., CRAFT, C. M. & SWAROOP, A. 2004. Transgenic mice expressing Cre-recombinase specifically in M- or S-cone photoreceptors. *Invest Ophthalmol Vis Sci,* 45**,** 42-7.

ALBRECHT, U. & FOSTER, R. G. 2002. Placing ocular mutants into a functional context: a chronobiological approach. *Methods,* 28**,** 465-477.

ALLEN, A. E., STORCHI, R., MARTIAL, F. P., PETERSEN, R. S., MONTEMURRO, M. A., BROWN, T. M. & LUCAS, R. J. 2014. Melanopsin-driven light adaptation in mouse vision. *Curr Biol,* 24**,** 2481-90.

ALTIMUS, C. M., GULER, A. D., ALAM, N. M., ARMAN, A. C., PRUSKY, G. T., SAMPATH, A. P. & HATTAR, S. 2010. Rod photoreceptors drive circadian photoentrainment across a wide range of light intensities. *Nat Neurosci,* 13**,** 1107-12.

ANAND, S. N., MAYWOOD, E. S., CHESHAM, J. E., JOYNSON, G., BANKS, G. T., HASTINGS, M. H. & NOLAN, P. M. 2013. Distinct and separable roles for endogenous CRY1 and CRY2 within the circadian molecular clockwork of the suprachiasmatic nucleus, as revealed by the Fbxl3(Afh) mutation. *J Neurosci,* 33**,** 7145-53.

ANDREWS, J. L., ZHANG, X., MCCARTHY, J. J., MCDEARMON, E. L., HORNBERGER, T. A., RUSSELL, B., CAMPBELL, K. S., ARBOGAST, S., REID, M. B., WALKER, J. R., HOGENESCH, J. B., TAKAHASHI, J. S. & ESSER, K. A. 2010. CLOCK and BMAL1 regulate MyoD and are necessary for maintenance of skeletal muscle phenotype and function. *Proc Natl Acad Sci U S A,* 107**,** 19090-5.

ANDRIEU-SOLER, C., BEJJANI, R. A., DE BIZEMONT, T., NORMAND, N., BENEZRA, D. & BEHAR-COHEN, F. 2006. Ocular gene therapy: a review of nonviral strategies. *Mol Vis,* 12**,** 1334-47.

APPLEBURY, M. L., ANTOCH, M. P., BAXTER, L. C., CHUN, L. L., FALK, J. D., FARHANGFAR, F., KAGE, K., KRZYSTOLIK, M. G., LYASS, L. A. & ROBBINS, J. T. 2000. The murine cone photoreceptor: a single cone type expresses both S and M opsins with retinal spatial patterning. *Neuron,* 27**,** 513-23.

ARSHAVSKY, V. Y. 2002. Rhodopsin phosphorylation: from terminating single photon responses to photoreceptor dark adaptation. *Trends Neurosci,* 25**,** 124-6.

ASARNOW, L. D., SOEHNER, A. M. & HARVEY, A. G. 2013. Circadian rhythms and psychiatric illness. *Curr Opin Psychiatry,* 26**,** 566-71.

ASCHOFF, J. 1960. Exogenous and endogenous components in circadian rhythms. *Cold Spring Harb Symp Quant Biol,* 25**,** 11-28.

ASCHOFF, J. 1979. Circadian rhythms: influences of internal and external factors on the period measured in constant conditions. *Z Tierpsychol,* 49**,** 225-49.

ASCHOFF, J. R. 1981. *Biological rhythms,* New York, Plenum Press.

ATKINSON, G. & REILLY, T. 1996. Circadian variation in sports performance. *Sports Med,* 21**,** 292-312.

AUBERT, C., VOS, M. H., MATHIS, P., EKER, A. P. & BRETTEL, K. 2000. Intraprotein radical transfer during photoactivation of DNA photolyase. *Nature,* 405**,** 586-90.

AYDIN, D., FEYCHTING, M., SCHUZ, J., TYNES, T., ANDERSEN, T. V., SCHMIDT, L. S., POULSEN, A. H., JOHANSEN, C., PROCHAZKA, M., LANNERING, B., KLAEBOE, L., EGGEN, T., JENNI, D., GROTZER, M., VON DER WEID, N., KUEHNI, C. E. & ROOSLI, M. 2011. Mobile phone use and brain tumors in children and adolescents: a multicenter case-control study. *J Natl Cancer Inst,* 103**,** 1264-76.

BABA, K., POZDEYEV, N., MAZZONI, F., CONTRERAS-ALCANTARA, S., LIU, C., KASAMATSU, M., MARTINEZ-MERLOS, T., STRETTOI, E., IUVONE, P. M. & TOSINI, G. 2009. Melatonin modulates visual function and cell viability in the mouse retina via the MT1 melatonin receptor. *Proc Natl Acad Sci U S A,* 106**,** 15043-8.

BALAGGAN, K. S. & ALI, R. R. 2012. Ocular gene delivery using lentiviral vectors. *Gene Ther,* 19**,** 145-53.

BALDI, I., COUREAU, G., JAFFRE, A., GRUBER, A., DUCAMP, S., PROVOST, D., LEBAILLY, P., VITAL, A., LOISEAU,

H. & SALAMON, R. 2011. Occupational and residential exposure to electromagnetic fields and risk of brain tumors in adults: a case-control study in Gironde, France. *Int J Cancer,* 129**,** 1477-84.

BALSALOBRE, A. 2002. Clock genes in mammalian peripheral tissues. *Cell Tissue Res,* 309**,** 193-9.

BALSALOBRE, A., DAMIOLA, F. & SCHIBLER, U. 1998. A serum shock induces circadian gene expression in mammalian tissue culture cells. *Cell,* 93**,** 929-37.

BAN, E. 1998. WHO funds mobile phone-cancer study. *Nat Med,* 4**,** 140.

BARLOW, H. B., HILL, R. M. & LEVICK, W. R. 1964. Retinal Ganglion Cells Responding Selectively to Direction and Speed of Image Motion in the Rabbit. *J Physiol,* 173**,** 377-407.

BARNARD, A. R., HATTAR, S., HANKINS, M. W. & LUCAS, R. J. 2006. Melanopsin regulates visual processing in the mouse retina. *Curr Biol,* 16**,** 389-95.

BAVER, S. B., PICKARD, G. E., SOLLARS, P. J. & PICKARD, G. E. 2008. Two types of melanopsin retinal ganglion cell differentially innervate the hypothalamic suprachiasmatic nucleus and the olivary pretectal nucleus. *Eur J Neurosci,* 27**,** 1763-70.

BEASON, R. & SEMM, P. 1996. Does the avian ophthalmic nerve carry magnetic navigational information? *J Exp Biol,* 199**,** 1241-4.

BEASON, R. C. & SEMM, P. 1991. Neuroethological aspects of avian orientation. *EXS,* 60**,** 106-27.

BEGALL, S., BURDA, H., CERVENY, J., GERTER, O., NEEF-WEISSE, J. & NEMEC, P. 2011. Further support for the alignment of cattle along magnetic field lines: reply to Hert *et al*. *J Comp Physiol A Neuroethol Sens Neural Behav Physiol,* 197**,** 1127-33; discussion 1135-6.

BEGALL, S., CERVENY, J., NEEF, J., VOJTECH, O. & BURDA, H. 2008. Magnetic alignment in grazing and resting cattle and deer. *Proc Natl Acad Sci U S A,* 105**,** 13451-5.

BENNETT, J. 2003. Immune response following intraocular delivery of recombinant viral vectors. *Gene Ther,* 10**,** 977-82.

BERSON, D. M., DUNN, F. A. & TAKAO, M. 2002. Phototransduction by retinal ganglion cells that set the circadian clock. *Science,* 295**,** 1070-3.

BESHARSE, J. C. & IUVONE, P. M. 1983. Circadian clock in Xenopus eye controlling retinal serotonin N-acetyltransferase. *Nature,* 305**,** 133-5.

BESOLUK, S., ONDER, I. & DEVECI, I. 2011. Morningness-eveningness preferences and academic achievement of university students. *Chronobiol Int,* 28**,** 118-25.

BHARDWAJ, S. K., STOJKOVIC, K., KIESSLING, S., SRIVASTAVA, L. K. & CERMAKIAN, N. 2015. Constant light uncovers behavioral effects of a mutation in the schizophrenia risk gene Dtnbp1 in mice. *Behav Brain Res,* 284**,** 58-68.

BLUM, I. D., ZHU, L., MOQUIN, L., KOKOEVA, M. V., GRATTON, A., GIROS, B. & STORCH, K. F. 2014. A highly tunable dopaminergic oscillator generates ultradian rhythms of behavioral arousal. *Elife,* 3.

BO, X. & VERHAAGEN, J. 2015. *Gene delivery and therapy for neurological disorders,* New York, Humana Press.

BOLTE, P., BLEIBAUM, F., EINWICH, A., GUNTHER, A., LIEDVOGEL, M., HEYERS, D., DEPPING, A., WOHLBRAND, L., RABUS, R., JANSSEN-BIENHOLD, U. & MOURITSEN, H. 2016. Localisation of the Putative Magnetoreceptive Protein Cryptochrome 1b in the Retinae of Migratory Birds and Homing Pigeons. *PLoS One,* 11**,** e0147819.

BONTEN, T. N., SARIS, A., VAN OOSTROM, M. J., SNOEP, J. D., ROSENDAAL, F. R., ZWAGINGA, J., EIKENBOOM, J., VAN DER MEER, P. F. & VAN DER BOM, J. G. 2014. Effect of aspirin intake at bedtime versus on awakening on circadian rhythm of platelet reactivity. A randomised cross-over trial. *Thromb Haemost,* 112**,** 1209-18.

BRAZARD, J., USMAN, A., LACOMBAT, F., LEY, C., MARTIN, M. M., PLAZA, P., MONY, L., HEIJDE, M., ZABULON, G. & BOWLER, C. 2010. Spectro-temporal characterization of the photoactivation mechanism of two new oxidized cryptochrome/photolyase photoreceptors. *J Am Chem Soc,* 132**,** 4935-45.

BROWN, K. T. 1968. The eclectroretinogram: its components and their origins. *Vision Res,* 8**,** 633-77.

BROWN, T. M., WYNNE, J., PIGGINS, H. D. & LUCAS, R. J. 2011. Multiple hypothalamic cell populations encoding distinct visual information. *J Physiol,* 589**,** 1173-94.

BUHR, E. D. & TAKAHASHI, J. S. 2013. Molecular components of the Mammalian circadian clock. *Handb Exp Pharmacol***,** 3-27.

BUHR, E. D. & VAN GELDER, R. N. 2014. Local photic entrainment of the retinal circadian oscillator in the absence of rods, cones, and melanopsin. *Proc Natl Acad Sci U S A,* 111**,** 8625-30.

BUHR, E. D., YUE, W. W., REN, X., JIANG, Z., LIAO, H. W., MEI, X., VEMARAJU, S., NGUYEN, M. T., REED, R. R., LANG, R. A., YAU, K. W. & VAN GELDER, R. N. 2015. Neuropsin (OPN5)-mediated photoentrainment of local circadian oscillators in mammalian retina and cornea. *Proc Natl Acad Sci U S A,* 112**,** 13093-8.

BUIJS, R. M. & KALSBEEK, A. 2001. Hypothalamic integration of central and peripheral clocks. *Nat Rev*

Neurosci, 2**,** 521-6.
BURDA, H., BEGALL, S., CERVENY, J., NEEF, J. & NEMEC, P. 2009. Extremely low-frequency electromagnetic fields disrupt magnetic alignment of ruminants. *Proc Natl Acad Sci U S A,* 106**,** 5708-13.
BURDA, H., MARHOLD, S., WESTENBERGER, T., WILTSCHKO, R. & WILTSCHKO, W. 1990. Magnetic compass orientation in the subterranean rodent Cryptomys hottentotus (Bathyergidae). *Experientia,* 46**,** 528-30.
CADIOU, H. & MCNAUGHTON, P. A. 2010. Avian magnetite-based magnetoreception: a physiologist's perspective. *J R Soc Interface,* 7 Suppl 2**,** S193-205.
CAHILL, G. M. & BESHARSE, J. C. 1989. Retinal melatonin is metabolized within the eye of xenopus laevis. *Proc Natl Acad Sci U S A,* 86**,** 1098-102.
CAHILL, G. M. & BESHARSE, J. C. 1990. Circadian regulation of melatonin in the retina of Xenopus laevis: limitation by serotonin availability. *J Neurochem,* 54**,** 716-9.
CAHILL, G. M. & BESHARSE, J. C. 1991. Resetting the circadian clock in cultured Xenopus eyecups: regulation of retinal melatonin rhythms by light and D2 dopamine receptors. *J Neurosci,* 11**,** 2959-71.
CAHILL, G. M., GRACE, M. S. & BESHARSE, J. C. 1991. Rhythmic regulation of retinal melatonin: metabolic pathways, neurochemical mechanisms, and the ocular circadian clock. *Cell Mol Neurobiol,* 11**,** 529-60.
CAMERON, M. A., BARNARD, A. R., HUT, R. A., BONNEFONT, X., VAN DER HORST, G. T., HANKINS, M. W. & LUCAS, R. J. 2008. Electroretinography of wild-type and Cry mutant mice reveals circadian tuning of photopic and mesopic retinal responses. *J Biol Rhythms,* 23**,** 489-501.
CAMERON, M. A., BARNARD, A. R. & LUCAS, R. J. 2008. The electroretinogram as a method for studying circadian rhythms in the mammalian retina. *J Genet,* 87**,** 459-66.
CAMERON, M. A., POZDEYEV, N., VUGLER, A. A., COOPER, H., IUVONE, P. M. & LUCAS, R. J. 2009. Light regulation of retinal dopamine that is independent of melanopsin phototransduction. *Eur J Neurosci,* 29**,** 761-7.
CASHMORE, A. R., JARILLO, J. A., WU, Y. J. & LIU, D. 1999. Cryptochromes: blue light receptors for plants and animals. *Science,* 284**,** 760-5.
CERIANI, M. F., DARLINGTON, T. K., STAKNIS, D., MAS, P., PETTI, A. A., WEITZ, C. J. & KAY, S. A. 1999. Light-dependent sequestration of TIMELESS by CRYPTOCHROME. *Science,* 285**,** 553-6.
CHALLET, E. 2007. Minireview: Entrainment of the suprachiasmatic clockwork in diurnal and nocturnal mammals. *Endocrinology,* 148**,** 5648-55.
CHAUDHURY, D. & COLWELL, C. S. 2002. Circadian modulation of learning and memory in fear-conditioned mice. *Behav Brain Res,* 133**,** 95-108.
CHEN, S. K., BADEA, T. C. & HATTAR, S. 2011. Photoentrainment and pupillary light reflex are mediated by distinct populations of ipRGCs. *Nature,* 476**,** 92-5.
CHUNG, S., SON, G. H. & KIM, K. 2011. Adrenal peripheral oscillator in generating the circadian glucocorticoid rhythm. *Ann N Y Acad Sci,* 1220**,** 71-81.
COOMANS, C. P., VAN DEN BERG, S. A., HOUBEN, T., VAN KLINKEN, J. B., VAN DEN BERG, R., PRONK, A. C., HAVEKES, L. M., ROMIJN, J. A., VAN DIJK, K. W., BIERMASZ, N. R. & MEIJER, J. H. 2013. Detrimental effects of constant light exposure and high-fat diet on circadian energy metabolism and insulin sensitivity. *FASEB J,* 27**,** 1721-32.
COOMBS, J., VAN DER LIST, D., WANG, G. Y. & CHALUPA, L. M. 2006. Morphological properties of mouse retinal ganglion cells. *Neuroscience,* 140**,** 123-36.
CRUMPTON, M. J. 2005. The Bernal Lecture 2004 Are low-frequency electromagnetic fields a health hazard? *Philos Trans R Soc Lond B Biol Sci,* 360**,** 1223-30.
CRUMPTON, M. J. & COLLINS, A. R. 2004. Are environmental electromagnetic fields genotoxic? *DNA Repair (Amst),* 3**,** 1385-7.
CZARNA, A., BERNDT, A., SINGH, H. R., GRUDZIECKI, A., LADURNER, A. G., TIMINSZKY, G., KRAMER, A. & WOLF, E. 2013. Structures of Drosophila cryptochrome and mouse cryptochrome1 provide insight into circadian function. *Cell,* 153**,** 1394-405.
DALLMANN, R., DEBRUYNE, J. P. & WEAVER, D. R. 2011. Photic resetting and entrainment in CLOCK-deficient mice. *J Biol Rhythms,* 26**,** 390-401.
DEBRUYNE, J. P., WEAVER, D. R. & REPPERT, S. M. 2007. CLOCK and NPAS2 have overlapping roles in the suprachiasmatic circadian clock. *Nat Neurosci,* 10**,** 543-5.
DEUTSCHLANDER, M. E., FREAKE, M. J., BORLAND, S. C., PHILLIPS, J. B., MADDEN, R. C., ANDERSON, L. E. & WILSON, B. W. 2003. Learned magnetic compass orientation by the Siberian hamster, Phodopus sungorus. *Animal Behaviour,* 65**,** 779-786.
DIBNER, C., SCHIBLER, U. & ALBRECHT, U. 2010. The mammalian circadian timing system: organization and coordination of central and peripheral clocks. *Annu Rev Physiol,* 72**,** 517-49.

DINET, V., ANSARI, N., TORRES-FARFAN, C. & KORF, H. W. 2007. Clock gene expression in the retina of melatonin-proficient (C3H) and melatonin-deficient (C57BL) mice. *J Pineal Res,* 42**,** 83-91.

DING, J. M., CHEN, D., WEBER, E. T., FAIMAN, L. E., REA, M. A. & GILLETTE, M. U. 1994. Resetting the biological clock: mediation of nocturnal circadian shifts by glutamate and NO. *Science,* 266**,** 1713-7.

DKHISSI-BENYAHYA, O., COUTANSON, C., KNOBLAUCH, K., LAHOUAOUI, H., LEVIEL, V., REY, C., BENNIS, M. & COOPER, H. M. 2013. The absence of melanopsin alters retinal clock function and dopamine regulation by light. *Cell Mol Life Sci,* 70**,** 3435-47.

DMITRIEV, A. V. & MANGEL, S. C. 2001. Circadian clock regulation of pH in the rabbit retina. *J Neurosci,* 21**,** 2897-902.

DO, M. T. & YAU, K. W. 2010. Intrinsically photosensitive retinal ganglion cells. *Physiol Rev,* 90**,** 1547-81.

DORENBOS, R., CONTINI, M., HIRASAWA, H., GUSTINCICH, S. & RAVIOLA, E. 2007. Expression of circadian clock genes in retinal dopaminergic cells. *Vis Neurosci,* 24**,** 573-80.

DOWSE, H., UMEMORI, J. & KOIDE, T. 2010. Ultradian components in the locomotor activity rhythms of the genetically normal mouse, Mus musculus. *Journal of Experimental Biology,* 213**,** 1788-1795.

DOYLE, S. E., GRACE, M. S., MCIVOR, W. & MENAKER, M. 2002. Circadian rhythms of dopamine in mouse retina: the role of melatonin. *Vis Neurosci,* 19**,** 593-601.

DOYLE, S. E., MCIVOR, W. E. & MENAKER, M. 2002. Circadian rhythmicity in dopamine content of mammalian retina: role of the photoreceptors. *J Neurochem,* 83**,** 211-9.

DUFFIELD, G. E. 2003. DNA microarray analyses of circadian timing: the genomic basis of biological time. *J Neuroendocrinol,* 15**,** 991-1002.

EBIHARA, S., MARKS, T., HUDSON, D. J. & MENAKER, M. 1986. Genetic control of melatonin synthesis in the pineal gland of the mouse. *Science,* 231**,** 491-3.

ECKER, J. L., DUMITRESCU, O. N., WONG, K. Y., ALAM, N. M., CHEN, S. K., LEGATES, T., RENNA, J. M., PRUSKY, G. T., BERSON, D. M. & HATTAR, S. 2010. Melanopsin-expressing retinal ganglion-cell photoreceptors: cellular diversity and role in pattern vision. *Neuron,* 67**,** 49-60.

EMERY, P., SO, W. V., KANEKO, M., HALL, J. C. & ROSBASH, M. 1998. CRY, a Drosophila clock and light-regulated cryptochrome, is a major contributor to circadian rhythm resetting and photosensitivity. *Cell,* 95**,** 669-79.

ERREN, T. C., FALATURI, P., MORFELD, P., KNAUTH, P., REITER, R. J. & PIEKARSKI, C. 2010. Shift work and cancer: the evidence and the challenge. *Dtsch Arztebl Int,* 107**,** 657-62.

EVANS, J. A., PAN, H., LIU, A. C. & WELSH, D. K. 2012. Cry1-/- circadian rhythmicity depends on SCN intercellular coupling. *J Biol Rhythms,* 27**,** 443-52.

FACER-CHILDS, E. & BRANDSTAETTER, R. 2015. The impact of circadian phenotype and time since awakening on diurnal performance in athletes. *Curr Biol,* 25**,** 518-22.

FAMIGLIETTI, E. V., JR. & KOLB, H. 1975. A bistratified amacrine cell and synaptic cirucitry in the inner plexiform layer of the retina. *Brain Res,* 84**,** 293-300.

FEDELE, G., EDWARDS, M. D., BHUTANI, S., HARES, J. M., MURBACH, M., GREEN, E. W., DISSEL, S., HASTINGS, M. H., ROSATO, E. & KYRIACOU, C. P. 2014. Genetic analysis of circadian responses to low frequency electromagnetic fields in Drosophila melanogaster. *PLoS Genet,* 10**,** e1004804.

FEDELE, G., GREEN, E. W., ROSATO, E. & KYRIACOU, C. P. 2014. An electromagnetic field disrupts negative geotaxis in Drosophila via a CRY-dependent pathway. *Nat Commun,* 5**,** 4391.

FEIGL, B., MATTES, D., THOMAS, R. & ZELE, A. J. 2011. Intrinsically photosensitive (melanopsin) retinal ganglion cell function in glaucoma. *Invest Ophthalmol Vis Sci,* 52**,** 4362-7.

FEIGL, B., ZELE, A. J., FADER, S. M., HOWES, A. N., HUGHES, C. E., JONES, K. A. & JONES, R. 2012. The post-illumination pupil response of melanopsin-expressing intrinsically photosensitive retinal ganglion cells in diabetes. *Acta Ophthalmol,* 90**,** e230-4.

FISHER, S. P., GODINHO, S. I., POTHECARY, C. A., HANKINS, M. W., FOSTER, R. G. & PEIRSON, S. N. 2012. Rapid assessment of sleep-wake behavior in mice. *J Biol Rhythms,* 27**,** 48-58.

FOLEY, L. E., GEGEAR, R. J. & REPPERT, S. M. 2011. Human cryptochrome exhibits light-dependent magnetosensitivity. *Nat Commun,* 2**,** 356.

FOSTER, R. G., PEIRSON, S. N., WULFF, K., WINNEBECK, E., VETTER, C. & ROENNEBERG, T. 2013. Sleep and circadian rhythm disruption in social jetlag and mental illness. *Prog Mol Biol Transl Sci,* 119**,** 325-46.

FOSTER, R. G., PROVENCIO, I., HUDSON, D., FISKE, S., DE GRIP, W. & MENAKER, M. 1991. Circadian photoreception in the retinally degenerate mouse (rd/rd). *J Comp Physiol A,* 169**,** 39-50.

FOULKES, N. S., BORJIGIN, J., SNYDER, S. H. & SASSONE-CORSI, P. 1996. Transcriptional control of circadian hormone synthesis via the CREM feedback loop. *Proc Natl Acad Sci U S A,* 93**,** 14140-5.

FRANKEL, R. B., BLAKEMORE, R. P. & WOLFE, R. S. 1979. Magnetite in freshwater magnetotactic bacteria.

Science, 203**,** 1355-6.

FREEDMAN, M. S., LUCAS, R. J., SONI, B., VON SCHANTZ, M., MUNOZ, M., DAVID-GRAY, Z. & FOSTER, R. 1999. Regulation of mammalian circadian behavior by non-rod, non-cone, ocular photoreceptors. *Science,* 284**,** 502-4.

FU, Y., ZHONG, H., WANG, M. H., LUO, D. G., LIAO, H. W., MAEDA, H., HATTAR, S., FRISHMAN, L. J. & YAU, K. W. 2005. Intrinsically photosensitive retinal ganglion cells detect light with a vitamin A-based photopigment, melanopsin. *Proc Natl Acad Sci U S A,* 102**,** 10339-44.

GAGLIARDO, A., IOALE, P., SAVINI, M. & WILD, M. 2008. Navigational abilities of homing pigeons deprived of olfactory or trigeminally mediated magnetic information when young. *Journal of Experimental Biology,* 211**,** 2046-2051.

GEGEAR, R. J., CASSELMAN, A., WADDELL, S. & REPPERT, S. M. 2008. Cryptochrome mediates light-dependent magnetosensitivity in Drosophila. *Nature,* 454**,** 1014-8.

GEGEAR, R. J., FOLEY, L. E., CASSELMAN, A. & REPPERT, S. M. 2010. Animal cryptochromes mediate magnetoreception by an unconventional photochemical mechanism. *Nature,* 463**,** 804-7.

GEKAKIS, N., STAKNIS, D., NGUYEN, H. B., DAVIS, F. C., WILSBACHER, L. D., KING, D. P., TAKAHASHI, J. S. & WEITZ, C. J. 1998. Role of the CLOCK protein in the mammalian circadian mechanism. *Science,* 280**,** 1564-9.

GHOSH, K. K., BUJAN, S., HAVERKAMP, S., FEIGENSPAN, A. & WASSLE, H. 2004. Types of bipolar cells in the mouse retina. *J Comp Neurol,* 469**,** 70-82.

GOTO, M., OSHIMA, I., TOMITA, T. & EBIHARA, S. 1989. Melatonin content of the pineal gland in different mouse strains. *J Pineal Res,* 7**,** 195-204.

GRACE, M. S., CHIBA, A. & MENAKER, M. 1999. Circadian control of photoreceptor outer segment membrane turnover in mice genetically incapable of melatonin synthesis. *Vis Neurosci,* 16**,** 909-18.

GRAHAM, D. M., WONG, K. Y., SHAPIRO, P., FREDERICK, C., PATTABIRAMAN, K. & BERSON, D. M. 2008. Melanopsin ganglion cells use a membrane-associated rhabdomeric phototransduction cascade. *J Neurophysiol,* 99**,** 2522-32.

GREEN, C. B. & BESHARSE, J. C. 2004. Retinal circadian clocks and control of retinal physiology. *J Biol Rhythms,* 19**,** 91-102.

GREENLAND, S., SHEPPARD, A. R., KAUNE, W. T., POOLE, C. & KELSH, M. A. 2000. A pooled analysis of magnetic fields, wire codes, and childhood leukemia. Childhood Leukemia-EMF Study Group. *Epidemiology,* 11**,** 624-34.

GRIFFIN, E. A., JR., STAKNIS, D. & WEITZ, C. J. 1999. Light-independent role of CRY1 and CRY2 in the mammalian circadian clock. *Science,* 286**,** 768-71.

GULER, A. D., ECKER, J. L., LALL, G. S., HAQ, S., ALTIMUS, C. M., LIAO, H. W., BARNARD, A. R., CAHILL, H., BADEA, T. C., ZHAO, H., HANKINS, M. W., BERSON, D. M., LUCAS, R. J., YAU, K. W. & HATTAR, S. 2008. Melanopsin cells are the principal conduits for rod-cone input to non-image-forming vision. *Nature,* 453**,** 102-5.

GUSTINCICH, S., CONTINI, M., GARIBOLDI, M., PUOPOLO, M., KADOTA, K., BONO, H., LEMIEUX, J., WALSH, P., CARNINCI, P., HAYASHIZAKI, Y., OKAZAKI, Y. & RAVIOLA, E. 2004. Gene discovery in genetically labeled single dopaminergic neurons of the retina. *Proc Natl Acad Sci U S A,* 101**,** 5069-74.

HACK, I., FRECH, M., DICK, O., PEICHL, L. & BRANDSTATTER, J. H. 2001. Heterogeneous distribution of AMPA glutamate receptor subunits at the photoreceptor synapses of rodent retina. *Eur J Neurosci,* 13**,** 15-24.

HANKINS, M. W., PEIRSON, S. N. & FOSTER, R. G. 2008. Melanopsin: an exciting photopigment. *Trends Neurosci,* 31**,** 27-36.

HANNIBAL, J. 2006. Regulation of melanopsin expression. *Chronobiol Int,* 23**,** 159-66.

HANNIBAL, J., GEORG, B., HINDERSSON, P. & FAHRENKRUG, J. 2005. Light and darkness regulate melanopsin in the retinal ganglion cells of the albino Wistar rat. *J Mol Neurosci,* 27**,** 147-55.

HANNIBAL, J., MOLLER, M., OTTERSEN, O. P. & FAHRENKRUG, J. 2000. PACAP and glutamate are co-stored in the retinohypothalamic tract. *J Comp Neurol,* 418**,** 147-55.

HANNIBAL, J., VRANG, N., CARD, J. P. & FAHRENKRUG, J. 2001. Light-dependent induction of cFos during subjective day and night in PACAP-containing ganglion cells of the retinohypothalamic tract. *J Biol Rhythms,* 16**,** 457-70.

HARDIN, P. E. 2005. The circadian timekeeping system of Drosophila. *Curr Biol,* 15**,** R714-22.

HARMAR, A. J., MARSTON, H. M., SHEN, S., SPRATT, C., WEST, K. M., SHEWARD, W. J., MORRISON, C. F., DORIN, J. R., PIGGINS, H. D., REUBI, J. C., KELLY, J. S., MAYWOOD, E. S. & HASTINGS, M. H. 2002. The VPAC(2) receptor is essential for circadian function in the mouse suprachiasmatic nuclei. *Cell,* 109**,** 497-508.

HARRIS, S. R., HENBEST, K. B., MAEDA, K., PANNELL, J. R., TIMMEL, C. R., HORE, P. J. & OKAMOTO, H. 2009. Effect of magnetic fields on cryptochrome-dependent responses in Arabidopsis thaliana. *J R Soc Interface,* 6**,** 1193-205.

HART, V., NOVAKOVA, P., MALKEMPER, E. P., BEGALL, S., HANZAL, V., JEZEK, M., KUSTA, T., NEMCOVA, V., ADAMKOVA, J., BENEDIKTOVA, K., CERVENY, J. & BURDA, H. 2013. Dogs are sensitive to small variations of the Earth's magnetic field. *Front Zool,* 10**,** 80.

HASTINGS, M. H., BRANCACCIO, M. & MAYWOOD, E. S. 2014. Circadian pacemaking in cells and circuits of the suprachiasmatic nucleus. *J Neuroendocrinol,* 26**,** 2-10.

HASTINGS, M. H., FIELD, M. D., MAYWOOD, E. S., WEAVER, D. R. & REPPERT, S. M. 1999. Differential regulation of mPER1 and mTIM proteins in the mouse suprachiasmatic nuclei: new insights into a core clock mechanism. *J Neurosci,* 19**,** RC11.

HASTINGS, M. H., REDDY, A. B., MCMAHON, D. G. & MAYWOOD, E. S. 2005. Analysis of circadian mechanisms in the suprachiasmatic nucleus by transgenesis and biolistic transfection. *Methods Enzymol,* 393**,** 579-92.

HATANAKA, F., MATSUBARA, C., MYUNG, J., YORITAKA, T., KAMIMURA, N., TSUTSUMI, S., KANAI, A., SUZUKI, Y., SASSONE-CORSI, P., ABURATANI, H., SUGANO, S. & TAKUMI, T. 2010. Genome-wide profiling of the core clock protein BMAL1 targets reveals a strict relationship with metabolism. *Mol Cell Biol,* 30**,** 5636-48.

HATTAR, S., LIAO, H. W., TAKAO, M., BERSON, D. M. & YAU, K. W. 2002. Melanopsin-containing retinal ganglion cells: architecture, projections, and intrinsic photosensitivity. *Science,* 295**,** 1065-70.

HATTAR, S., LUCAS, R. J., MROSOVSKY, N., THOMPSON, S., DOUGLAS, R. H., HANKINS, M. W., LEM, J., BIEL, M., HOFMANN, F., FOSTER, R. G. & YAU, K. W. 2003. Melanopsin and rod-cone photoreceptive systems account for all major accessory visual functions in mice. *Nature,* 424**,** 76-81.

HAVERKAMP, S. & WASSLE, H. 2000. Immunocytochemical analysis of the mouse retina. *J Comp Neurol,* 424**,** 1-23.

HEISE, I., FISHER, S. P., BANKS, G. T., WELLS, S., PEIRSON, S. N., FOSTER, R. G. & NOLAN, P. M. 2015. Sleep-like behavior and 24-h rhythm disruption in the Tc1 mouse model of Down syndrome. *Genes Brain Behav,* 14**,** 209-16.

HELLSTROM, M., RUITENBERG, M. J., POLLETT, M. A., EHLERT, E. M., TWISK, J., VERHAAGEN, J. & HARVEY, A. R. 2009. Cellular tropism and transduction properties of seven adeno-associated viral vector serotypes in adult retina after intravitreal injection. *Gene Ther,* 16**,** 521-32.

HEPWORTH, S. J., SCHOEMAKER, M. J., MUIR, K. R., SWERDLOW, A. J., VAN TONGEREN, M. J. & MCKINNEY, P. A. 2006. Mobile phone use and risk of glioma in adults: case-control study. *BMJ,* 332**,** 883-7.

HERT, J., JELINEK, L., PEKAREK, L. & PAVLICEK, A. 2011. No alignment of cattle along geomagnetic field lines found. *J Comp Physiol A Neuroethol Sens Neural Behav Physiol,* 197**,** 677-82.

HIRANO, A., YUMIMOTO, K., TSUNEMATSU, R., MATSUMOTO, M., OYAMA, M., KOZUKA-HATA, H., NAKAGAWA, T., LANJAKORNSIRIPAN, D., NAKAYAMA, K. I. & FUKADA, Y. 2013. FBXL21 regulates oscillation of the circadian clock through ubiquitination and stabilization of cryptochromes. *Cell,* 152**,** 1106-18.

HONMA, K., HONMA, S. & HIROSHIGE, T. 1986. Disorganization of the rat activity rhythm by chronic treatment with methamphetamine. *Physiol Behav,* 38**,** 687-95.

HONMA, K., HONMA, S. & HIROSHIGE, T. 1987. Activity rhythms in the circadian domain appear in suprachiasmatic nuclei lesioned rats given methamphetamine. *Physiol Behav,* 40**,** 767-74.

HUGHES, A. T., CROFT, C. L., SAMUELS, R. E., MYUNG, J., TAKUMI, T. & PIGGINS, H. D. 2015. Constant light enhances synchrony among circadian clock cells and promotes behavioral rhythms in VPAC2-signaling deficient mice. *Sci Rep,* 5**,** 14044.

HUGHES, S., HANKINS, M. W., FOSTER, R. G. & PEIRSON, S. N. 2012. Melanopsin phototransduction: slowly emerging from the dark. *Prog Brain Res,* 199**,** 19-40.

HUGHES, S., JAGANNATH, A., HANKINS, M. W., FOSTER, R. G. & PEIRSON, S. N. 2015. Photic regulation of clock systems. *Methods Enzymol,* 552**,** 125-43.

HUGHES, S., JAGANNATH, A., HICKEY, D., GATTI, S., WOOD, M., PEIRSON, S. N., FOSTER, R. G. & HANKINS, M. W. 2015. Using siRNA to define functional interactions between melanopsin and multiple G Protein partners. *Cell Mol Life Sci,* 72**,** 165-79.

HUGHES, S., WATSON, T. S., FOSTER, R. G., PEIRSON, S. N. & HANKINS, M. W. 2013. Nonuniform distribution and spectral tuning of photosensitive retinal ganglion cells of the mouse retina. *Curr Biol,* 23**,** 1696-701.

HUGHES, S., WELSH, L., KATTI, C., GONZALEZ-MENENDEZ, I., TURTON, M., HALFORD, S., SEKARAN, S., PEIRSON, S. N., HANKINS, M. W. & FOSTER, R. G. 2012. Differential expression of melanopsin isoforms Opn4L and Opn4S during postnatal development of the mouse retina. *PLoS One,* 7**,** e34531.

HUT, R. A. & BEERSMA, D. G. 2011. Evolution of time-keeping mechanisms: early emergence and adaptation to photoperiod. *Philos Trans R Soc Lond B Biol Sci,* 366**,** 2141-54.

HWANG, C. K., CHAURASIA, S. S., JACKSON, C. R., CHAN, G. C., STORM, D. R. & IUVONE, P. M. 2013. Circadian rhythm of contrast sensitivity is regulated by a dopamine-neuronal PAS-domain protein 2-adenylyl cyclase 1 signaling pathway in retinal ganglion cells. *J Neurosci,* 33**,** 14989-97.

IARC 2002. Non-ionizing radiation, Part 1: static and extremely low-frequency (ELF) electric and magnetic fields. *IARC Monogr Eval Carcinog Risks Hum,* 80**,** 1-395.

INOUYE, S. T. & KAWAMURA, H. 1979. Persistence of circadian rhythmicity in a mammalian hypothalamic "island" containing the suprachiasmatic nucleus. *Proc Natl Acad Sci U S A,* 76**,** 5962-6.

INTERPHONE STUDY GROUP 2010. Brain tumour risk in relation to mobile telephone use: results of the INTERPHONE international case-control study. *Int J Epidemiol,* 39**,** 675-94.

ISHIDA, A., MUTOH, T., UEYAMA, T., BANDO, H., MASUBUCHI, S., NAKAHARA, D., TSUJIMOTO, G. & OKAMURA, H. 2005. Light activates the adrenal gland: timing of gene expression and glucocorticoid release. *Cell Metab,* 2**,** 297-307.

IVANOVA, E., HWANG, G. S. & PAN, Z. H. 2010. Characterization of transgenic mouse lines expressing Cre recombinase in the retina. *Neuroscience,* 165**,** 233-43.

JACKSON, C. R., CAPOZZI, M., DAI, H. & MCMAHON, D. G. 2014. Circadian perinatal photoperiod has enduring effects on retinal dopamine and visual function. *J Neurosci,* 34**,** 4627-33.

JACKSON, C. R., RUAN, G. X., ASEEM, F., ABEY, J., GAMBLE, K., STANWOOD, G., PALMITER, R. D., IUVONE, P. M. & MCMAHON, D. G. 2012. Retinal dopamine mediates multiple dimensions of light-adapted vision. *J Neurosci,* 32**,** 9359-68.

JACOBS, G. H., NEITZ, J. & DEEGAN, J. F., 2ND 1991. Retinal receptors in rodents maximally sensitive to ultraviolet light. *Nature,* 353**,** 655-6.

JAEGER, C., SANDU, C., MALAN, A., MELLAC, K., HICKS, D. & FELDER-SCHMITTBUHL, M. P. 2015. Circadian organization of the rodent retina involves strongly coupled, layer-specific oscillators. *FASEB J,* 29**,** 1493-504.

JAGANNATH, A., HUGHES, S., ABDELGANY, A., POTHECARY, C. A., DI PRETORO, S., PIRES, S. S., VACHTSEVANOS, A., PILORZ, V., BROWN, L. A., HOSSBACH, M., MACLAREN, R. E., HALFORD, S., GATTI, S., HANKINS, M. W., WOOD, M. J., FOSTER, R. G. & PEIRSON, S. N. 2015. Isoforms of Melanopsin Mediate Different Behavioral Responses to Light. *Curr Biol,* 25**,** 2430-4.

JAGANNATH, A., PEIRSON, S. N. & FOSTER, R. G. 2013. Sleep and circadian rhythm disruption in neuropsychiatric illness. *Curr Opin Neurobiol,* 23**,** 888-94.

JALIFFA, C. O., SAENZ, D., RESNIK, E., KELLER SARMIENTO, M. I. & ROSENSTEIN, R. E. 2001. Circadian activity of the GABAergic system in the golden hamster retina. *Brain Res,* 912**,** 195-202.

JIANG, Z. G., YANG, Y., LIU, Z. P. & ALLEN, C. N. 1997. Membrane properties and synaptic inputs of suprachiasmatic nucleus neurons in rat brain slices. *J Physiol,* 499 (Pt 1)**,** 141-59.

JOHNSON, C. H., ELLIOTT, J. A. & FOSTER, R. 2003. Entrainment of circadian programs. *Chronobiol Int,* 20**,** 741-74.

JUD, C., SCHMUTZ, I., HAMPP, G., OSTER, H. & ALBRECHT, U. 2005. A guideline for analyzing circadian wheel-running behavior in rodents under different lighting conditions. *Biol Proced Online,* 7**,** 101-16.

KABACIK, S., KIRSCHENLOHR, H., RAFFY, C., WHITEHILL, K., COSTER, M., ABE, M., BRINDLE, K., BADIE, C., SIENKIEWICZ, Z. & BOUFFLER, S. 2013. Investigation of transcriptional responses of juvenile mouse bone marrow to power frequency magnetic fields. *Mutat Res,* 745-746**,** 40-5.

KAMPHUIS, W., CAILOTTO, C., DIJK, F., BERGEN, A. & BUIJS, R. M. 2005. Circadian expression of clock genes and clock-controlled genes in the rat retina. *Biochem Biophys Res Commun,* 330**,** 18-26.

KANKIPATI, L., GIRKIN, C. A. & GAMLIN, P. D. 2010. Post-illumination pupil response in subjects without ocular disease. *Invest Ophthalmol Vis Sci,* 51**,** 2764-9.

KASAHARA, T., ABE, K., MEKADA, K., YOSHIKI, A. & KATO, T. 2010. Genetic variation of melatonin productivity in laboratory mice under domestication. *Proc Natl Acad Sci U S A,* 107**,** 6412-7.

KENNAWAY, D. J. 2005. The role of circadian rhythmicity in reproduction. *Hum Reprod Update,* 11**,** 91-101.

KHEIFETS, L., AHLBOM, A., CRESPI, C. M., DRAPER, G., HAGIHARA, J., LOWENTHAL, R. M., MEZEI, G., OKSUZYAN, S., SCHUZ, J., SWANSON, J., TITTARELLI, A., VINCETI, M. & WUNSCH FILHO, V. 2010. Pooled analysis of recent studies on magnetic fields and childhood leukaemia. *Br J Cancer,* 103**,** 1128-35.

KIMCHI, T. & TERKEL, J. 2001. Magnetic compass orientation in the blind mole rat Spalax ehrenbergi. *J Exp Biol,* 204**,** 751-8.

KIRSCHVINK, J. L. & GOULD, J. L. 1981. Biogenic magnetite as a basis for magnetic field detection in animals. *Biosystems,* 13**,** 181-201.

KIRSCHVINK, J. L., WALKER, M. M. & DIEBEL, C. E. 2001. Magnetite-based magnetoreception. *Curr Opin Neurobiol,* 11**,** 462-7.

KLEIN, D. C., MOORE, R. Y. & REPPERT, S. M. 1991. *Suprachiasmatic nucleus : the mind's clock,* New York, Oxford University Press.

KOIKE, N., YOO, S. H., HUANG, H. C., KUMAR, V., LEE, C., KIM, T. K. & TAKAHASHI, J. S. 2012. Transcriptional architecture and chromatin landscape of the core circadian clock in mammals. *Science,* 338**,** 349-54.

KONDRATOV, R. V., KONDRATOVA, A. A., GORBACHEVA, V. Y., VYKHOVANETS, O. V. & ANTOCH, M. P. 2006. Early aging and age-related pathologies in mice deficient in BMAL1, the core componentof the circadian clock. *Genes Dev,* 20**,** 1868-73.

KONDRATOV, R. V., SHAMANNA, R. K., KONDRATOVA, A. A., GORBACHEVA, V. Y. & ANTOCH, M. P. 2006. Dual role of the CLOCK/BMAL1 circadian complex in transcriptional regulation. *FASEB J,* 20**,** 530-2.

KUHLMAN, S. J., QUINTERO, J. E. & MCMAHON, D. G. 2000. GFP fluorescence reports Period 1 circadian gene regulation in the mammalian biological clock. *Neuroreport,* 11**,** 1479-82.

KUME, K., ZYLKA, M. J., SRIRAM, S., SHEARMAN, L. P., WEAVER, D. R., JIN, X., MAYWOOD, E. S., HASTINGS, M. H. & REPPERT, S. M. 1999. mCRY1 and mCRY2 are essential components of the negative limb of the circadian clock feedback loop. *Cell,* 98**,** 193-205.

LACY-HULBERT, A., METCALFE, J. C. & HESKETH, R. 1998. Biological responses to electromagnetic fields. *FASEB J,* 12**,** 395-420.

LALL, G. S., REVELL, V. L., MOMIJI, H., AL ENEZI, J., ALTIMUS, C. M., GULER, A. D., AGUILAR, C., CAMERON, M. A., ALLENDER, S., HANKINS, M. W. & LUCAS, R. J. 2010. Distinct contributions of rod, cone, and melanopsin photoreceptors to encoding irradiance. *Neuron,* 66**,** 417-28.

LAMIA, K. A., PAPP, S. J., YU, R. T., BARISH, G. D., UHLENHAUT, N. H., JONKER, J. W., DOWNES, M. & EVANS, R. M. 2011. Cryptochromes mediate rhythmic repression of the glucocorticoid receptor. *Nature,* 480**,** 552-6.

LAMIA, K. A., SACHDEVA, U. M., DITACCHIO, L., WILLIAMS, E. C., ALVAREZ, J. G., EGAN, D. F., VASQUEZ, D. S., JUGUILON, H., PANDA, S., SHAW, R. J., THOMPSON, C. B. & EVANS, R. M. 2009. AMPK regulates the circadian clock by cryptochrome phosphorylation and degradation. *Science,* 326**,** 437-40.

LAMONT, E. W., JAMES, F. O., BOIVIN, D. B. & CERMAKIAN, N. 2007. From circadian clock gene expression to pathologies. *Sleep Med,* 8**,** 547-56.

LE, Y. Z., ASH, J. D., AL-UBAIDI, M. R., CHEN, Y., MA, J. X. & ANDERSON, R. E. 2004. Targeted expression of Cre recombinase to cone photoreceptors in transgenic mice. *Mol Vis,* 10**,** 1011-8.

LEE, H. S., NELMS, J. L., NGUYEN, M., SILVER, R. & LEHMAN, M. N. 2003. The eye is necessary for a circadian rhythm in the suprachiasmatic nucleus. *Nat Neurosci,* 6**,** 111-2.

LEFELDT, N., HEYERS, D., SCHNEIDER, N. L., ENGELS, S., ELBERS, D. & MOURITSEN, H. 2014. Magnetic field-driven induction of ZENK in the trigeminal system of pigeons (Columba livia). *J R Soc Interface,* 11**,** 20140777.

LEGATES, T. A. & ALTIMUS, C. M. 2011. Measuring circadian and acute light responses in mice using wheel running activity. *J Vis Exp*.

LEGATES, T. A., ALTIMUS, C. M., WANG, H., LEE, H. K., YANG, S., ZHAO, H., KIRKWOOD, A., WEBER, E. T. & HATTAR, S. 2012. Aberrant light directly impairs mood and learning through melanopsin-expressing neurons. *Nature,* 491**,** 594-8.

LEGATES, T. A., DUNN, D. & WEBER, E. T. 2009. Accelerated re-entrainment to advanced light cycles in BALB/cJ mice. *Physiol Behav,* 98**,** 427-32.

LEHMAN, M. N., SILVER, R., GLADSTONE, W. R., KAHN, R. M., GIBSON, M. & BITTMAN, E. L. 1987. Circadian rhythmicity restored by neural transplant. Immunocytochemical characterization of the graft and its integration with the host brain. *J Neurosci,* 7**,** 1626-38.

LIEDVOGEL, M., MAEDA, K., HENBEST, K., SCHLEICHER, E., SIMON, T., TIMMEL, C. R., HORE, P. J. & MOURITSEN, H. 2007. Chemical magnetoreception: bird cryptochrome 1a is excited by blue light and forms long-lived radical-pairs. *PLoS One,* 2**,** e1106.

LIEDVOGEL, M. & MOURITSEN, H. 2010. Cryptochromes--a potential magnetoreceptor: what do we know and what do we want to know? *J R Soc Interface,* 7 Suppl 2**,** S147-62.

LIPINSKI, D. M., YUSUF, M., BARNARD, A. R., DAMANT, C., CHARBEL ISSA, P., SINGH, M. S., LEE, E., DAVIES, W. L., VOLPI, E. V. & MACLAREN, R. E. 2011. Characterization of a dominant cone degeneration in a green fluorescent protein-reporter mouse with disruption of Loci associated with human dominant retinal dystrophy. *Invest Ophthalmol Vis Sci,* 52**,** 6617-23.

LIU, C., WEAVER, D. R., STROGATZ, S. H. & REPPERT, S. M. 1997. Cellular construction of a circadian clock: period determination in the suprachiasmatic nuclei. *Cell,* 91**,** 855-60.

LIU, X., ZHANG, Z. & RIBELAYGA, C. P. 2012. Heterogeneous expression of the core circadian clock proteins among neuronal cell types in mouse retina. *PLoS One,* 7**,** e50602.

LONN, S., AHLBOM, A., HALL, P., FEYCHTING, M. & SWEDISH INTERPHONE STUDY, G. 2005. Long-term mobile phone use and brain tumor risk. *Am J Epidemiol,* 161**,** 526-35.

LUCAS, R. J., DOUGLAS, R. H. & FOSTER, R. G. 2001. Characterization of an ocular photopigment capable of driving pupillary constriction in mice. *Nat Neurosci,* 4**,** 621-6.

LUCAS, R. J., FREEDMAN, M. S., MUNOZ, M., GARCIA-FERNANDEZ, J. M. & FOSTER, R. G. 1999. Regulation of the mammalian pineal by non-rod, non-cone, ocular photoreceptors. *Science,* 284**,** 505-7.

LUCAS, R. J., HATTAR, S., TAKAO, M., BERSON, D. M., FOSTER, R. G. & YAU, K. W. 2003. Diminished pupillary light reflex at high irradiances in melanopsin-knockout mice. *Science,* 299**,** 245-7.

LUCAS, R. J., LALL, G. S., ALLEN, A. E. & BROWN, T. M. 2012. How rod, cone, and melanopsin photoreceptors come together to enlighten the mammalian circadian clock. *Prog Brain Res,* 199**,** 1-18.

LUPI, D., OSTER, H., THOMPSON, S. & FOSTER, R. G. 2008. The acute light-induction of sleep is mediated by OPN4-based photoreception. *Nat Neurosci,* 11**,** 1068-73.

LYUBARSKY, A., NOKONOV, S., DANIELLE, L. & PUGH, E. 2004. Recent advances in the investigation of mouse cone photoreceptors. *In:* CHALUPA, L. & WILLIAMS, R. (eds.) *Eye, Retina, and Visual System of the Mouse.* MIT Press.

MALIK, A., KONDRATOV, R. V., JAMASBI, R. J. & GEUSZ, M. E. 2015. Circadian Clock Genes Are Essential for Normal Adult Neurogenesis, Differentiation, and Fate Determination. *PLoS One,* 10**,** e0139655.

MASU, M., IWAKABE, H., TAGAWA, Y., MIYOSHI, T., YAMASHITA, M., FUKUDA, Y., SASAKI, H., HIROI, K., NAKAMURA, Y., SHIGEMOTO, R. & *ET AL*. 1995. Specific deficit of the ON response in visual transmission by targeted disruption of the mGluR6 gene. *Cell,* 80**,** 757-65.

MATEJU, K., SUMOVA, A. & BENDOVA, Z. 2010. Expression and light sensitivity of clock genes Per1 and Per2 and immediate-early gene c-fos within the retina of early postnatal Wistar rats. *J Comp Neurol,* 518**,** 3630-44.

MATHES, A., ENGEL, L., HOLTHUES, H., WOLLOSCHECK, T. & SPESSERT, R. 2007. Daily profile in melanopsin transcripts depends on seasonal lighting conditions in the rat retina. *J Neuroendocrinol,* 19**,** 952-7.

MAYNARD, M. L., ZELE, A. J. & FEIGL, B. 2015. Melanopsin-Mediated Post-Illumination Pupil Response in Early Age-Related Macular Degeneration. *Invest Ophthalmol Vis Sci,* 56**,** 6906-13.

MAYWOOD, E. S., CHESHAM, J. E., MENG, Q. J., NOLAN, P. M., LOUDON, A. S. & HASTINGS, M. H. 2011. Tuning the period of the mammalian circadian clock: additive and independent effects of CK1epsilonTau and Fbxl3Afh mutations on mouse circadian behavior and molecular pacemaking. *J Neurosci,* 31**,** 1539-44.

MCCLUNG, C. A., SIDIROPOULOU, K., VITATERNA, M., TAKAHASHI, J. S., WHITE, F. J., COOPER, D. C. & NESTLER, E. J. 2005. Regulation of dopaminergic transmission and cocaine reward by the Clock gene. *Proc Natl Acad Sci U S A,* 102**,** 9377-81.

MCGREGOR, A. 1998. WHO launches mobile-phone hazards study. *Lancet,* 351**,** 276.

MCMAHON, D. G., IUVONE, P. M. & TOSINI, G. 2014. Circadian organization of the mammalian retina: from gene regulation to physiology and diseases. *Prog Retin Eye Res,* 39**,** 58-76.

MCNEILL, D. S., SHEELY, C. J., ECKER, J. L., BADEA, T. C., MORHARDT, D., GUIDO, W. & HATTAR, S. 2011. Development of melanopsin-based irradiance detecting circuitry. *Neural Dev,* 6**,** 8.

MCWATTERS, H. G., BASTOW, R. M., HALL, A. & MILLAR, A. J. 2000. The ELF3 zeitnehmer regulates light signalling to the circadian clock. *Nature,* 408**,** 716-20.

MEIJER, J. H. & SCHWARTZ, W. J. 2003. In search of the pathways for light-induced pacemaker resetting in the suprachiasmatic nucleus. *J Biol Rhythms,* 18**,** 235-49.

MEIJER, J. H., WATANABE, K., DETARI, L. & SCHAAP, J. 1996. Circadian rhythm in light response in suprachiasmatic nucleus neurons of freely moving rats. *Brain Res,* 741**,** 352-5.

MEIJER, J. H., WATANABE, K., SCHAAP, J., ALBUS, H. & DETARI, L. 1998. Light responsiveness of the suprachiasmatic nucleus: long-term multiunit and single-unit recordings in freely moving rats. *J Neurosci,* 18**,** 9078-87.

MELYAN, Z., TARTTELIN, E. E., BELLINGHAM, J., LUCAS, R. J. & HANKINS, M. W. 2005. Addition of human melanopsin renders mammalian cells photoresponsive. *Nature,* 433**,** 741-5.

MERROW, M., BRUNNER, M. & ROENNEBERG, T. 1999. Assignment of circadian function for the Neurospora clock gene frequency. *Nature,* 399**,** 584-6.

MERROW, M., DRAGOVIC, Z., TAN, Y., MEYER, G., SVERIC, K., MASON, M., RICKEN, J. & ROENNEBERG, T. 2003. Combining theoretical and experimental approaches to understand the circadian clock. *Chronobiol Int,* 20**,** 559-75.

MILLER, B. H., OLSON, S. L., TUREK, F. W., LEVINE, J. E., HORTON, T. H. & TAKAHASHI, J. S. 2004. Circadian

clock mutation disrupts estrous cyclicity and maintenance of pregnancy. *Curr Biol,* 14**,** 1367-73.
MITSUI, H., MAEDA, T., YAMAGUCHI, C., TSUJI, Y., WATARI, R., KUBO, Y., OKANO, K. & OKANO, T. 2015. Overexpression in yeast, photocycle, and in vitro structural change of an avian putative magnetoreceptor cryptochrome4. *Biochemistry,* 54**,** 1908-17.
MIYAMOTO, Y. & SANCAR, A. 1998. Vitamin B2-based blue-light photoreceptors in the retinohypothalamic tract as the photoactive pigments for setting the circadian clock in mammals. *Proc Natl Acad Sci U S A,* 95**,** 6097-102.
MOHAWK, J. A., BAER, M. L. & MENAKER, M. 2009. The methamphetamine-sensitive circadian oscillator does not employ canonical clock genes. *Proc Natl Acad Sci U S A,* 106**,** 3519-24.
MOORE, R. Y. & EICHLER, V. B. 1972. Loss of a circadian adrenal corticosterone rhythm following suprachiasmatic lesions in the rat. *Brain Res,* 42**,** 201-6.
MORGAN, L. L., MILLER, A. B., SASCO, A. & DAVIS, D. L. 2015. Mobile phone radiation causes brain tumors and should be classified as a probable human carcinogen (2A) (review). *Int J Oncol,* 46**,** 1865-71.
MORSE, D., HASTINGS, J. W. & ROENNEBERG, T. 1994. Different phase responses of the two circadian oscillators in Gonyaulax. *J Biol Rhythms,* 9**,** 263-74.
MOURITSEN, H., HEYERS, D. & GUNTURKUN, O. 2016. The Neural Basis of Long-Distance Navigation in Birds. *Annu Rev Physiol,* 78**,** 133-54.
MOURITSEN, H. & HORE, P. J. 2012. The magnetic retina: light-dependent and trigeminal magnetoreception in migratory birds. *Curr Opin Neurobiol,* 22**,** 343-52.
MOURITSEN, H., JANSSEN-BIENHOLD, U., LIEDVOGEL, M., FEENDERS, G., STALLEICKEN, J., DIRKS, P. & WEILER, R. 2004. Cryptochromes and neuronal-activity markers colocalize in the retina of migratory birds during magnetic orientation. *Proc Natl Acad Sci U S A,* 101**,** 14294-9.
MROSOVSKY, N. 1999. Masking: history, definitions, and measurement. *Chronobiol Int,* 16**,** 415-29.
MUHEIM, R., EDGAR, N. M., SLOAN, K. A. & PHILLIPS, J. B. 2006. Magnetic compass orientation in C57BL/6J mice. *Learn Behav,* 34**,** 366-73.
MUKHERJEE, S., COQUE, L., CAO, J. L., KUMAR, J., CHAKRAVARTY, S., ASAITHAMBY, A., GRAHAM, A., GORDON, E., ENWRIGHT, J. F., 3RD, DILEONE, R. J., BIRNBAUM, S. G., COOPER, D. C. & MCCLUNG, C. A. 2010. Knockdown of Clock in the ventral tegmental area through RNA interference results in a mixed state of mania and depression-like behavior. *Biol Psychiatry,* 68**,** 503-11.
MULLER, P., YAMAMOTO, J., MARTIN, R., IWAI, S. & BRETTEL, K. 2015. Discovery and functional analysis of a 4th electron-transferring tryptophan conserved exclusively in animal cryptochromes and (6-4) photolyases. *Chem Commun (Camb),* 51**,** 15502-5.
MUNOZ, M., PEIRSON, S. N., HANKINS, M. W. & FOSTER, R. G. 2005. Long-term constant light induces constitutive elevated expression of mPER2 protein in the murine SCN: a molecular basis for Aschoff's rule? *J Biol Rhythms,* 20**,** 3-14.
NELSON, R. J. & ZUCKER, I. 1981. Absence of Extra-Ocular Photoreception in Diurnal and Nocturnal Rodents Exposed to Direct Sunlight. *Comparative Biochemistry and Physiology a-Physiology,* 69**,** 145-148.
NIESSNER, C., DENZAU, S., MALKEMPER, E. P., GROSS, J. C., BURDA, H., WINKLHOFER, M. & PEICHL, L. 2016. Cryptochrome 1 in Retinal Cone Photoreceptors Suggests a Novel Functional Role in Mammals. *Sci Rep,* 6**,** 21848.
NIESSNER, C., DENZAU, S., STAPPUT, K., AHMAD, M., PEICHL, L., WILTSCHKO, W. & WILTSCHKO, R. 2013. Magnetoreception: activated cryptochrome 1a concurs with magnetic orientation in birds. *J R Soc Interface,* 10**,** 20130638.
NIKONOV, S. S., KHOLODENKO, R., LEM, J. & PUGH, E. N., JR. 2006. Physiological features of the S- and M-cone photoreceptors of wild-type mice from single-cell recordings. *J Gen Physiol,* 127**,** 359-74.
NIR, I., HAQUE, R. & IUVONE, P. M. 2000. Diurnal metabolism of dopamine in the mouse retina. *Brain Res,* 870**,** 118-25.
OBRIETAN, K., IMPEY, S. & STORM, D. R. 1998. Light and circadian rhythmicity regulate MAP kinase activation in the suprachiasmatic nuclei. *Nat Neurosci,* 1**,** 693-700.
OHTA, H., YAMAZAKI, S. & MCMAHON, D. G. 2005. Constant light desynchronizes mammalian clock neurons. *Nat Neurosci,* 8**,** 267-9.
OLVECZKY, B. P., BACCUS, S. A. & MEISTER, M. 2003. Segregation of object and background motion in the retina. *Nature,* 423**,** 401-8.
ONO, D., HONMA, S. & HONMA, K. 2013. Postnatal constant light compensates Cryptochrome1 and 2 double deficiency for disruption of circadian behavioral rhythms in mice under constant dark. *PLoS One,* 8**,** e80615.
OWENS, L., BUHR, E., TU, D. C., LAMPRECHT, T. L., LEE, J. & VAN GELDER, R. N. 2012. Effect of circadian clock

gene mutations on nonvisual photoreception in the mouse. *Invest Ophthalmol Vis Sci,* 53**,** 454-60.
OZTURK, N., LEE, J. H., GADDAMEEDHI, S. & SANCAR, A. 2009. Loss of cryptochrome reduces cancer risk in p53 mutant mice. *Proc Natl Acad Sci U S A,* 106**,** 2841-6.
PANDA, S., NAYAK, S. K., CAMPO, B., WALKER, J. R., HOGENESCH, J. B. & JEGLA, T. 2005. Illumination of the melanopsin signaling pathway. *Science,* 307**,** 600-4.
PANDA, S., PROVENCIO, I., TU, D. C., PIRES, S. S., ROLLAG, M. D., CASTRUCCI, A. M., PLETCHER, M. T., SATO, T. K., WILTSHIRE, T., ANDAHAZY, M., KAY, S. A., VAN GELDER, R. N. & HOGENESCH, J. B. 2003. Melanopsin is required for non-image-forming photic responses in blind mice. *Science,* 301**,** 525-7.
PANDA, S., SATO, T. K., CASTRUCCI, A. M., ROLLAG, M. D., DEGRIP, W. J., HOGENESCH, J. B., PROVENCIO, I. & KAY, S. A. 2002. Melanopsin (Opn4) requirement for normal light-induced circadian phase shifting. *Science,* 298**,** 2213-6.
PAPP, S. J., HUBER, A. L., JORDAN, S. D., KRIEBS, A., NGUYEN, M., MORESCO, J. J., YATES, J. R. & LAMIA, K. A. 2015. DNA damage shifts circadian clock time via Hausp-dependent Cry1 stabilization. *Elife,* 4.
PARTCH, C. L., GREEN, C. B. & TAKAHASHI, J. S. 2014. Molecular architecture of the mammalian circadian clock. *Trends Cell Biol,* 24**,** 90-9.
PEIRSON, S. N., BUTLER, J. N., DUFFIELD, G. E., TAKHER, S., SHARMA, P. & FOSTER, R. G. 2006. Comparison of clock gene expression in SCN, retina, heart, and liver of mice. *Biochem Biophys Res Commun,* 351**,** 800-7.
PEIRSON, S. N., BUTLER, J. N. & FOSTER, R. G. 2003. Experimental validation of novel and conventional approaches to quantitative real-time PCR data analysis. *Nucleic Acids Res,* 31**,** e73.
PEIRSON, S. N., THOMPSON, S., HANKINS, M. W. & FOSTER, R. G. 2005. Mammalian photoentrainment: results, methods, and approaches. *Methods Enzymol,* 393**,** 697-726.
PERLMAN, I. & NORMANN, R. A. 1998. Light adaptation and sensitivity controlling mechanisms in vertebrate photoreceptors. *Prog Retin Eye Res,* 17**,** 523-63.
PETRS-SILVA, H., DINCULESCU, A., LI, Q., DENG, W. T., PANG, J. J., MIN, S. H., CHIODO, V., NEELEY, A. W., GOVINDASAMY, L., BENNETT, A., AGBANDJE-MCKENNA, M., ZHONG, L., LI, B., JAYANDHARAN, G. R., SRIVASTAVA, A., LEWIN, A. S. & HAUSWIRTH, W. W. 2011. Novel properties of tyrosine-mutant AAV2 vectors in the mouse retina. *Mol Ther,* 19**,** 293-301.
PHILLIPS, J. B., YOUMANS, P. W., MUHEIM, R., SLOAN, K. A., LANDLER, L., PAINTER, M. S. & ANDERSON, C. R. 2013. Rapid learning of magnetic compass direction by C57BL/6 mice in a 4-armed 'plus' water maze. *PLoS One,* 8**,** e73112.
PICKARD, G. E., BAVER, S. B., OGILVIE, M. D. & SOLLARS, P. J. 2009. Light-induced fos expression in intrinsically photosensitive retinal ganglion cells in melanopsin knockout (opn4) mice. *PLoS One,* 4**,** e4984.
PIRES, S. S., HUGHES, S., TURTON, M., MELYAN, Z., PEIRSON, S. N., ZHENG, L., KOSMAOGLOU, M., BELLINGHAM, J., CHEETHAM, M. E., LUCAS, R. J., FOSTER, R. G., HANKINS, M. W. & HALFORD, S. 2009. Differential expression of two distinct functional isoforms of melanopsin (Opn4) in the mammalian retina. *J Neurosci,* 29**,** 12332-42.
PITTENDRIGH, C. S. 1960. Circadian rhythms and the circadian organization of living systems. *Cold Spring Harb Symp Quant Biol,* 25**,** 159-84.
POTHECARY, C. A., WONG, J., RODGERS, J., HANKINS, M. W., FOSTER, R. G. & PEIRSON, S. In preparation. Characterisation of circadian and post-illumination pupillary responses in melanopsin-deficient mice.
PRITCHETT, D., WULFF, K., OLIVER, P. L., BANNERMAN, D. M., DAVIES, K. E., HARRISON, P. J., PEIRSON, S. N. & FOSTER, R. G. 2012. Evaluating the links between schizophrenia and sleep and circadian rhythm disruption. *J Neural Transm (Vienna),* 119**,** 1061-75.
PROVENCIO, I., JIANG, G., DE GRIP, W. J., HAYES, W. P. & ROLLAG, M. D. 1998. Melanopsin: An opsin in melanophores, brain, and eye. *Proc Natl Acad Sci U S A,* 95**,** 340-5.
PROVENCIO, I., ROLLAG, M. D. & CASTRUCCI, A. M. 2002. Photoreceptive net in the mammalian retina. This mesh of cells may explain how some blind mice can still tell day from night. *Nature,* 415**,** 493.
PRUSKY, G. T., ALAM, N. M., BEEKMAN, S. & DOUGLAS, R. M. 2004. Rapid quantification of adult and developing mouse spatial vision using a virtual optomotor system. *Invest Ophthalmol Vis Sci,* 45**,** 4611-6.
PRUSKY, G. T. & DOUGLAS, R. M. 2004. Characterization of mouse cortical spatial vision. *Vision Res,* 44**,** 3411-8.
QIN, S., YIN, H., YANG, C., DOU, Y., LIU, Z., ZHANG, P., YU, H., HUANG, Y., FENG, J., HAO, J., HAO, J., DENG, L., YAN, X., DONG, X., ZHAO, Z., JIANG, T., WANG, H. W., LUO, S. J. & XIE, C. 2016. A magnetic protein biocompass. *Nat Mater,* 15**,** 217-26.
QIU, X., KUMBALASIRI, T., CARLSON, S. M., WONG, K. Y., KRISHNA, V., PROVENCIO, I. & BERSON, D. M. 2005. Induction of photosensitivity by heterologous expression of melanopsin. *Nature,* 433**,** 745-9.

RALPH, M. R., FOSTER, R. G., DAVIS, F. C. & MENAKER, M. 1990. Transplanted suprachiasmatic nucleus determines circadian period. *Science,* 247**,** 975-8.

REFINETTI, R. 2006. *Circadian physiology,* Boca Raton, CRC Press/Taylor & Francis Group.

REICK, M., GARCIA, J. A., DUDLEY, C. & MCKNIGHT, S. L. 2001. NPAS2: an analog of clock operative in the mammalian forebrain. *Science,* 293**,** 506-9.

REPPERT, S. M. & WEAVER, D. R. 2002. Coordination of circadian timing in mammals. *Nature,* 418**,** 935-41.

RIBELAYGA, C., CAO, Y. & MANGEL, S. C. 2008. The circadian clock in the retina controls rod-cone coupling. *Neuron,* 59**,** 790-801.

RICHTER, C. P. 1971. Inborn nature of the rat's 24-hour clock. *J Comp Physiol Psychol,* 75**,** 1-4.

RITZ, T., ADEM, S. & SCHULTEN, K. 2000. A model for photoreceptor-based magnetoreception in birds. *Biophys J,* 78**,** 707-18.

RITZ, T., AHMAD, M., MOURITSEN, H., WILTSCHKO, R. & WILTSCHKO, W. 2010. Photoreceptor-based magnetoreception: optimal design of receptor molecules, cells, and neuronal processing. *J R Soc Interface,* 7 Suppl 2**,** S135-46.

RITZ, T., THALAU, P., PHILLIPS, J. B., WILTSCHKO, R. & WILTSCHKO, W. 2004. Resonance effects indicate a radical-pair mechanism for avian magnetic compass. *Nature,* 429**,** 177-80.

RITZ, T., WILTSCHKO, R., HORE, P. J., RODGERS, C. T., STAPPUT, K., THALAU, P., TIMMEL, C. R. & WILTSCHKO, W. 2009. Magnetic compass of birds is based on a molecule with optimal directional sensitivity. *Biophys J,* 96**,** 3451-7.

RITZ, T., YOSHII, T., HELFRICH-FOERSTER, C. & AHMAD, M. 2010. Cryptochrome: A photoreceptor with the properties of a magnetoreceptor? *Commun Integr Biol,* 3**,** 24-7.

RODGERS, C. T. & HORE, P. J. 2009. Chemical magnetoreception in birds: the radical pair mechanism. *Proc Natl Acad Sci U S A,* 106**,** 353-60.

RODIECK, R. W. 1998. *The first steps in seeing,* Sunderland, Mass., Sinauer Associates.

ROECKLEIN, K., WONG, P., ERNECOFF, N., MILLER, M., DONOFRY, S., KAMARCK, M., WOOD-VASEY, W. M. & FRANZEN, P. 2013. The post illumination pupil response is reduced in seasonal affective disorder. *Psychiatry Res,* 210**,** 150-8.

ROENNEBERG, T., DAAN, S. & MERROW, M. 2003. The art of entrainment. *J Biol Rhythms,* 18**,** 183-94.

ROENNEBERG, T. & MERROW, M. 1998. Molecular circadian oscillators: an alternative hypothesis. *J Biol Rhythms,* 13**,** 167-79.

ROENNEBERG, T. & MORSE, D. 1993. 2 Circadian Oscillators in One Cell. *Nature,* 362**,** 362-364.

ROENNEBERG, T. & TAYLOR, W. 1994. Light-induced phase responses in Gonyaulax are drastically altered by creatine. *J Biol Rhythms,* 9**,** 1-12.

ROENNEBERG, T., WIRZ-JUSTICE, A. & MERROW, M. 2003. Life between clocks: daily temporal patterns of human chronotypes. *J Biol Rhythms,* 18**,** 80-90.

ROHLICH, P., VAN VEEN, T. & SZEL, A. 1994. Two different visual pigments in one retinal cone cell. *Neuron,* 13**,** 1159-66.

RUAN, G. X., ALLEN, G. C., YAMAZAKI, S. & MCMAHON, D. G. 2008. An autonomous circadian clock in the inner mouse retina regulated by dopamine and GABA. *PLoS Biol,* 6**,** e249.

RUAN, G. X., GAMBLE, K. L., RISNER, M. L., YOUNG, L. A. & MCMAHON, D. G. 2012. Divergent roles of clock genes in retinal and suprachiasmatic nucleus circadian oscillators. *PLoS One,* 7**,** e38985.

RUAN, G. X., ZHANG, D. Q., ZHOU, T., YAMAZAKI, S. & MCMAHON, D. G. 2006. Circadian organization of the mammalian retina. *Proc Natl Acad Sci U S A,* 103**,** 9703-8.

RUDIC, R. D., MCNAMARA, P., CURTIS, A. M., BOSTON, R. C., PANDA, S., HOGENESCH, J. B. & FITZGERALD, G. A. 2004. BMAL1 and CLOCK, two essential components of the circadian clock, are involved in glucose homeostasis. *PLoS Biol,* 2**,** e377.

SACK, R. L., AUCKLEY, D., AUGER, R. R., CARSKADON, M. A., WRIGHT, K. P., JR., VITIELLO, M. V., ZHDANOVA, I. V. & AMERICAN ACADEMY OF SLEEP, M. 2007. Circadian rhythm sleep disorders: part II, advanced sleep phase disorder, delayed sleep phase disorder, free-running disorder, and irregular sleep-wake rhythm. An American Academy of Sleep Medicine review. *Sleep,* 30**,** 1484-501.

SAHA, S., WOODBINE, L., HAINES, J., COSTER, M., RICKET, N., BARAZZUOL, L., AINSBURY, E., SIENKIEWICZ, Z. & JEGGO, P. 2014. Increased apoptosis and DNA double-strand breaks in the embryonic mouse brain in response to very low-dose X-rays but not 50 Hz magnetic fields. *J R Soc Interface,* 11**,** 20140783.

SAINI, C., SUTER, D. M., LIANI, A., GOS, P. & SCHIBLER, U. 2011. The mammalian circadian timing system: synchronization of peripheral clocks. *Cold Spring Harb Symp Quant Biol,* 76**,** 39-47.

SAKAMOTO, K., LIU, C., KASAMATSU, M., POZDEYEV, N. V., IUVONE, P. M. & TOSINI, G. 2005. Dopamine regulates melanopsin mRNA expression in intrinsically photosensitive retinal ganglion cells. *Eur J*

Neurosci, 22**,** 3129-36.
SANCAR, A. 2000. Cryptochrome: the second photoactive pigment in the eye and its role in circadian photoreception. *Annu Rev Biochem,* 69**,** 31-67.
SANCAR, A. 2003. Structure and function of DNA photolyase and cryptochrome blue-light photoreceptors. *Chem Rev,* 103**,** 2203-37.
SANDU, C., HICKS, D. & FELDER-SCHMITTBUHL, M. P. 2011. Rat photoreceptor circadian oscillator strongly relies on lighting conditions. *Eur J Neurosci,* 34**,** 507-16.
SAPER, C. B. 2005. An open letter to our readers on the use of antibodies. *J Comp Neurol,* 493**,** 477-8.
SCHMIDT, T. M., ALAM, N. M., CHEN, S., KOFUJI, P., LI, W., PRUSKY, G. T. & HATTAR, S. 2014. A role for melanopsin in alpha retinal ganglion cells and contrast detection. *Neuron,* 82**,** 781-8.
SCHMIDT, T. M., CHEN, S. K. & HATTAR, S. 2011. Intrinsically photosensitive retinal ganglion cells: many subtypes, diverse functions. *Trends Neurosci,* 34**,** 572-80.
SCHMIDT, T. M., TANIGUCHI, K. & KOFUJI, P. 2008. Intrinsic and extrinsic light responses in melanopsin-expressing ganglion cells during mouse development. *J Neurophysiol,* 100**,** 371-84.
SCHULTEN, K., SWENBERG, C. E. & WELLER, A. 1978. Biomagnetic Sensory Mechanism Based on Magnetic-Field Modulated Coherent Electron-Spin Motion. *Zeitschrift Fur Physikalische Chemie-Frankfurt,* 111**,** 1-5.
SEKARAN, S., FOSTER, R. G., LUCAS, R. J. & HANKINS, M. W. 2003. Calcium imaging reveals a network of intrinsically light-sensitive inner-retinal neurons. *Curr Biol,* 13**,** 1290-8.
SEKARAN, S., LUPI, D., JONES, S. L., SHEELY, C. J., HATTAR, S., YAU, K. W., LUCAS, R. J., FOSTER, R. G. & HANKINS, M. W. 2005. Melanopsin-dependent photoreception provides earliest light detection in the mammalian retina. *Curr Biol,* 15**,** 1099-107.
SELBY, C. P., THOMPSON, C., SCHMITZ, T. M., VAN GELDER, R. N. & SANCAR, A. 2000. Functional redundancy of cryptochromes and classical photoreceptors for nonvisual ocular photoreception in mice. *Proc Natl Acad Sci U S A,* 97**,** 14697-702.
SEMM, P. & BEASON, R. C. 1990. Responses to small magnetic variations by the trigeminal system of the bobolink. *Brain Res Bull,* 25**,** 735-40.
SEMO, M., LUPI, D., PEIRSON, S. N., BUTLER, J. N. & FOSTER, R. G. 2003. Light-induced c-fos in melanopsin retinal ganglion cells of young and aged rodless/coneless (rd/rd cl) mice. *Eur J Neurosci,* 18**,** 3007-17.
SEMO, M., PEIRSON, S., LUPI, D., LUCAS, R. J., JEFFERY, G. & FOSTER, R. G. 2003. Melanopsin retinal ganglion cells and the maintenance of circadian and pupillary responses to light in aged rodless/coneless (rd/rd cl) mice. *Eur J Neurosci,* 17**,** 1793-801.
SENGUPTA, A., BABA, K., MAZZONI, F., POZDEYEV, N. V., STRETTOI, E., IUVONE, P. M. & TOSINI, G. 2011. Localization of melatonin receptor 1 in mouse retina and its role in the circadian regulation of the electroretinogram and dopamine levels. *PLoS One,* 6**,** e24483.
SHAW, J., BOYD, A., HOUSE, M., WOODWARD, R., MATHES, F., COWIN, G., SAUNDERS, M. & BAER, B. 2015. Magnetic particle-mediated magnetoreception. *J R Soc Interface,* 12**,** 0499.
SHEARMAN, L. P., SRIRAM, S., WEAVER, D. R., MAYWOOD, E. S., CHAVES, I., ZHENG, B., KUME, K., LEE, C. C., VAN DER HORST, G. T., HASTINGS, M. H. & REPPERT, S. M. 2000. Interacting molecular loops in the mammalian circadian clock. *Science,* 288**,** 1013-9.
SIEPKA, S. M., YOO, S. H., PARK, J., SONG, W., KUMAR, V., HU, Y., LEE, C. & TAKAHASHI, J. S. 2007. Circadian mutant Overtime reveals F-box protein FBXL3 regulation of cryptochrome and period gene expression. *Cell,* 129**,** 1011-23.
SMITH, L. & CANAL, M. M. 2009. Expression of circadian neuropeptides in the hypothalamus of adult mice is affected by postnatal light experience. *J Neuroendocrinol,* 21**,** 946-53.
SMITH, R. S., EFRON, B., MAH, C. D. & MALHOTRA, A. 2013. The impact of circadian misalignment on athletic performance in professional football players. *Sleep,* 36**,** 1999-2001.
SOKOLOVE, P. G. & BUSHELL, W. N. 1978. The chi square periodogram: its utility for analysis of circadian rhythms. *J Theor Biol,* 72**,** 131-60.
SOLOV'YOV, I. A., MOURITSEN, H. & SCHULTEN, K. 2010. Acuity of a cryptochrome and vision-based magnetoreception system in birds. *Biophys J,* 99**,** 40-9.
SOMERS, D. E., DEVLIN, P. F. & KAY, S. A. 1998. Phytochromes and cryptochromes in the entrainment of the Arabidopsis circadian clock. *Science,* 282**,** 1488-90.
SON, G. H., CHUNG, S. & KIM, K. 2011. The adrenal peripheral clock: glucocorticoid and the circadian timing system. *Front Neuroendocrinol,* 32**,** 451-65.
SOUCY, E., WANG, Y., NIRENBERG, S., NATHANS, J. & MEISTER, M. 1998. A novel signaling pathway from rod photoreceptors to ganglion cells in mammalian retina. *Neuron,* 21**,** 481-93.

STAIGER, D. & GREEN, R. 2011. RNA-based regulation in the plant circadian clock. *Trends Plant Sci,* 16**,** 517-23.

STANEWSKY, R., KANEKO, M., EMERY, P., BERETTA, B., WAGER-SMITH, K., KAY, S. A., ROSBASH, M. & HALL, J. C. 1998. The cryb mutation identifies cryptochrome as a circadian photoreceptor in Drosophila. *Cell,* 95**,** 681-92.

STEPHAN, F. K. & ZUCKER, I. 1972. Circadian rhythms in drinking behavior and locomotor activity of rats are eliminated by hypothalamic lesions. *Proc Natl Acad Sci U S A,* 69**,** 1583-6.

STORCH, K. F., PAZ, C., SIGNOROVITCH, J., RAVIOLA, E., PAWLYK, B., LI, T. & WEITZ, C. J. 2007. Intrinsic circadian clock of the mammalian retina: importance for retinal processing of visual information. *Cell,* 130**,** 730-41.

STRAIF, K., BAAN, R., GROSSE, Y., SECRETAN, B., EL GHISSASSI, F., BOUVARD, V., ALTIERI, A., BENBRAHIM-TALLAA, L. & COGLIANO, V. 2007. Carcinogenicity of shift-work, painting, and fire-fighting. *Lancet Oncol,* 8**,** 1065-6.

STRETTOI, E., RAVIOLA, E. & DACHEUX, R. F. 1992. Synaptic connections of the narrow-field, bistratified rod amacrine cell (AII) in the rabbit retina. *J Comp Neurol,* 325**,** 152-68.

SUDO, M., SASAHARA, K., MORIYA, T., AKIYAMA, M., HAMADA, T. & SHIBATA, S. 2003. Constant light housing attenuates circadian rhythms of mPer2 mRNA and mPER2 protein expression in the suprachiasmatic nucleus of mice. *Neuroscience,* 121**,** 493-9.

TAKAHASHI, J. S., HONG, H. K., KO, C. H. & MCDEARMON, E. L. 2008. The genetics of mammalian circadian order and disorder: implications for physiology and disease. *Nat Rev Genet,* 9**,** 764-75.

TEIRSTEIN, P. S., GOLDMAN, A. I. & O'BRIEN, P. J. 1980. Evidence for both local and central regulation of rat rod outer segment disc shedding. *Invest Ophthalmol Vis Sci,* 19**,** 1268-73.

TERMAN, J. S., REME, C. E. & TERMAN, M. 1993. Rod outer segment disk shedding in rats with lesions of the suprachiasmatic nucleus. *Brain Res,* 605**,** 256-64.

THALAU, P., RITZ, T., STAPPUT, K., WILTSCHKO, R. & WILTSCHKO, W. 2005. Magnetic compass orientation of migratory birds in the presence of a 1.315 MHz oscillating field. *Naturwissenschaften,* 92**,** 86-90.

THOMPSON, C. L., BOWES RICKMAN, C., SHAW, S. J., EBRIGHT, J. N., KELLY, U., SANCAR, A. & RICKMAN, D. W. 2003. Expression of the blue-light receptor cryptochrome in the human retina. *Invest Ophthalmol Vis Sci,* 44**,** 4515-21.

THOMPSON, C. L., SELBY, C. P., VAN GELDER, R. N., BLANER, W. S., LEE, J., QUADRO, L., LAI, K., GOTTESMAN, M. E. & SANCAR, A. 2004. Effect of vitamin A depletion on nonvisual phototransduction pathways in cryptochromeless mice. *J Biol Rhythms,* 19**,** 504-17.

THRESHER, R. J., VITATERNA, M. H., MIYAMOTO, Y., KAZANTSEV, A., HSU, D. S., PETIT, C., SELBY, C. P., DAWUT, L., SMITHIES, O., TAKAHASHI, J. S. & SANCAR, A. 1998. Role of mouse cryptochrome blue-light photoreceptor in circadian photoresponses. *Science,* 282**,** 1490-4.

TODA, K., BUSH, R. A., HUMPHRIES, P. & SIEVING, P. A. 1999. The electroretinogram of the rhodopsin knockout mouse. *Vis Neurosci,* 16**,** 391-8.

TONETTI, L., NATALE, V. & RANDLER, C. 2015. Association between circadian preference and academic achievement: A systematic review and meta-analysis. *Chronobiol Int,* 32**,** 792-801.

TOSINI, G., DAVIDSON, A. J., FUKUHARA, C., KASAMATSU, M. & CASTANON-CERVANTES, O. 2007. Localization of a circadian clock in mammalian photoreceptors. *FASEB J,* 21**,** 3866-71.

TOSINI, G., KASAMATSU, M. & SAKAMOTO, K. 2007. Clock gene expression in the rat retina: effects of lighting conditions and photoreceptor degeneration. *Brain Res,* 1159**,** 134-40.

TOSINI, G. & MENAKER, M. 1996. Circadian rhythms in cultured mammalian retina. *Science,* 272**,** 419-21.

TOSINI, G., POZDEYEV, N., SAKAMOTO, K. & IUVONE, P. M. 2008. The circadian clock system in the mammalian retina. *Bioessays,* 30**,** 624-33.

TU, D. C., BATTEN, M. L., PALCZEWSKI, K. & VAN GELDER, R. N. 2004. Nonvisual photoreception in the chick iris. *Science,* 306**,** 129-31.

TU, D. C., ZHANG, D., DEMAS, J., SLUTSKY, E. B., PROVENCIO, I., HOLY, T. E. & VAN GELDER, R. N. 2005. Physiologic diversity and development of intrinsically photosensitive retinal ganglion cells. *Neuron,* 48**,** 987-99.

TUREK, F. W., JOSHU, C., KOHSAKA, A., LIN, E., IVANOVA, G., MCDEARMON, E., LAPOSKY, A., LOSEE-OLSON, S., EASTON, A., JENSEN, D. R., ECKEL, R. H., TAKAHASHI, J. S. & BASS, J. 2005. Obesity and metabolic syndrome in circadian Clock mutant mice. *Science,* 308**,** 1043-5.

VAN DER HORST, G. T., MUIJTJENS, M., KOBAYASHI, K., TAKANO, R., KANNO, S., TAKAO, M., DE WIT, J., VERKERK, A., EKER, A. P., VAN LEENEN, D., BUIJS, R., BOOTSMA, D., HOEIJMAKERS, J. H. & YASUI, A. 1999. Mammalian Cry1 and Cry2 are essential for maintenance of circadian rhythms. *Nature,* 398**,** 627-30.

VAN DER VINNE, V., ZERBINI, G., SIERSEMA, A., PIEPER, A., MERROW, M., HUT, R. A., ROENNEBERG, T. & KANTERMANN, T. 2015. Timing of examinations affects school performance differently in early and late chronotypes. *J Biol Rhythms,* 30**,** 53-60.

VAN GELDER, R. N., WEE, R., LEE, J. A. & TU, D. C. 2003. Reduced pupillary light responses in mice lacking cryptochromes. *Science,* 299**,** 222.

VAN HOOK, M. J., WONG, K. Y. & BERSON, D. M. 2012. Dopaminergic modulation of ganglion-cell photoreceptors in rat. *Eur J Neurosci,* 35**,** 507-18.

VANDESOMPELE, J., DE PRETER, K., PATTYN, F., POPPE, B., VAN ROY, N., DE PAEPE, A. & SPELEMAN, F. 2002. Accurate normalization of real-time quantitative RT-PCR data by geometric averaging of multiple internal control genes. *Genome Biol,* 3**,** RESEARCH0034.

VANVICKLE-CHAVEZ, S. J. & VAN GELDER, R. N. 2007. Action spectrum of Drosophila cryptochrome. *The Journal of biological chemistry,* 282**,** 10561-6.

VETTER, C., FISCHER, D., MATERA, J. L. & ROENNEBERG, T. 2015. Aligning work and circadian time in shift workers improves sleep and reduces circadian disruption. *Curr Biol,* 25**,** 907-11.

VETTER, C., JUDA, M. & ROENNEBERG, T. 2012. The influence of internal time, time awake, and sleep duration on cognitive performance in shiftworkers. *Chronobiol Int,* 29**,** 1127-38.

VITATERNA, M. H., SELBY, C. P., TODO, T., NIWA, H., THOMPSON, C., FRUECHTE, E. M., HITOMI, K., THRESHER, R. J., ISHIKAWA, T., MIYAZAKI, J., TAKAHASHI, J. S. & SANCAR, A. 1999. Differential regulation of mammalian period genes and circadian rhythmicity by cryptochromes 1 and 2. *Proc Natl Acad Sci U S A,* 96**,** 12114-9.

VOLGYI, B., CHHEDA, S. & BLOOMFIELD, S. A. 2009. Tracer coupling patterns of the ganglion cell subtypes in the mouse retina. *J Comp Neurol,* 512**,** 664-87.

VUGLER, A. A., REDGRAVE, P., SEMO, M., LAWRENCE, J., GREENWOOD, J. & COFFEY, P. J. 2007. Dopamine neurones form a discrete plexus with melanopsin cells in normal and degenerating retina. *Exp Neurol,* 205**,** 26-35.

WAITE, E. J., MCKENNA, M., KERSHAW, Y., WALKER, J. J., CHO, K., PIGGINS, H. D. & LIGHTMAN, S. L. 2012. Ultradian corticosterone secretion is maintained in the absence of circadian cues. *Eur J Neurosci,* 36**,** 3142-50.

WATARI, R., YAMAGUCHI, C., ZEMBA, W., KUBO, Y., OKANO, K. & OKANO, T. 2012. Light-dependent structural change of chicken retinal Cryptochrome4. *J Biol Chem,* 287**,** 42634-41.

WELSH, D. K., LOGOTHETIS, D. E., MEISTER, M. & REPPERT, S. M. 1995. Individual neurons dissociated from rat suprachiasmatic nucleus express independently phased circadian firing rhythms. *Neuron,* 14**,** 697-706.

WENG, S., WONG, K. Y. & BERSON, D. M. 2009. Circadian modulation of melanopsin-driven light response in rat ganglion-cell photoreceptors. *J Biol Rhythms,* 24**,** 391-402.

WILTSCHKO, R., SCHIFFNER, I., FUHRMANN, P. & WILTSCHKO, W. 2010. The role of the magnetite-based receptors in the beak in pigeon homing. *Curr Biol,* 20**,** 1534-8.

WILTSCHKO, R. & WILTSCHKO, W. 2012. Magnetoreception. *Adv Exp Med Biol,* 739**,** 126-41.

WILTSCHKO, R. & WILTSCHKO, W. 2013. The magnetite-based receptors in the beak of birds and their role in avian navigation. *J Comp Physiol A Neuroethol Sens Neural Behav Physiol,* 199**,** 89-98.

WILTSCHKO, W. & WILTSCHKO, R. 2002. Magnetic compass orientation in birds and its physiological basis. *Naturwissenschaften,* 89**,** 445-52.

WITKOVSKY, P. 2004. Dopamine and retinal function. *Doc Ophthalmol,* 108**,** 17-40.

WITKOVSKY, P., VEISENBERGER, E., LESAUTER, J., YAN, L., JOHNSON, M., ZHANG, D. Q., MCMAHON, D. & SILVER, R. 2003. Cellular location and circadian rhythm of expression of the biological clock gene Period 1 in the mouse retina. *J Neurosci,* 23**,** 7670-6.

XING, W., BUSINO, L., HINDS, T. R., MARIONNI, S. T., SAIFEE, N. H., BUSH, M. F., PAGANO, M. & ZHENG, N. 2013. SCF(FBXL3) ubiquitin ligase targets cryptochromes at their cofactor pocket. *Nature,* 496**,** 64-8.

XUE, T., DO, M. T., RICCIO, A., JIANG, Z., HSIEH, J., WANG, H. C., MERBS, S. L., WELSBIE, D. S., YOSHIOKA, T., WEISSGERBER, P., STOLZ, S., FLOCKERZI, V., FREICHEL, M., SIMON, M. I., CLAPHAM, D. E. & YAU, K. W. 2011. Melanopsin signalling in mammalian iris and retina. *Nature,* 479**,** 67-73.

YAMAGUCHI, S., KOBAYASHI, M., MITSUI, S., ISHIDA, Y., VAN DER HORST, G. T., SUZUKI, M., SHIBATA, S. & OKAMURA, H. 2001. View of a mouse clock gene ticking. *Nature,* 409**,** 684.

YAMAZAKI, S., ALONES, V. & MENAKER, M. 2002. Interaction of the retina with suprachiasmatic pacemakers in the control of circadian behavior. *J Biol Rhythms,* 17**,** 315-29.

YANG, X. L. & WU, S. M. 1991. Feedforward lateral inhibition in retinal bipolar cells: input-output relation of the horizontal cell-depolarizing bipolar cell synapse. *Proc Natl Acad Sci U S A,* 88**,** 3310-3.

YOO, S. H., MOHAWK, J. A., SIEPKA, S. M., SHAN, Y., HUH, S. K., HONG, H. K., KORNBLUM, I., KUMAR, V., KOIKE, N., XU, M., NUSSBAUM, J., LIU, X., CHEN, Z., CHEN, Z. J., GREEN, C. B. & TAKAHASHI, J. S. 2013. Competing E3 ubiquitin ligases govern circadian periodicity by degradation of CRY in nucleus and cytoplasm. *Cell,* 152**,** 1091-105.

YOO, S. H., YAMAZAKI, S., LOWREY, P. L., SHIMOMURA, K., KO, C. H., BUHR, E. D., SIEPKA, S. M., HONG, H. K., OH, W. J., YOO, O. J., MENAKER, M. & TAKAHASHI, J. S. 2004. PERIOD2::LUCIFERASE real-time reporting of circadian dynamics reveals persistent circadian oscillations in mouse peripheral tissues. *Proc Natl Acad Sci U S A,* 101**,** 5339-46.

YOUNG, M. 2005. *Circadian Rhythms: Methods in Enzymology*, Elsevier Science.

YUJNOVSKY, I., HIRAYAMA, J., DOI, M., BORRELLI, E. & SASSONE-CORSI, P. 2006. Signaling mediated by the dopamine D2 receptor potentiates circadian regulation by CLOCK:BMAL1. *Proc Natl Acad Sci U S A,* 103**,** 6386-91.

ZAVADA, A., GORDIJN, M. C., BEERSMA, D. G., DAAN, S. & ROENNEBERG, T. 2005. Comparison of the Munich Chronotype Questionnaire with the Horne-Ostberg's Morningness-Eveningness Score. *Chronobiol Int,* 22**,** 267-78.

ZELE, A. J., FEIGL, B., SMITH, S. S. & MARKWELL, E. L. 2011. The circadian response of intrinsically photosensitive retinal ganglion cells. *PLoS One,* 6**,** e17860.

ZHANG, D. Q., BELENKY, M. A., SOLLARS, P. J., PICKARD, G. E. & MCMAHON, D. G. 2012. Melanopsin mediates retrograde visual signaling in the retina. *PLoS One,* 7**,** e42647.

ZHANG, D. Q., WONG, K. Y., SOLLARS, P. J., BERSON, D. M., PICKARD, G. E. & MCMAHON, D. G. 2008. Intraretinal signaling by ganglion cell photoreceptors to dopaminergic amacrine neurons. *Proc Natl Acad Sci U S A,* 105**,** 14181-6.

ZHANG, R., LAHENS, N. F., BALLANCE, H. I., HUGHES, M. E. & HOGENESCH, J. B. 2014. A circadian gene expression atlas in mammals: implications for biology and medicine. *Proc Natl Acad Sci U S A,* 111**,** 16219-24.

ZHENG, B., ALBRECHT, U., KAASIK, K., SAGE, M., LU, W., VAISHNAV, S., LI, Q., SUN, Z. S., EICHELE, G., BRADLEY, A. & LEE, C. C. 2001. Nonredundant roles of the mPer1 and mPer2 genes in the mammalian circadian clock. *Cell,* 105**,** 683-94.